

Towards an EEG cap: A study of electrode ability under non-ideal conditions

ROSHAN FEDRIC COELHO
MASTERS OF ENGINEERING (BIOMEDICAL)

SUPERVISOR: DOCTOR KENNETH J. POPE
SUBMISSION: 19TH MAY 2019

Submitted to the College of Science and Engineering in partial fulfillment of the requirements for the degree of Masters of Engineering (Biomedical) at Flinders University – Adelaide, Australia

Declaration

I certify that this work does not incorporate without acknowledgement any material previously submitted for a degree or diploma in any university, and that to the best of my knowledge and belief it does not contain any material previously published or written by another person except where due reference is made in text.

A handwritten signature in black ink, appearing to read 'Roshan', with a long horizontal stroke extending to the right. The signature is set against a light, textured background.

Roshan Fedric Coelho

19th May 2019

Acknowledgements

I would like to acknowledge the technical and academic encouragement and assistance shown by Professor Kenneth J. Pope for the duration of my thesis. I would also like to thank Professor Trent Lewis for assisting in the experimental work in the laboratory. I would also like to express my appreciation to Professor John Willoughby and my peer Andrew J. Lelei for agreeing to participate in the experimental phase.

Table of Contents

1. Abstract	7
2. Introduction	8
3. Literature Review	10
3.1. EEG analysis	10
3.1.1. ICA/CCA analysis	10
3.1.2. Source analysis	12
3.2. Laplacian transform	14
3.3. Types of Electrodes.....	15
3.3.1. Passive wet electrodes	15
3.3.2. Dry electrodes.....	18
3.3.3. tCRE electrodes.....	19
3.4. Optimal experimental electrode parameters.....	22
3.4.1. Frequency response of different types of electrodes	22
3.4.2. Effect of site of electrodes.....	23
3.4.3. Effect of number of electrodes.....	24
3.5. Neurological disorders.....	25
3.5.1. Bipolar disorder	25
3.5.2. Schizophrenia	27
4. Method	29
4.1. 20 tCRE electrodes with 108 passive wet electrodes.....	30
4.2. tCRE electrodes periphery test (9 central + 11 peripheral electrodes).....	31
4.3. 20 tCRE electrodes used 'dry' in the cap	34
4.4. 20 tCRE electrodes used 'dry' under the cap	34
4.5. 20 tCRE electrodes used in cap with saline filled foam in the cap	35
4.6. 20 tCRE electrodes used in the cap with foam cap underneath	37
4.6.1. 20 tCRE electrodes with foam cap used on subject with thick hair	37
4.6.2. 20 tCRE electrodes with foam cap used on subject with short, curly, stiff hair.....	38
4.7. 20 ring electrodes used 'dry' in the cap	39
4.8. 8 SAHARA electrode used 'dry' in the cap.....	40
4.8.1. SAHARA electrodes used on subject with thick hair	41

4.8.2.	SAHARA electrodes used on subject with short, curly, stiff hair	42
4.9.	5mm dry comb electrodes used with ring electrodes in cap	42
4.9.1.	Dry comb electrodes used on subject with thick hair	43
4.9.2.	Dry comb electrodes used on subject with short, curly, stiff hair.....	44
5.	Results	45
5.1.	20 tCRE electrodes with 108 passive wet electrodes.....	45
5.2.	tCRE electrodes periphery test (9 central + 11 peripheral electrodes).....	48
5.2.1.	tCRE electrode periphery test on subject with thin, wispy hair	48
5.2.2.	tCRE electrode periphery test on subject with short, stiff curly hair	50
5.3.	20 tCRE electrodes used 'dry' in the cap	53
5.3.1.	20 tCRE electrodes used 'dry' in cap on subject with thick hair.....	53
5.3.2.	20 tCRE electrodes used 'dry' in cap on subject with short, stiff curly hair	55
5.4.	20 tCRE electrodes used 'dry' under the cap	57
5.5.	20 tCRE electrodes used in cap with saline filled foam infills in the cap.....	59
5.5.1.	20 tCRE electrodes used in cap with saline filled foam infills in cap used on subject with thin, wispy hair	59
5.5.2.	20 tCRE electrodes used in cap with saline filled foam infills in cap used on subject with thick hair	61
5.6.	20 tCRE electrodes used in cap with foam cap underneath.....	63
5.6.1.	20 tCRE electrodes used in cap with foam cap underneath on subject with thick hair	63
5.6.2.	20 tCRE electrodes with foam cap used on subject with short, stiff curly hair.....	65
5.7.	20 ring electrodes used 'dry' in the cap	67
5.8.	8 SAHARA electrodes used dry in the cap	69
5.8.1.	SAHARA electrodes used on subject with thick hair	69
5.8.2.	SAHARA electrodes used on subject with short, stiff curly hair	71
5.9.	5mm dry comb electrodes used with ring electrodes in cap	73
5.9.1.	Dry comb electrodes with ring electrodes used on subject with thick hair with lights on	73
5.9.2.	Dry comb electrodes with ring electrodes used on subject with thick hair with lights off.....	75
5.9.3.	Dry comb electrodes with ring electrodes used on subject with short, stiff curly hair	77
6.	Discussion	79
6.1.	20 tCRE electrodes with 108 passive wet electrodes.....	80

6.2.	tCRE electrodes periphery test (9 central + 11 peripheral electrodes)	81
6.2.1.	tCRE electrode periphery test on subject with thin, wispy hair	81
6.2.2.	tCRE electrode periphery test on subject with short, stiff curly hair	83
6.3.	20 tCRE electrodes used 'dry' in the cap	84
6.3.1.	20 tCRE electrodes used 'dry' in cap on subject with thick hair	84
6.3.2.	20 tCREs used 'dry' in cap on subject with short, stiff, curly hair	85
6.4.	20 tCRE electrodes used 'dry' under the cap	85
6.5.	20 tCRE electrodes used in cap with saline filled foam in the cap	86
6.5.1.	20 tCRE electrodes used in cap with saline filled foam in cap used on subject with thin, wispy hair	86
6.5.2.	20 tCRE electrodes used in cap with saline filled foam in cap used on subject with thick hair	87
6.6.	20 tCRE electrodes used in cap with saline soaked foam cap underneath	88
6.6.1.	20 tCRE electrodes with foam cap used on subject with thick hair	88
6.6.2.	20 tCRE electrodes with foam cap used on subject with short, thick, stiff curly hair	89
6.7.	20 ring electrodes used 'dry' in the cap	89
6.8.	8 SAHARA electrodes used dry in the cap	90
6.8.1.	SAHARA electrodes used on subject with thick hair	90
6.8.2.	SAHARA electrodes used on subject with short, stiff curly hair	91
6.9.	5mm dry comb electrodes used with ring electrodes in cap	92
6.9.1.	Dry comb electrodes with ring electrodes used on subject with thick hair with lights on	92
6.9.2.	Dry comb electrodes with ring electrodes used on subject with thick hair with lights off	93
6.9.3.	Dry comb electrodes with ring electrodes used on subject with short, stiff curly hair	94
7.	Conclusion	96
8.	Bibliography	98
9.	Appendix	103
9.1.	Appendix A	103
9.1.1.	Loading the data	103
9.1.2.	Find the tCRE electrodes	104
9.1.3.	Extract task specific data	104
9.1.4.	Separating the EEG and the tCRE EEG electrodes	105
9.1.5.	Calculate the Spectra	105

9.1.6.	Berger Effect	106
9.1.7.	Laplacian of EEG from selected electrodes	106
9.1.8.	Display Spectra	107
9.1.9.	Topographies of Muscle, Relative Muscle between Laplacian of EEG and electrode EEG	108
9.2.	Appendix B.....	109
9.2.1.	20 tCRE electrodes with 108 passive wet electrodes.....	110
9.2.2.	tCRE electrodes periphery test (9 central + 11 peripheral electrodes).....	127
9.2.3.	20 tCRE electrodes used 'dry' in the cap	151
9.2.4.	20 tCRE electrodes used 'dry' under the cap	154
9.2.5.	20 tCRE electrodes used in cap with saline filled foam in the cap	156
9.2.6.	20 tCRE electrodes used in cap with foam cap underneath.....	165
9.2.7.	20 ring electrodes used 'dry' in the cap	178
9.2.8.	8 SAHARA electrodes used dry in the cap	184
9.2.9.	5mm dry comb electrodes used with ring electrodes in cap	189

1. Abstract

Introduction: The absence of definitive data and EEG acquisition methods to diagnose schizophrenia and bipolar disorder (BP) is seen to be a hindrance in the early treatment and management of the diseases. A primary concern in the existing field of studies, shows the absence of data showing the differentiation of EEG patterns between schizophrenia and BP. This thesis aims at experimenting with the effectiveness of different electrode types under non-ideal conditions, towards building a new EEG cap, that will be used to diagnose schizophrenia and BP.

Methods: Thesis first experimented on 3 willing subjects, with varying degrees of hair volume and type, acquired EEG data off the participants and then visualized the data by running it through pre-existing code, before analysis was done by the author. The experiments attempted to place electrode types on at least 2 subjects per experiment, in order to increase sample size as well as compare effects of hair. The primary outcome measure was the successful acquisition of neural biology from a non-ideal electrode setup.

Results/Discussion: Data from experiments show us the effectiveness of wet passive electrode system over others, and draws special interest to tCRE electrodes which show the ability to ignore the effects of muscle on the acquired EEG. Combination of wet and dry electrodes also showed evidence of neural activity. Berger effect was used to compare muscle seen in the software laplacian of the EEG acquired and the acquired EEG itself. This allowed for a visual study of areas of interest.

Conclusion: Our study found that wet passive electrodes were best suited to non-ideal conditions, due to their ability to maintain contact with the scalp under duress. A combination of dry and wet electrodes was also seen to show some promise and required further experiments to confirm efficacy. tCREs were especially noted to be able to acquire data under difficult conditions. The use of tCREs also reduced the number of electrodes required for clinical EEG, from 128 to about 4-8 depending on the area of interest. Additionally, hair was seen to be major factor in the successful acquisition of data, not only with regard to volume, but also type. Future studies are expected to improve on sample size, electrode types their combinations and conclusively lay framework for the electrodes used in the EEG cap.

2. Introduction

The brain is a complex organ that shows continuous electrical activity while active and even in the state of sleep. Brain signals are created when interconnected neurons, transferring information to one another in the brain, fire impulses. These electrical impulses are the product of chemical changes in the neuron ends. The detection of these signals on the surface of the head or intra-cranially, was first proposed by (Berger, 1929) and was called electroencephalography. An electroencephalogram (EEG) is a method of measuring brain activity using electrodes. EEG detects brain waves produced by the interaction of neurons in the brain. There are many different reasons to conduct an EEG test, like diagnosis of epilepsy, assessment of brain function etc. (Weatherspoon, 2017). The skull is a solid structure with very low conductivity, this results in the signal being obtained from the brain through the scalp and skull being highly attenuated (Thulasidas, 2006). Additionally, the movement of muscles like eye blinks, jaw movements and eye movements, on the face and the neck, result in muscle artefact being introduced into the EEG.

A standard non-invasive outpatient EEG takes between 20-30 minutes (Peters, 2018), while a clinical EEG takes from between 30-60 minutes (St.Vincent's Hospital, Melbourne, 2014), and involves a technician applying a gel or a paste on the scalp and the electrodes, before placing the electrodes on the scalp to acquire EEG. In a standard clinical EEG test, the technician may ask the patient to undergo baseline tests like keeping their eyes open and closed, followed by tests to compare them against like blink their eyes, or look into flashing lights etc. (Vrocher III, 2017). The process of acquiring EEGs tend to apply many limitations to the participant, like the need for declaration of medications being used by the patient, the abstinence from caffeine for a period of time before the EEG and the need to wash participant's hair the previous night (Weatherspoon, 2017). As these are issues that are impossible to achieve satisfactorily for patients suffering from schizophrenia or bipolar disorder without a caregiver present, or if the patient is in a catatonic state (episode), the need for an alternative method that requires as little patient preparation as possible is necessary.

Studies done in the 1990s by (Sponheim, 1994) showed that there was a conclusive difference between the EEGs of schizophrenic patients and non-diseased patients. Their studies showed that first-episode patients (patients who have had only one episode) and chronic patients shared similar EEG patterns, with no significant variations. But, there was no differentiation between mental diseases done to confirm EEG differences due to schizophrenia. This implied that the conclusive differences seen in the study could have been as a result of any of multiple diseases. This was confirmed by a study done by (Boutros, 2008), which showed that schizophrenia is one of several mental diseases that may be seen in the spectral EEG of the brain. For bipolar disorder, study done by (Kam, 2013) showed that the power spectra of bipolar disorder was higher than that of schizophrenia, but also stated that more sensitive measurements would have to be developed in order to effectively differentiate and diagnose both schizophrenia and bipolar disorder. Another issue seen was most studies on bipolar disorder were sleep studies requiring longer

periods of EEG acquisition. This along with no conclusive data to show that the diseases could be differentiated from one another, was seen as a major stumbling block to the successful diagnosis of schizophrenia and bipolar disorder.

As no specific technique is available for the successful diagnosis of schizophrenia or bipolar disorder, there is a need for a re-think of how EEGs are acquired off the head. As the centre (top) of the head is the furthest from any muscle allowing for clear EEG detection with minimal muscle interference, it is seen as the optimal location for EEG acquisition for schizophrenia and bipolar disorder detection. Study of the ability of electrodes to acquire EEG data off the top of the head while under stress (non-ideal conditions), is seen as the first step towards developing improved systems for diagnosing schizophrenia and bipolar disorder.

3. Literature Review

3.1. EEG analysis

Ordinarily, preparation for an EEG is a time intensive process. It requires the patient to sit still for a long period of time while a technician applies a gel to the scalp/skin to improve electrical conductivity, and then attaches each individual electrode to a fixed point on the scalp. An experienced technician can apply a 128 passive electrode system in about 30 minutes before readings may be taken (personal communication, Pope K.J., 2019).

In EEG, muscle artefact is a major issue that occurs at higher frequencies. Frequencies above 15 Hz see a gradual rise in muscle artefact exceeding the desired neural signal. This is due to the overlap of neural activity with muscle activity in bandwidth (20-300 Hz) (Muthukumaraswamy, 2013). This is minimized as we move closer to the top of the head, as the effects of muscle activity are diminished due to the distance to the muscles.

The analysis of EEG is important to help understand how the brain functions under specific conditions like sleep, visual stimuli or auditory stimuli. It also improves our understanding of the effects of diseases like bipolar disorder and schizophrenia on the brain. Analysis of brain activity helps us better understand the cognitive behaviour of the brain under normal function and compare it to brain activity under diseased conditions. This helps the diagnosis and treatment processes by providing a clear picture of the brains condition and provides physicians the ability to treat patients. The EEG is obviously difficult to obtain due to the inherent low amplitude of the EEG signal and having the ability to separate the actual EEG signal from the obtained signal, allows us to remove noise from external sources and see effects of stimuli and inherent behaviour of the brain like alpha, beta waves etc. Some methods used for this include,

3.1.1. ICA/CCA analysis

The ICA method, first proposed by Herault and Jutten in 1988, as cited in (Mansour, 2000) showed the possibility of separating out individual components of signals and the removal of artefacts from signals. ICA or independent component analysis relied on applying an un-mixing matrix to EEG signals, which gave us statistically-independent components of the EEG signal. As the algorithm for the un-mixing matrix was not optimal, the process was not optimal for the separation of independent components. The issue with the matrix was its invertibility, by which the independent signals passed through the inverse matrix would return the original signal. ICA was seen as a method to 'clean' the EEG signal, where separated out components could be then analysed and discarded per the discretion of the analyst. This allowed for removal of components in signals due to muscle, eye blinks etc. The idea was

improved on by (Bell, 1995), proposing algorithms for the un-mixing matrix which allowed for the improved segregation of individual signals from the EEG, from a linear mix of signals. The figure below shows a visual of this process. Alpha and theta wave activity was separated out in individual traces and muscular signals like eye blinks or head movements were filtered. This showed there was little importance for system memory when using ICA transforms. As the process required either a human element or a software function to distinguish between noise component and EEG signal component, there was the need for the signals to be perfectly distinct from each other to reduce the chances of loss of brains signal due to either human error, study parameters or software parameters. This was confirmed by (Mammone, 2012) et.al, who showed that the tendency of analysts to remove some EEG signal due to imperfect separation of signals, which resulted in noise and brain signals being shown in the same component was a negative that needed to be addressed. Djuwari et.al, showed that for ICA analysis, if the number of source signals was more than the number of recordings being used for the analysis, then ICA will only be able to separate out components with high magnitude relative to other components in the linear mix (Djuwari, 2005).

<Image has been removed due to copyright restriction>

Figure 1. ICA decomposition of EEG signals. (left) Signals taken from 5 different electrodes are unmixed to give 4 component signals (middle) with their scalp maps (right). This allows for classification of components as neurogenic (i.e. from the brain and to be retained), or artefactual (i.e. not from the brain and to be removed) (Jung, n.d.).

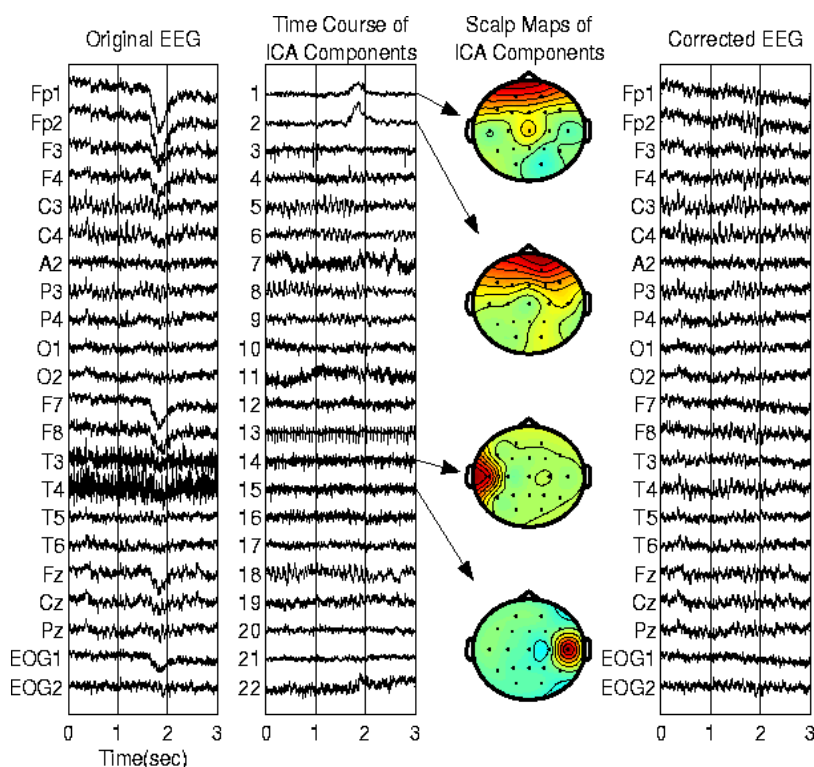


Figure 2. (left) The original EEG signal acquired from the scalp. (center) The ICA components separated out by the un-mixing matrix, and the 4 components of interest are visualised. These 4 components show characteristics of noise and are thus chosen to be discarded. (right) The corrected EEG signal after the removal of the 4 noise components and the application of the mixing matrix

Canonical Component Analysis (CCA) is a method to get maximally correlated sets of variables by transforming 2 sets of variables. This method was first proposed by (Hotelling, 1935) and is seen as the basis for BSS-CCA. Blind Source Separation – Canonical Component Analysis (BSS-CCA) is a method first proposed by De Clercq et.al., in 2005, and published in 2006, which assumed sources of activity in the brain, without knowing any parameters related to these sources. CCA uses 2 signals that are maximally correlated with each other, which in this case would be an EEG signal, and a time shifted version of the same signal. The sources are assumed to be uncorrelated and are ordered by autocorrelation coefficient. Signals in BSS-CCA are maximally uncorrelated compared to ICA method, where they are independent. Muscle artefacts in EEG signals have the lowest autocorrelation, which means they are lowest in the decreasing-order. They are then easy to separate out, but, had the same issues as the ICA method, where the analyst had to be careful to choose parameters for segregation of noise signals from the EEG signals.

Study by Vergult et.al, as cited in (Vergult, 2007) showed that BSS-CCA performs exceedingly well in muscle artefact affected signal (97% of signals contaminated), being able to identify EEG signal from the same. In their study, when BSS-CCA was applied to a patient (35-year-old woman with 'refractory left mesial temporal lobe epilepsy with hippocampal sclerosis), a comparatively clean EEG signal was easily visible. Assigning values to the correlation between the different signals received from 'sources' allows for removal of lowest correlation until the EEG signal appears as shown by (De Clercq, 2006). Weight matrices derived from blocks of EEG signal, showed correlation levels of 0.894 and above, indicating very little deviation (Makeig, 1996). Djuwari et.al. showed that due to assumptions made about sources, the process is not accurate.

3.1.2. Source analysis

Due to the low spatial resolution of EEG, discriminating between signals close to each other becomes a problem. This issue is addressed by modelling the EEG by a set of dipoles inside the head, i.e. these dipoles are considered the source of the signal being measured by the electrodes. This is a time and resource intensive process due to the nonlinear optimisation required to determine the best location and orientation of each source. Source analysis focuses on sources of signals rather than the EEG signal acquired allowing for better discrimination between signals at individual electrodes at the cost of EEG quality (Congedo, 2017).

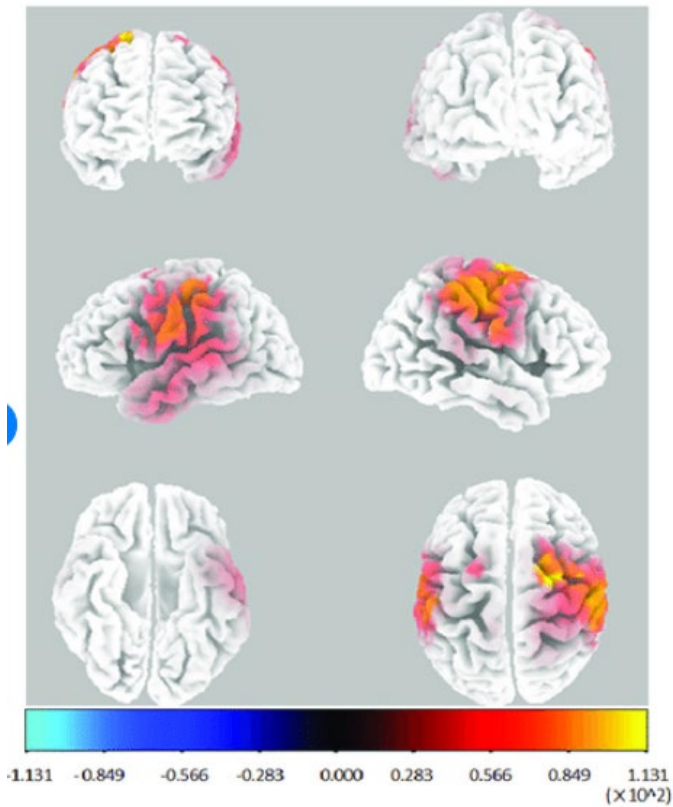


Figure 3. Sources seen in the brain after the application of source analysis on EEG signal.

A study by Michel et.al, that applied varying number of electrodes to subjects, from 25 to 181, showed that there is a marked rise in quality of signal obtained between 31 and 68 electrodes as compared to 68 and above (Michel, 2004). The limitation of the study was the size of the electrodes involved. The authors theorized that smaller distances between the electrodes would vastly improve the spatial resolution. While these methods of analysis are very useful in giving us locations of sources of electrical activity within the brain, they rely on assumptions and thus aren't exactly accurate. An alternate method that uses the surface potentials of the scalp is seen as a better method to analyse brain signals and estimate sources within the brain.

3.2. Laplacian transform

The surface Laplacian is a method to find the underlying current from the potentials found on the surface. It was first proposed in 1973 by (Nicholson, 1973) and showed the usefulness of surface Laplacian in determining current density under the scalp. Laplacian uses a second derivative of the surface potentials to provide an idea about the activity of the cortex. Unlike other methods of EEG analysis, there is no need for assumptions regarding sources or modelling of the head. This is offset by the loss in ability to distinguish between depths in the brain. Surface Laplacian is based on the volume Laplacian and uses its connections to electric fields and surface potentials and the relationship between electric field and scalar potentials to predict current density at a given point. As brain functions result in electrical activity, the current density on the scalp is proportional to the electric field in the brain. The potentials seen on the scalp are not related to the electric field but to a reference electrode placed on the scalp.

Spatial resolution of brain signals is important to distinguish the sources of electrode signals. Increasing the number of electrodes does not improve signal quality due to the attenuation effect of the cerebrospinal fluid (CSF), the brain and the skull, Due to this poor conductance, the potential seen at the surface will be radial in nature (Srinivasan, 1999). Muscle artefact is another major parameter for the accurate acquisition of brain signals. Muscle signals from eye blinks, neck movements and facial muscle result in distorted signals being acquired by the electrodes on the surface of the scalp. Laplacian transform is not a direct representation of the current density of the brain, but a second order partial differential of the voltages on the surfaces. The idea is to 'deblur' the signal rather than estimate a source. This would improve spatial resolution while removing any uncertainty over estimates (Babiloni, 2001). Additionally, study by Fitzgibbon et.al, showed Laplacian is indifferent to muscle artefacts when used centrally on the scalp. (Fitzgibbon, 2013)

The Laplacian transform was first proposed for use with EEG by Hjorth et.al, in 1975, to use a mathematical theory to estimate EEG potentials on the scalp (Hjorth, 1975). As the Laplacian negated the need for assumptions as well as using Ohm's Law to predict underlying current density, it showed improved accuracy in signal quality than previous methods. The volume conduction of electrical signal in the brain means there is radial dissipation of the signal which reaches multiple electrodes on the surface of the scalp. As the transform is sensitive to neural activity that is directed perpendicular to the scalp. The amplitude of the Laplacian at an electrode therefore depends on the orientation of the neural activity, and the distance from the electrode. As the angle of the potential changes with respect to the perpendicular, the value of the Laplacian changes.

Laplacian Transform of EEG is visualized in 2-dimensions as a graph of current density and frequency. It assumes that the brain-skull combination has a fixed resistance and that the voltage potential found on the surface has to correspond to the current density below the skull on the surface of the brain. (Carvalhoes, 2014). Surface current density refers to the density of current that is present at spatial points on the surface. This seems a better representation of brain activity due to its direct correlation to electrical activity in the brain (Kamarajan, 2016), which is considered a function of the brain.

<Image has been removed due to copyright restriction>

Figure 4. (left)Artificial sources in the brain modelled, black dots indicate negative sources and white indicates positive. (centre)Scalp potential seen in standard EEG of the model. (right)The sources seen after Laplacian applied on signals acquired from the model (Srinivasan, 1999)

As the Laplacian transform uses nearby signals to predict a signal at a given point on the scalp, muscle artefacts play a major role in altering acquired signal by masking any signals of interest with a high amplitude. As previously stated, Laplacian can ignore muscle artefacts from distance sources as seen by Fitzgibbon et.al. As Laplacian at electrodes showing muscle activity will in all probability enhance muscle artefact, the application of Laplacian to electrodes on the scalp, that are maximally distal from muscle, will see improved signal quality due to reduced muscle artefact. Thus, Laplacians are best when taken centrally on the head.

As most electrodes require software Laplacian to be applied to the signal, in order to achieve visualization of the brain activity and Laplacian in software is a time intensive process as the number of electrodes increases which is necessary as the Laplacian is optimal when maximum number of electrodes is used, this becomes a major problem for analysts and researchers when using Laplacian transform. A system that automatically applied Laplacian transform to the electrode signal at acquisition would be a major improvement in EEG analysis methods using Laplacian transform.

3.3. Types of Electrodes

3.3.1. Passive wet electrodes

These are electrodes that require a gel or paste to be applied to their surface as well as the scalp location where they have to be placed. The gel/paste acts as a medium for transmission of EEG signals from the scalp. As the gel/paste replaces the gaps between the electrodes and the scalp, the signal transmission is of a good quality. But, this is met by the process of applying the gel/paste to the scalp is time intensive and usually unpleasant to the participants involved.

Passive wet electrodes are limited by the need for a gel/paste in order to achieve satisfactory connections between the electrodes and the scalp. They are also vastly different in the type of connectors used between different manufacturers, resulting in electrodes having different methods of connections that may not be compatible across the board with other manufacturers. The process of setting up a wet passive electrode interface is also comparatively longer than one with dry electrodes. Even with all these minor limitations, the benefits far outweigh the negatives, as the signal quality is better, while the participant's level of comfort is satisfactory. Additionally, study by (Saab, 2011) et al., show that the wet electrodes have a higher classification accuracy than the dry electrodes.

The electrodes used in this case are usually classified into 2 types

3.3.1.1. Ring electrodes

Ring electrodes are the most common type of electrode in use in passive systems. Ring electrodes comprise of a ring of metal with a connector attached, allowing for signal transmission. The space in the ring allows for

application of the gel/paste on the scalp directly, making it easier to ensure adequate volume of gel/paste to allow for good connection between the scalp and the ring electrode.

<Image has been removed due to copyright restriction>

Figure 5. Figure shows ring electrodes connected to an adapter cable. The electrodes in this case are made of Ag/AgCl. They have rough inner surfaces which are in contact with the cap, and smooth outer surfaces (Villamar, 2013)

3.3.1.2. *Disc Electrodes*

Disc electrodes are another type of passive electrodes in use in EEG systems. They consist of a disc of metal packed in a plastic header that uses either a pin type or touch-proof connector. Disc electrodes have a larger surface area than ring electrodes allowing for better signal acquisition.

<Image has been removed due to copyright restriction>

Figure 6. Disposable disc EEG electrodes from FixXLLtd (FixXL Ltd., 2018).

Disc electrodes are limited by the possibility of dislocation of the electrode due to a combination of gel and movement. If too many of them are used at once (>64), there is a chance the applied gel at one electrode location comes into contact with the one nearest to it, and forms a bridge, forming a single electrode rather than 2 distinct ones.

3.3.2. Dry electrodes

Dry electrodes are electrodes that do not require a layer of gel or electro-conductive surface to acquire signals from the scalp. Since these electrodes do not have a conductive layer between them and the scalp, the signal quality is not very good compared to wet electrodes. Without a conductive interspace, the resistance seen is about 150-200k Ω (ALopez-Gordo, 2014), which drops by a magnitude of 10 when an interface is set up. An interface refers to the space between the scalp and the electrode. In the case of 'dry' electrodes, direct contact between the 2 is sufficient to acquire data, but in the case of 'wet' electrodes, there is a need for a conductive paste/gel to improve acquisition ability of the electrode. The drop of 10 was seen to be due to the removal of air pockets by the presence of a paste/gel and assurance of complete connections, irrespective of scalp surface shape.

Limitations seen with dry electrodes include,

- Using spiked electrodes might result in electrical bridges which interfere with the actual signal acquired.
- Spiked electrodes are optimally suited for signal acquisition but may be invasive depending on rigorousness of the test.
- Frequency Response tests for the comparison of Wet and Dry electrodes have not been validated.
- Dry Electrodes are large in size and do not improve on the comfort of wet electrodes

There are different types of dry electrodes

3.3.2.1. Spiked electrodes

In this type of electrode, long rod like metal contacts are placed in close proximity to each other on the scalp as seen in the figure below. The distance between the contacts may range from the nano to the milli scale. Tests conducted showed that impedance was down to around 1k Ω and visual comparison showed no discernible variation from signal acquired from wet electrodes (Griss, 2002).

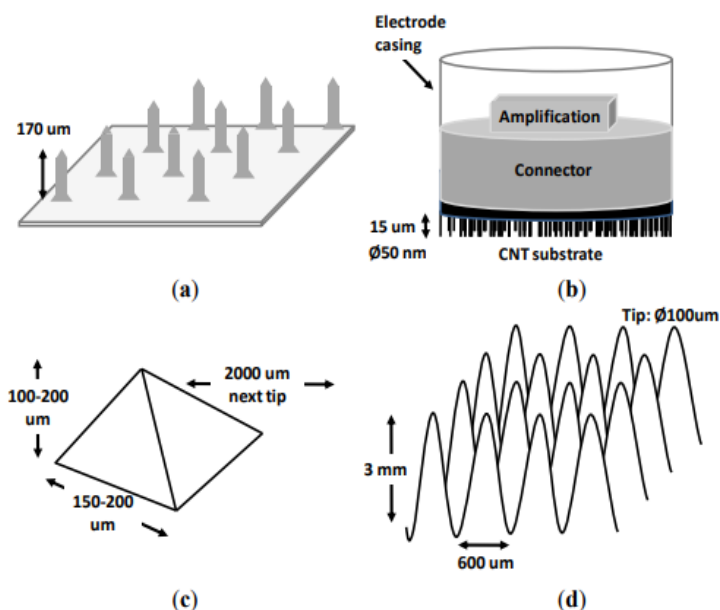


Figure 7. shows the spiked array used for the testing done in (2). (a) Shows silicon microneedles, (b) shows carbon nanotube electrodes, (c) shows a micro tip in detail and (d) shows 3D printed microneedles

A study by Liao et. al., showed that the impedance seen at the skin-electrode interface in a dry and wet electrode setup, without preparation of the scalp, was dependent on time and were reversed for both types (Liao, 2011). The dry electrodes showed a reduction in impedance as time progressed. This was shown in the figure below,

<Image has been removed due to copyright restriction>

Figure 8. Image above plots impedances as a function of time, the red line indicates the impedance with respect to time of the wet electrodes without gel being applied to skin surface. The blue line indicates the impedance with respect to time of dry electrodes without any gel applied, plot obtained from study by (Liao, 2011)

3.3.2.2. Capacitive electrodes

Like the non-contact electrodes, the capacitive electrodes too have a flat contact surface, similar to passive electrodes. These electrodes primarily sit on the skin/scalp to measure signals.

<Image has been removed due to copyright restriction>

Figure 9. shows capacitive dry electrodes that are used on the skin from Cognionics (CGX, 2019)

All of the above have shown limitations in both hardware design and the obvious issue of needing additional help to be able to achieve EEG signal without muscle noise. There is a need for an electrode system that can perform muscle signal reduction inherently in order to save time in the analysis process.

3.3.3. tCRE electrodes

The tCRE electrodes radically change how signal acquisition of EEGs is done. The Tripolar Concentric Ring Electrode (CREmedical, 2018) consists of 2 outer rings surrounding a central disc. The electrode detects current density rather than voltages and measures it by comparing the density differences across the 3 'rings'. The tCRE is also highly efficient and directly calculates the Laplacian of the signal achieved, thus providing 2 outputs, the original EEG signal and a Laplacian version of the data. The tCRE system sold by CREmedical, provides 20 electrodes (CREmedical, n.d.), with the connectors and headbox. The headbox called the t-Interface, has 20 connectors and acts as both a router and a pre-amplifier. This headbox gives an output of 40 channels, 20 emulated EEGs and 20 Laplacian signals.



Figure 10. *tCRE electrodes used for experiments. 2 rings (gold) visible in image concentric around central disc*

The tCRE electrodes are faster with respect to total time taken for signal acquisition and Laplacian transform application than ordinary wet passive electrodes as they immediately process Laplacians of the acquired signals, which usually takes a long period of time to achieve in software, irrespective of the multiple signals that the transform has to be applied towards. Laplacian transform has a few limitations, like, it has to be kept away from muscle artefact in order to avoid masking of required EEG signals, and that it requires many electrodes as close to each other in order to interpolate for a specific point. This problem is negated with the tCRE due to their construction and inherent Laplacian transformation of the signal. The tCRE uses a weighted second derivative Laplacian formula to get a representation of the electrode signal. The following simplified version of a more complex formula is used to determine the differences in the potentials seen across the rings of the tCRE electrode.

$$16*[(M-D)-(O-D)] \text{ (Besio, 2014)}$$

Where, M = Potential of Middle Ring

D = Potential of Central Disc

O = Potential of Outer Ring

Studies by (Besio, 2014) showed that unlike other Laplacian systems, which require the signal to be taken between electrodes placed at least 1 cm apart, the tCREs use a smaller area and are potentially more effective in acquiring the same Laplacian signal in a shorter period of time. Besio et.al, also showed that the Signal-to-Noise-Ratio (SNR) is almost 4-fold better than any existing system, while reducing the effect of neighbouring tCREs to almost a tenth of what is expected of wet passive electrodes. As Besio et.al, were also involved in the development of the tCRE system, the need for a neutral third party to verify claims is needed. The system used in the studies is as shown below,

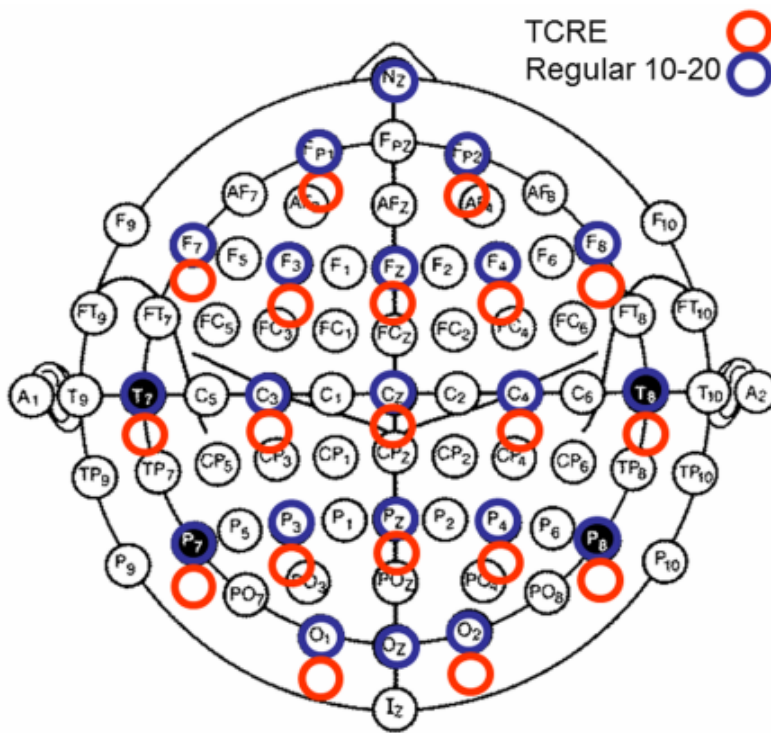


Figure 11. A visualization of the 10-5 system used for the placement of the electrodes on the scalp. The red electrodes indicate tCRE electrodes, while the blue refer to ordinary passive electrodes in a 10-20 system.

The tCREs work by detecting perpendicular currents at the scalp, these currents hit the scalp and radiate over the scalp. These currents dissipate as they travel. The 3 rings of the tCREs help in the measurement of these currents. When the currents spread, the current vectors are picked up by the closely placed rings and provide a Laplacian signal, due to their vertical components. The difference in the signal picked up across the 3 rings is a characteristic of the signal acquired. Signals from further away spread and become flat, losing their vertical component, thus negating their effect on the electrode. This gives tCREs the ability to highly localise acquisition of the current densities rather than voltages. Thus, tCREs do not acquire EEG signals, but a Laplacian of the EEG signals and an emulated signal.

3.4. Optimal experimental electrode parameters

3.4.1. Frequency response of different types of electrodes

Frequency response is an important factor in the construction of electrodes, as most biological signals received from the brain are of low frequency. The figure below derived from experiments conducted by (Wycoff, 2015), shows that due to a 1Hz high pass filter, the delta wave patterns which are of lower frequency were cut off in the dry electrode system (Versus) while a lower High pass filter (Mitsar) for the wet electrodes showed a better frequency response. The study was limited by a small sample size of only 9 participants, and the prevalence of wet electrodes meant electrode systems with low HPF's were easy to find as compared to dry electrode systems.

<Image has been removed due to copyright restriction>

Figure 12. Validation of a wireless dry electrode system for electroencephalography. Graph shows filters need to be as low as possible in order to obtain low frequency signals of interest. - Scientific Figure on ResearchGate (Sherlin, 2015).

Another study performed by Xing et.al, (Xing, 2018) compared the signal quality between wet and dry electrodes by placing them at a distance of 2cm from each other on the scalp and taking simultaneous data recordings. The SNR of the signals was compared from the correlation coefficient calculations; Fig. 4 shows the comparison as a function of the temporal waveform.

<Image has been removed due to copyright restriction>

Figure 13. (a) shows a plot of amplitude of signal with respect to time, at earlier times, the amplitude of wet electrodes is more positive than dry ones, while at later times, the mean amplitudes of both match. (b) Shows the mean amplitude as a function of frequency, which shows us that the mean amplitude of dry electrodes has a large spike at 10 Hz, with decreasing harmonics at 10 Hz intervals. (Xing, 2018)

The study concluded that dry electrode accuracy was very close to wet electrode and could be realistically used for brain interface applications. The study was limited by the interference at low frequencies in the amplitude spectrum, where the dry electrodes signal was suppressed at 0-5 Hz. This was addressed by the authors as a function of the electrode-skin contact issue, and solutions were presented to fix the same.

3.4.2. Effect of site of electrodes

It is common knowledge that muscle is absent at the top of the head. Muscle artefacts come into play when the sites of electrodes are closer to the periphery of the skull i.e. near the face or the back of the neck. As this will cause distortion of the signal due to the masking of important EEG activity, the need for study of the effect of the site of electrodes is important for any EEG analysis. Digitization of locations of electrodes on the head is a practice that allows for easier determination of signal source localization. Towle et.al., proposed the used of digitalization (Towle, 1993) in order to both, avoid long periods of time placing electrodes at exact pre-determined locations as well as to avoid having to use a 3-D localizer described by Echallier et.al. (Echallier, 1992). While this may not allow custom-fits for patients, it makes the process of setting up EEG, simpler and faster.

As the study by (Kim, 2013) showed, there was clear clustering of signal in the region at the top of the head around Cz, in bipolar disorder patients, this allowed for a quality EEG to be obtained from the patients. Additionally, the top of the head is the furthest point on the scalp from muscle activity. This reduces muscle artefact and its masking effects on low amplitude signals.

References for the system usually are placed at the mastoid or the ear, but the best location was seen to be Cz, in the centre of the scalp due to large reduction in muscle, there is also precedent for using the average of the signals from the whole head using the Common Average Reference system (CAR), where no physical reference is present, but the incoming signals from the electrodes is averaged to form a reference signal (Teplan, 2002). Studies by (Ludwig, 2009) on 21 male rats implanted with microelectrodes, showed the effectiveness of the CAR reference system, vastly reducing noise by more than 30%. The study used microelectrodes instead of ordinary electrodes and the subjects were placed in a Faraday cage, reducing ambient noise, suggesting biological signals might have been greater if they were placed in a non-shielded area.

3.4.3. Effect of number of electrodes

The effect electrodes have on the signal acquired is dependent on a wide range of factors, the size of the electrodes, the construction of the electrodes etc. Thus, when the question of the number of electrodes arises, the issue is firstly, what type of electrode should be used?

The tCRE or the Tripolar Concentric Ring Electrode consists of 3 concentric rings. Each ring will acquire signals from the scalp which will depend on their distance from the origin. Since the signals will be compared between all 3 rings to provide an output, common noise and distant muscle artefacts are effectively nullified. The tCRE also provides a direct Laplacian of the signal acquired, an improvement over traditional electrodes. Due to its use of Laplacian and 3 ring system, it is assumed that fewer tCREs may be used to acquire the same signal.

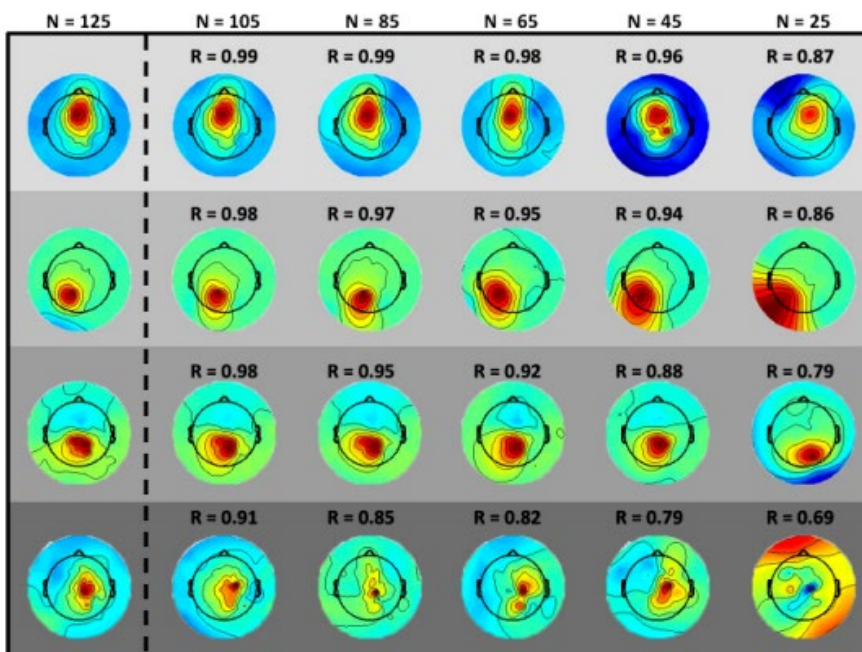


Figure 14. Graph from study by (Lau, 2012), shows the signal acquired by 125, 105, 65, 45 and 25 electrode systems of the same area of the brain. As we see the quality of the signal and the spatial resolution show a large drop that is attributed to the spaces between electrodes requiring system to interpolate.

Study done by (Lau, 2012) used a 256 channel EEG on subjects, retaining 125 channels after rejecting low quality channels, and then applied ICA analysis on the remaining channels starting from 125 and reducing them concurrently to 25. Their experiment showed that with the reduction in number of electrodes, the topography of the brain activity also radically changed. This was seen as an effect of the absence of electrodes that would otherwise have detected impulses in empty spots on the scalp, changing the signal visualization. The graph above shows the comparison between the number of electrodes. While the number of electrodes changed, the distances between them also dropped, this resulted in an increase in the estimation of intermediate points on the head through interpolation. Thus, the density of electrodes placed on the head also affects the EEG acquired, as a higher density with low quality electrodes will lead to redundant signals. Improvements in the accuracy and size of electrodes will help improve this.

3.5. Neurological disorders

3.5.1. Bipolar disorder

Bipolar Disorder is a chronic disorder where afflicted patients can have extreme mood swings. The Black Dog Institute states that 1 in 50 Australians are affected by the disorder each year (Black Dog Institute, 2018). Symptoms of the disorder include loss of appetite, irritability, poor concentration etc. Hypomania is considered to be an early warning sign of bipolar disorder. Currently the disorder is not very well understood with long term management its only treatment options. A study conducted by (Kim, 2013) showed that the resting state EEG for Bipolar disorder showed a reduction in the alpha peaks as compared to ordinary EEG's

As the condition is not very well understood, the underlying neural aspects are not very accurate. As the traditional method of identifying brain structures which use the lobes (frontal, temporal, parietal etc.) do not give an exact picture of the areas of the brains activity, where the disorder affects specifically, the primary issue is identifying a method of differentiating areas of the brain by their neural activity. Brodmann areas are a better visualization of the brain regions due to their dependence on neural connections. Figure shows the Brodmann area distribution across the brain.

<Image has been removed due to copyright restriction>

Figure 15. Images show the distribution of Brodmanns area in the cortex. Brodmann area 4 and beyond are considered to be motor regions of the brain, while area 6 and ahead are considered prefrontal. This is not a highly defined distinction, but overlaps dependent on the underlying neural connections (Gage, 2018)

Brodmann area 6 has shown to have a rise in beta wave activity (McDermid, 2014). This area is shown in figure below, providing further evidence to support further investigations into EEG acquisition at the top of the head. The absence of muscle involvement means Brodmann's Area 6 and its surrounding areas are an optimal spot for signal acquisition.

<Image has been removed due to copyright restriction>

Figure 16. Brodmann's Area 6 (Wikimedia, 2011) which is in the area of interest as seen by (Kim, 2013)

Visuospatial processing is the ability to process visual cues or stimuli and process the relationship between their spatial coordinates (Tres, 2014). It is an important part of the brain's functions allowing subjects to interact with their surroundings. Visuospatial processing requires the interconnected use of multiple brain centres. In bipolar disorder, this ability of visuospatial processing is considered an important part of understanding how the disease affects brain centres. Study by (Lera-Miguel, 2011) showed there was a significant drop in executive functions and visuospatial processing than the control group. Also, study conducted by (Degabrielle, 2009), showed a clear distinction in the delta and theta waves with rises seen during resting EEGs alongside the drop in alpha wave activity. Additionally, (El-Badri, 2001) showed a rise in power across all 4 bands, and provided further evidence of effect of the changes on the wave bands on the visuospatial processing of the brain.

(Kam, 2013) showed that there is an increase in beta and gamma power in Bipolar disorder. This led them to conclude that due to the links between beta power and mind wandering, bipolar disorder patients show a marked response to novel/new stimuli at rest. They were unable to explain the increased muscle artefact present in their study, even after the use of ICA to negate ocular artefacts. Another study by (Lagopoulos et.al) show that there is a rise in wave activity. This however, is not sufficient information to diagnose bipolar disorder in patients using EEG alone. Following thesis will attempt to clarify parameters of wave activity and any related changes in EEG signals in order to create a basis for diagnosis of bipolar disorder using EEG if possible.

3.5.2. Schizophrenia

SANE Australia defines Schizophrenia as “an illness that disrupts the functioning of the human mind. It causes intense episodes of psychosis involving delusions and hallucinations, and longer periods of reduced expression, motivation and functioning” (SANE Australia, 2017)

The symptoms of schizophrenia including hallucinations and delusions have been linked to inability for areas of the brain to communicate with each other. A study by (Di Blaise, 2018) showed that in younger patients, there was a marked decrease in grey matter in the frontal region of the brain and in older patients there was a strong decrease in connections in white matter in the frontal region of the brain. This is linked to the loss of cognitive impairments which worsen with age. Schizophrenia diagnosis is a difficult process, as it may take up to 6 months to get a positive diagnosis, as the progressive decline of the subject is one of few indicators for physicians. Treatment is currently possible and lasts from 2-5 years (SANE Australia, 2017). As the period of diagnosis is too long for an illness as serious as schizophrenia, there is a need for quick diagnosis of the disease. As seen in the study by (Dvey-Aharon, 2015) the best position for EEG was seen at the top of the head. The study compared the EEG signals of healthy patients with those of patients suffering from schizophrenia. Earlier studies by Merrin et.al, in which subjects were seated in a sound-proof (sound attenuated) chamber with eyes open and 2 tasks of copying text and design were conducted. 9 electrode positions around the centre of the head were taken, referenced to the z-line of the head (Fz or Cz depending on patient), showed that there is a high coherence in EEG in un-medicated schizophrenic patients, which was theorized with no factual evidence to be as a result of highly undifferentiated cortical organization (Merrin, 1989)

<Image has been removed due to copyright restriction>

Figure 17. Graph shows a color-coded representation of the signal received from the brain. The electrode scalp location shows greater SNR in the signal seen at AFz to FCz. The presence of high SNR with the reduction in muscle activity means the centre of the head is the optimal spot for signal acquisition (Dvey-Aharon, 2015).

Earlier studies by Giannitrapani et.al, had shown that the EEG spectra had some correlation to subjects with schizophrenia, encouraging further investigation into use of EEG spectra as a form of diagnosis for schizophrenia (Giannitrapani, 1974). In contrast, study by Boutros et.al, showed there was no clear indicator of schizophrenic behaviour from the EEG spectra, to differentiate schizophrenia from other similar psychiatric disorders (Boutros, 2008), however, they also concluded that the abnormalities seen in spectral EEG of schizophrenic patients was repeated in their studies when compared to previous studies they had reviewed. This indicated that there is a need for further studies to verify if changes in EEG were sufficient as a stand-alone diagnosis method to diagnose schizophrenia in patients.

4. Method

The primary aim was to conduct experiments with different types of electrodes on subjects, to verify the ability of electrodes to acquire EEG data. The experiments were run in a Faraday cage in the Multimodal Recording Facility at the Tonsley campus of Flinders University. The faraday cage allowed for the attenuation of outside interference from electrical, auditory and physical noise. The cage required the participation of at least 2 participants, the subject and the researcher. This was due to the absence of safety equipment within the cage, in order to avoid any interference in function. This made it dangerous to operate in isolation. The experiments involved the author, Professor Kenneth Pope, Professor Trent Lewis, Professor John Willoughby and fellow student Andrew J. Lelei. The setup included 2 computer terminals outside the faraday cage, which each ran the mirror terminal within the cage. The test simulation was coded on Python and run through the mirror computer after the setup had been completed. The setup was coded on Matlab and involved code written by Professor Kenneth (included in the appendix).

The experiments involved a number of devices, like electrodes, amplifiers and headboxes. Each of which, had limited connection options. The standard g.Hlamp (Figure 18) was used as a bio-signal amplifier, as it allowed connections of about 256 channels.

<Image has been removed due to copyright restriction>

Figure 18. g. Hlamp as seen in gtecs device brochure

The Hlamp consists of ADC convertors to improve signal quality and a high sensitivity to pick up a wide range of bio-signals (EEG, ECG, EMG etc.). It supports active and passive electrodes and can configure with Matlab's Simulink. Artefact removal is also seen through a hold channel. The Hlamp allows for impedance checking by showing a colour coded chart on the connected terminal, allowing for manual improvement of skin-electrode interface. It comes with a choice of active or passive headboxes (Figure 19), to connect electrodes as shown in figure.

<Image has been removed due to copyright restriction>

Figure 19. Passive(left) and Active(right) headboxes as seen in the gtec device brochure

The electrodes used for these experiments varied depending on the experiment. The tCREs were used due to their potential ability and compared to several types of electrodes like the ring electrode, the spiked dry electrodes and the SAHARA dry electrodes (Figure 20). The SAHARA electrodes were active dry electrodes sold by gtec, which allowed the easy usage with the Hlamp. Gtec states that it has a range of 0.1 to 40 Hz, while being a dry electrode negating the time taken for setup of cap. It uses a GAMMAcap, which has a total of 160 positions in a variation of the 10/20 system.

<Image has been removed due to copyright restriction>

Figure 20. The SAHARA electrode allows for the separation of a snap connector from the electrode, which allows for the placement of the electrode under a cap, in direct contact with the participant.

The experiments were run with these devices correctly setup before each experiment. The experiment itself consisted of 5 blocks or parts.

- Baseline Eyes Closed

The participant was asked to keep his eyes closed for 30 seconds. At the end of the 30 seconds, a chime sounded to indicate completion of the baseline eyes open test.

- Baseline Eyes Open

The participant was asked to keep his eyes open for a period of 30 seconds. At the end of the 30 seconds, a chime sounded to indicate completion of the baseline eyes open test.

- Auditory MMN Test

Participant was asked to listen to a set of tones. These tones were varied to allow the participant to recognize any changes associated. The participant was asked to keep track of the number of tones. This was repeated 6 times, and the sounds were different in both pitch and number in each test block. The participant was asked to provide a fatigue rating after each set.

- Muscle Test

This test consisted of 4 subsets. The participant was asked to make muscular changes like, clenching the jaw, raising eyebrows, coughing intermittently and tightening shoulders.

- Motor Imagery Test

Participant was asked to respond to visual cues by imagining corresponding muscle movement. The visual cues provided a Left/Right symbol, which corresponded to the movement of hands. The cues were separated by a neutral cue of a cross.

The test took an estimated 20 minutes to complete and at least an hour to setup, which included, planning of the experiment, the setup of the software for the variation in ordinary testing conditions as well as the physical setup of the cap on the patient's head. The location of electrode positions is shown in Figure 123 in the appendix. The application of gel after the placement of the electrodes as needed, also extended the time for some experiments. The test itself was much shorter, as it was continuously done, with each test block being followed by the next, with only a short break that was dependent on the participant. Following the first few experiments, only the baseline and muscle tasks were run as they gave us the data required. Cases where the full sets of experimental tasks were not run, are stated in the following.

4.1. 20 tCRE electrodes with 108 passive wet electrodes

Experiment was conducted with Prof John Willoughby as a participant. The participant was asked to put on an EEG cap, and 108 wet electrodes were placed before the application of gel. The electrodes were individually displaced to gel electrode location. This allowed for the gel volume and contact to be optimally decided. The tCRE electrodes were then placed in positions centred around the top of the head (at F4, F2, Fz, F1, F3, C4, C2, Cz, C1, C3, P8, P6, P4, P2, Pz, P1, P3, P5, P7, O1, Oz, O2). The tCRE electrodes used a specific gel called TD-246 (Skin Resistance/Conductance Electrode Paste) that had a white pasty texture as compared to the ordinary EEG

electrodes that used Abralyt, which was grey and had a grainy texture. Once the electrodes were placed securely in the cap, the passive electrodes were connected to a headboard while the tCREs were connected to provided headboard.

Lab Recorder was used to record EEG signals from the participant. The experiment setup included the use of multiple applications to achieve signal acquisition. First the HIampRunner was run, to allow the connection between the HIamp and the computer. This gave us the HIamp signal with the EEG. The mirror computer used for the test had Python run to execute the test programs. Following which, Matlab was run, to turn on SNAPviewer and VisStream. It was indicated to the author, that in order for the experiment to successfully run, the computers would have to be connected only to the local room connections and not the University server, meaning a static IP would have to be used.

The next step was to check impedance of the electrodes with the headboard. The wet passive electrodes were impedance checked through the traditional 128 channel headbox, with the hiAMP used, while the tCREs had to be individually checked. A tCRE electrodes was attached to the wet EEG headboard and a signal sent through it, the return was through a reference line, which was used to calculate the resistance seen at the skin-electrode interface. The impedance testing was seen by observer on the system, with a color-coded system that visualized the resistances seen at interface. On impedance reaching within sufficient ranges, the experiment was begun.

4.2. tCRE electrodes periphery test (9 central + 11 peripheral electrodes)

The second experiment was conducted 2 weeks after the first. Professor John Willoughby once again volunteered to participate in the experiment. The EEG cap was placed on the participant's head and the 20 tCRE electrodes were then placed on the head at intervals that allowed data acquisition from both the top of the head as well as the perimeter (at Fp1, Fp2, F7, F3, Fz, F4, F8, T7, C3, Cz, C4, T8, P7, P3, Pz, P4, P8, O1, Oz and O2). There were no wet EEG electrodes used this time. External reference and ground were used for the experiment. These 2 were connected to a wet EEG headboard connected to a High Amplifier.

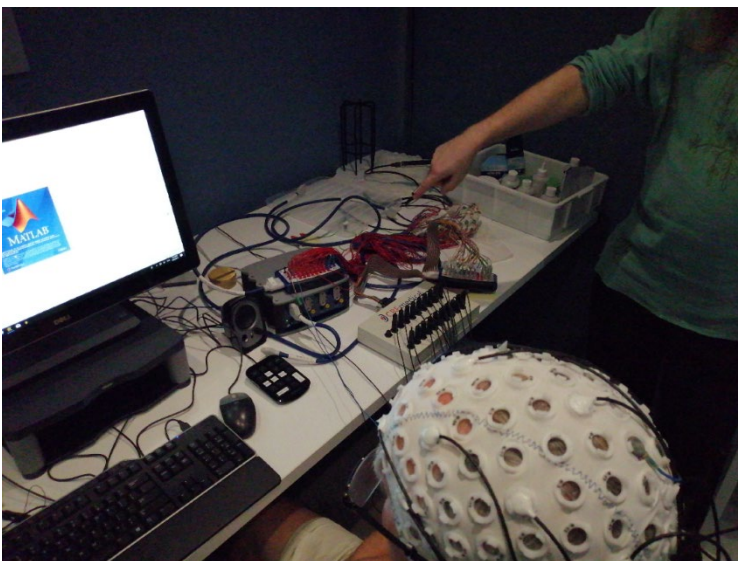


Figure 21. Cap connected to the tCRE headbox (white box, centre frame), and the references connected to the wet EEG electrode headbox (white box with red wires, center-left frame)



Figure 22. TCRE headbox from CREmedical, allows for 20 channels. The open channel (top left) is being impedance tested with the 128 channel headbox, as shown in next image.

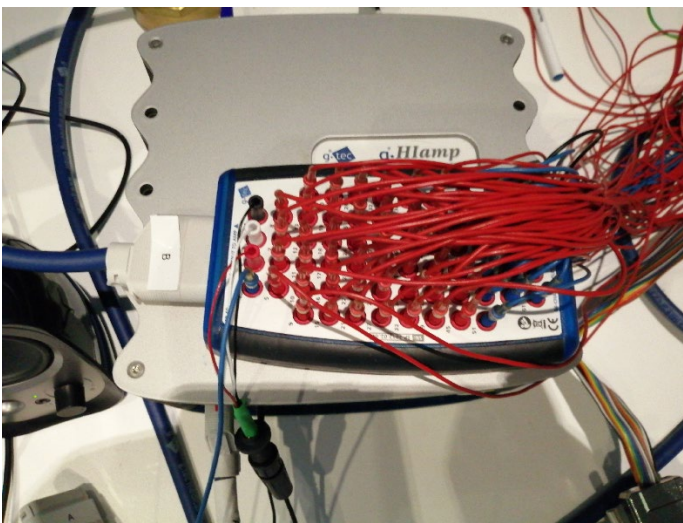


Figure 23. Wet EEG headbox, with the top 4 connectors being used to impedance match the tCRE electrodes. The tCRE connector was converted to a 3 wire system (red, white and black), while the blue wire is the reference feeding back for the test.

Once impedance testing was completed, the experiment was begun. Two steps were taken before the experiment,

- Lights turned off in Faraday cage
- Door shut in Faraday cage



Figure 24. Participant being prepared for experiment start. Devices being powered up for the start of the experiment. Pad on right side of keyboard for stimuli response.

Before the experiment was begun, Professor Trent made sure signals from 2 events were visibly recorded by the system, namely,

- Jaw clench artefact visible
- Alpha frequencies of 10-12 Hz clearly visible at Pz and beyond

A trigger was setup between the mirrored computer in the Faraday cage and the external computer and the Hlamp to get marked events in data acquired. As with the previous experiment, the participant was asked to respond to stimuli in 5 different tests.

- Baseline eyes open

The participant was asked to keep eyes open for 30 seconds. A chime announced when the test was completed. Participant was asked to use pad to continue when ready.

- Baseline eyes closed

Participant was asked to close his eyes for 30 seconds. A chime announced when the test was completed. Participant was asked to use pad to indicate readiness to continue.

- Auditory MMN Test

Participant was required to count the auditory 'target' signals, and to ignore everything else. This was done in batches of 8 tests, where the frequency and order of the 'target' was randomized.

- Motor Imagery Test

This test required the participant to follow instructions. Participant was asked to imagine the actions being shown on the screen.

- Muscle Test

Participant was asked to make changes corresponding to screen instructions. These included jaw clench, eyebrow raises, coughing intermittently and shoulder tightening. Data was collected for subject as shown in figure below.

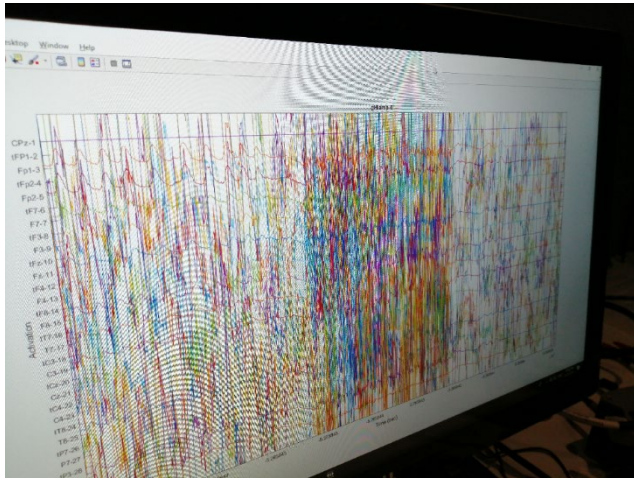


Figure 25. *Massive congregation of spikes in frequency and amplitude detected on jaw clench portion of the Muscle test*

On completion of the test, the cap was removed and data analysis was begun. The running EEG was not a great indicator of alpha peaks, the spectrum analyser was used to visualize this better

4.3. 20 tCRE electrodes used 'dry' in the cap

tCRE electrodes were placed on the cap, with no gel underneath, and the reference and ground were kept the same. 'Dry' tCREs were used to get a comparison to 'wet' tCREs EEG signal. A new headbox was used to connect the tCREs as they had dual channel properties, where they gave us both emulated EEG signal as well as a Laplacian.

As the previous tests had shown extremely high impedances, there was little need for another impedance test, with the obvious visible air gap. Test blocks were then run with the lights turned off and the faraday cage closed. Error was detected in the connection of the HiAMP, showing accumulative fatigue for all involved in the multiple tests conducted on the same day. The error was fixed and tests run again.

4.4. 20 tCRE electrodes used 'dry' under the cap

Following the test with the tCRE on the cap, the next test was to see if tCRE was able to make any contact with the scalp and get a viable signal. The tCRE was placed under the cap (Figure 26), and held in place by the cap connectors. Problem was encountered when the electrodes were lost under hair and had to be placed again in the right position, which took a long time. The electrodes on the posterior side were found to be relatively loose, while the top and the anterior were found to be a tight fit. The lights were turned off and the faraday cage sealed. 3 test blocks were run with no errors detected.

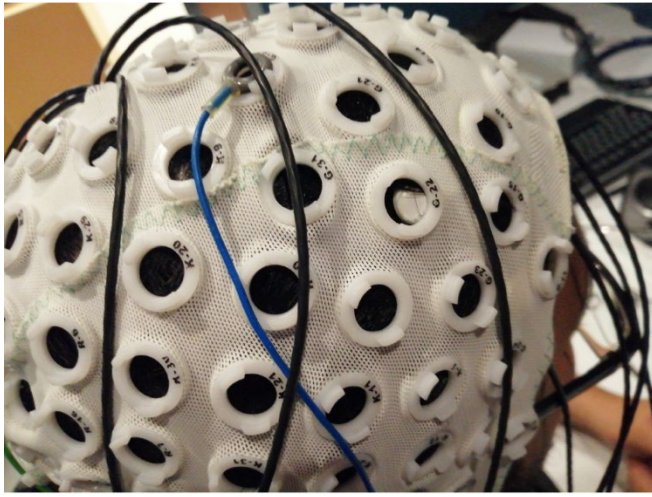


Figure 26. The tCREs are barely visible under the cap due to participant's hair volume, the visible tCRE had to be displaced for this image to show the placement

4.5. 20 tCRE electrodes used in cap with saline filled foam in the cap

Experiment was conducted in 2 parts. The first part had Professor Willoughby who once again volunteered to participate in the experiment, put on an EasyCap. The cap had been constructed the previous day with foam placed in the central electrode locations and the tCRE electrodes placed over them, this reduced time needed for construction of the cap.

Once placed on the head of the professor to confirm that the foam would not move under the lateral movement of the cap, it was taken off and then flipped, and saline applied to the foam using a syringe (Figure 27).

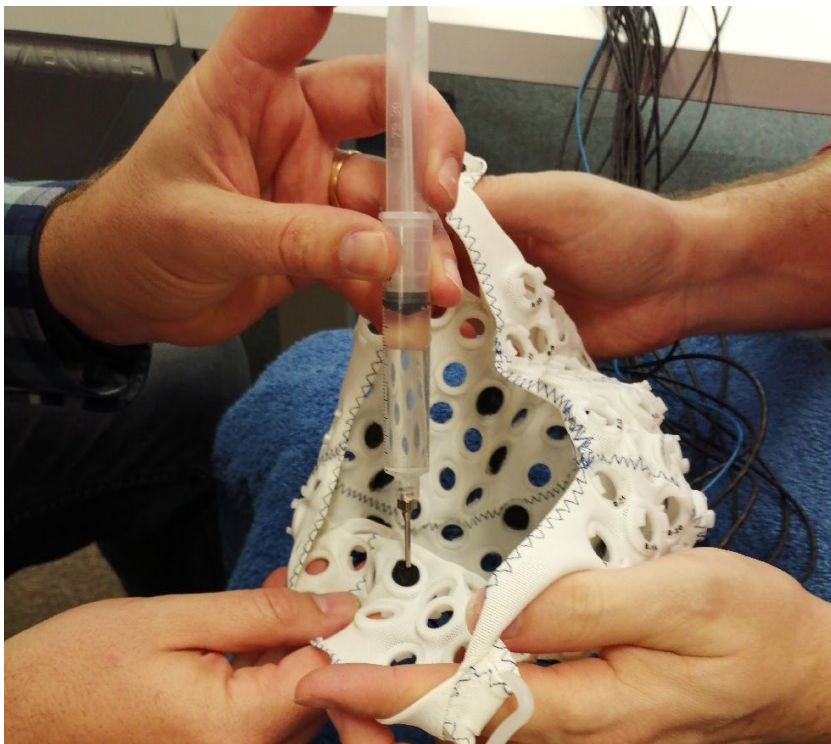


Figure 27. Professor Lewis applied saline to the foam under the cap. Participants stated that the cap was comfortable and that the saline filled foam was felt under the cap.

The reference and ground electrodes were considered, and chosen to be ring electrodes with the foam sitting in the space in the ring. This allowed for direct application of saline to the foam without the movement of the cap (Figure 28). It was also decided to use foam rather than gel with them in order to maintain consistency.



Figure 28. Application of saline to the foam placed in the space in a ring electrode, used as reference/ground in experiment 4

Since the impedance was logically assumed to be better than the previous experiment, there was no check done for the setup. Test parameters were set up as before, with 3 test blocks being run, baseline eyes open, baseline eyes closed and muscle tests. These were run with lights off and cage closed.

The test was then run again with author participating, in order to see the difference hair volume would make in the signal acquisition. This experiment was conducted with lights on and cage shut.



Figure 29. Test 2 run with author as participant to verify effect of hair volume on interface connection quality

4.6. 20 tCRE electrodes used in the cap with foam cap underneath

The author constructed a foam cap using a foam sheet. The dimensions were taken from that of a snapback cap. The amateur quality of the stitching made the cap imperfect, but suitable for the test. The cap was soaked in saline, and then placed on the subject's head. The cap itself had foam fillings in the electrode holders, filled with saline.

4.6.1. 20 tCRE electrodes with foam cap used on subject with thick hair



Figure 30. Subject with thick hair with the foam cap under the tCRE cap. The electrode holders under the tCRE electrodes have foam fillings (black bits sticking out) filled with saline.

The saline soaked foam cap got the subjects hair wet under the cap, giving us a better connection with the scalp than expected, and fit as expected. There was a concern about bridging (connection of multiple electrodes to each other through an interface) and the test was conducted to verify its effect on the EEG acquisition. The setup for the experiment was done as before, and the 3 test blocks run with the lights turned off and the faraday cage shut.

4.6.2. 20 tCRE electrodes with foam cap used on subject with short, curly, stiff hair



Figure 31. Subject with short, curly, stiff hair with foam cap under tCRE cap, with foam infills under the tCRE electrodes in the electrode holder

To compare the effects of hair, subject with short, curly stiff hair underwent the experiment. The subject with the short, curly stiff hair had issues with the fitting, which resulted in the foam cap being stretched out and seams opening at the edges. The electrodes were placed after the cap was moved to give good connections to the scalp for the electrodes above it. The foam infills were soaked in saline with a syringe and the tests were run. The setup for the experiment was done as before, and the 3 test blocks run with the lights turned off and the faraday cage shut.

4.7. 20 ring electrodes used 'dry' in the cap

This test was conducted on the 12th of February 2019, earlier than some of the previous tCRE tests, as it helped the author understand the limitations of a wet passive electrode system. It consisted of 4 distinct electrodes being tested. Author volunteered to participate in the experiment to better understand the tests from the participant's view. The test required changes to be made to testing parameters due to both time constraint and perceived effects on multiple long tests on the participant's EEG. The test blocks were reduced to just 3, the baseline eyes open, the baseline eyes closed and the muscle tests. This experiment was done to verify if any dry configuration of the electrodes being tested had comparable EEG signals that showed viability.



Figure 32. Size 58 EasyCap used for Experiment 3 on a dummy head model.

A size 58 EasyCap (Figure 32) cap was used for the tests, which applied 20 ring electrodes to the same locations as the tCRE electrodes. The ring electrodes connected to the headbox with touch-proof connectors, which had a female lead and connected to the headboxes male leads, as shown in figure below. The cap label was different from standard cap designs and thus used terminology that had to be converted to traditional electrode locations. R14 (Cpz in traditional EEG setups) was used as reference to the system, while G30 (FFC2h) was used as ground.



Figure 33. On the left, the ring electrode. On the right, the touch-proof connector that connects to the headbox

Impedance checking was done for the ring electrodes and the impedances seen were astronomically high. This was attributed to the air gap between the scalp and electrode due to participant's hair volume. The lights were turned off and faraday cage shut. The test was begun for the participant.

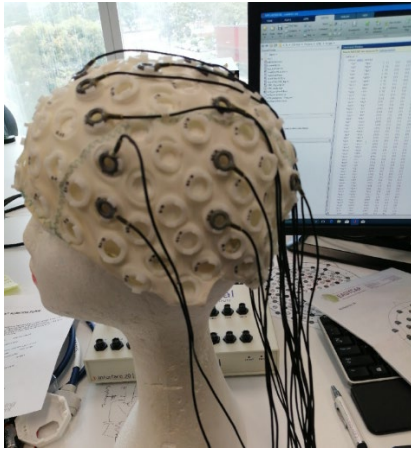


Figure 34. Ring electrodes connected to the EasyCap before the experiment.

4.8. 8 SAHARA electrode used 'dry' in the cap

As there were a limited number of SAHARA electrodes (8), the locations for their placements had to be chosen carefully, the positions chosen were F3, Fz, F4, FCz, C4, Cz, C3 and Pz. The SAHARA electrodes were bulky and spiked. They had 2 parts, the long spiked electrode end with a male connector, and a snap female lead connector. The electrode was placed under the cap, while the snap connector was placed above and connected through the cap. 3 electrodes had longer spikes than the rest and were thus, placed at the frontal locations at F3, Fz and F4 in order to tighten the cap. The electrodes were plugged into a SAHARA headbox, which allowed 16 channels (Figure 35). The headbox was then plugged into the Hlamp.



Figure 35. 16 channel SAHARA electrode headbox, with incoming electrode connectors (black) and outgoing channel to the Hlamp (white)

4.8.1. SAHARA electrodes used on subject with thick hair

Author volunteered for this experiment, with the electrodes showing a drift on the EEG signal monitor from the 'Hlamp Runner'. It was indicated to the author that the SAHARA dry electrodes took a period of time to settle down from the drift to show viable EEG signals. The setup itself took a fair bit of time, as the cap was seen to be loose for the subject in the posterior region. The longer spiked SAHARA electrodes were placed in the front in order to tighten the cap as seen in the figure below. After a wait of about 10 minutes, with the SAHARA electrodes being uncomfortable as seen in Figure 36, the signal was checked again and the experiment run. The lights were turned off and the cage closed. The test blocks were run.

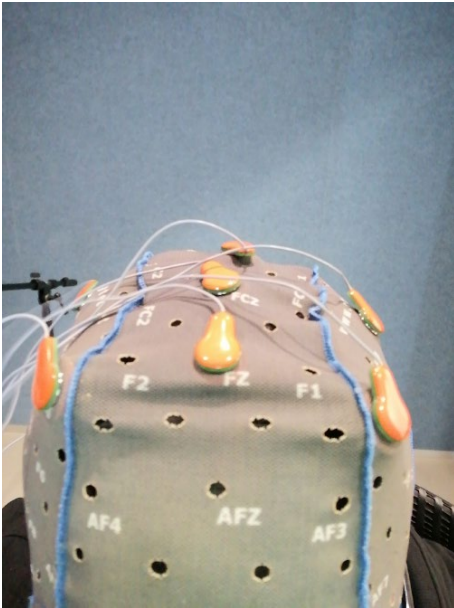


Figure 36. Placement of SAHARA electrodes on gtec cap. The orange snap electrodes are visible here and the bulk of the electrodes can be seen by the shape of the cap

4.8.2. SAHARA electrodes used on subject with short, curly, stiff hair



Figure 37. Subject with short, stiff, curly hair with the SAHARA electrode gtec cap fit on

The SAHARA electrodes fit better on the subject with short, stiff, curly hair as seen in Figure 37. The electrodes were loose at the posterior end and showed signs of not sitting on the scalp perfectly. After letting the SAHARA electrodes settle for a short period of time, to avoid electrode drift, the experiment was run.

4.9. 5mm dry comb electrodes used with ring electrodes in cap

Initial attempts to place the comb electrodes in the cap, resulted in a loose cap, with no acquisition possible. This was compounded by the shortage of comb electrode connectors for the experiment. This was remedied by out of the box thinking, where the comb electrodes would be paired with the 'wet' passive ring electrodes. The 5 mm dry comb electrodes were placed under the cap and held in place by the ring electrodes. The idea was that the dry comb electrodes would make contact with the scalp through participant's hair and the ring electrodes would then transmit the signal. This was due to a shortage in the number of connectors available for the dry 5mm comb electrodes. The setup resulted in the cap being slightly raised over the scalp as it sat on the dry electrodes. The process was laborious for the professors placing the electrodes and uncomfortable for the participant. As placing new electrodes resulted in former placements being displaced, the process was lengthened for double checking. The participant was found to have stronger connections in the center of the

head as compared to the periphery, due to cap being slightly loose. The impedance tests showed practically no changes to the impedance from the first test.

4.9.1. Dry comb electrodes used on subject with thick hair

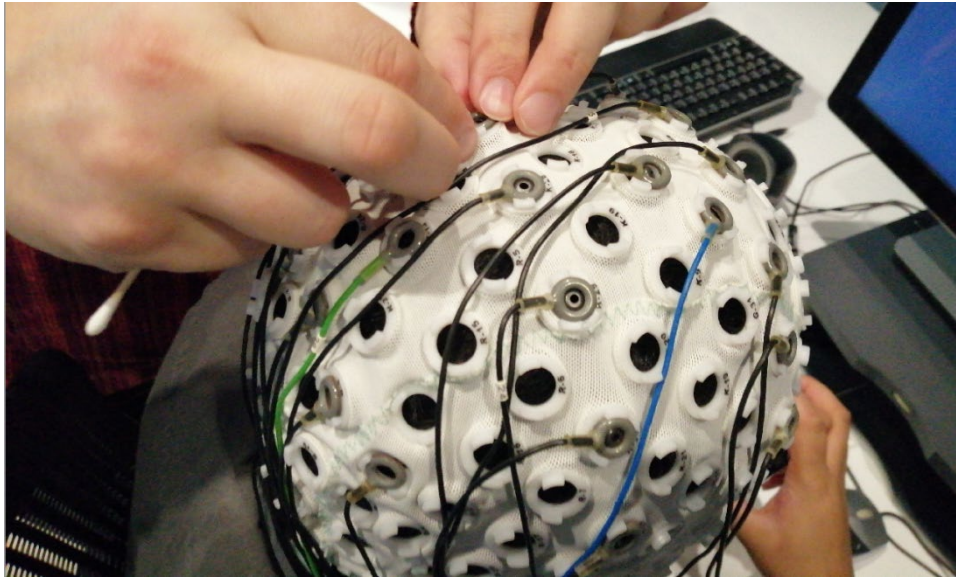


Figure 38. Image shows the ring electrodes sitting around the head of the 5mm comb electrodes. The process was time intensive due to the restrictions in cap design to movement of electrodes in the cap

The cap was lifted off the subject's hair due to the comb electrodes lifting the cap up. There was also the issue of the thick hair making it difficult for the electrodes to be correctly placed. An error at the start of the experiment, resulted in the test being conducted with the lights turned on. The test was then re-conducted with the lights turned off, allowing for an additional parameter to be analysed.

4.9.2. Dry comb electrodes used on subject with short, curly, stiff hair



Figure 39. Subject with short, curly, stiff hair with the ring and comb electrode combination set in the cap

The cap was easier to setup on the subjects head due to lesser volume of hair as seen in Figure 39. The electrodes were easier to setup for this experiment reducing time required for the setup. The electrodes were seen to make incomplete connections with the scalp due to the stiff hair blocking the electrode spikes (5mm). The longer spikes of the SAHARA electrodes were seen to improve connections.

5. Results

In this section, author will present the data acquired from the subjects. Analysis of the data will be continued in the [Discussion](#) section of the thesis. Graphs from electrode positions not crucial to the data analysis, but important as evidence of the results and analysis are included in the [Appendix](#). During period of data analysis, the spectra of the EEG signal were used to compare the effects of each experiment. The colour coded graphs show traces of either the hardware EEG directly taken from the electrodes or the software laplacian of the EEG taken from electrodes. The latter usually indicated by the RBY (Red-Blue-Yellow) coloured traces, while the electrode EEGs usually indicated by PGB (purple-green-light blue). Three tasks were run for each experiment where the eyes closed task was indicated by Blue and Purple traces, the eyes open by Red and Green traces and muscle tasks by Yellow and Light Blue traces respectively.

5.1. 20 tCRE electrodes with 108 passive wet electrodes

The first experiment involved using tCRE electrodes interspersed between passive wet electrodes. Central 20 passive wet electrodes were replaced with tCRE electrodes. The montage in figure 36, gives us the legend for our traces, as explained below.

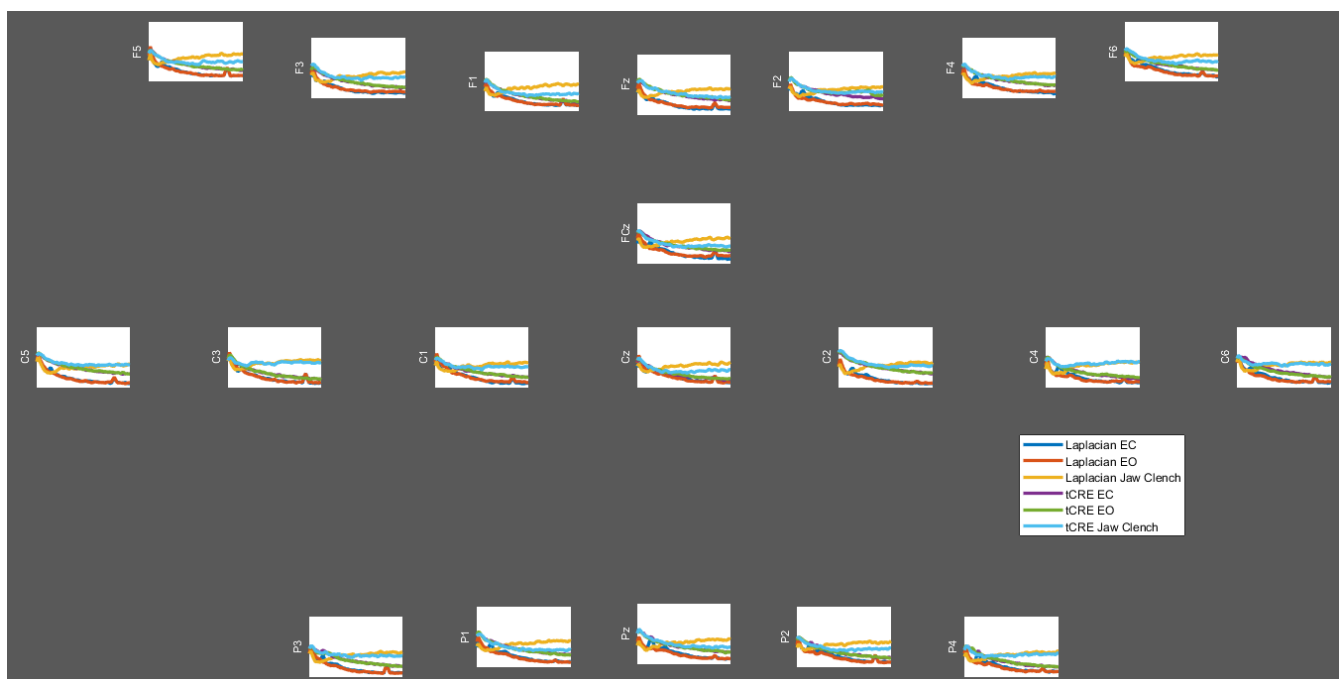


Figure 40. Figure shows montage of electrodes on the head with the colour coded legend

Figure 40 shows the montage of the electrodes placed on the head. The 108 ring electrodes were placed around these tCRE electrodes in order to compare the acquired EEGs. As seen in the legend, blue trace represents the laplacian eyes closed EEG trace, red trace represents the laplacian eyes open EEG trace, yellow trace represents the muscle task EEG trace. Similarly, for the tCRE EEG, purple trace represents tCRE eyes closed task, green trace represents tCRE eyes open task and light blue represents the tCRE muscle task.

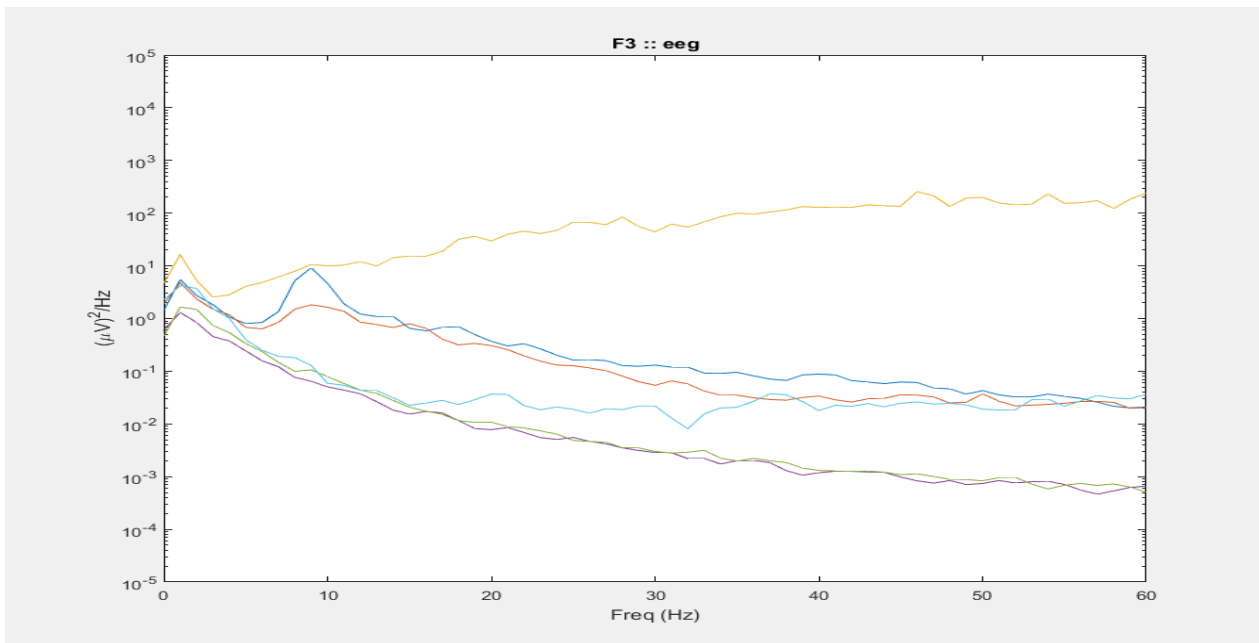


Figure 41. Graph shows EEG at F3 electrode position, 3 traces (dark blue, red, yellow) show emulated EEG and 3 traces (maroon, green, light blue) show EEG from tCRE electrodes

From Figure 41, we see 6 traces. Red, Blue and Yellow refer to software Laplacian eyes closed, eyes open and muscle tasks. The purple, green and light blue traces refer to the tCRE eyes closed, eyes open and muscle tasks. As seen in the traces, the muscle traces (light blue and yellow) show a large divergence from their baseline green-purple and red-blue traces. There is also a large spike seen at 10Hz with regard to the software Laplacian EEG, but not in the tCRE electrodes.

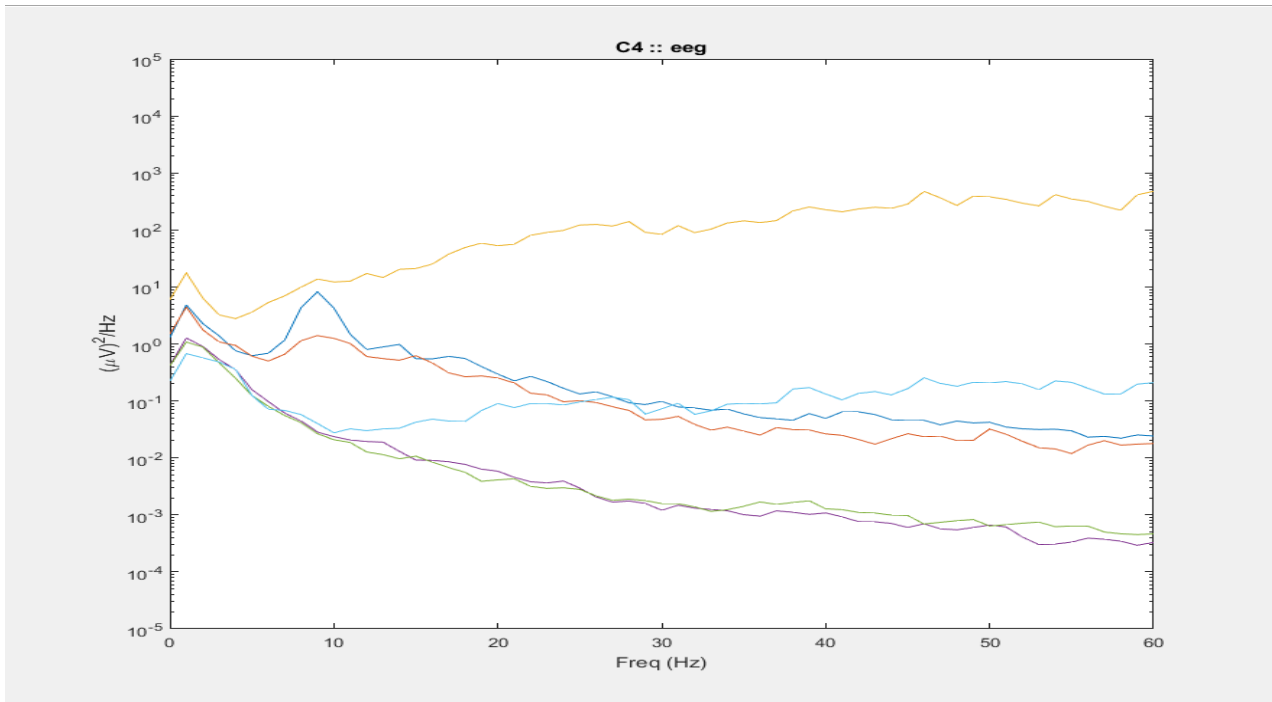


Figure 42. Graph shows EEG traces at C4 electrode position., 3 traces (dark blue, red, yellow) show emulated EEG and 3 traces (maroon, green, light blue) show EEG from tCRE electrodes

From Figure 42, we see the traces from electrode at position C4 on the head. The muscle task traces show a large divergence from the baseline tasks. There is an alpha peak seen at 10 Hz for the Laplacian software EEG, but absent in the tCRE electrodes.

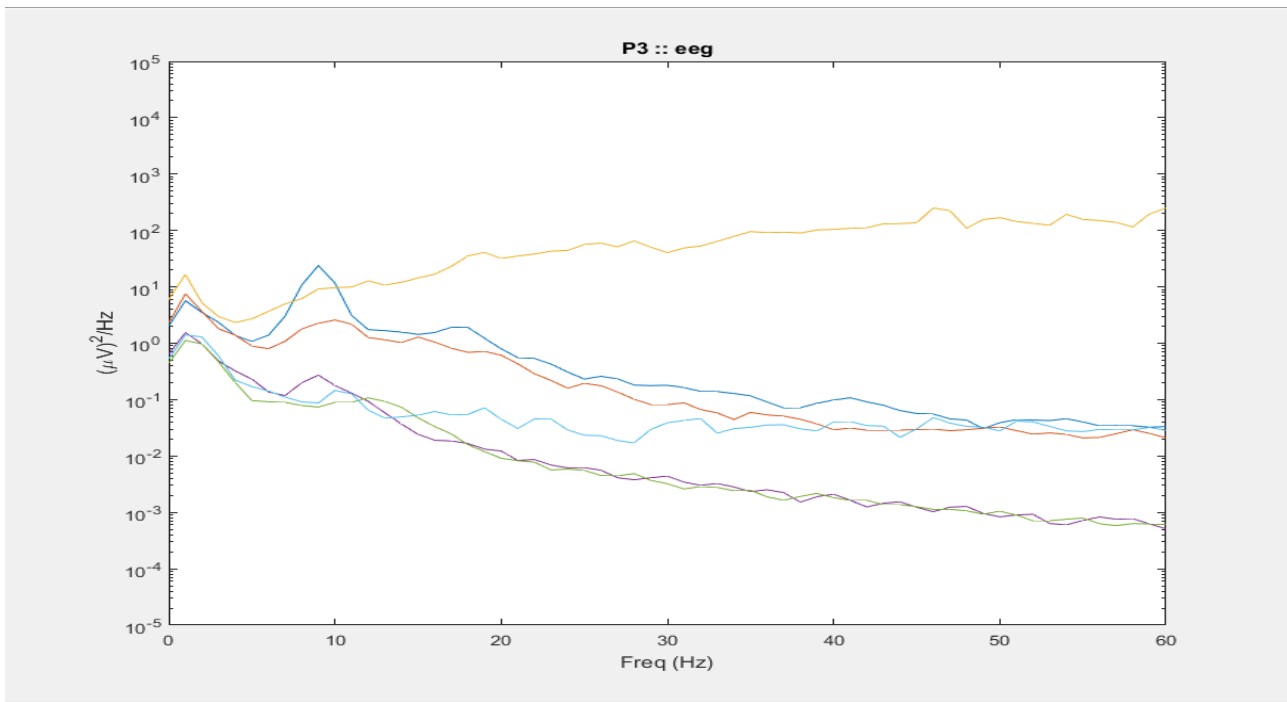


Figure 43. Graph shows EEG at P3 electrode location, 3 traces (dark blue, red, yellow) show emulated EEG and 3 traces (maroon, green, light blue) show EEG from tCRE electrodes

Figure 43 shows traces taken from electrodes at position P3 on the head. Muscle task traces show divergence from their baseline. There is also a 10Hz peak seen in both eyes closed tasks for the software laplacian and the tCRE electrode EEG. The amplitude of the tCRE electrodes signal is seen to be lower than the Laplacian version of the traces.

5.2. tCRE electrodes periphery test (9 central + 11 peripheral electrodes)

The tCREs were distributed over the scalp, with 9 tCREs placed centrally and 11 peripherally, to measure the effect of muscle on EEG acquisition by the tCREs as seen in Figure 44.

5.2.1. tCRE electrode periphery test on subject with thin, wispy hair



Figure 44. Montage of tCRE electrode layout on subject's head for test, with 9 central and 11 peripheral electrodes

The montage of electrodes placed on the head centrally and peripherally is shown in Figure 44, where we see that the electrodes are placed as far as the occipital and temporal regions of the head.

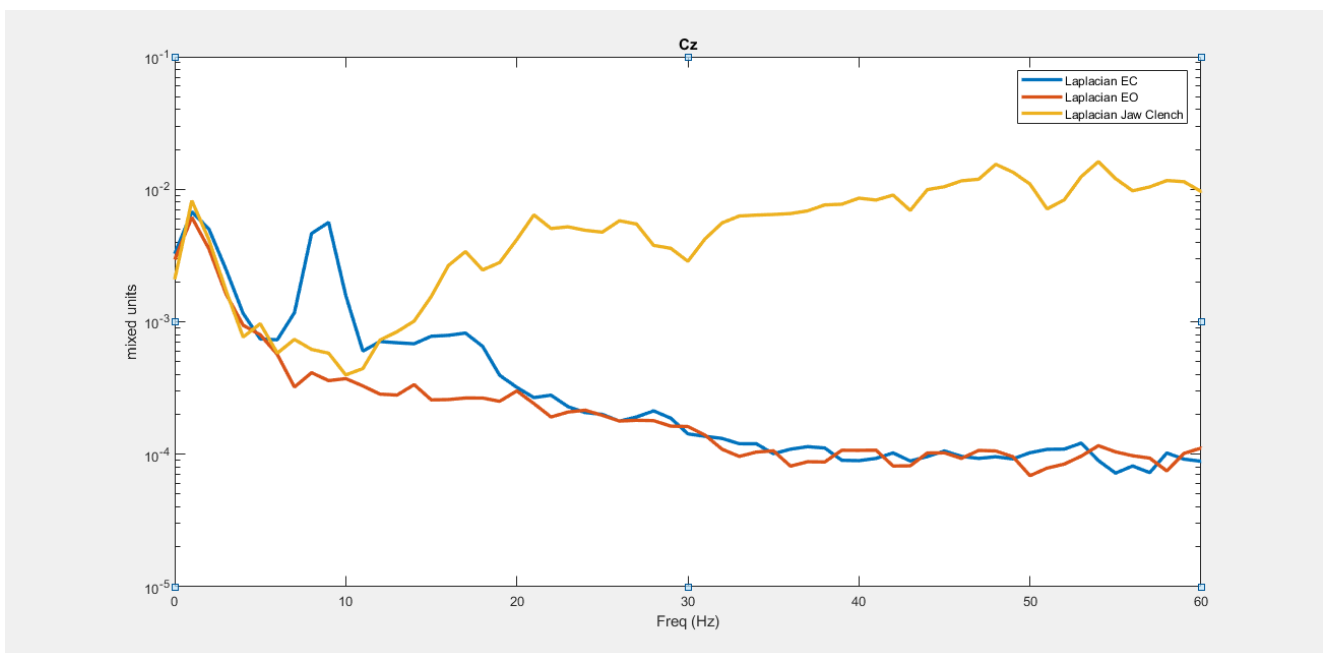


Figure 45. Graph shows software Laplacian traces from electrode at Cz locations

Figure 45 shows us the alpha peak at 10 Hz for eyes closed (blue traces) and the muscle task (yellow trace) divergence from the baseline.

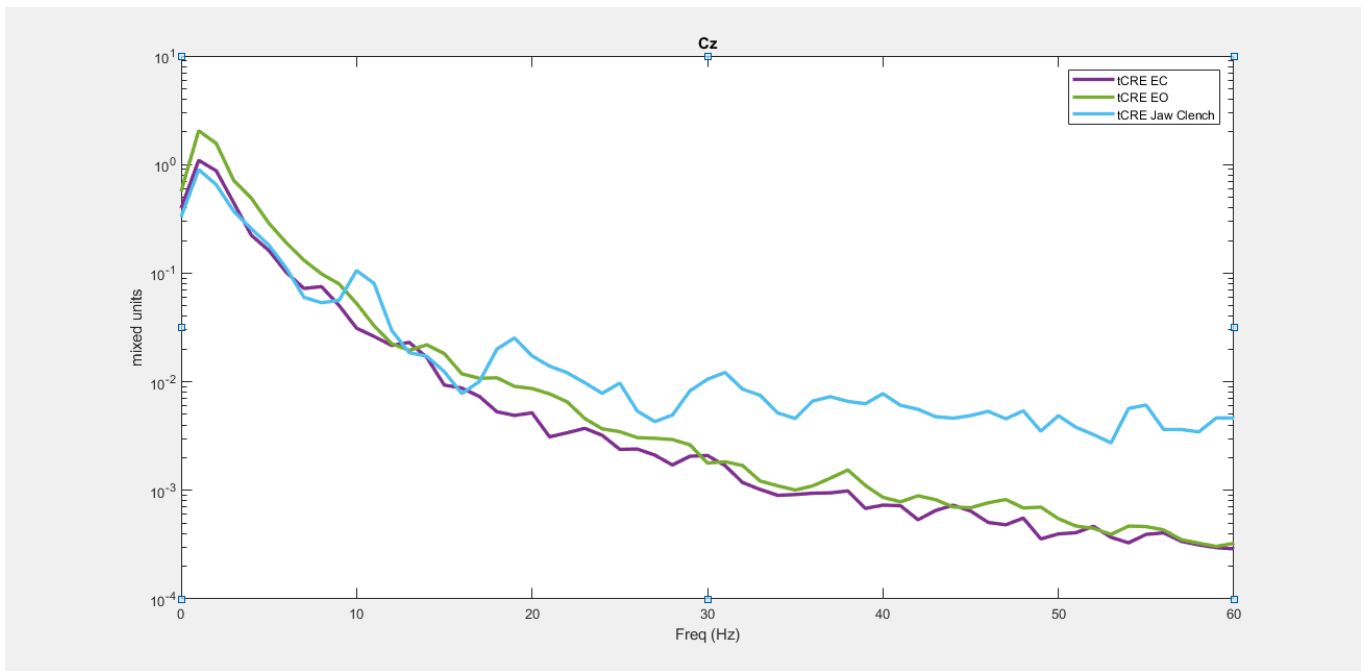


Figure 46. Graph show tCRE electrode traces at Cz location

In Figure 46, there is no alpha peak seen in 10Hz with eyes closed. Light blue trace shows muscle task divergence from the baseline. There is also a large 10Hz spike seen in the muscle task (light blue trace).

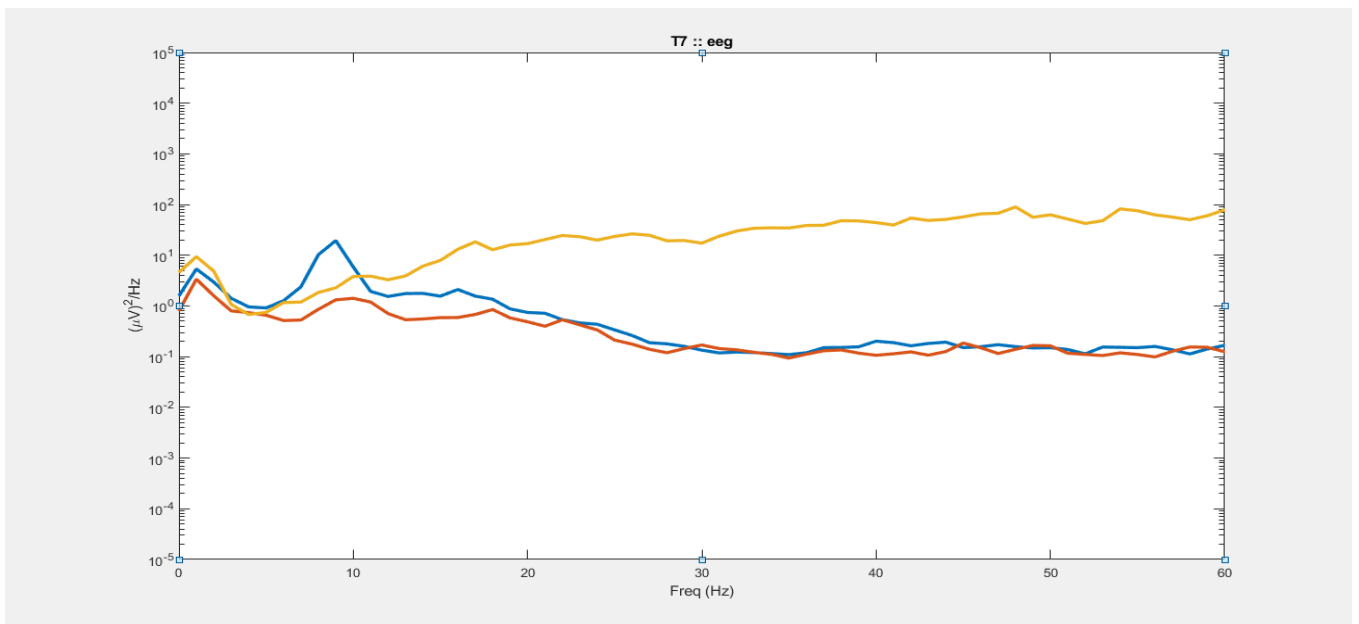


Figure 47. Graph shows Laplacian of EEG at electrode location T7

As Figure 47 shows, the Laplacian version of the EEG gives us an alpha peak at eyes closed (blue trace) and the muscle task (yellow trace) shows a divergence from the baseline.

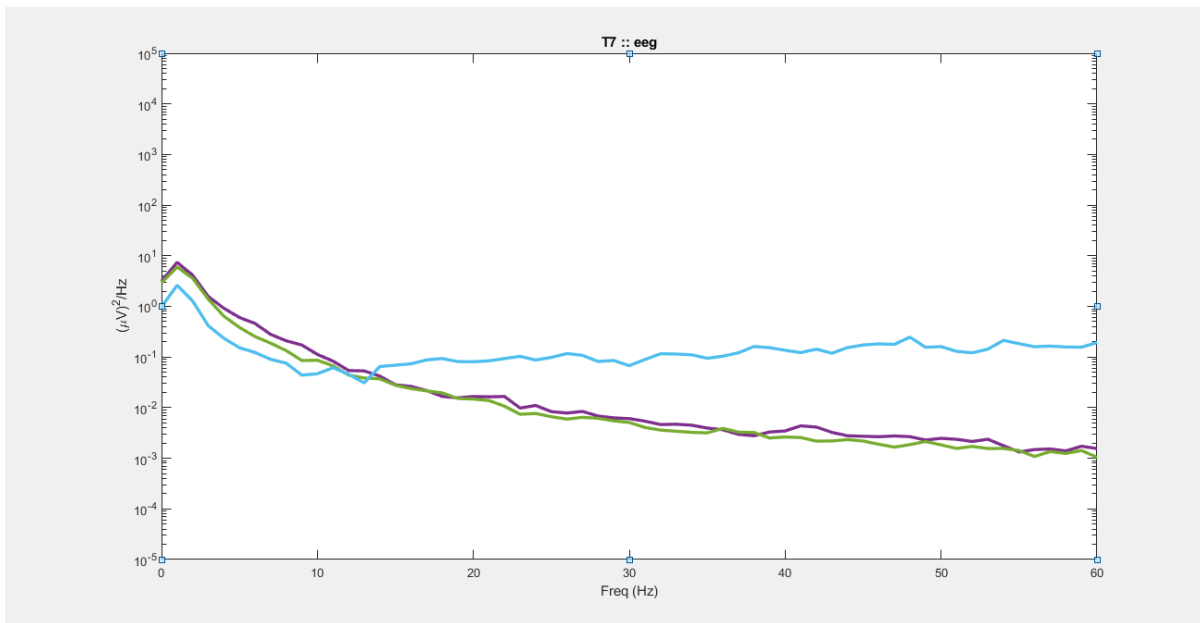


Figure 48. Graph shows tCRE electrode EEG at electrode location T7

Figure 48 shows the tCRE EEG of T7, where we do not see an alpha peak during eyes closed (purple trace) and the muscle task (light blue trace) shows similar divergence from baseline as spectra at electrode location Cz.

5.2.2. tCRE electrode periphery test on subject with short, stiff curly hair

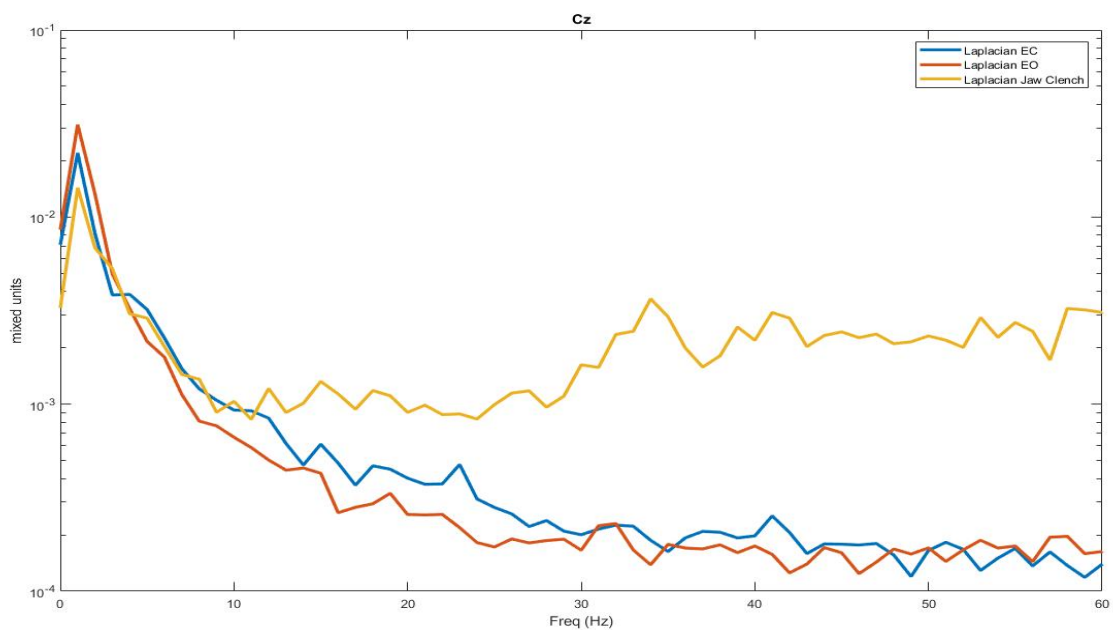


Figure 49. Graph shows Laplacian of EEG at electrode location Cz

Figure 49 shows laplacian of EEG at Cz, where we see the absence of an alpha peak (blue trace) at 10 Hz and the divergence of the muscle task (yellow trace) from the baseline.

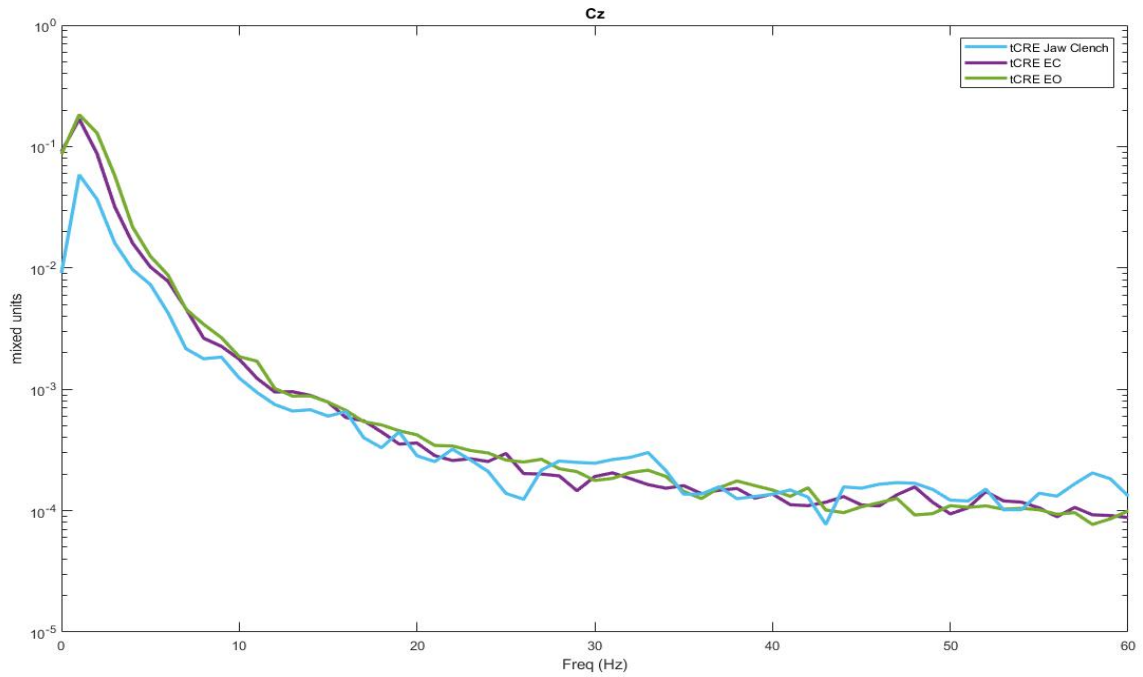


Figure 50. Graph shows tCRE EEG at electrode location Cz

Figure 50 shows tCRE EEG at Cz, where there is an absence of alpha peaks at 10 Hz in eyes closed (purple trace) and no evidence of muscle task (light blue trace) divergence from the baseline.

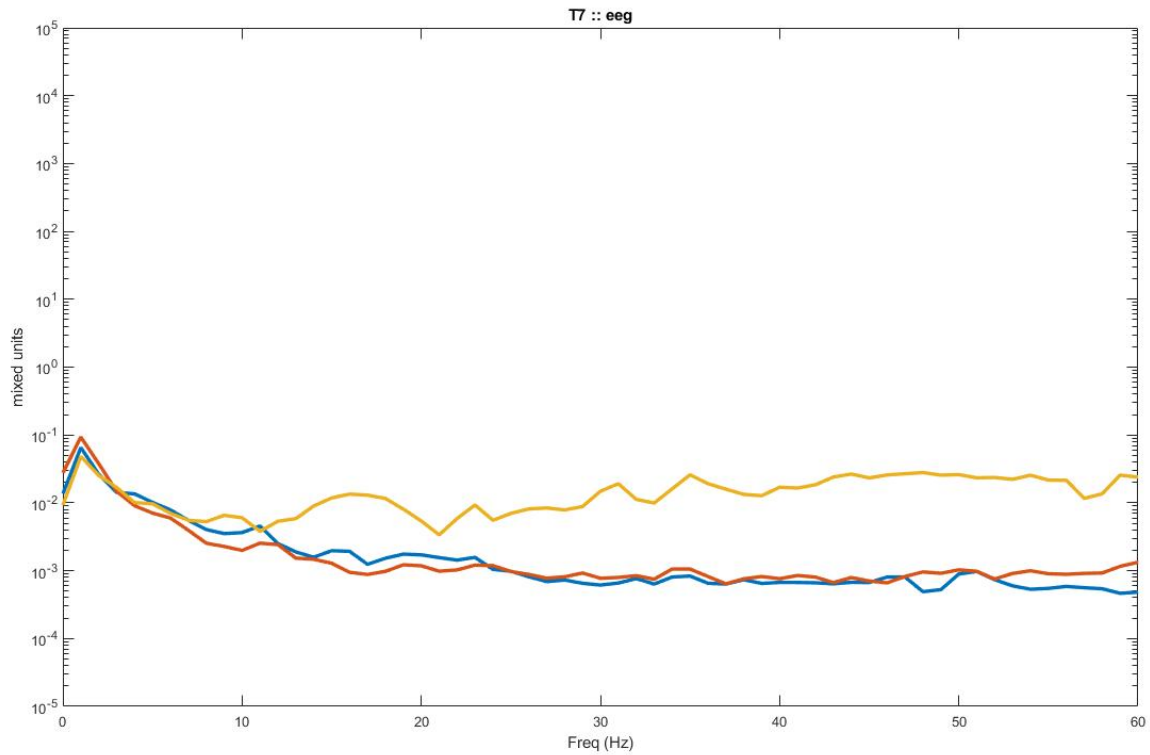


Figure 51. Graph shows Laplacian of EEG at electrode location T7

Figure 51 shows the laplacian of EEG at T7, where there is a slight bump at 10 Hz for eyes closed (Blue trace) and there is muscle task (yellow trace) divergence seen, from the baseline.

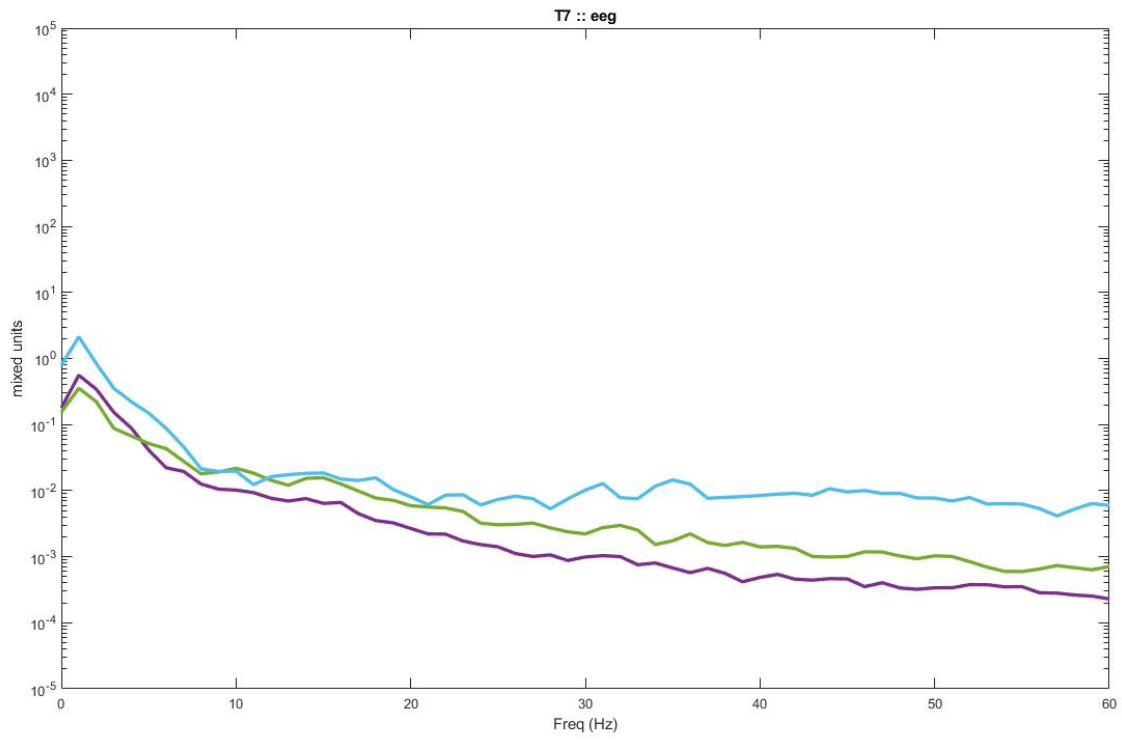


Figure 52. Graph shows tCRE EEG at electrode location T7

Figure 52 shows tCRE EEG at T7, where we see the absence of 10 Hz alpha peak at eyes closed (blue trace) and a slight divergence of muscle task (yellow task) from the baseline.

5.3. 20 tCRE electrodes used 'dry' in the cap

The tCREs were placed on the cap, with no interface connecting them to the scalp. This was done to verify the ability of tCREs in the absence of good connections.

5.3.1. 20 tCRE electrodes used 'dry' in cap on subject with thick hair

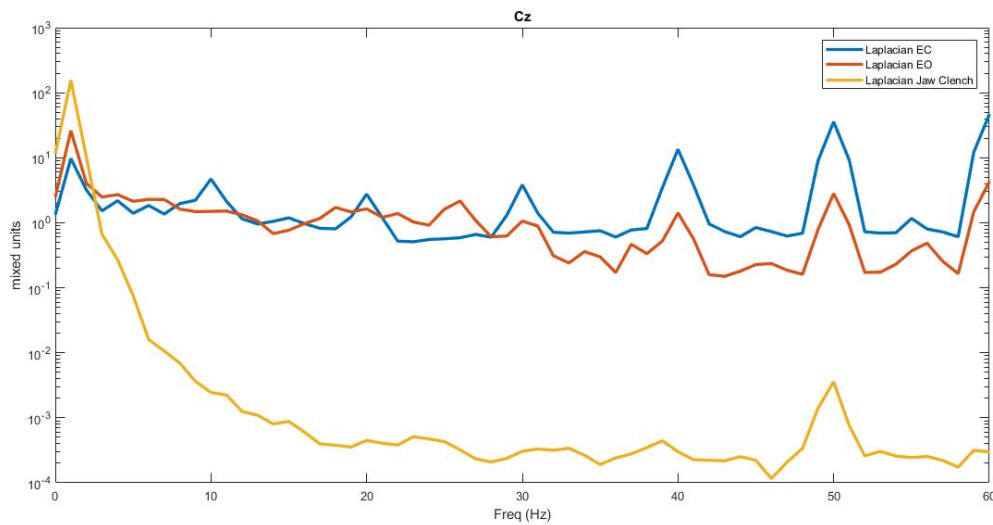


Figure 53. Graph shows laplacian of EEG at electrode location Cz

Figure 53 shows the laplacian of EEG at Cz, where we see the absence of alpha peaks at 10 Hz in eyes closed (blue traces), instead seeing a harmonic created in both eyes closed and eyes open tasks. The muscle task (yellow trace) seems suppressed.

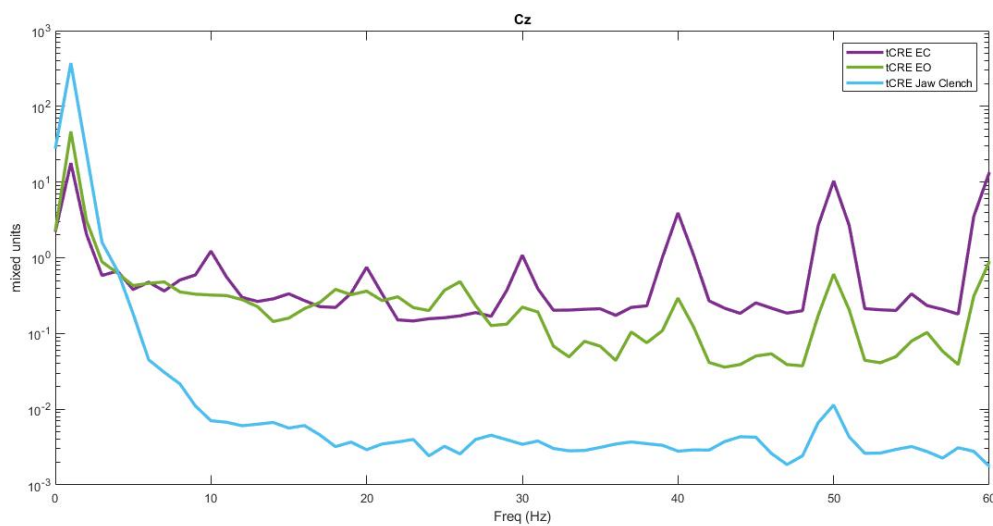


Figure 54. Graph shows tCRE EEG at electrode location Cz

Large harmonics are seen in the eyes open (green) and eyes closed (purple) tasks and the muscle (light blue) is seen to be suppressed in Figure 54

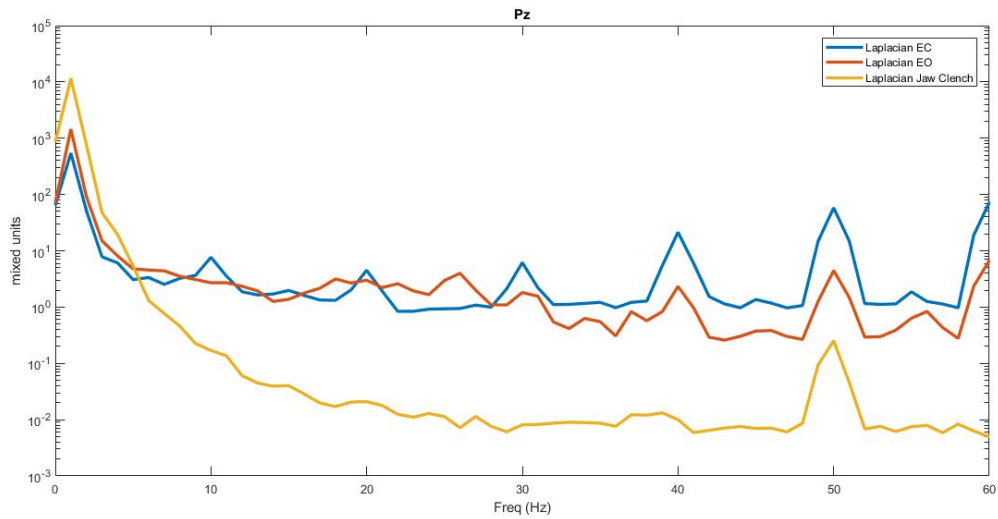


Figure 55. Graph shows Laplacian of EEG at electrode location Pz

At Pz, the harmonics are seen again during eyes closed tasks every 10 Hz, and in eyes open task from 40Hz. The muscle is depressed below the baseline in Figure 55

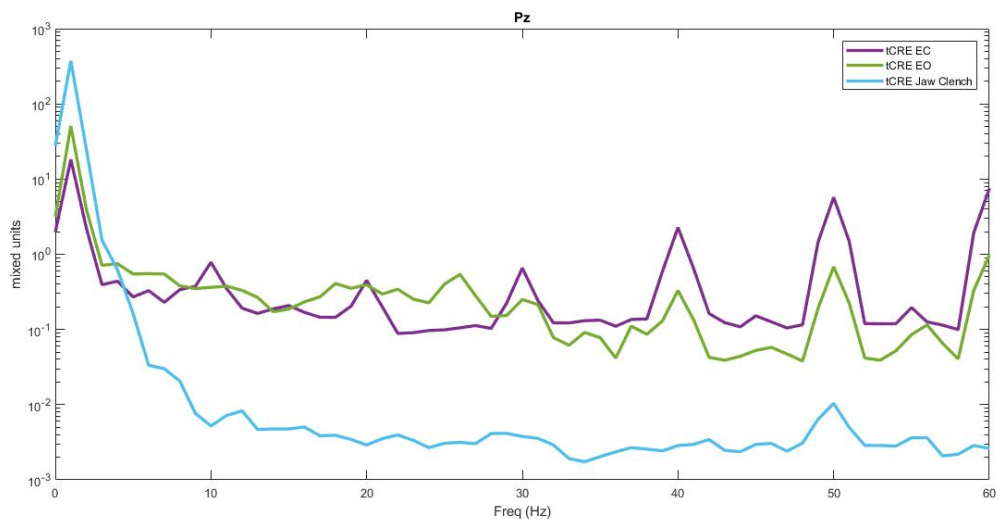


Figure 56. Graph shows tCRE EEG at electrode location Pz

In Figure 56, we see the prevalence of an increasing harmonic in the eyes closed task every 10 Hz, and the same for the eyes open task starting from 40 Hz. The muscle task is once again suppressed compared to the baseline.

5.3.2. 20 tCRE electrodes used 'dry' in cap on subject with short, stiff curly hair

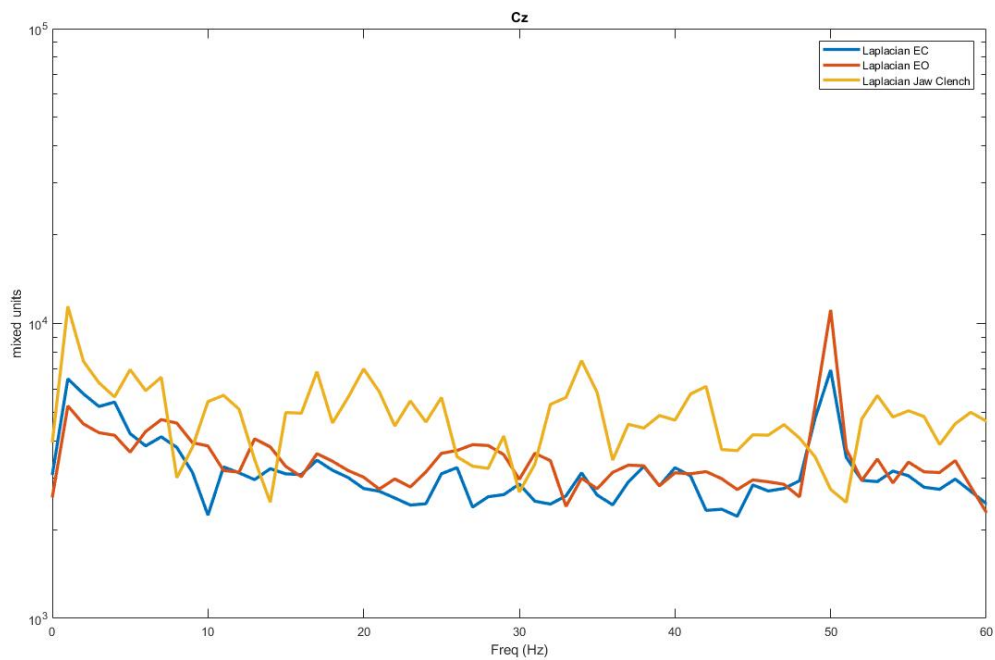


Figure 57. Graph shows Laplacian of EEG at electrode location Cz

Subject with short, curly, stiff hair showed large resistance to 'dry' tCREs and thus gave us absolutely no biological signal, as seen in Figure 57. Muscle showed some variation from the baseline.

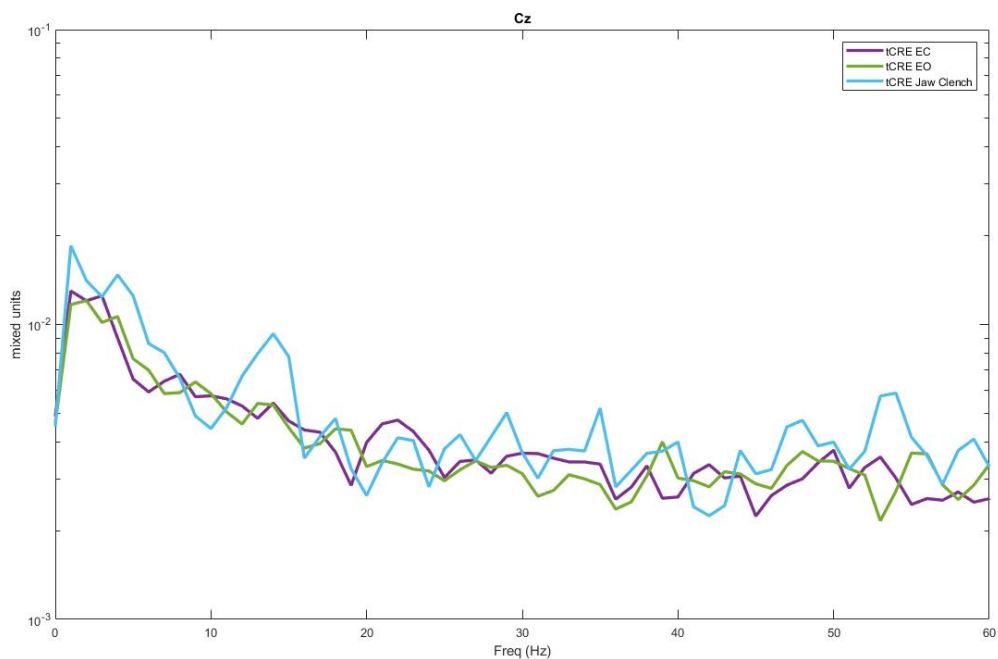


Figure 58. Graph shows tCRE EEG at electrode location Cz

As seen in Figure 58, the tCRE electrodes did not provide a valid biological signal, and showed depressed muscle traces

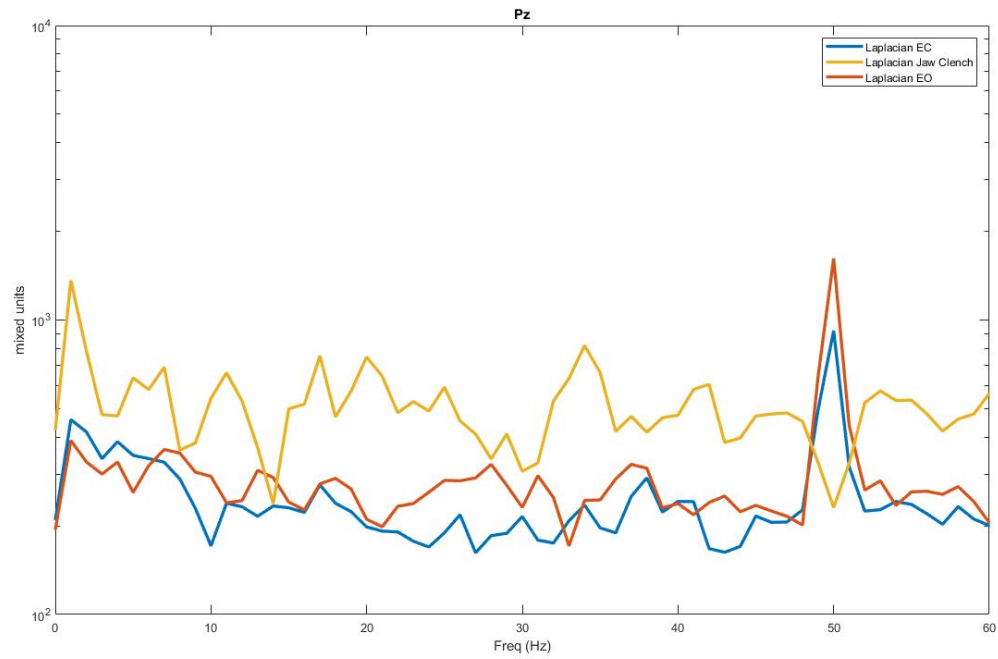


Figure 59. Graph shows Laplacian of EEG at electrode location Pz

In Figure 59, At Pz, closer to the back of the head, we see the muscle task shows separation from the baseline, but no biological signal is visible.

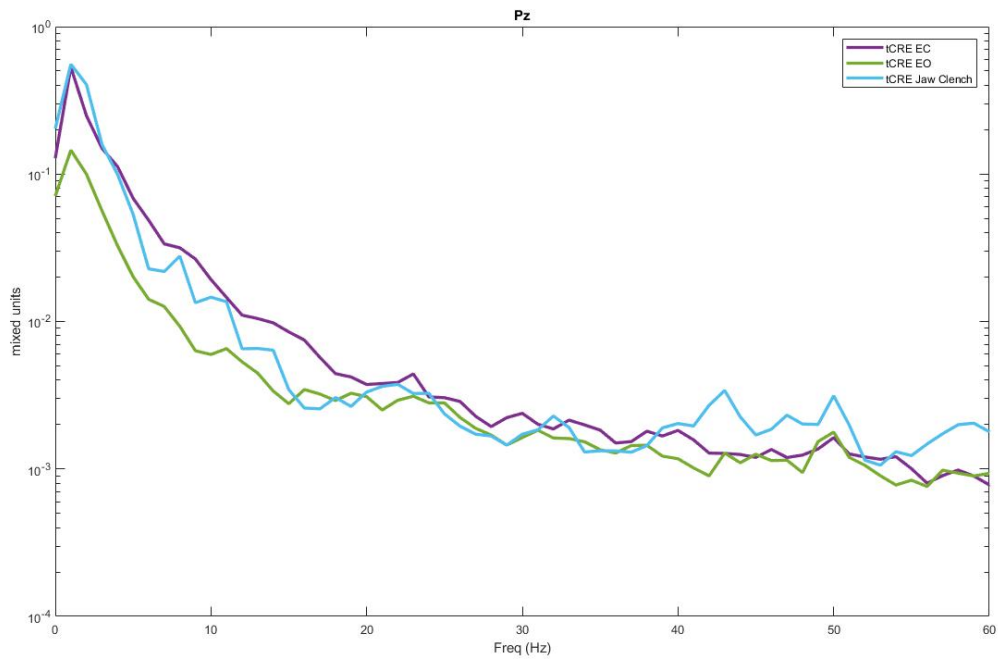


Figure 60. Graph shows tCRE EEG at electrode location Pz

In Figure 60, we see there is no biology seen and muscle doesn't show any reliable variation from baseline.

5.4. 20 tCRE electrodes used 'dry' under the cap

This experiment was conducted only on the subject with thick hair due to scheduling constraints. It placed the tCREs closer to the scalp under the cap in order to improve connections, and see if the tCREs were able to acquire any EEG signal.

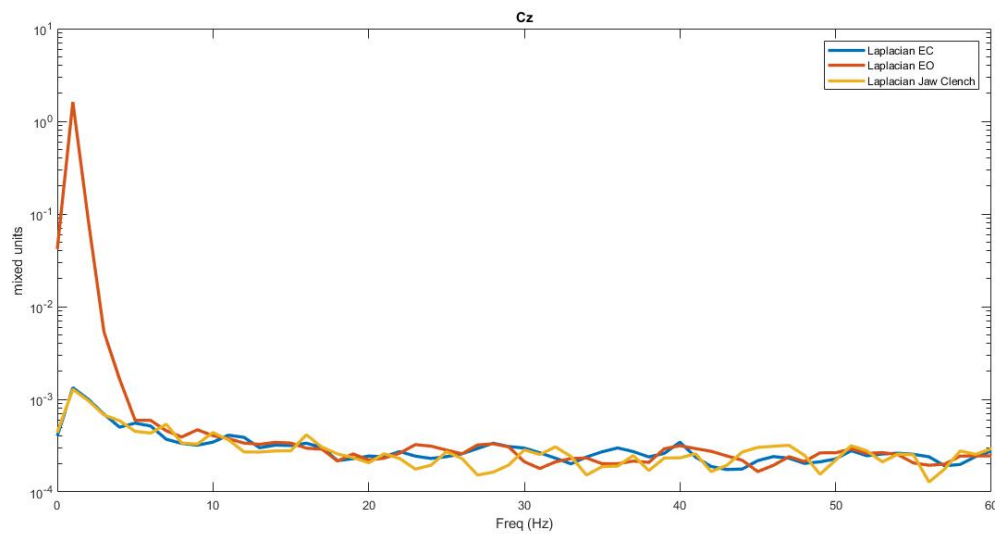


Figure 61. Graph shows Laplacian of EEG at electrode location Cz

From Figure 61, we see there is absolutely no biology detected by the electrodes, muscle is not detected and neither is the 50Hz mains noise prevalent in the other experiments

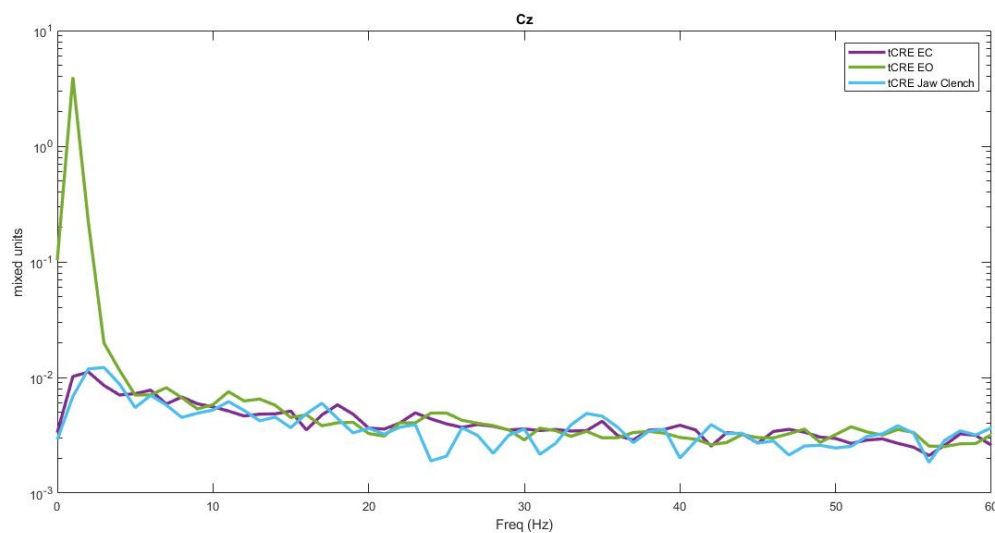


Figure 62. Graph shows tCRE EEG at electrode location Cz

In Figure 62, we see similar traces as the Laplacian version, with the absence of any form of biology, artefact or otherwise.

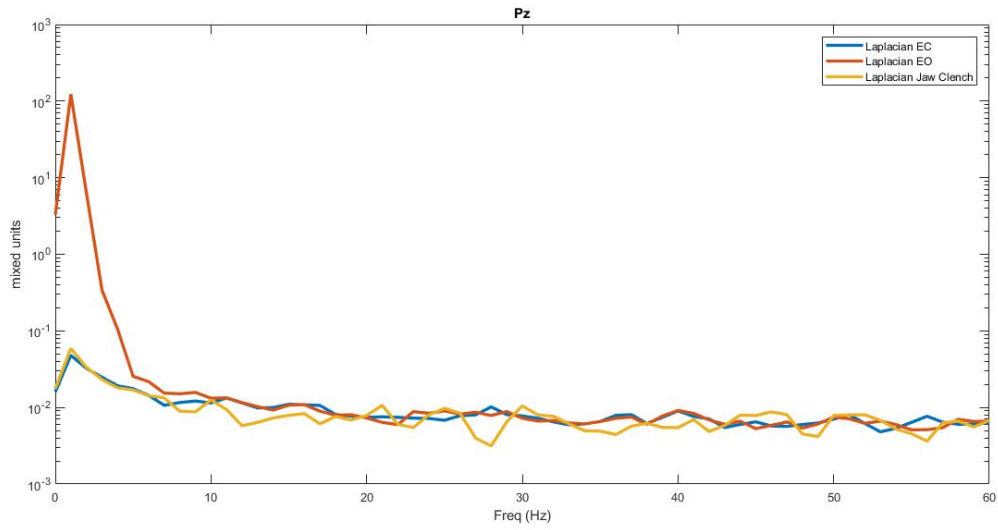


Figure 63. Graph shows Laplacian of EEG at electrode location Pz

In Figure 63, moving closer to muscle on the head has no effect on the electrode, with no biology seen.

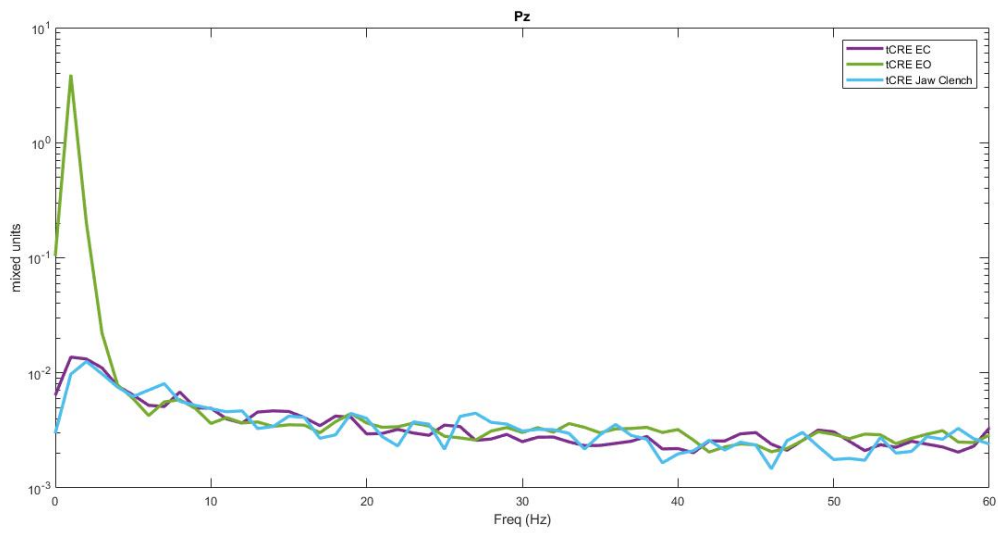


Figure 64. Graph shows tCRE EEG at electrode location Pz

No biology is seen in Figure 64, and muscle (light blue) is absent too.

5.5. 20 tCRE electrodes used in cap with saline filled foam infills in the cap

The tCREs were placed on the cap, with saline filled foam infills connecting the electrodes to the scalp. This replaced the traditional gel used by the tCREs for their ideal function.

5.5.1. 20 tCRE electrodes used in cap with saline filled foam infills in cap used on subject with thin, wispy hair

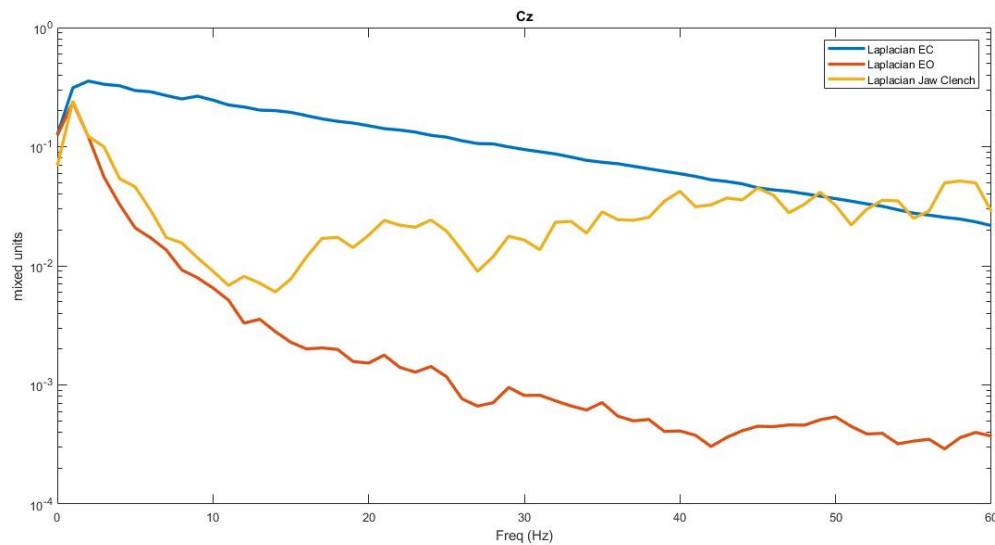


Figure 65. Graph shows Laplacian of EEG at electrode location Cz

In Figure 65, there is an error with the eyes closed task (blue trace) but the muscle task (yellow trace) shows divergence from baseline eyes open (red)

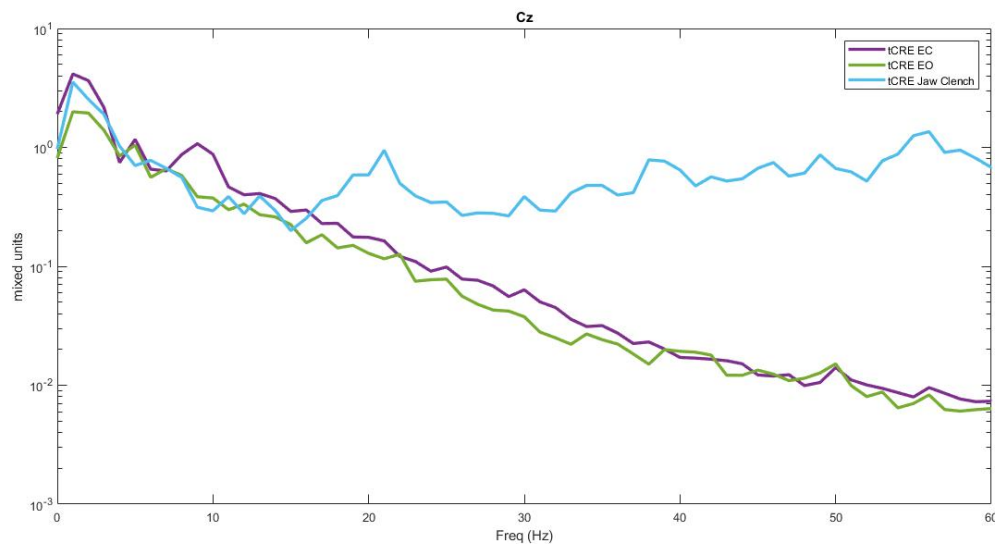


Figure 66. Graph shows tCRE EEG at electrode location Cz

In tCRE EEG, we see that there is a slight bump of eyes closed (purple trace) at 10Hz alpha peak, and a divergence from baseline of the muscle tasks (light blue trace) as seen in Figure 66

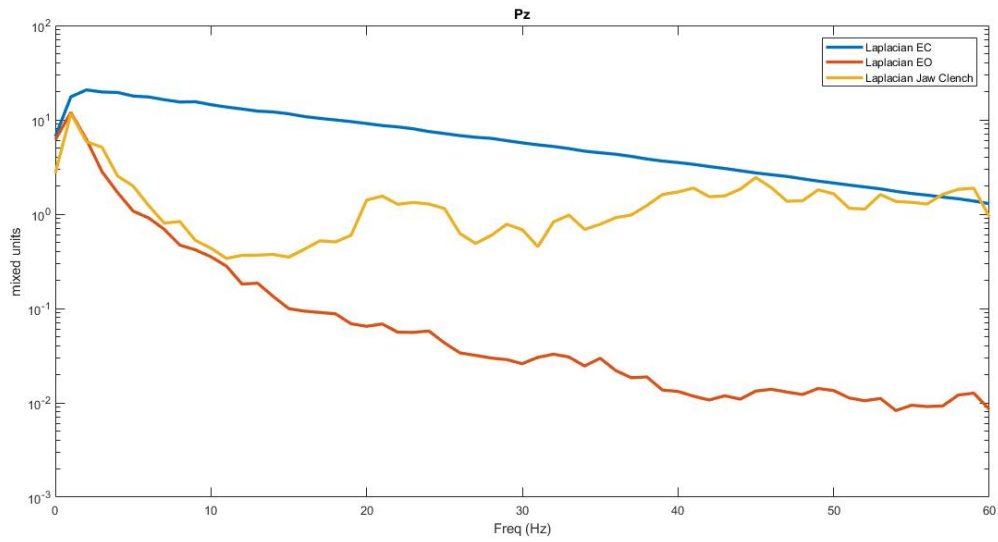


Figure 67. Graph shows Laplacian of EEG at electrode location Pz

Figure 67 shows the same error seen in Laplacian of Cz, at eyes closed (blue trace), and the muscle task (yellow trace) shows divergence from baseline eyes open.

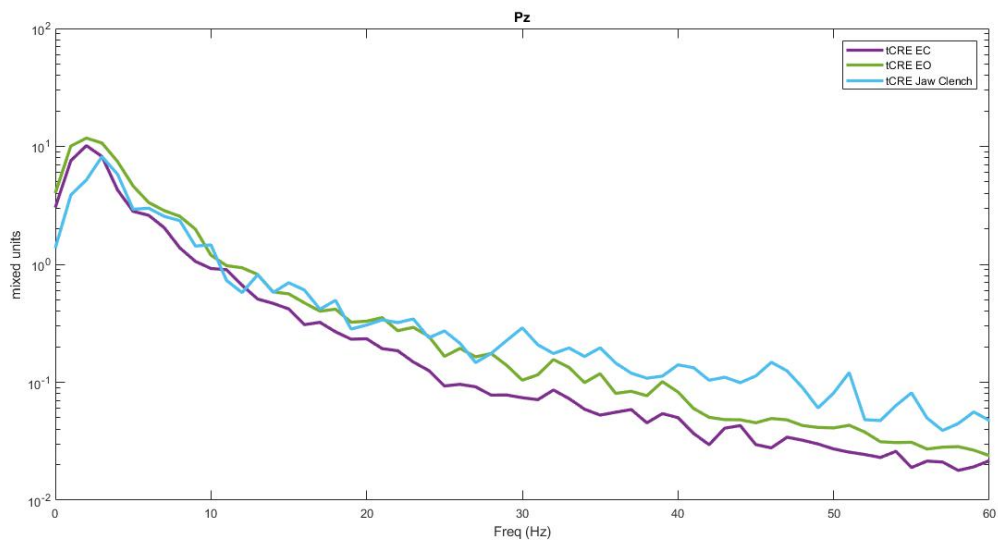


Figure 68. Graph shows tCRE EEG at electrode location Pz

There is no biology visible in the tCRE EEG at Pz, but a slight divergence is seen in the muscle task (light blue trace) from the baseline as seen in Figure 68

5.5.2. 20 tCRE electrodes used in cap with saline filled foam infills in cap used on subject with thick hair

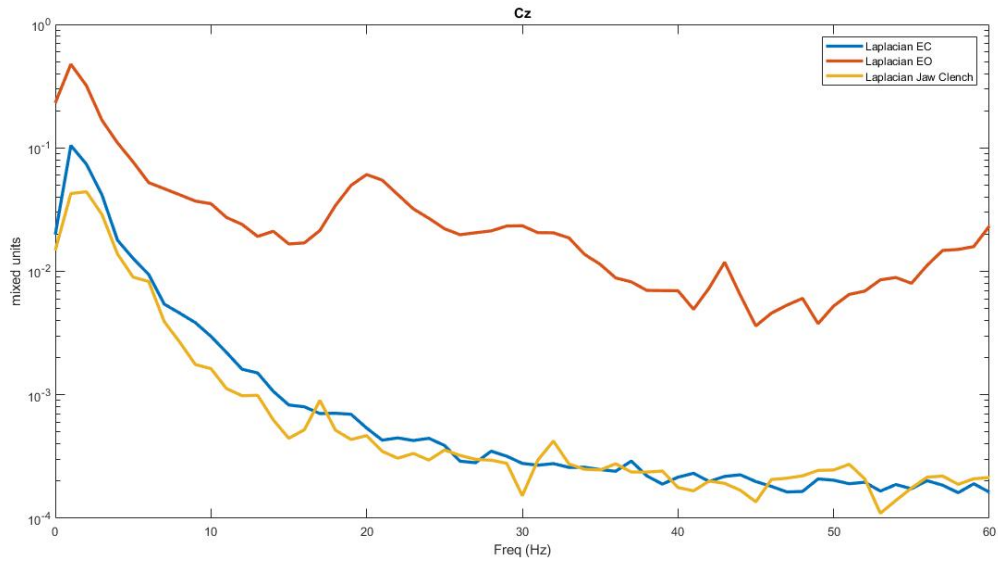


Figure 69. Graph shows Laplacian of EEG at electrode location Cz

Figure 69 shows laplacian of EEG at Cz. The eyes open (red trace) is unusually high, but no biology is seen with respect to the muscle task (yellow trace) or the eyes closed (blue trace)

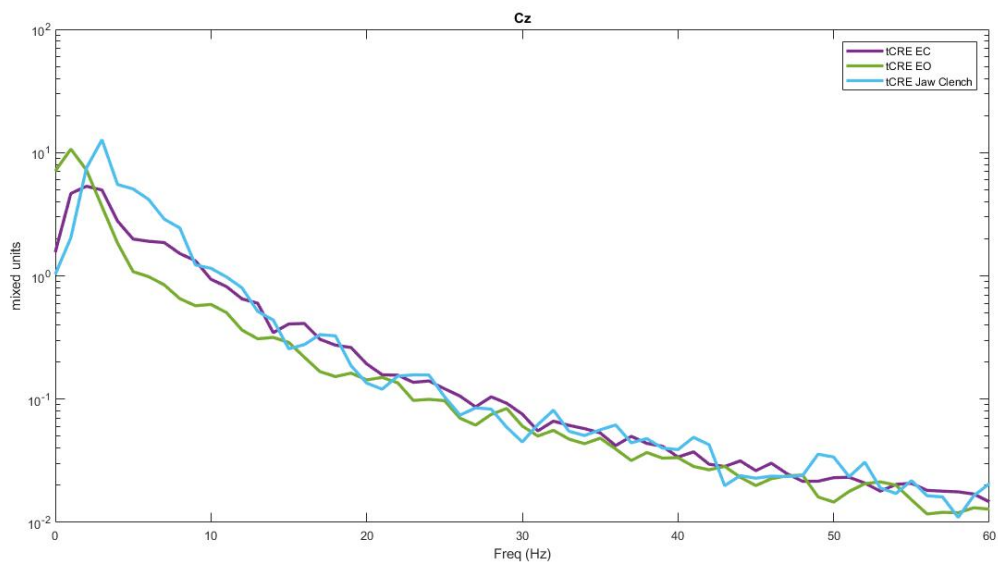


Figure 70. Graph shows tCRE EEG at electrode location Pz

Figure 70 shows no neural or muscular biology from the EEG taken at electrode Pz.

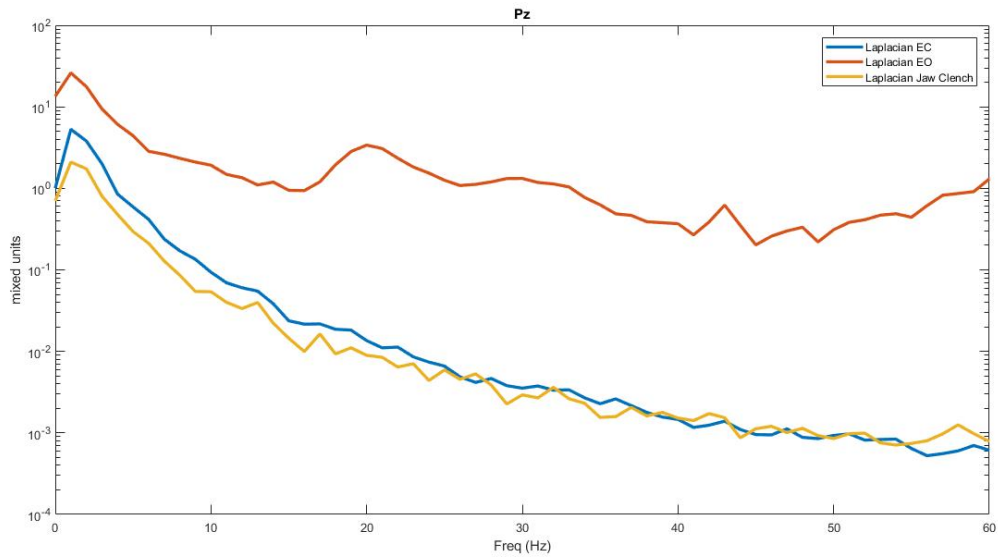


Figure 71. Graph shows Laplacian of EEG at electrode location Pz

As seen in Cz, Pz also sees no biology and there an unusually high eyes open (red trace) signal seen.

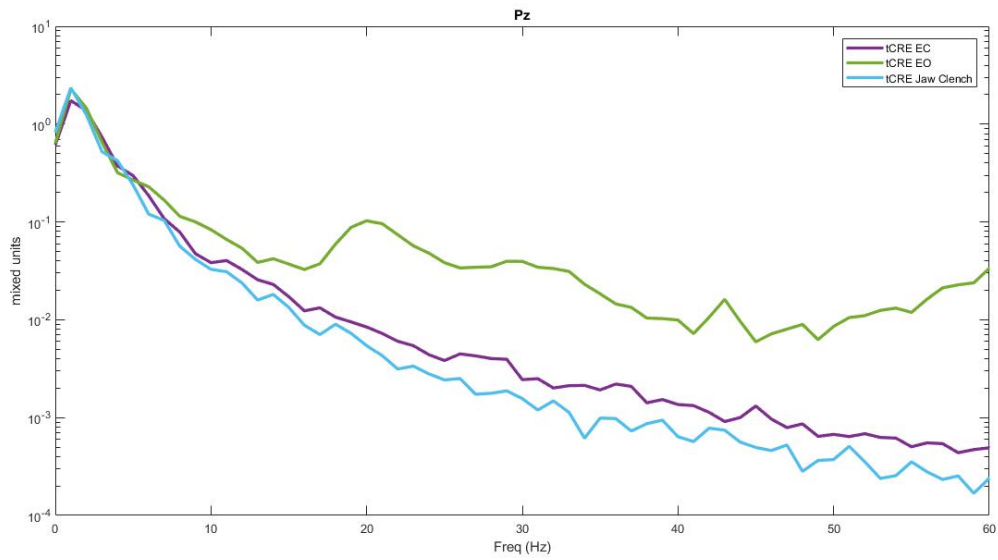


Figure 72. Graph shows tCRE EEG at electrode location Pz

The tCRE EEG of Pz, shows absence of muscle task (light blue) but shows the unusual variation at eyes open (green trace) in Figure 72

5.6. 20 tCRE electrodes used in cap with foam cap underneath

The tCRE electrodes were placed on the cap, with a saline soaked foam cap underneath the cap, with saline filled foam infills placed between the electrodes and the foam cap. This replaced the gel interface used in ideal connections.

5.6.1. 20 tCRE electrodes used in cap with foam cap underneath on subject with thick hair

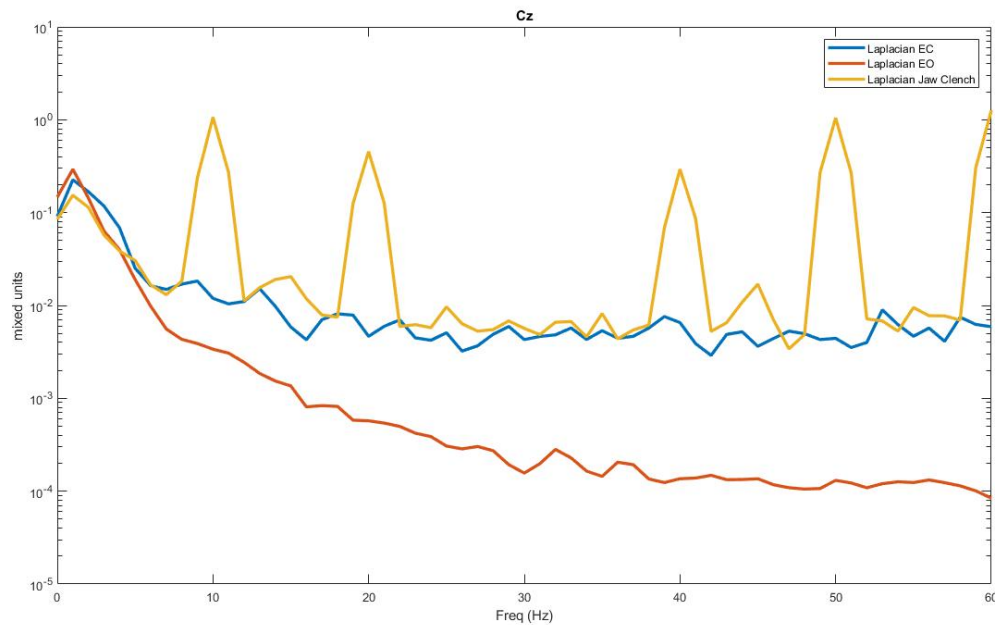


Figure 73. Graph shows Laplacian of EEG at electrode location Cz

Figure 73 shows us a harmonic in the muscle task (yellow trace), that has a missing harmonic at 30Hz. The eyes closed and eyes open baselines also show variation from one another and no biology. There is also a variation seen between eyes open (red trace) and eyes closed (blue trace).

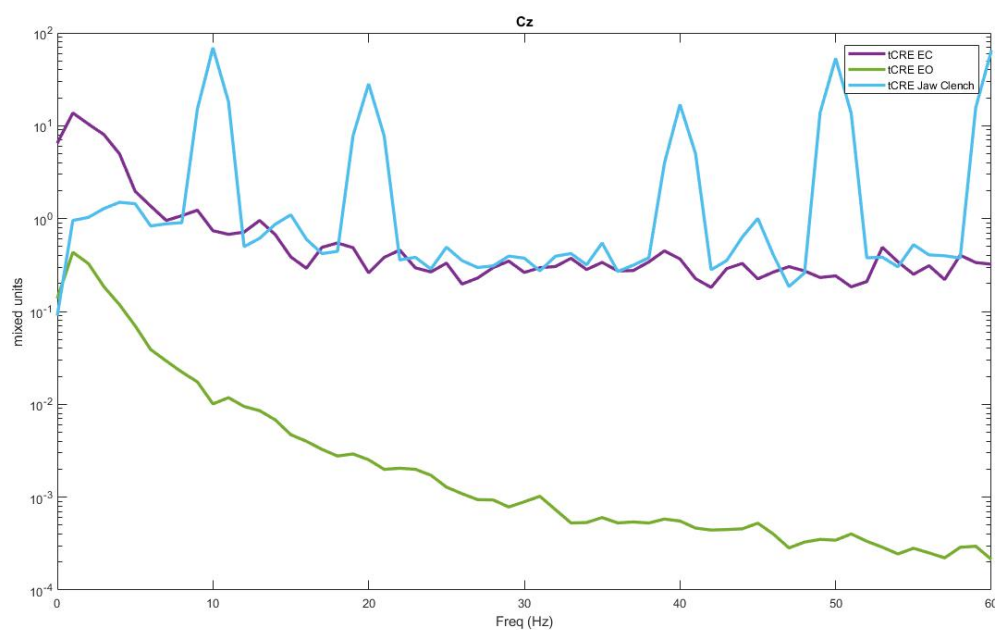


Figure 74. Graph shows tCRE EEG at electrode location Cz

The tCRE EEG in Figure 74, shows us a similar graph to that of Figure 73, with a missing 30Hz harmonic in the muscle task (light blue trace) and the variation between eyes open (green trace) and eyes closed (purple trace) with no biology visible.

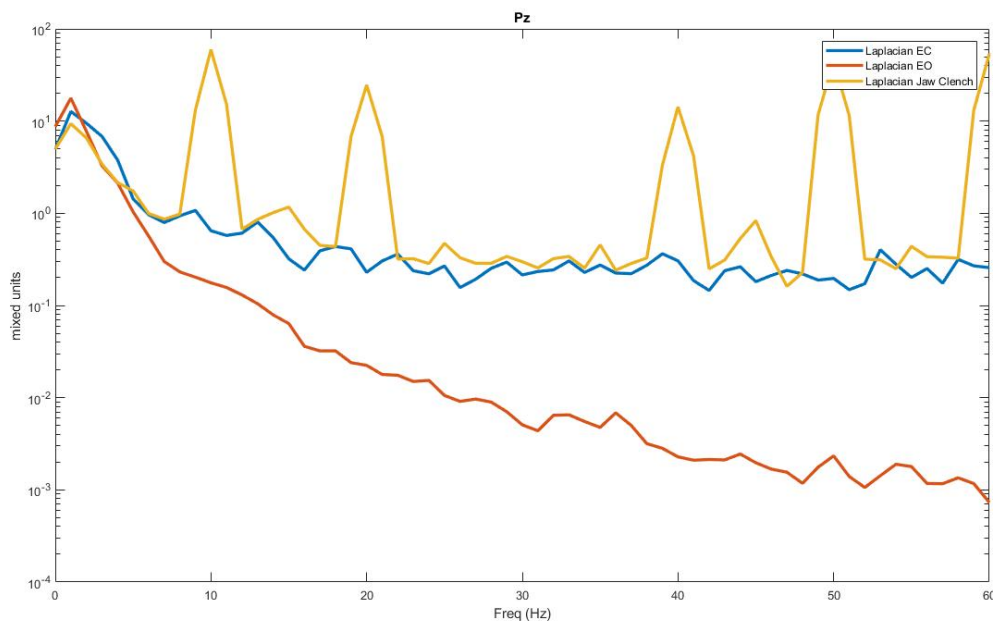


Figure 75. Graph shows Laplacian of EEG at electrode location Pz

In Figure 75, At location Pz, we see the same missing 30Hz harmonic, in the sequence of harmonics every 10 Hz, in the muscle task (yellow trace). There is also no biology seen in either the eyes open (red trace) or the eyes closed (blue trace)

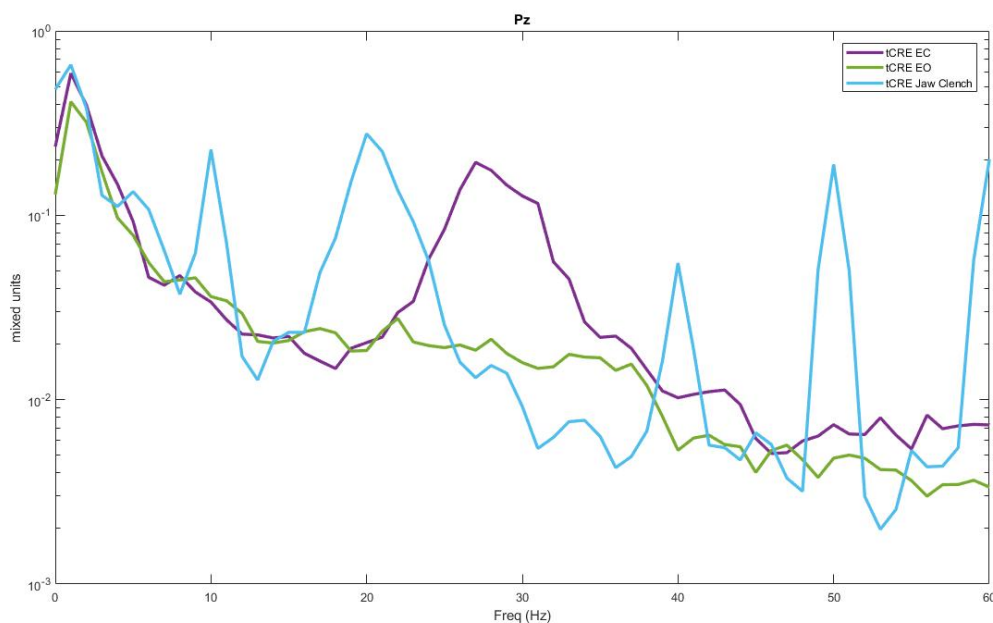


Figure 76. Graph shows tCRE EEG at electrode location Pz

A large variance is seen in the eyes closed task (purple trace) at 30 Hz, in Figure 76, with the missing harmonic at 30Hz in muscle task (light blue trace). The muscle task is also suppressed and in proximity to the baseline tasks.

5.6.2. 20 tCRE electrodes with foam cap used on subject with short, stiff curly hair

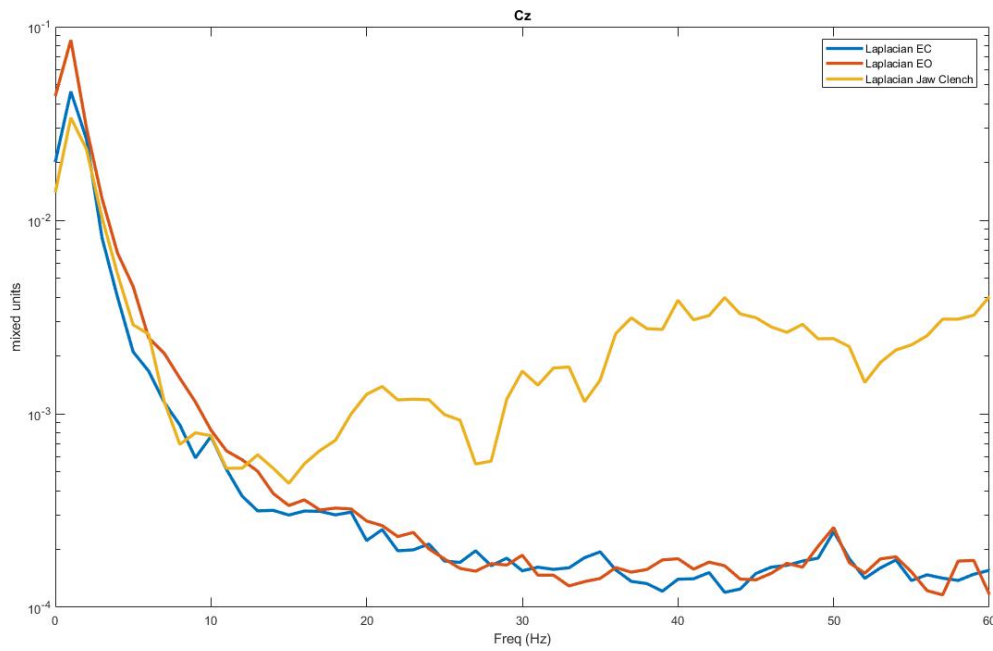


Figure 77. Graph shows Laplacian of EEG at electrode location Cz

The patient with short, stiff, curly hair showed better compatibility with the foam cap, the laplacian of the EEG at Cz shown in Figure 77, gives us a short bump at 10Hz (alpha peak) in the eyes closed phase (blue trace), while there is a muscle divergence seen in the yellow trace (muscle task). The 50Hz mains noise is also seen to be suppressed.

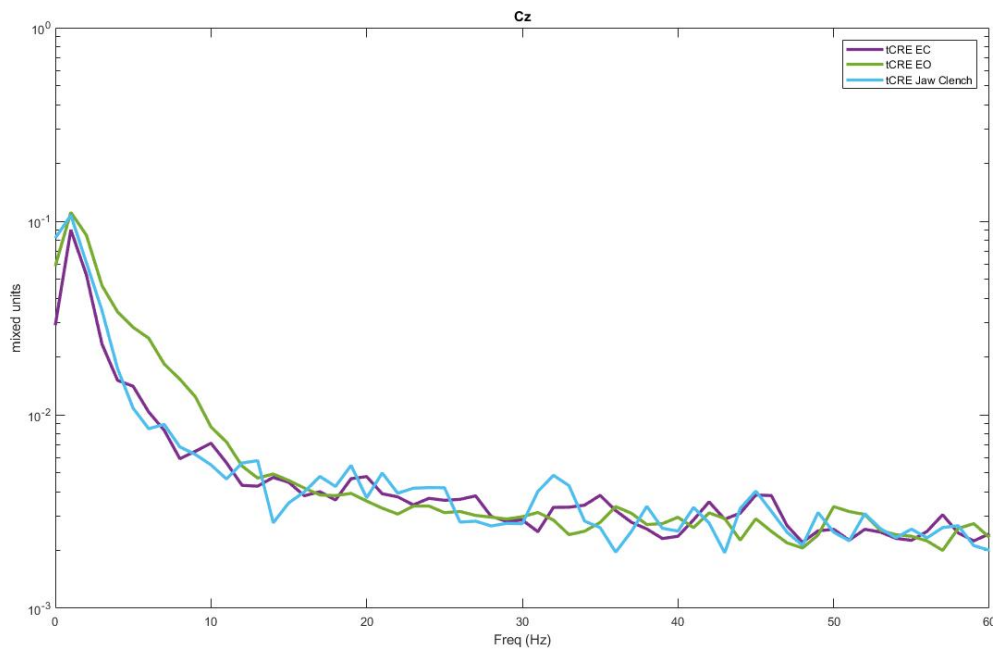


Figure 78. Graph shows tCRE EEG at electrode location Cz

The tCRE version of the EEG shown in Figure 78, shows a spike at 10 Hz (alpha peak), and a suppression of the muscle task (light blue trace).

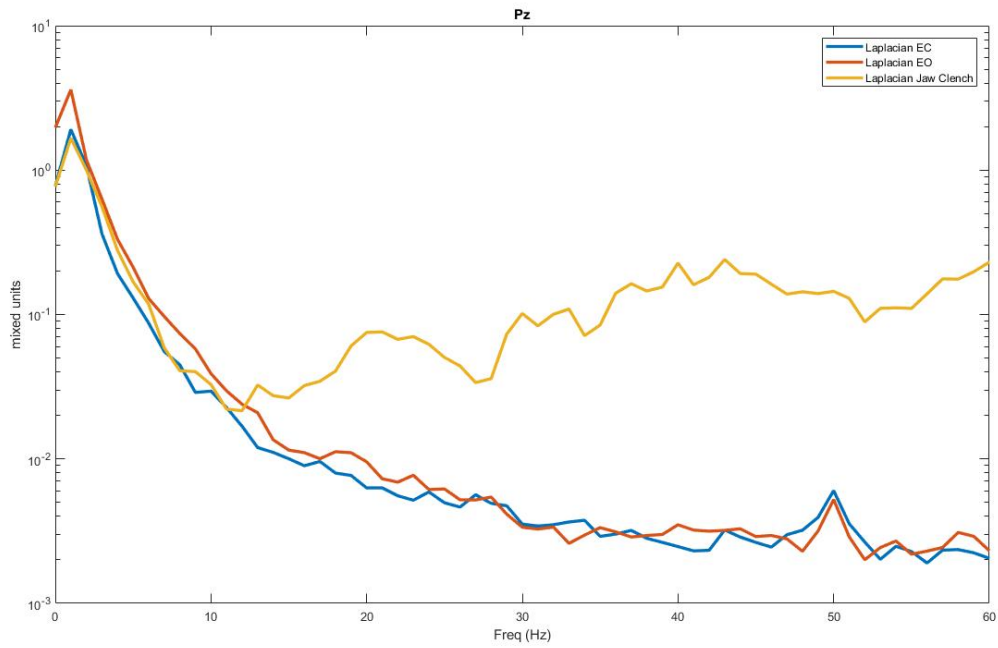


Figure 79. Graph shows Laplacian of EEG at electrode location Pz

The Laplacian version of the EEG at electrode location Pz, as seen in Figure 79, shows absence of a 10 Hz peak (alpha peak) in the eyes closed task (blue trace) but a large divergence in muscle task (yellow trace).

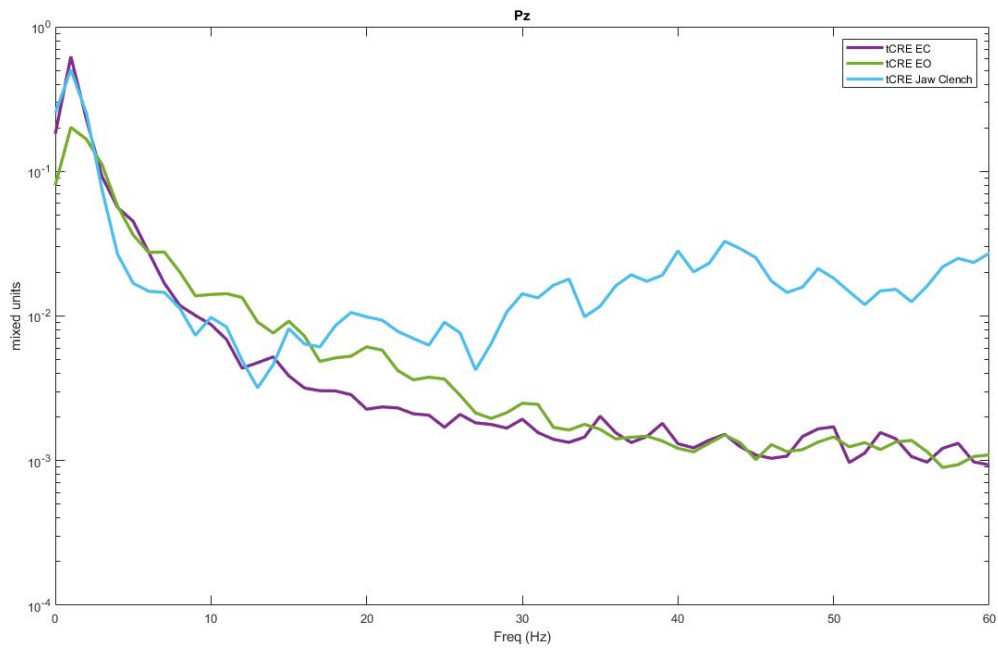


Figure 80. Graph shows tCRE EEG at electrode location Pz

The tCRE EEG of the Pz electrode shows no alpha peaks in the eyes closed task (purple trace) but the muscle divergence from the baseline is seen in the muscle task (light blue trace)

5.7. 20 ring electrodes used 'dry' in the cap

Ring electrodes were placed in the cap with no gel interface. This was done to measure the electrodes ability to acquire signals off the head.

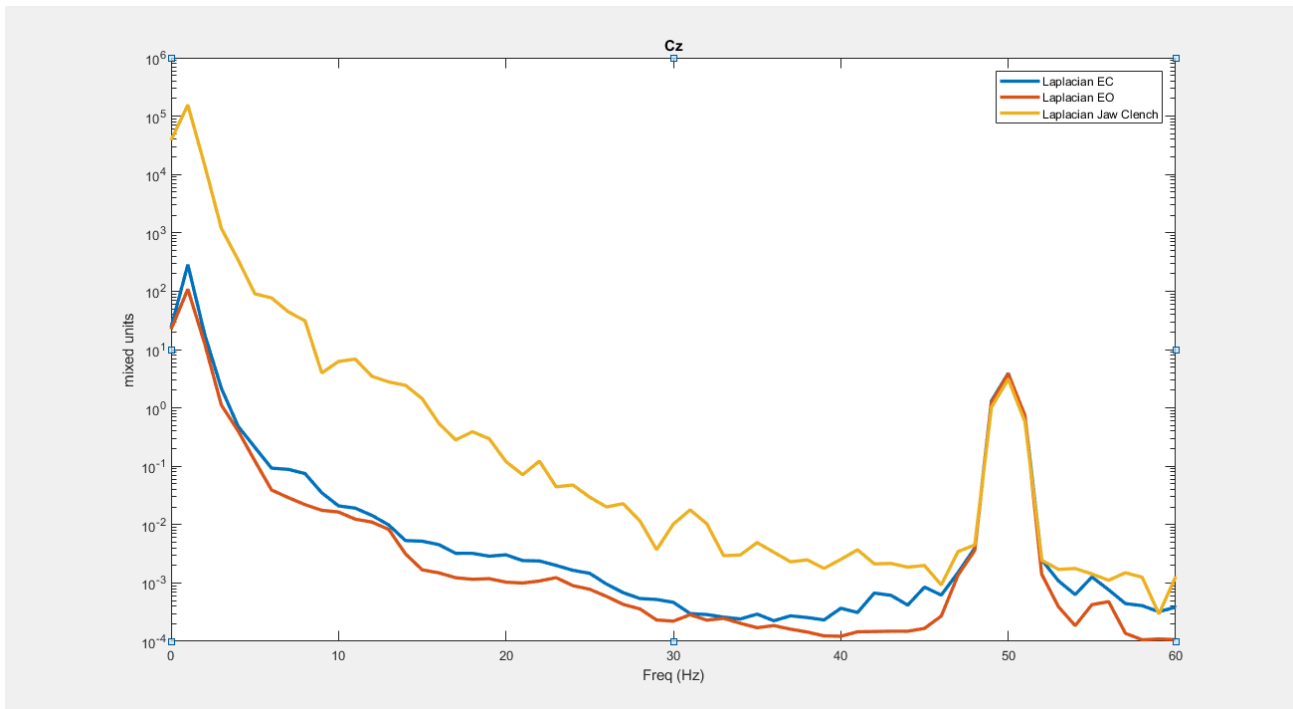


Figure 81. Graph shows Laplacian EEG traces at electrode position Cz

Figure 81 showed the software laplacian of the EEG at Cz, there was no evidence of any biological signal from ring electrodes used 'dry' on the head.

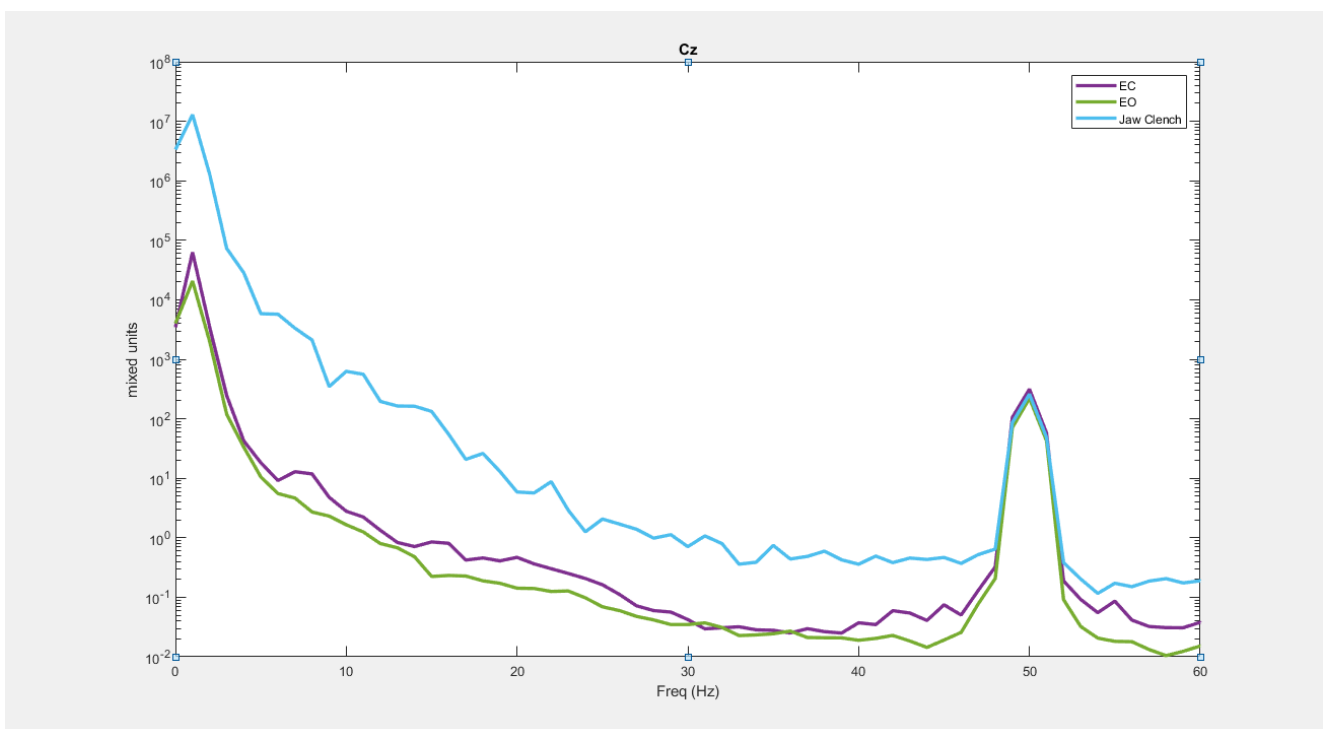


Figure 82. Graph shows ring electrode EEG at electrode location Cz

The electrode EEG at location Cz, seen in Figure 82, showed no biology.

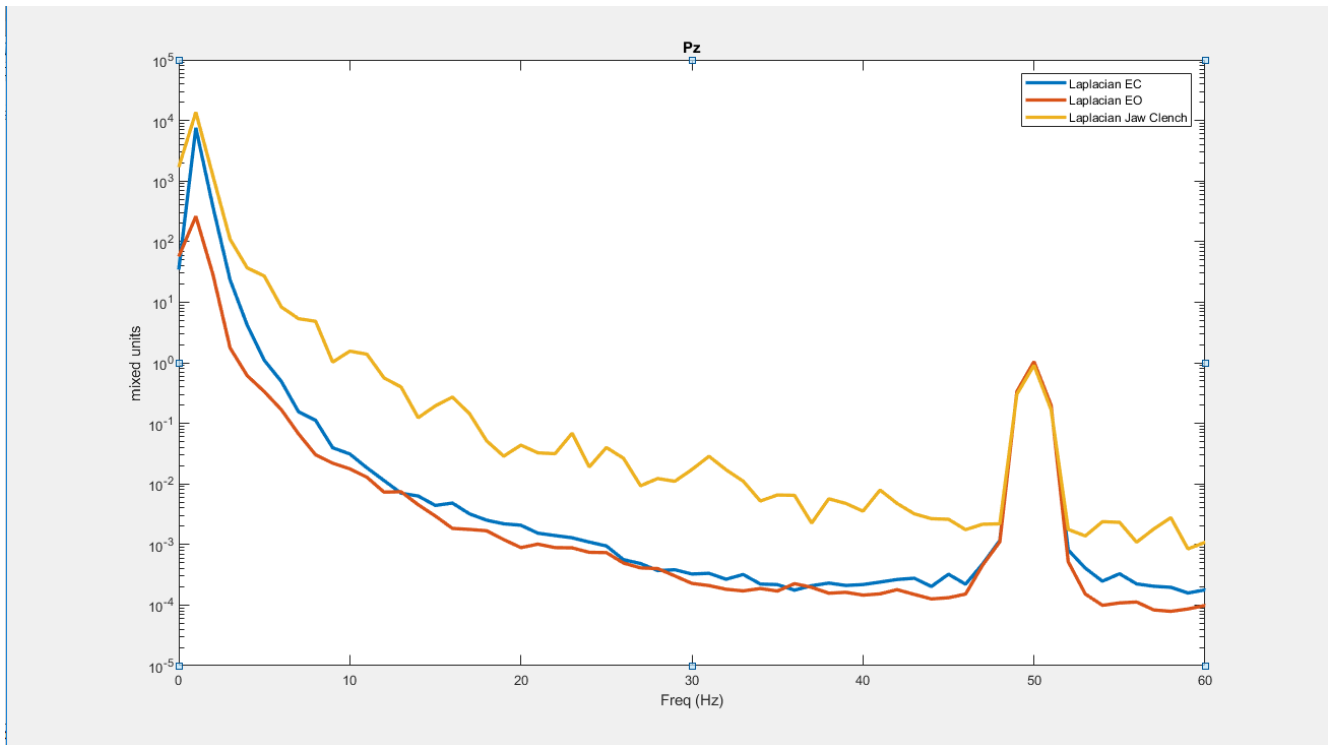


Figure 83. Graph shows ring electrode EEG at electrode location Pz

The electrode at Pz, showed what looks like evidence of muscle (yellow trace) as seen in Figure 83 above, but there was a complete absence of any neural biology.

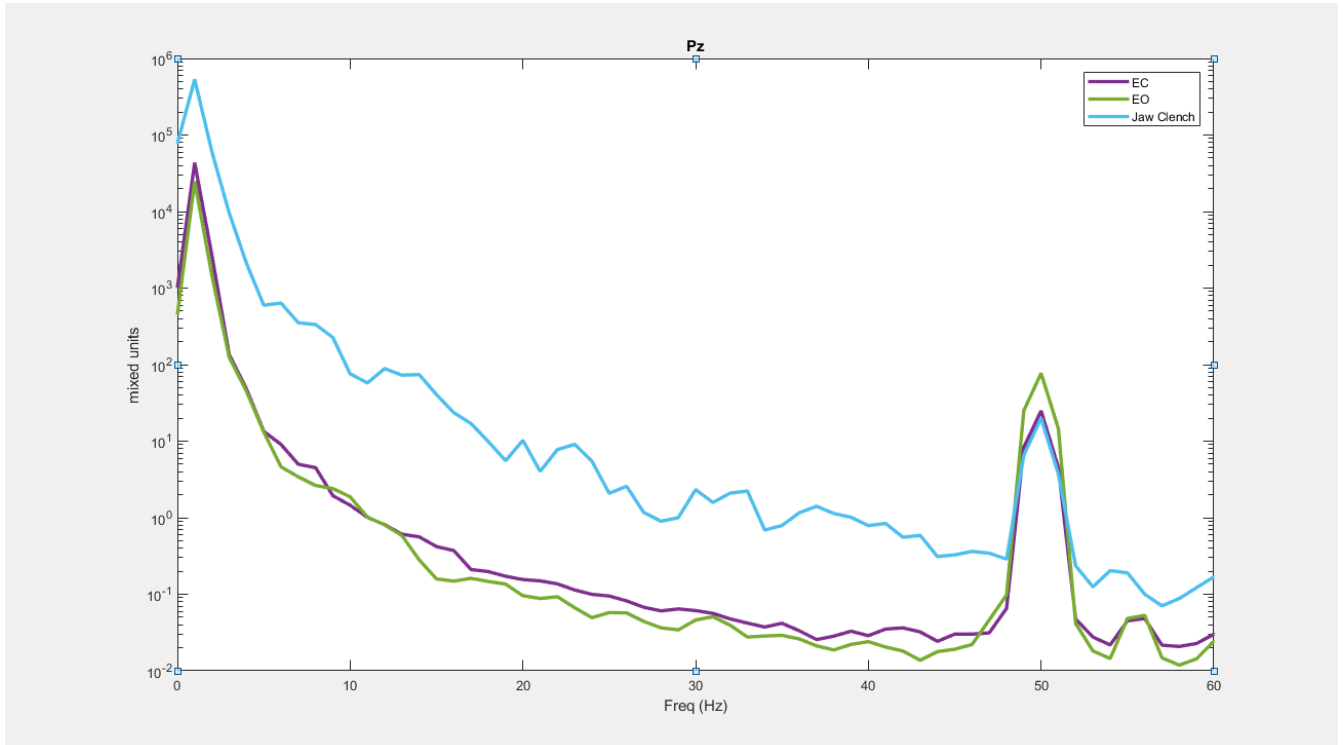


Figure 84. Graph shows ring electrode EEG at electrode location Pz

The electrode EEG at Pz, showed the same possibility of muscle activity (light blue trace), but no neural biology.

5.8. 8 SAHARA electrodes used dry in the cap

5.8.1. SAHARA electrodes used on subject with thick hair

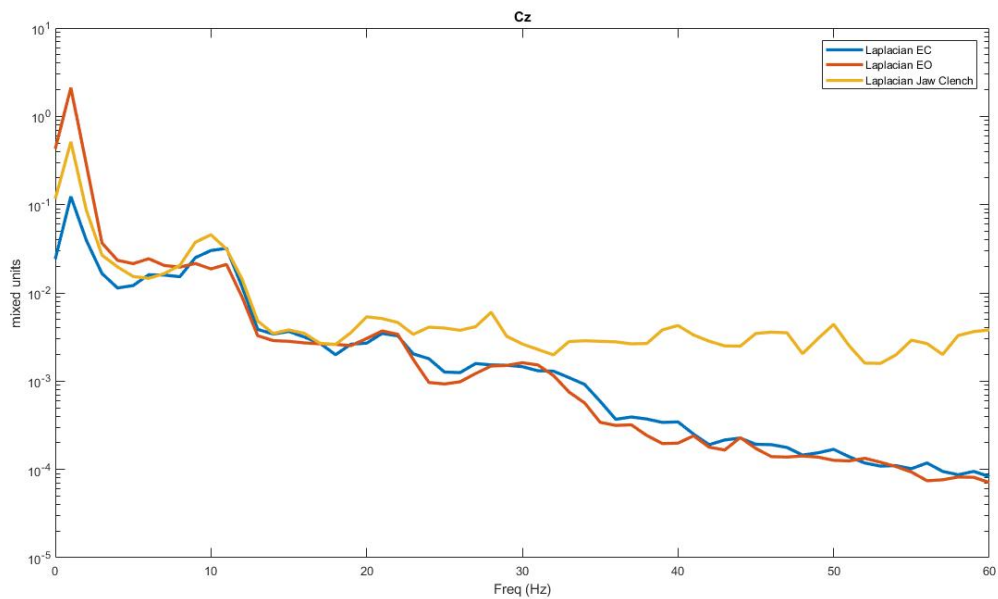


Figure 85. Graph shows Laplacian of EEG at electrode location Cz

As seen in Figure 85, at electrode location Cz, there is a 10 Hz spike seen in the eyes closed (blue trace), but also in the muscle and eyes open task (red trace). There is a slight divergence of muscle (yellow trace) from the baseline.

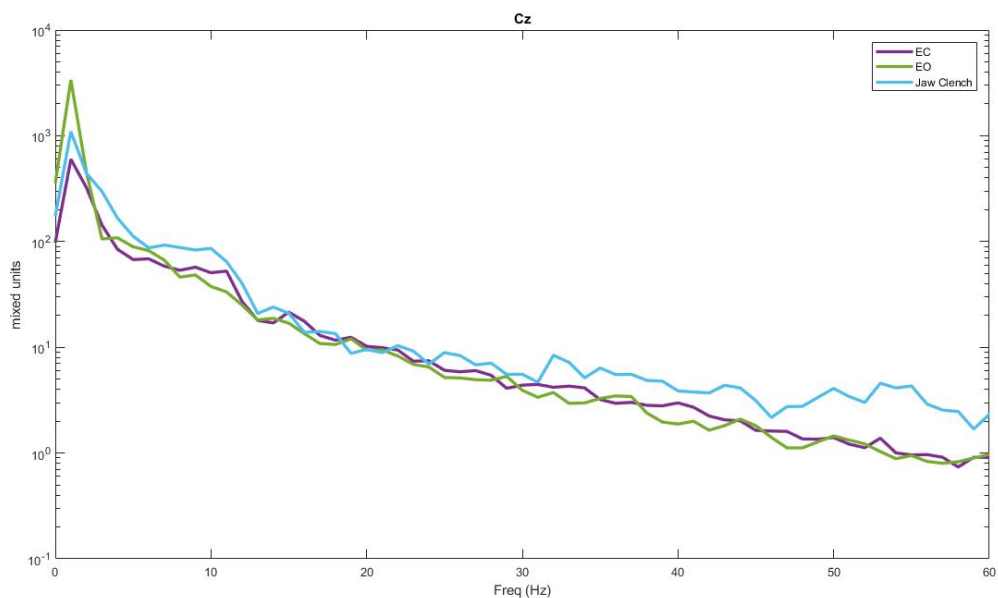


Figure 86. Graph shows SAHARA EEG at electrode location Cz

The SAHARA EEG shown in Figure 86, at Cz, shows a clear spike at 10 Hz (alpha peak) in the eyes closed task (purple trace), but the muscle (light blue trace) divergence is reduced.

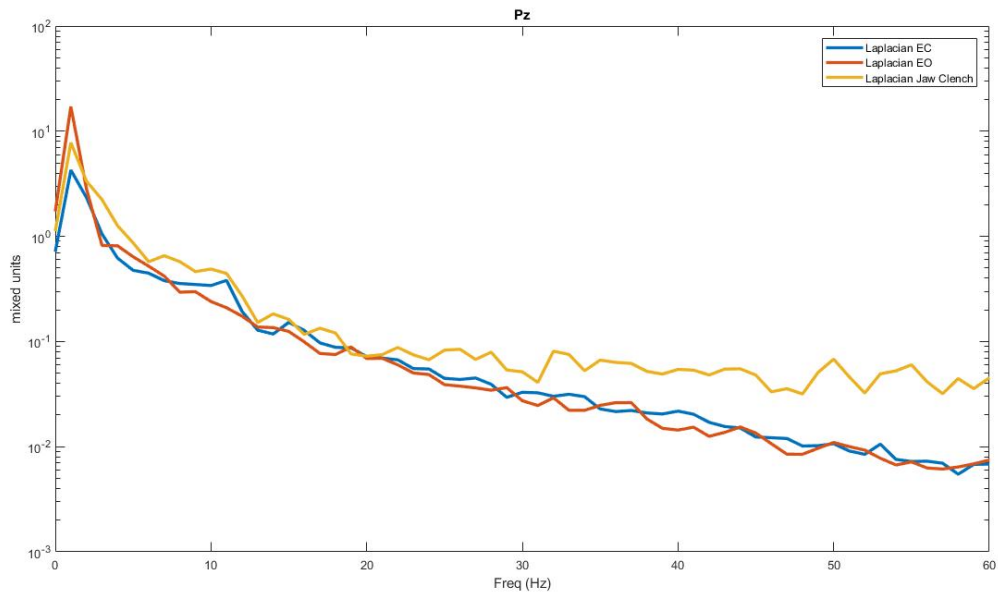


Figure 87. Graph shows Laplacian of EEG at electrode location Pz

The Laplacian of the EEG at location Pz, shows a spike at 10 Hz (alpha peak) in the eyes closed task (blue trace), and a divergence from the baseline of the muscle task (yellow trace)

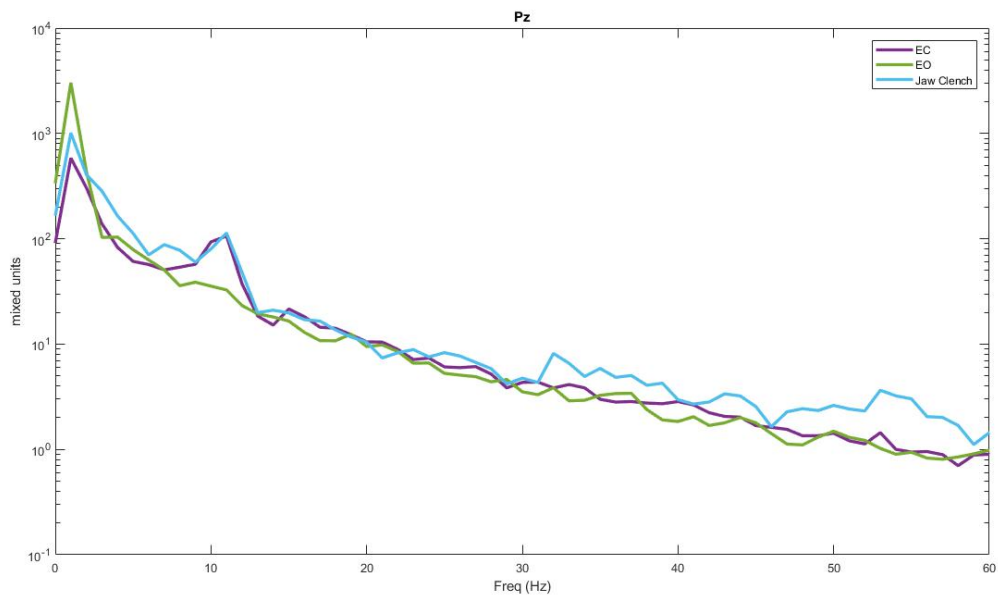


Figure 88. Graph shows SAHARA EEG at electrode location Pz

The SAHARA EEG of Pz, shows a clear and strong spike at 10 Hz (alpha peak) in the eyes closed task (purple trace), but there is very little divergence of the muscle task (light blue trace) from the baseline, as seen in Figure 88

5.8.2. SAHARA electrodes used on subject with short, stiff curly hair

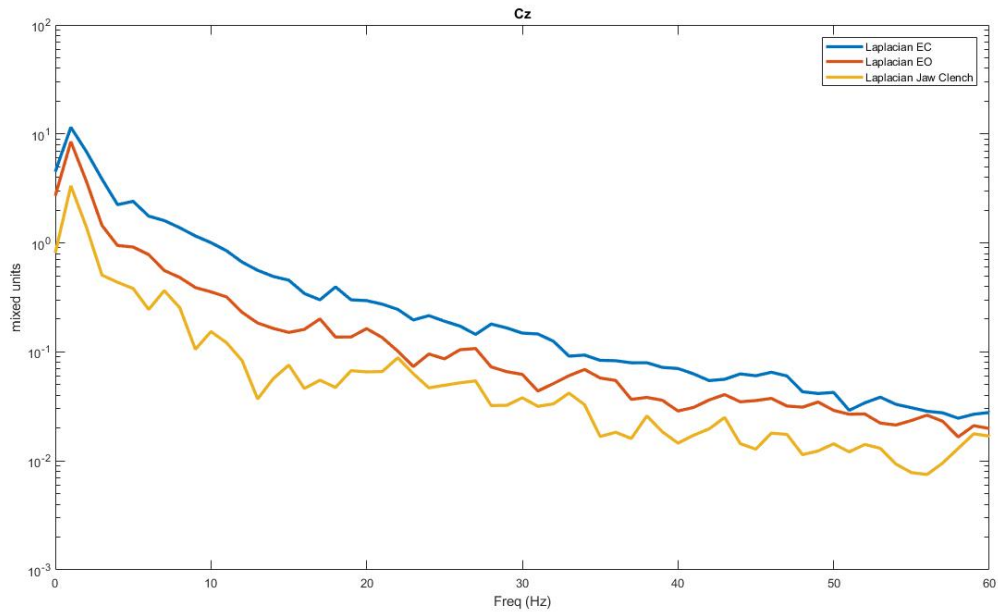


Figure 89. Graph shows Laplacian of EEG at electrode location Cz

Figure 89 shows us no evidence of any sort of biology at electrode location Cz. The muscle task (yellow trace) is seen to be lower than the baseline.

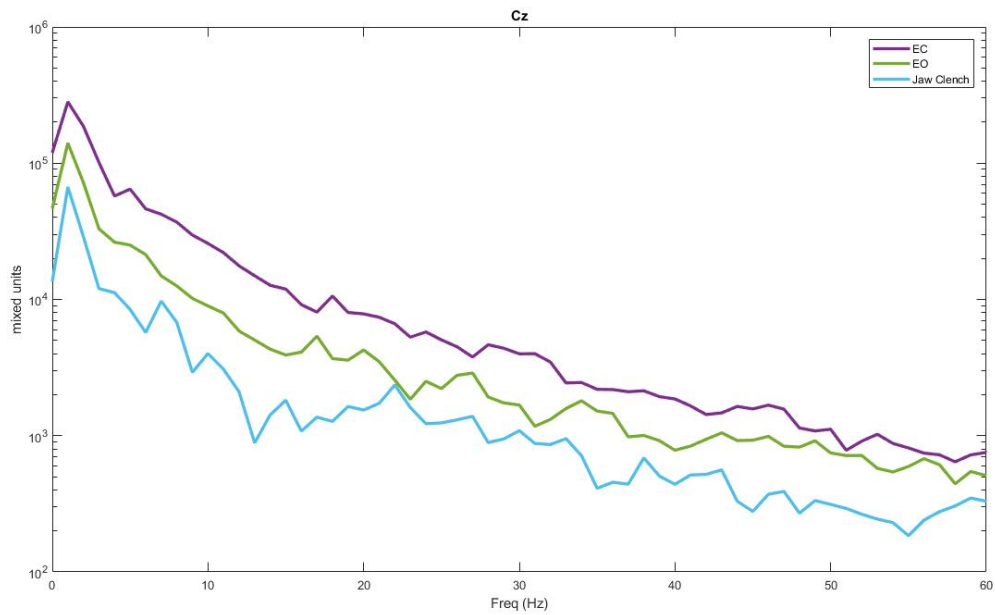


Figure 90. Graph shows SAHARA EEG at electrode location Cz

Figure 90 shows no evidence of biology at electrode location Cz and shows muscle task (light blue trace) lower than the baseline tasks.

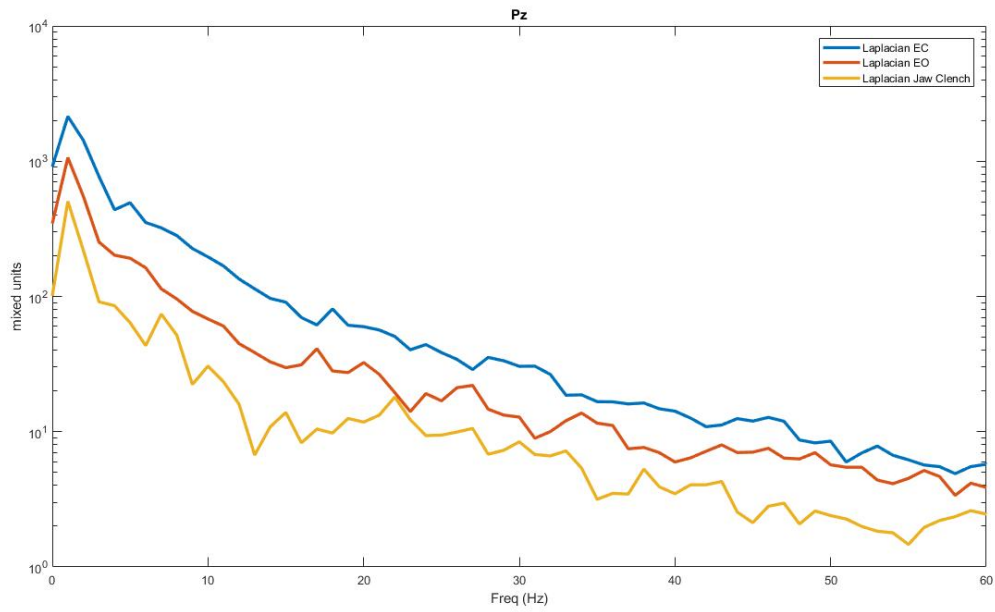


Figure 91. Graph shows Laplacian of EEG at electrode location Pz

Electrode location Pz, shows us no evidence of biology as seen in Figure 91, with the muscle task (yellow trace) seen below the baseline tasks.

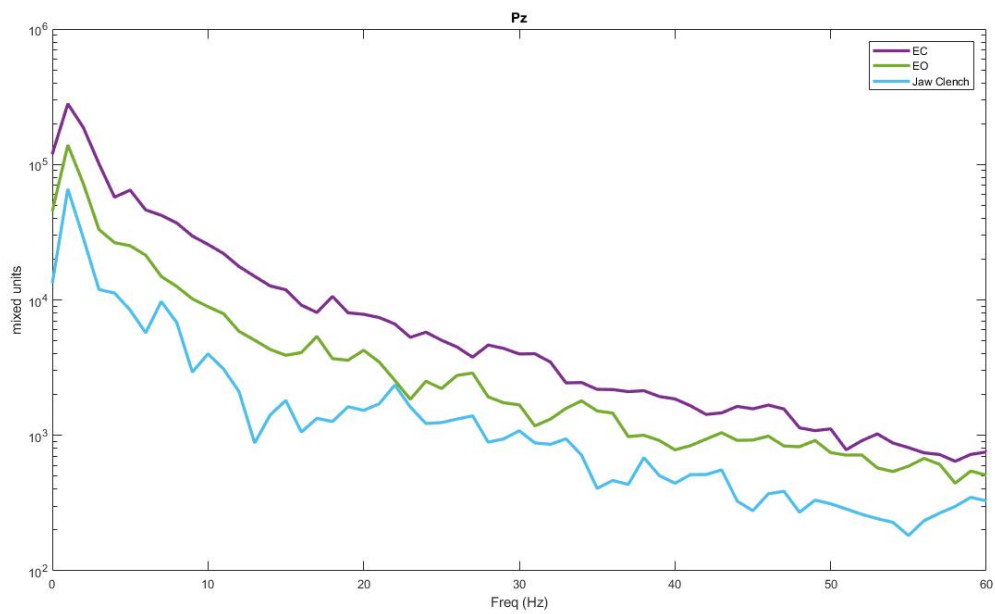


Figure 92. Graph shows SAHARA EEG at electrode location Pz

Figure 92 shows no evidence of biology at electrode location Pz. The muscle is also seen below the baseline tasks.

5.9. 5mm dry comb electrodes used with ring electrodes in cap

Dry comb electrodes were seen to not fit the EEG cap perfectly and showed movement from electrode location when tasks were run. This prompted the combination of dry comb electrodes with the 'wet' ring electrodes being used 'dry'.

5.9.1. Dry comb electrodes with ring electrodes used on subject with thick hair with lights on

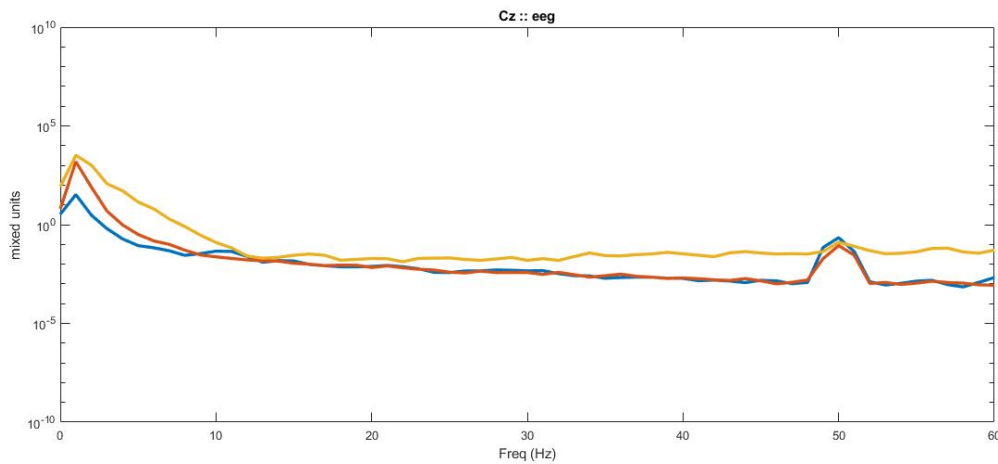


Figure 93. Graph shows Laplacian of EEG at electrode location Cz

Figure 93 shows a slight bump at 10Hz (alpha peaks) in the eyes closed task (blue trace), while also showing a divergence of the muscle task (yellow trace) from the baseline tasks.

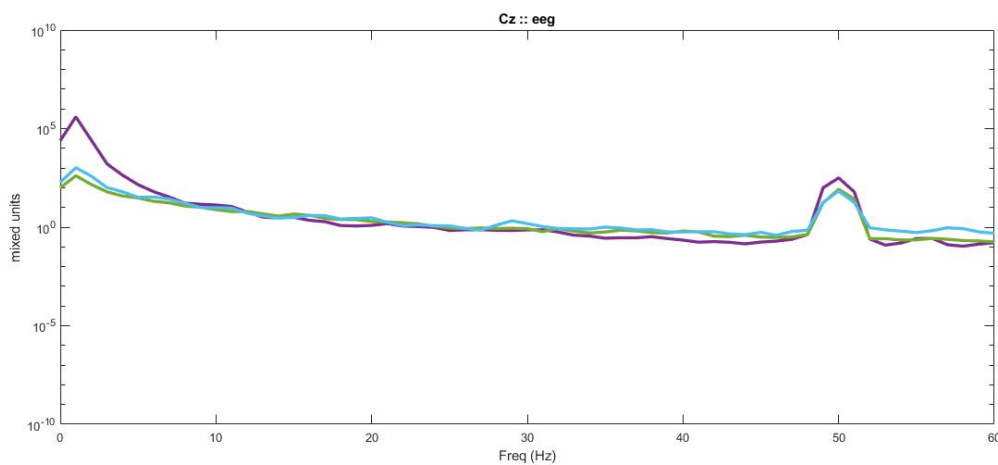


Figure 94. Graph shows electrode EEG at electrode location Cz

The tCRE EEG at electrode location Cz, shows very little evidence of biology, with the muscle divergence (light blue trace) also seen to be reduced.

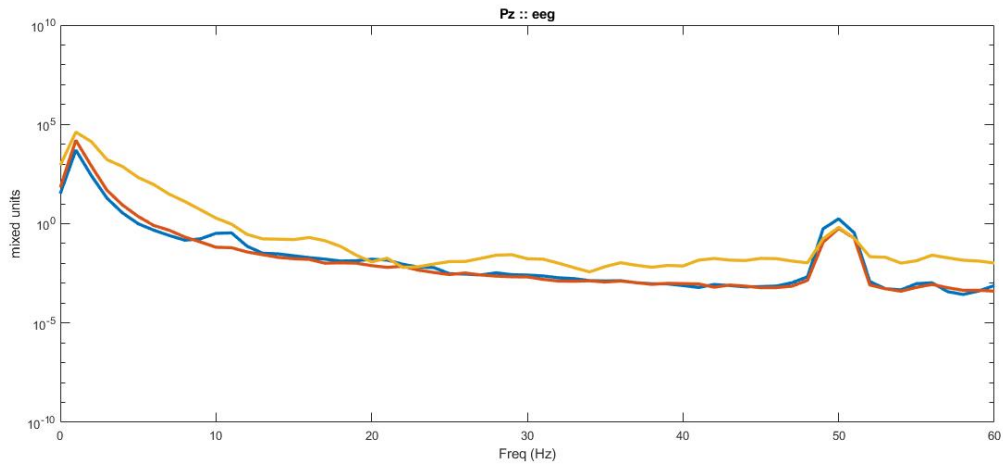


Figure 95. Graph shows Laplacian of EEG at electrode location Pz

The graph in Figure 95, shows the electrode location Pz. There is a clear spike at 10 Hz (alpha peak) in the eyes closed task (blue trace). There is a slight divergence seen in the muscle task (yellow trace) from the baseline.

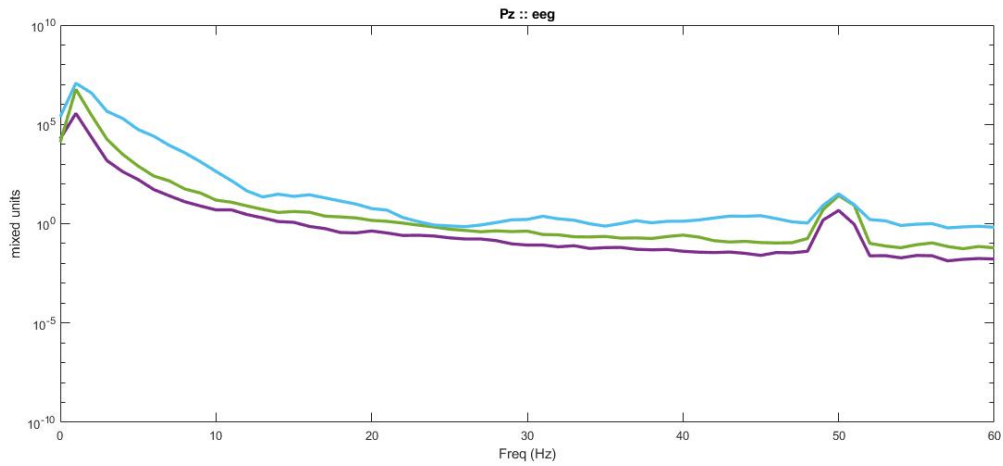


Figure 96. Graph shows electrode EEG at electrode location Pz

Figure 96 shows us the absence of any neural biology at electrode location Pz in the tCRE electrodes. There is a muscle biology (light blue trace) seen with the divergence away from the baseline tasks.

5.9.2. Dry comb electrodes with ring electrodes used on subject with thick hair with lights off

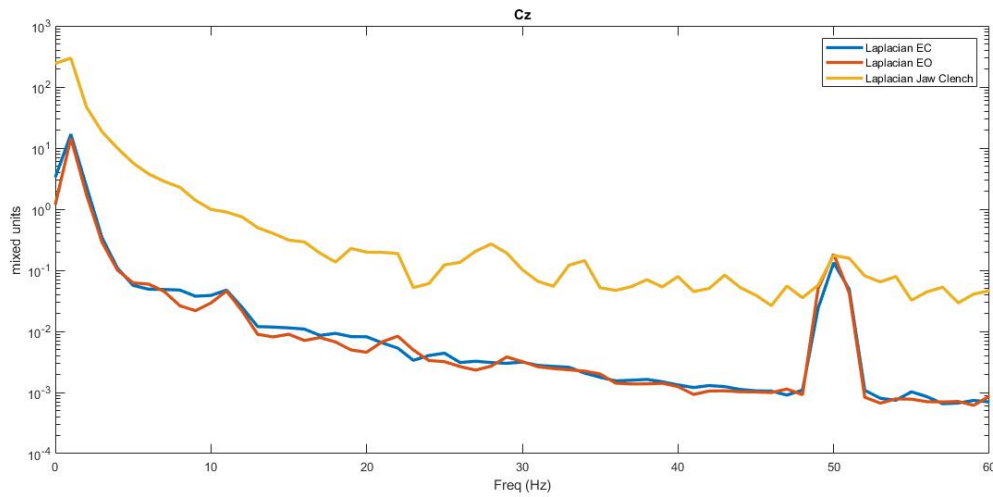


Figure 97. Graph shows Laplacian of EEG at electrode location Cz

In Figure 97, there is a 10 Hz spike seen in the eyes closed (blue trace) and eyes open task (red trace). The muscle task (yellow trace) shows a large variation but very little divergence.

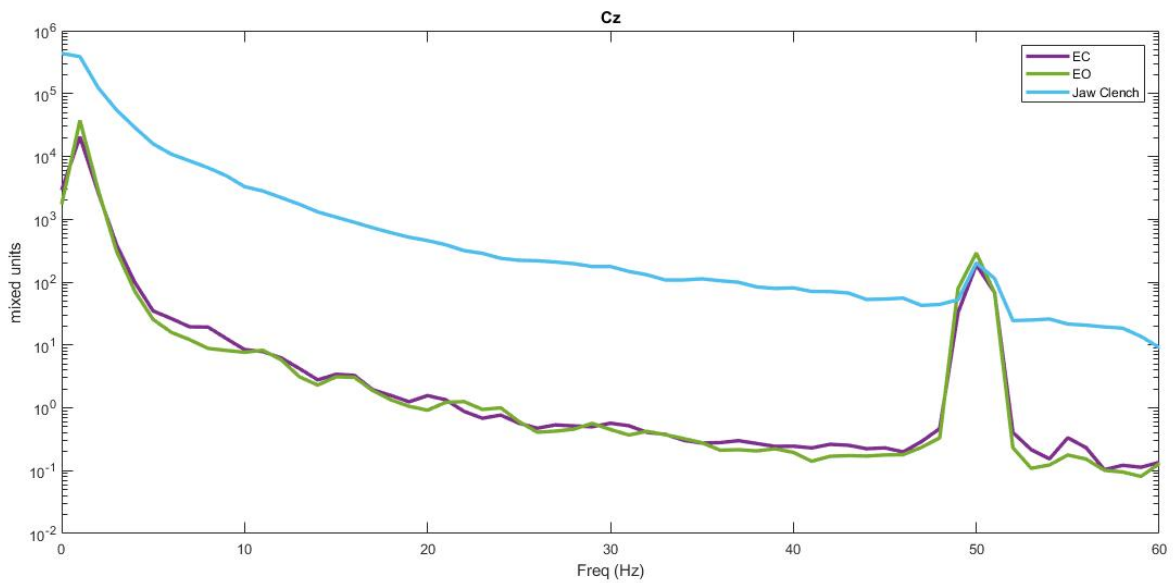


Figure 98. Graph shows electrode EEG at electrode location Cz

In Figure 98 at electrode location Cz, the electrode EEG shows very little neural biology and an amplified muscle task (light blue trace)

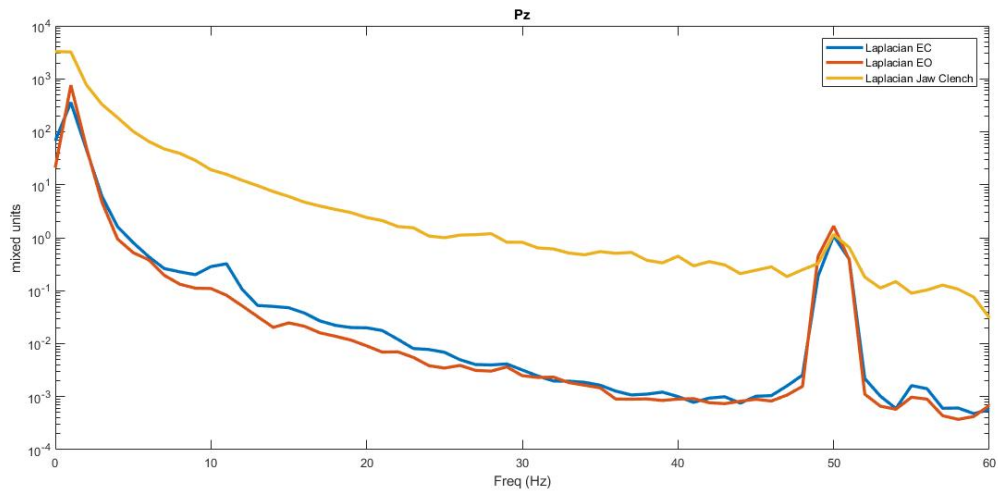


Figure 99. Graph shows Laplacian of EEG at electrode location Pz

At electrode location Pz, as seen in Figure 99, the laplacian version of the EEG shows us a 10Hz spike (alpha peak) in the eyes closed task (blue trace), and a large divergence of the muscle task (yellow trace) from the baseline.

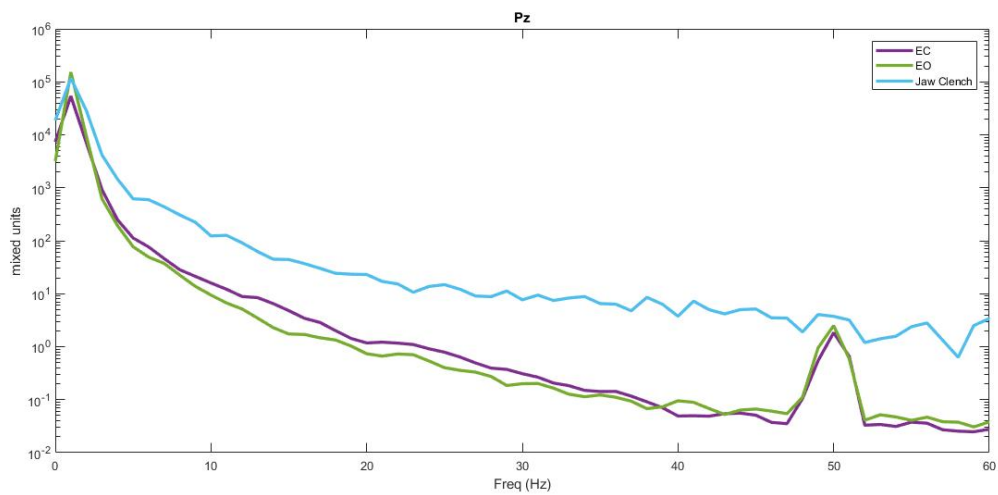


Figure 100. Graph shows electrode EEG at electrode location Pz

Figure 100 shows the absence of neural biology in the electrode EEG, but shows evidence of muscular biology (light blue trace) diverging from the baseline tasks.

5.9.3. Dry comb electrodes with ring electrodes used on subject with short, stiff curly hair

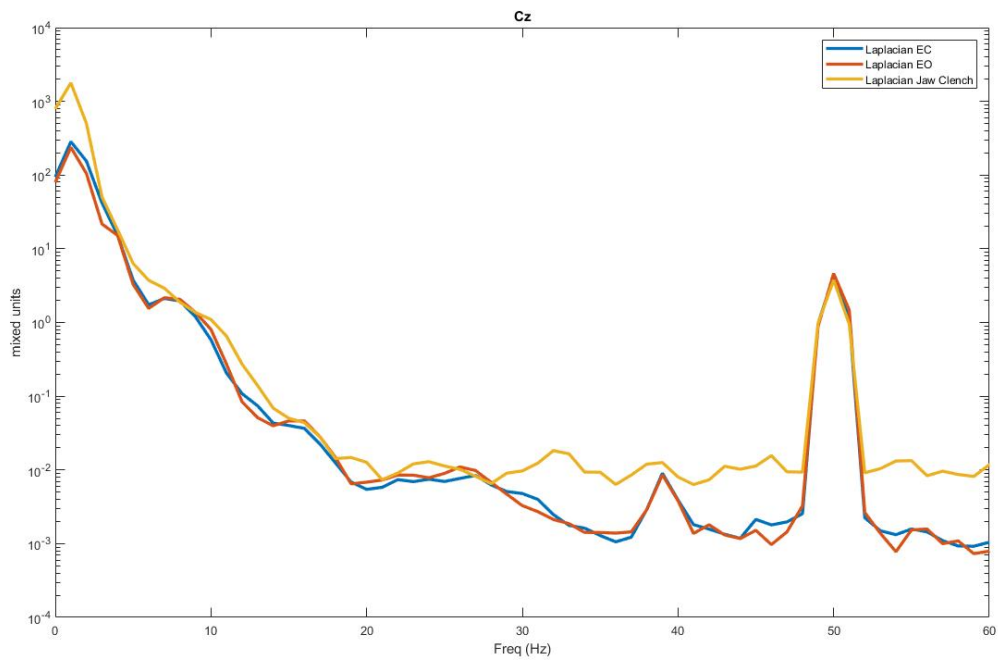


Figure 101. Graph shows Laplacian of EEG at electrode location Cz

Figure 101 shows Laplacian of EEG acquired from electrode at Cz. It shows the absence of an alpha peak, but the divergence of muscle task (yellow task) from the baseline task. There is also an unusual spike at 39Hz seen.

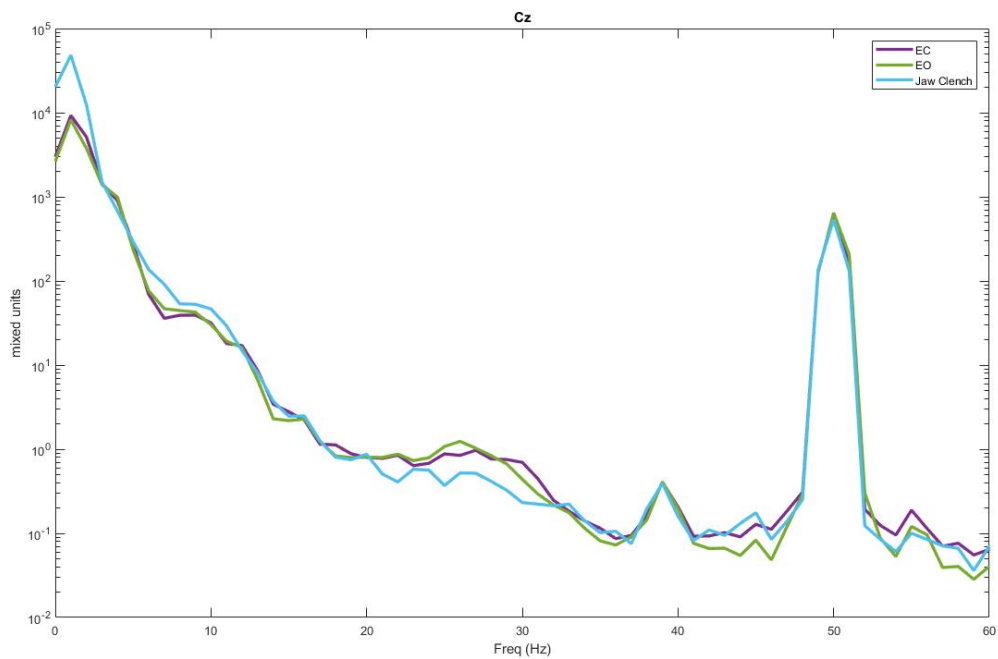


Figure 102. Graph shows electrode EEG at electrode location Cz

The electrode EEG seen in Figure 102 of electrode at Cz, shows a slight bump at 10Hz across all 3 traces. The muscle divergence is absent and an unusual spike at 39Hz is seen.

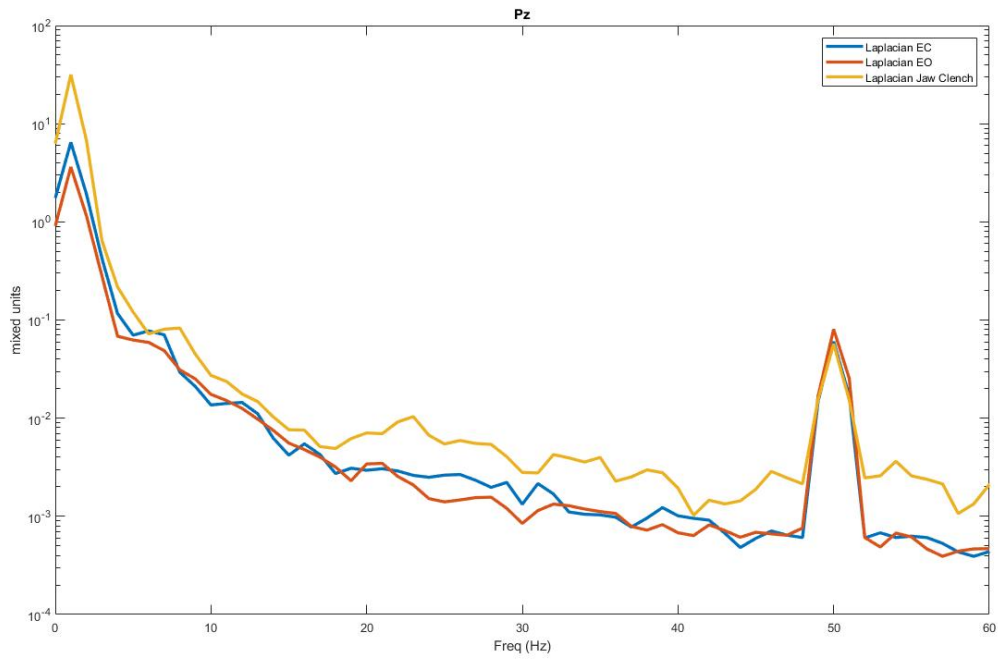


Figure 103. Graph shows Laplacian of EEG at electrode location Pz

Figure 103 shows evidence of muscle divergence (yellow trace) but no evidence of an alpha peak at 10 Hz. The 39Hz spike is absent in the laplacian version of the EEG at Pz.

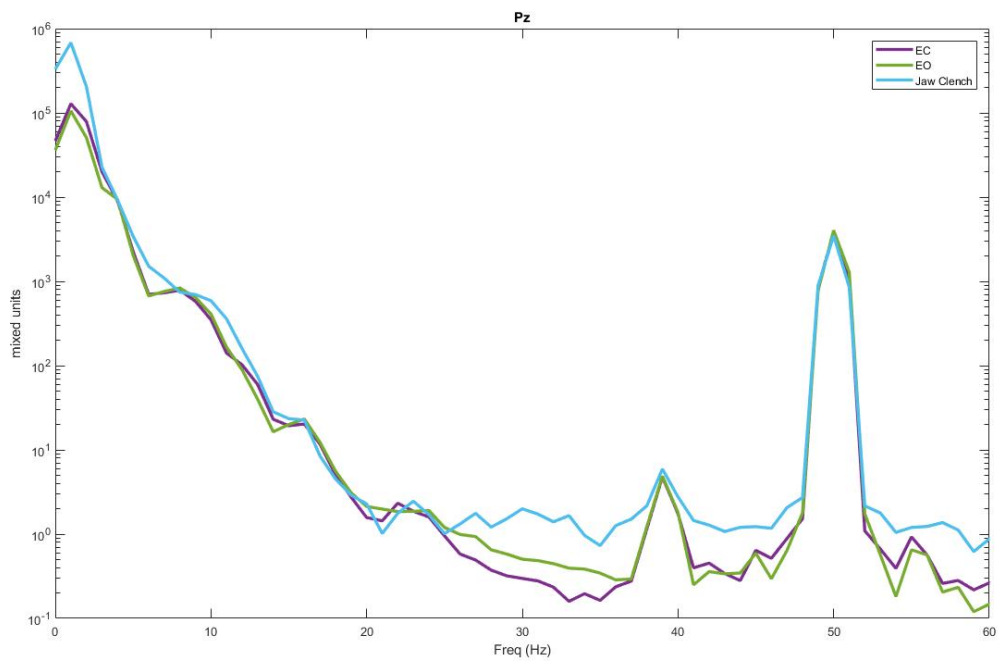


Figure 104. Graph shows electrode EEG at electrode location Pz

Figure 104 shows electrode EEG at location Pz, there is no clear indication of the alpha peak, but muscle divergence (light blue) is seen, and the unusual spike at 39Hz is seen again.

6. Discussion

The Berger effect as applied to the experiments conducted, refers to the relational variation of muscle effects in the acquired signal between the software laplacian of EEG signals and the hardware Laplacians from the tCREs. A colour scale is used to improve visualization of the effect.

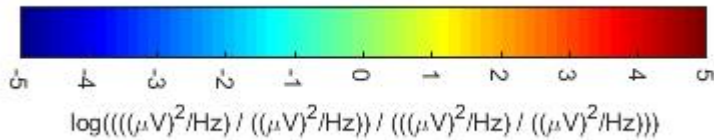


Figure 105. Figure shows colour bar for Berger effect graphs used for analysis

As seen in Figure 105, the extremes represent excess or no muscle effect. The extreme right (dark red) represents a multi-fold increase in the effect of muscle on the acquired signal, when compared to EEG signals acquired from the electrodes, that may overshadow the neural bio-signal required. The extreme left (dark blue) represents a drop in muscle effect when compared to EEG signals acquired from the electrodes, which may help justify the use of software Laplacian to extract signals of interest. Due to the inherent ability of the tCREs to acquire Laplacian signals, we expect the range of the Berger effect with respect to the tCRE electrodes to be within the -1 to 1 range (light blue to yellow). If the Berger effect is seen to be in the dark blues (extreme left), it implies that the tCREs have a large muscle presence in the acquired signal, which is absent in the software laplacian of EEG. Similarly, if the Berger effect is seen to be in the dark reds (extreme right), it means the tCREs have negated a large amount of muscle which even the software laplacian has been unable to accomplish.

The main parameter used to define successful neural bio-signal acquisition for these experiments is the presence of alpha peaks. Alpha peaks are seen in the range of 8-12 Hz, but usually occur at 10 Hz. These peaks are produced when the participant closes their eyes. This effect is produced in the occipital regions of the head (back of the head), and is an indicator of functioning of the visual cortex, when no sensory input is inbound. With the detection of these waves being possible over a lower range of the head when tCREs are used as compared to when passive ring electrodes (most common) are used, the presence of alpha peaks alone cannot be used as an indicator for forward located electrodes (Fz/FCz/Cz). This lower range is due to the claims by the inventors of localization of the tCRE electrodes due to their functioning ability to detect current density.

To avoid this, the shape of the Laplacian graph is also taken into account. The software laplacian of the passive ring electrodes used in the first electrode are taken as a baseline, in order to visually compare and analyse the shape assumed by acquired laplacian of EEG. This allows us to disqualify signals which do not conform to traditional shapes but show a peak/spike at 10Hz, when laplacian of EEG is acquired.

6.1. 20 tCRE electrodes with 108 passive wet electrodes

The 20 tCREs replaced 20 central passive wet electrodes in the central locations in the head as seen in the montage in Figure 40. EEGs taken from electrodes at locations, F3, C4 and P3, showed that a single tCRE electrode could acquire EEG data from the scalp without the need for multiple electrodes. As seen in Figure 41, the tCRE version of the graph shows no alpha peaks, as compared to the emulated software laplacian version. This is attributed to the highly localized ability of the tCREs to acquire signals, which results in signals beyond its range being negated. This means that the tCREs places away from the back of the head will not pick up alpha peaks like ordinary electrode systems. The same is seen in Figure 42, where the alpha peak spike is pronounced in the software laplacian version of the EEG, but suppressed in tCRE EEG. Comparing EEG at location F3 and C4, we see the pronounced difference in the muscle detected by the tCREs. In C4, the muscle detected shows a large deviation from the baseline eyes closed and eyes open tests, but in F3, the deviation is average. In Figure 43, at P3, closer to the occipital region of the brain, we see the alpha spike starting to be detected by the tCREs (purple trace) and the deviation of the muscle from baseline is suppressed again. Additionally, EEGs from lateral electrode locations showed no special variations. The difference in muscle variation seen comparatively between software laplacian of EEG and the tCRE hardware laplacian is very positive for our aim of reducing effects of muscle on acquired signal. The only negative seen is the reduction in amplitude of the tCRE signal, which is of about 100 times smaller than the software laplacian. EEGs taken from other locations at the central locations of the head are shown in Appendix B

From Figure 106, we see that the relative muscle in software laplacian EEG compared to tCRE EEG is seen in the yellow spectrum of the colour-bar. This tells us that the muscle seen in software laplacian EEG is higher than that seen in the tCRE EEG, which shows us that the tCREs do a stellar job reducing muscle in the signal acquired.

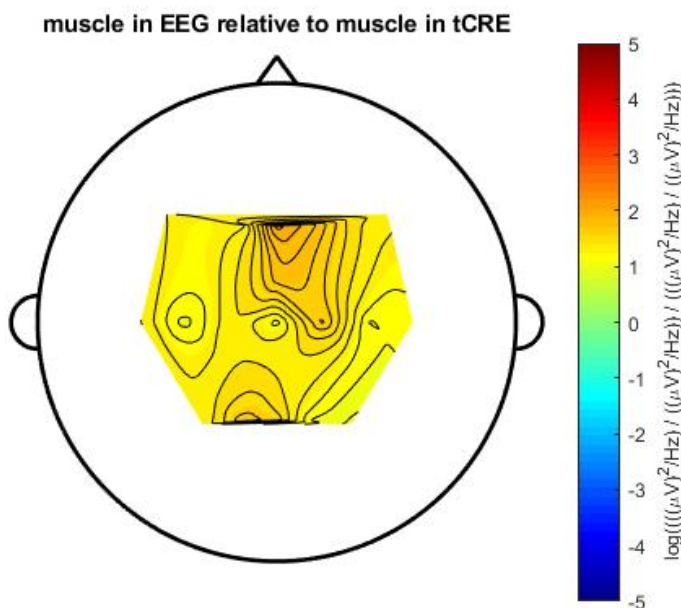


Figure 106. Figure shows the relative muscle in the laplacian EEG to that in the tCRE EEG, the colour-bar is a scale, where no relative muscle is shown by green, higher relative muscle by yellow through red, and lower relative muscle by light blue through dark blue

6.2. tCRE electrodes periphery test (9 central + 11 peripheral electrodes)

The montage in Figure 44 shows the locations of the tCRE electrodes on the head. On verifying the efficacy of the tCRE electrodes with the previous experiment, and noticing the suppressed effect of muscle on the tCRE electrodes, the tCREs were then placed peripherally alongside the central locations to compare the acquired signal and the effects of muscle on them with signals acquired more centrally on the head.

6.2.1. tCRE electrode periphery test on subject with thin, wispy hair

The first subject had thin, wispy hair and thus allowed for excellent contact between the tCRE wet electrodes and the scalp. As Figure 45 shows us, the software laplacian version of the EEG at Cz location, acquired biology as expected, with a strong alpha peak and good divergence in muscle from baseline tasks detected. The presence of a strong alpha peak, when the same was vaguely visible in the previous experiment, was attributed to the split of the graphs, allowing the restructuring of the X and Y limits of the graphs, improving resolution. The tCRE EEG on the other hand showed no alpha peaks and a suppressed muscle divergence when compared to the laplacian EEG (Figure 46). A sharp peak is seen at 10 Hz in the muscle task, but absent in the eyes closed task. The participant stated they had their eyes closed during the eyes closed task, thus making the spike in the muscle task an anomaly. Future studies could incorporate visual checks to ensure participants follow instructions and provide physical evidence to assist in determination of neural events.

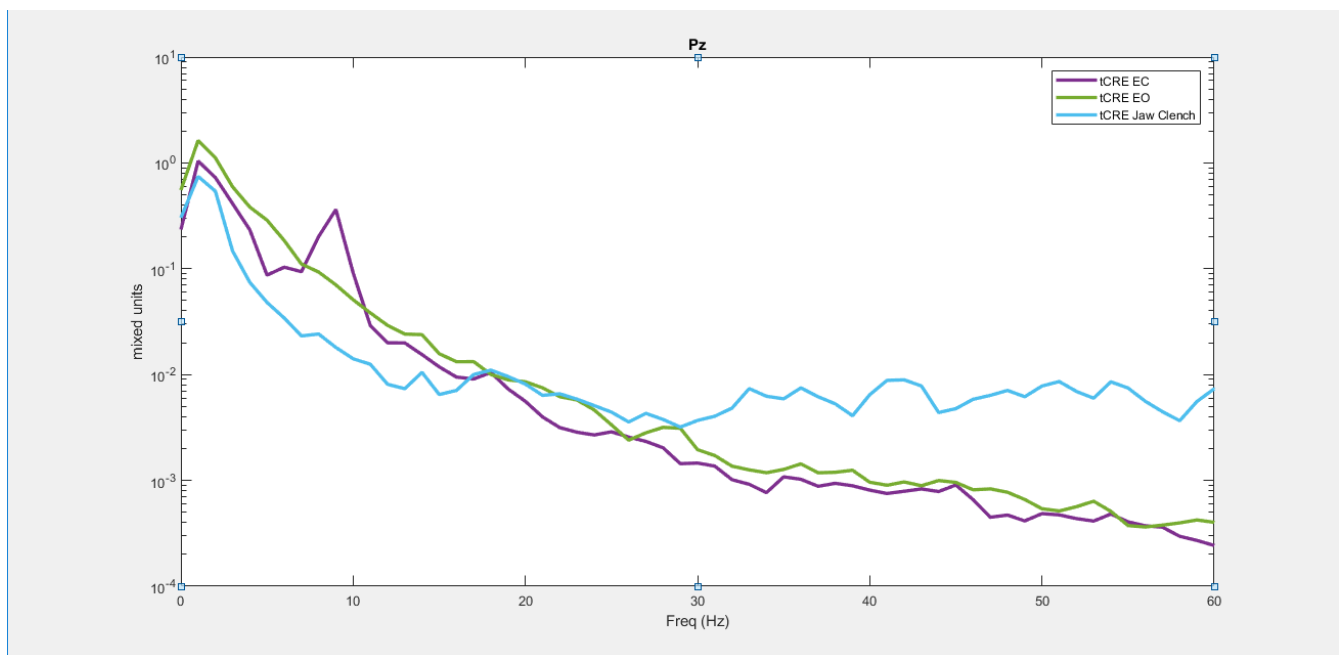


Figure 107. Figure shows tCRE EEG at Pz electrode location

As we move further back on the head, at Pz, (Figure 107), we see that the tCRE is able to pick up alpha peaks, and the muscle is suppressed when compared to laplacian versions of the EEG. A clear separation of the alpha peak and the shape of the graph confirms positive neural signal acquisition.

When the central electrodes were compared to the peripheral electrodes at T7 (Figure 47 & Figure 48), we see that the T7 software laplacian EEG, showed an alpha peak and muscle divergence. The graph showed signs of levelling off earlier than previous experiments had shown. The tCRE EEG showed very little muscle divergence and no alpha peaks. The muscle suppression seen was a positive indicator towards the efficacy of the tCREs in

reducing the effect of muscle even when placed on locations with high muscle activity. This was attributed to the suppression of acquired signal by the tCREs, and the highly localized ability of the tCREs.

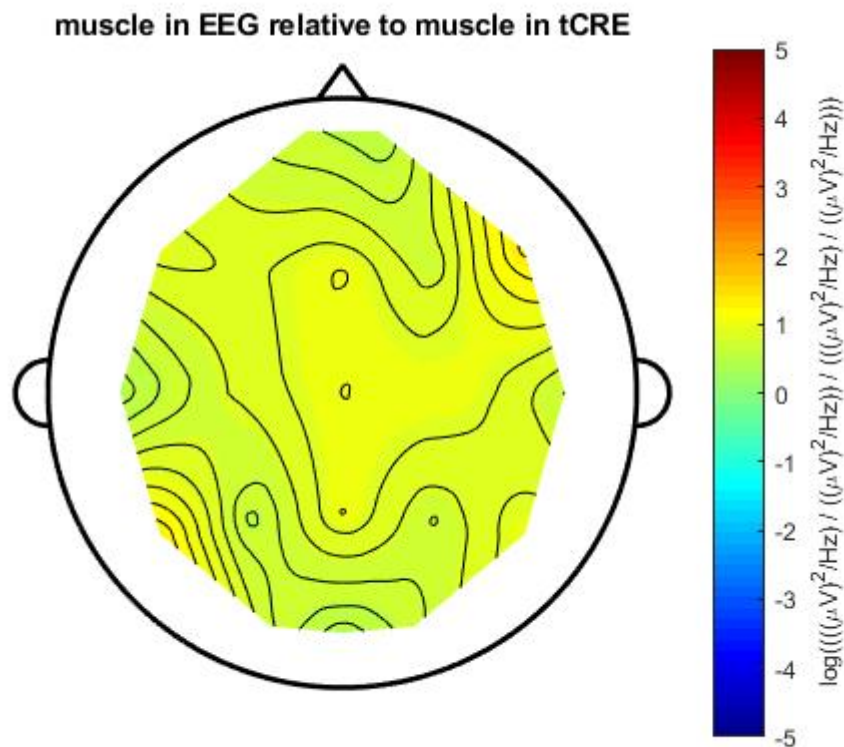


Figure 108. Figure shows relative muscle in software laplacian EEG to the muscle seen in tCRE EEG

The Berger effect seen in the peripheral electrodes remains the same as that seen in the central electrodes. There is no variation seen even with electrodes being placed on muscle. While, Figure 108 does not show the peripheral regions, the nearly constant colour spectrum predicts that there is very little variation laterally, as the colour scheme shows a tendency to move towards 0 (green) which implies reducing muscle variation. This shows that the tCREs might be able to remove muscle satisfactorily in the peripheral regions and can replace traditional software laplacian removing the need for digital computation and extended wait times.

6.2.2. tCRE electrode periphery test on subject with short, stiff curly hair

The subject with short, curly stiff hair showed very good muscle biology but suppressed neural biology even in the software laplacian EEG. Figure 49 and Figure 50 showed the muscle divergence of the software laplacian EEG and tCRE EEG respectively. No alpha peak was seen in either, and the muscle divergence in the tCRE EEG (Figure 50) was negligible. This was attributed to the location of the tCREs as well as the subject's hair, which made connections with the scalp difficult.

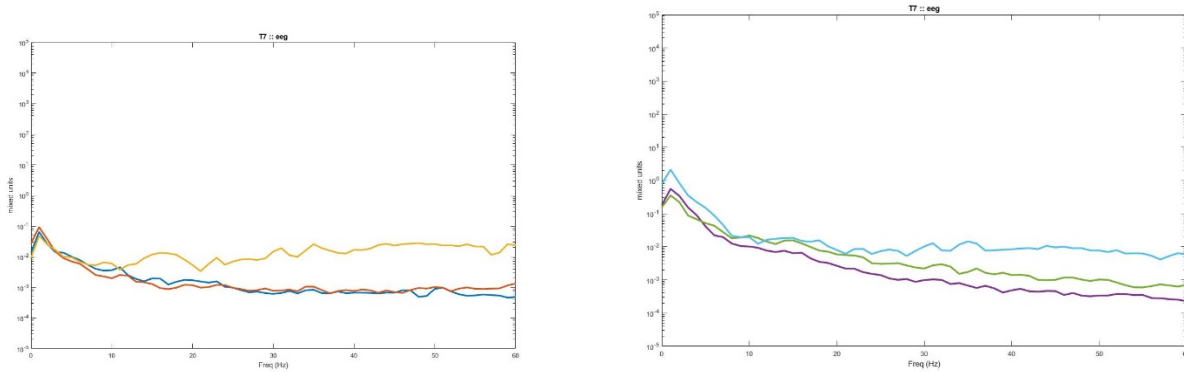


Figure 109. Figures show software laplacian EEG (left) at electrode location T7 and tCRE EEG at electrode location T7 (right)

As seen in Figure 109, the electrode at peripheral location T7, showed better connection due to reduction in volume of hair, this allowed for a better connection with the scalp and the acquisition of a short alpha peak at 10 Hz (blue trace) on the software laplacian EEG (left graph) and the visualization of muscle divergence at the peripherals. This showed that the tCREs were able to suppress or ignore most muscle effects even when placed directly on muscle (T7-T8 electrode locations). There was some suppression of neural data seen, which was attributed to the subject's hair rather than the ability of the tCREs themselves.

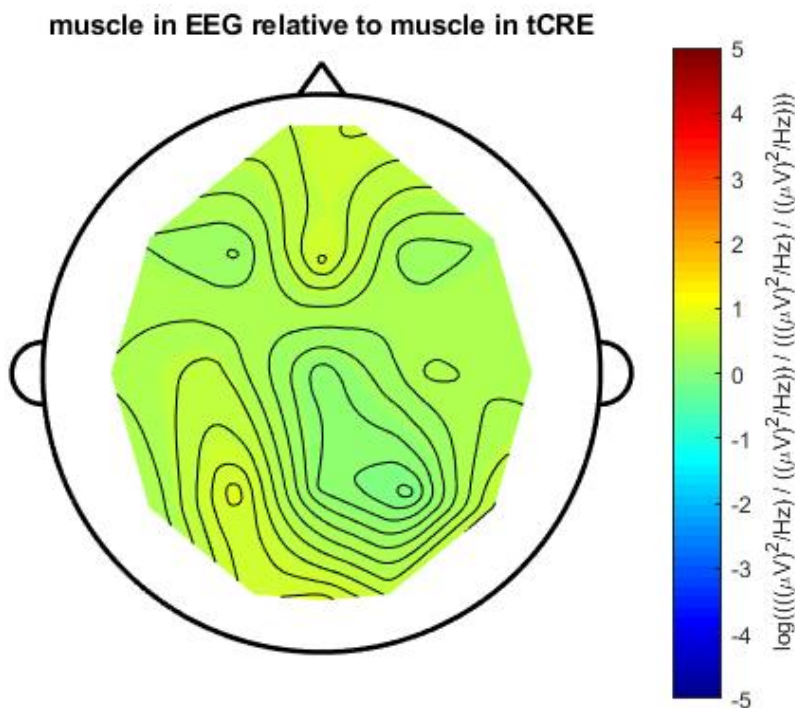


Figure 110. Figure shows relative muscle in software laplacian EEG to that of tCRE EEG

Berger effect seen in subject with short, stiff curly hair varies from the previous experimental subjects. Here we see that the colour spectrum is closer to green than yellow, indicating that the muscle seen in the software laplacian and the tCRE EEG are similar to each other. The yellow tinge seen towards the front and back of the head is predicted to be due to lessening hair volume allowing for better direct connection of the electrode with the scalp.

6.3. 20 tCRE electrodes used 'dry' in the cap

Having seen that the tCRE electrodes worked excellently even when placed on muscle, stress testing for the electrodes was taken further by testing the tCRE electrodes without the gel interface. The 'dry' tCRE electrodes made no contact with the scalp for both subjects and thus showed us very little in the form of neural biology

6.3.1. 20 tCRE electrodes used 'dry' in cap on subject with thick hair

Subject with thick hair prevented any sort of contact being made with the scalp due to the formation of hair-air gap interface between the scalp and the electrode. As seen in Figure 53 and Figure 54, when the tCREs at Cz, were not in contact with the scalp, they showed presence of an increasing harmonic every 10 Hz. The muscle task was also seen to be suppressed excessively in both the software laplacian EEG and the tCRE EEG. Moving further backwards did not help, as the loose cap at the posterior did not improve contact ability of the tCREs. Figure 55 and Figure 56 showed the increasing harmonics every 10 Hz as well.

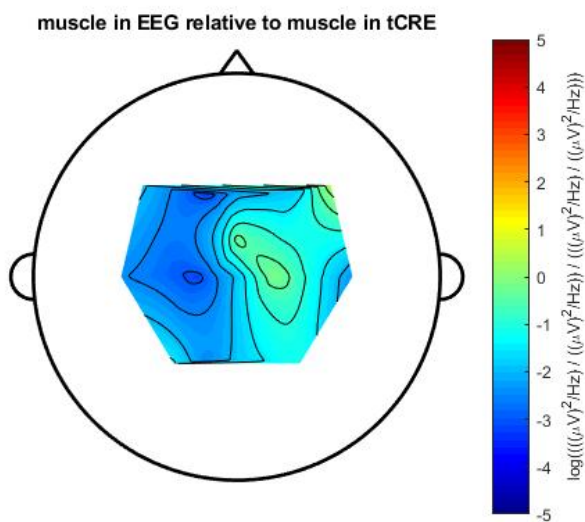


Figure 111. Figure shows muscle in software laplacian EEG to that in tCRE EEG

Figure 111 shows that the muscle seen in software laplacian is less than that seen in the tCRE EEG. This is attributed to the 'dry' usage of the tCREs and their inherent ability to acquire signal in difficult situations.

6.3.2. 20 tCREs used 'dry' in cap on subject with short, stiff, curly hair

The subject with short, stiff, curly hair showed absolutely no signs of biology, as the cap were held off the scalp by the hair and prevented any meaningful connection. The graphs seen in Figure 57, Figure 58, Figure 59 and Figure 60 showed the complete absence of any biology. Only a 50 Hz mains noise was visible.

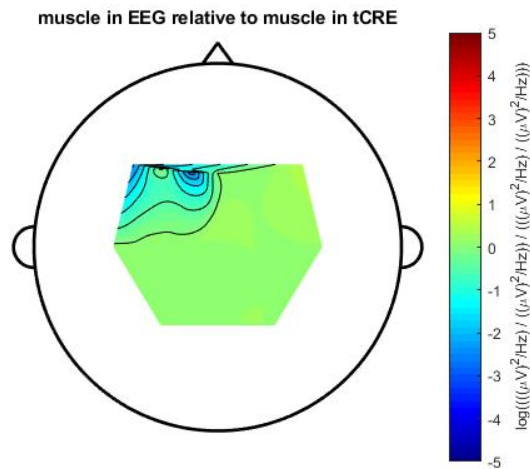


Figure 112. Figure shows muscle in software laplacian EEG to that in tCRE EEG

Figure 112 shows that the muscle seen in software laplacian EEG is the same as that seen in the tCRE EEGs. There is a slight drop in the muscle signal acquired at the frontal-left-lateral side of the head. The equal muscle signal seen in both software laplacian and tCRE EEG is attributed to the cap on the subject's head moving, due to the cap being held off the scalp by the subject's hair, and this being acquired as muscle signal.

6.4. 20 tCRE electrodes used 'dry' under the cap

As this experiment took a long time to setup, due to the difficulty in setting up electrodes under the cap accurately, this experiment was conducted on only one subject, with thick hair. The electrodes were placed under the electrode holders at the central electrode locations and held in place by the cap. There was very little connection with the scalp due to the volume of hair. As seen in Figure 61, Figure 62, Figure 63 and Figure 64 there was little to no biological signal seen from electrodes placed centrally. The 50 Hz mains noise was also seen to be absent.

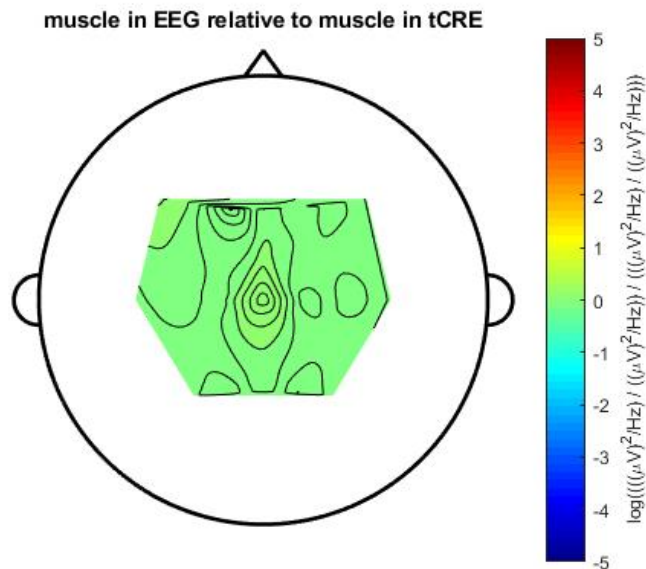


Figure 113. Figure shows muscle in software laplacian EEG to that in tCRE EEG

As seen in Figure 113, there is equal muscle seen in both software laplacian EEG and the tCRE EEG. This is attributed to poor connection with the scalp and no signal being acquired.

6.5. 20 tCRE electrodes used in cap with saline filled foam in the cap

Having seen that the tCRE electrodes were of no practical use without an interface, this experiment attempted to use alternate interfaces to verify efficacy of the tCRE electrodes.

6.5.1. 20 tCRE electrodes used in cap with saline filled foam in cap used on subject with thin, wispy hair

Subject with this, wispy hair showed best connection when used in cap with saline filled foam. The connection quality did not influence the outcome, as there was an error seen in the eyes closed task thus negating any attempts at verifying neural biological signal (Figure 65). The tCRE EEG (Figure 66) was much more conclusive, with the eyes closed task (purple trace) showing an alpha peak at 10Hz and both graphs showing muscle divergence from baseline tasks. At Pz, the same error was seen with the software laplacian EEG, which was absent in the tCRE EEG. A point of interest is the absence of the alpha peak at 10 Hz in the tCRE EEG graph of Pz. This is assumed to be due to the higher amplitude of the eyes closed signal masking the alpha peak at 10 Hz.

6.6. 20 tCRE electrodes used in cap with saline soaked foam cap underneath

Having seen that the saline filled foam was of some use in subjects with lesser volume of hair, but showed little to no penetration on subjects with higher volumes, this test attempted to place a saline soaked foam cap on the head to improve the connection of the tCRE electrodes with the scalp. The foam cap was first soaked in saline, wringed and then placed on the head.

6.6.1. 20 tCRE electrodes with foam cap used on subject with thick hair

As the subject with thick hair stated that the saline soaked foam cap was making good contact and that the subject's hair was also wet due to the contact, the EEG was expected to be improved. But, as seen in Figure 73 electrode at Cz, showed that the data acquired was not suitable for biological signals. A large harmonic was seen every 10 Hz, which showed a missing harmonic at 30 Hz. The same was seen in the tCRE EEG (Figure 74), with no biology visible. Moving further back on the head did not improve signal, as seen in Figure 75 and Figure 76.

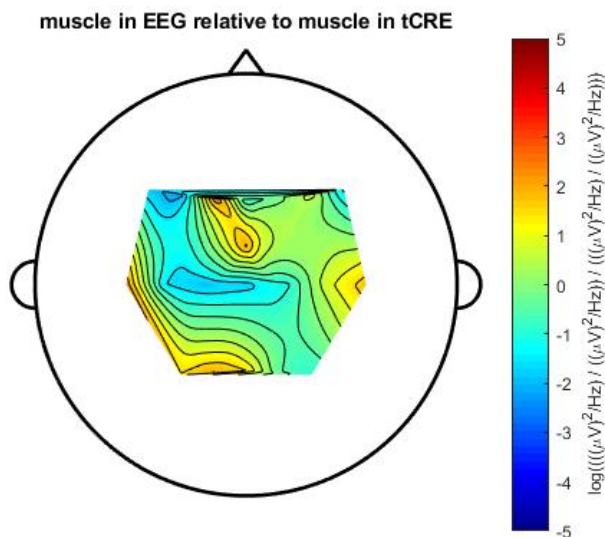


Figure 116. Figure shows muscle in software laplacian EEG to that in tCRE EEG

As seen in the previous saline filled foam inserts in cap test, there was a randomness in the Berger effect due to the poor connections being made with the head. This resulted in a mixture of very low and high relative muscle seen in the software laplacian EEG when compared to the tCRE EEG. Berger effect showed vast variations in line with the poor connection made with the scalp. Sharp edges between locations of comparative muscle meant the 'signals' acquired might not be viable as bio-neural signals.

6.6.2. 20 tCRE electrodes with foam cap used on subject with short, thick, stiff curly hair

The saline soaked foam cap was predicted to be more accurate with the subject with short, stiff curly hair due to the lesser volume of hair. This was seen to be true, as in Figure 77, we see a slight alpha peak at 10Hz (blue trace) and a large deviation from the baseline tasks of the muscle signal (yellow trace). Figure 78 showed the tCRE EEG, where no muscle-deviation was seen, but an alpha peak was visible, contrary to the norm of no alpha peaks being visible at Cz for tCRE EEGs. The absence of alpha peak in the tCRE EEG of electrode at location Pz, also contradicted the norm. Muscle deviations was seen as expected in both the software laplacian (Figure 79) and the tCRE EEGs (Figure 80). The absence of harmonics indicated that the cap was not undergoing bridging. The absence of neural bio-signal was attributed to the cap being raised above the scalp by the stiff hair, allowing for muscle signals but not neural ones.

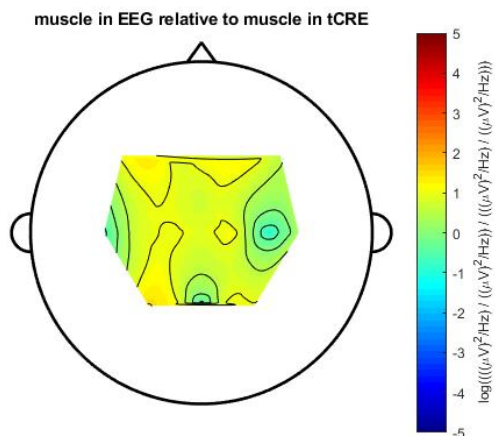


Figure 117. Figure shows muscle in software laplacian EEG to that in tCRE EEG

Berger effect seen in Figure 117 was seen to be a slight increase in muscle detected in software laplacian EEG when compared to the tCRE EEG. This indicated that the tCREs had improved ability to suppress muscle than the software laplacian method. There were slight drops in these muscle signals at the peripherals, showing that the tCREs might not suppress muscle activity completely at the peripherals..

6.7. 20 ring electrodes used 'dry' in the cap

The ring electrodes were then tested 'dry'. As they were not expected to be used in this manner, and the placement on the cap showed us that no contact was made between the head and the electrodes, no EEG signal was expected. This was confirmed, as seen in Figure 81 and Figure 82, where the electrode EEG at electrode location Cz and the software laplacian of the electrode EEG were shown respectively. No biology is seen, and there is a separation of muscle task trace (yellow trace) from the baseline that can be attributed to the movement of the cap. A large 50 Hz mains noise was seen, which was seen to be amplified, as no biology was detected, and the acquired signal was suppressed. The waveforms shape implied some sort of connection but not of a high enough quality to be useful for EEG acquisition. As the cap was loose posteriorly, the graphs seen in Figure 83 and Figure 84, at electrode location Pz, show similar absence in neural biology and 'muscle' separation.

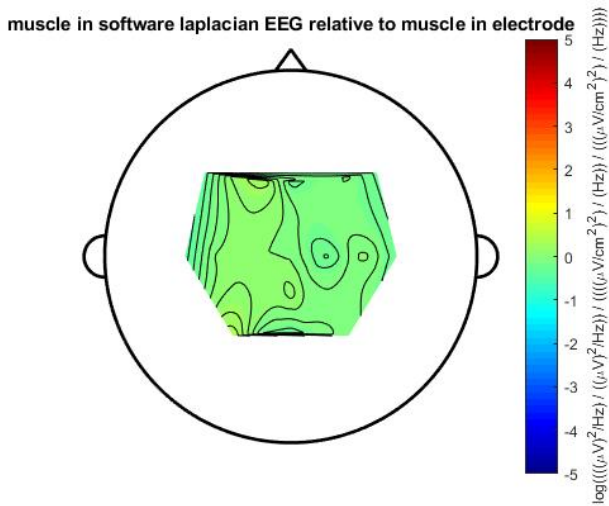


Figure 118. Figure shows comparison of muscle in software laplacian of electrode EEG and the muscle in electrode EEG

Berger effect (Figure 118) between electrode EEG and laplacian of the EEG show very little muscle being suppressed or acquired from the scalp. The range extended between -1 (light blue) to 0 (green), again showing the clear importance of software laplacian to EEG analysis and muscle removal. Peripheral regions showed no gradual change, indicating the muscle activity was minimized, mainly due to the absence of a clear bio-neural signal and the general space between the electrode and scalp for all electrodes on the head.

6.8. 8 SAHARA electrodes used dry in the cap

Having tested wet passive electrodes in a variety of stressful conditions for the electrodes and their ability to acquire data under the same, the dry active electrodes were the next experiment conducted. The SAHARAs were highly uncomfortable and required a cool-down period after being placed on the head of about 10 minutes to avoid electrode drift (Guger, 2012).

6.8.1. SAHARA electrodes used on subject with thick hair

Subject with thick hair was seen to have the most difficulty with placement of electrodes to make good contact with the scalp. After a period of ensuring good connections pre-test, the test was conducted. As seen in Figure 85, there was a 10Hz spike seen across all 3 traces, thus making it difficult to confirm the presence of an alpha peak solely from the software laplacian of the electrode EEG. The electrode EEG (Figure 86) showed a sharp peak in the eyes closed task (purple trace) at the 10 Hz mark, confirming the presence of alpha peak. There was poor divergence seen in the muscle task from the baseline (light blue trace). Moving backward on the head towards Pz improved the acquisition of neural signal with alpha peaks clearly visible in both electrode EEG (Figure 88) and software laplacian of electrode EEG (Figure 87). Poor divergence of muscle is once again seen in the electrode EEG (light blue trace). This poor muscle detection extends to laplacian electrode EEG too, where suppressed muscle is seen, this is confirmed by the Berger effect seen in Figure 119.

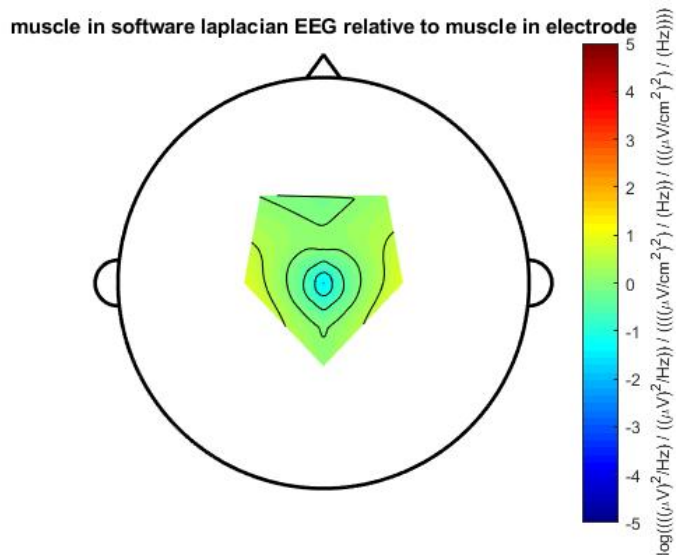


Figure 119. Figure shows comparison of muscle in software laplacian of electrode EEG and electrode EEG

From Figure 119, the central location was seen to show reduced comparative muscle due to the reduction in muscle at the scalp in the location, but muscle was seen to affect the rest of the head. While there is a clear distinction between the muscle at central locations and otherwise, it is important to note that the muscle seen is still at a range between -1 to 0, where the presence of muscle in software laplacian of EEG is seen to vary from less than the electrode EEG to almost the same. This is a positive, as dry electrodes are expected to show a lot more muscle interference in the acquired signal. Closer inspection, shows the periphery increases to the +1 range (yellow) implying higher muscle in software laplacian of EEG.

6.8.2. SAHARA electrodes used on subject with short, stiff curly hair

Subject with short, curly stiff hair was expected to have better connections with the electrodes than previous subject. Placement of electrodes on the head revealed that the stiffness of the hair was a major hindrance towards making a quality connection. The electrodes were mostly held off the scalp even with multiple readjustments. Figure 89 and Figure 90 show us the complete absence of neural biology with the muscle task (yellow trace) being suppressed below baselines. Same was visible further back on the head at Pz, as seen in Figure 91 and Figure 92. With the absence of any viable signal, the Berger effect was not important in any form of analysis.

Experiments were seen to be limited in some cases by,

1. As the experiments were performed on 3 willing participants only, the sample size used for the analysis is smaller than expected of a publishing-worthy thesis. Future work done in this field will increase the sample size and perform the experiments to confirm findings.
2. As these experiments were performed for the first time by the author, the time taken and the experience needed to reproduce the experiments was gained over the experimental period. The lessons learned over this period should make the reproducibility of the experiments easier.
3. Some of the electrodes had fewer accessories available than necessary to run the experiments, necessitating the use of non-ideal accessories. While this gave us an extra condition to study, it did not allow for the study and comparison of these electrodes under ideal conditions.

Comparing the tCRE electrodes to the wet passive ring electrodes by using them simultaneously showed that the tCRE electrodes were excellent in acquiring laplacian's of the acquired signal. Each tCRE showed the tendency to compensate for multiple wet passive electrodes in a localized area, which improved the case for fewer electrodes in an EEG cap. The tCREs showed muscle suppression even in the peripheries when compared to the central areas of the head, providing evidence of their usefulness. The wet electrodes were seen to be nearly useless when used without a gel interface, compounding the issues related to their use. Comparing the ability to acquire neural signals between wet and dry electrodes was seen to be important due to the variation in the set-up time for both. We saw that while the dry electrodes performed surprisingly well, they had issues with hair types as in the case of the subject with short, stiff curly hair and showed a tendency to mask the signal (highly suppressed signal or artefacts blurring bio-neural signals). This was seen to be caused by the loose fit of the cap on the participants head. The dry electrodes gave us a suppressed signal as compared to the wet passive electrodes, but also showed muscle suppression. While the muscle suppression was not of the same quality as that of the tCREs, it allowed for the acquisition of neural data in a few experiments, providing an alternate path for future studies into cap electrodes. The use of foam and saline as an alternative interface showed some promise and further studies into the efficacy of well modelled foam cap as an interface should improve our understanding of why the presence of a uniform interface connecting multiple electrodes doesn't cause consistent bridging on the scalp. The presence of harmonics in the experiment using the foam cap on thick haired subject, led the author to assume the effects of bridging on the participant. Subsequent experiments on participant with short, stiff curly hair showed the absence of such harmonics drawing into question the bridging effect attributed to the failure of previous experiment to acquire biological signals. As the same harmonics were seen when the wet passive electrodes were used on the scalp without a gel interface, the alternate theory was the insufficient soaking of the foam in saline, must have caused dry foam spots on the cap, resulting in an open circuit as seen with the wet passive electrode experiment.

7. Conclusion

The experiments conducted, attempted to use electrodes in non-ideal conditions, with poor scalp connections or with the wrong physical setup. This was done to form a basis for further studies, on the ability of individual electrode types under stressful conditions (for the electrode). As the experiments pre-empt the construction of an EEG cap used to diagnose schizophrenia and bipolar disorder, there is a need for electrodes that are not affected or show very little effects under stress (patient episodes). The following conclusions were reached,

Electrode types showed vastly different times required for their set up and data acquisition. Dry electrodes were seen to reduce time required for cap building on the participants head, but required team for electrode drift to subside. Wet electrodes extended times due to the need for application of gel. A combination of comb and ring electrodes showed the least delay, once the process of connecting the 2 was learned, but showed suppressed signal acquisition. Individually, each type showed characteristics as discussed below,

Dry electrodes were seen to be worth further studies as they showed signs of neural signal in situations where we did not expect to see any. The combination of dry comb electrodes with the wet passive ring electrodes also showed some surprising results even in the absence of gel. Poor connections between the ring and comb electrodes did not seem to affect the acquisition and transmission of EEG signal. The SAHARA electrodes worked well when used on a subject with thick voluminous hair, but seemed to be restricted in ability when used on stiff haired subject. Lateral electrodes showed better connections than the posterior electrodes due to the poor cap fit on both subjects tested, which was corrected in the post-experimental phase by using equal sized electrodes on the head rather than attempting to compensate for head shape.

Wet passive electrodes showed better ability to make connections with the scalp when used ideally. In non-ideal situations, they were seen to be practically open circuit with no real signal of any quality. Changes in interface (scalp-electrode) also did not seem to affect the wet passive electrodes with the ring electrodes even performing well when used in combination with the comb electrodes. Harmonics were seen consistently when ring electrodes were used without a gel. In one case, a harmonic was seen to be missing at 30Hz, which implied that the harmonics were not symmetric.

The tCRE electrodes were found to be excellent in acquisition of neural bio-signals. A single tCRE electrode was seen to give us a localized EEG signal. Using 4-8 of the tCREs spaced to cover areas of interest on the entire surface of the head was postulated to provide sufficient data for a scalp EEG. This confirmed the theory that the usage of tCREs can reduce the number of electrodes used for EEG acquisition to single digits from the current clinical ideal of 128 electrode systems. The tCREs also showed the ability to suppress muscle even when used on muscle, which implied its viability for usage in cases where a subject is undergoing an episode. The tCREs were only seen to be useful when used with a gel interface. As the system was new, the author was asked not to experiment with gels for use with the tCREs, thus making it impossible to discuss the effect of different gels on the ability of the tCREs. To avoid this, foam was used as an interface.

Factors outside of the electrodes also played a major part in the acquisition of EEG under non-ideal conditions, Muscle, played a large part in the successful neural bio-signal acquisitions and was seen to be highly suppressed by the tCREs and even by the dry comb and SAHARA electrodes. The wet passive ring electrodes showed no such signs and were thus seen to be the least useful for reduction in muscle. The comb electrodes were used in a non-ideal way using ring electrodes as connectors rather than the provided ones due to constraint in their numbers. Even with these issues, the comb electrodes acquired EEG signals off the head, with minimal muscle interference, although the amplitude of the signal acquired was reduced. This was seen as a hurdle during the analysis, as the successful classification of alpha peaks was difficult with reduced amplitudes.

With an interface between the scalp and electrode seen to be vital for the proper functioning of the wet passive electrodes and the absence of alternate gels, foam was used as an intermediate interface. The use of foam as a connective interface between the scalp and the electrodes was non-ideal but seen to function well. The issue of cross-bridging (shorting of electrodes due to common connections - foam) was brought up, and was assumed to show its effects on the experiment, but no bridging was seen, implying the foam cap soaked in saline did not short the electrodes. As the 'saline' used in the foam cap and the foam infills was water, further studies looking into different fluids to improve the conductivity of the cap/infills would be useful. As the author had no experience with sewing, an improved cap constructed by a professional or more experienced individual would improve the experiments. The different head sizes of the participants was seen to be an issue with the construction of a single universal 'cap' and affected the experiments negatively.

Another factor noticed during the experimental phases was the effect of hair on the ability of the electrodes to acquire EEG signal. Not only was the volume of hair an important factor, the type of hair was also seen to be important. Stiff hair was seen to be detrimental in all cases, while thick hair was seen to be detrimental to passive wet electrodes due to their flat construction. We see that thick hair and short, stiff curly hair showed the ability to resist electrode placement, this led to an open circuit between dry electrodes and the scalp, preventing acquisition of neural bio-signals. Thin or no hair was seen to be the best scenario for EEG acquisition as excellent scalp contact was maintained. The presence of external stimuli in an experiment suggested the negative effects on the acquisition of EEG, implying the need for a sealed environment, which may not be possible as a large-scale solution.

The experiments improved the authors understanding of how different electrode systems work to acquire signals and how the ideal set up can be tweaked to test said systems. Future studies of dry electrodes under stress with a large study group, might provide concrete evidence of their abilities under stress. Including participants with different hair types should be an important concern as a few experiments provided no bio-signal due to specific hair types. The tCREs were seen to be the best, when used with the correctly prescribed gel, even over muscle (periphery) and are recommended as the preference for the electrodes to be used for the EEG cap for diagnosis of schizophrenia and bipolar disorder.

8. Bibliography

ALopez-Gordo, D.-M. a. F. V., 2014. Dry EEG Electrodes. *sensors*, Issue 14, pp. 12847-12870.

American Clinical Neurophysiology Society, 2006. *Guidelines*. [Online] Available at: <https://www.acns.org/pdf/guidelines/Guideline-5.pdf> [Accessed 18 May 2019].

Babiloni, C. C. R. B., 2001. *Spatial enhancement of EEG data by surface Laplacian estimation: the use of magnetic resonance imaging-based head models*, Rome: Clinical Neurophysiology.

Bell, S. T., 1995. *An information-maximisation approach to blind separation and blind deconvolution*, San Diego, CA: Institute for Neural Computation.

Berger, 1929. uber das electrenkephalogram des menschen. *Arch. Psychiatr Nervenkr*, Issue 87, pp. 527-570.

Besio, M.-J. I. M. O. G. J. B. A. F. R. M. A.-V., 2014. High-Frequency Oscillations Recorded on the Scalp of Patients with Epilepsy using Tripolar Concetric Ring Electrodes. *Neurovascular Devices and Systems*, Volume 4.

Black Dog Institute, 2018. *What is bipolar disorder ?*. [Online] Available at: <https://www.blackdoginstitute.org.au/clinical-resources/bipolar-disorder/what-is-bipolar-disorder> [Accessed 17 February 2019].

Boutron N.N., A. C. G. S. W. J. P. g. I. W., 2008. The status of spectral EEG abnormality as a diagnostic test for schizophrenia. *Schizophrenia Research*, 99(1-3), pp. 225-237.

Boutros, A. C. G. S. W. J. P. F. I. W., 2008. The status of spectral EEG abnormality as a diagnostic test for schizophrenia. *Schizophrenia Research*, 99(1-3), pp. 225-237.

Carvalhaes, B. J., 2014. The Surface Laplacian Technique in EEG: Theory and Methods. *International Journal of Psychophysiology*, Volume 2.

CGX, 2019. *Drypad Sensors*. [Online] Available at: <https://www.cognionics.net/drypad-sensors> [Accessed 17 February 2019].

Compumedica NeuroScan, n.d. *Curry 7 - Signal Processing & Basic Source Analysis*. [Online] Available at: <https://compumedicsneuroscan.com/curry-7-signal-processing-and-basic-source-analysis/> [Accessed 17 February 2019].

Congedo, 2017. *EEG Source Analysis*. Grenoble: HAL archives-ouvertes.

CREmedical, 2018. *What is the TCRE*. [Online] Available at: <https://cremedical.com/tcre/> [Accessed 17 February 2019].

CREmedical, n.d. *t-Lead: Tripolar Concentric Ring Electrode (TCRE)-based sensor*. [Online] Available at: <https://cremedical.com/product-2/> [Accessed 17 February 2019].

De Clercq, V. A. V. B. V. P. W. V. H. S., 2006. Canonical correlation analysis applied to remove muscle artifacts from the electroencephalogram. *IEEE Transactions on Biomedical Engineering*, Issue 53, pp. 2583-2587.

De Vos, R. S. V. K. V. B. V. H. S. B. B., 2010. Removal of Muscle Artifacts from EEG recordings of spoken language production. *Neuroinformatics*, 135(50).

Degabrielle, L. J., 2009. A review of EEG and ERP studies in bipolar disorder. *Acta Neuropsychiatrica*, 21(2), pp. 58-66.

Di Blaise, C. V. L. F. A. C. F. G. E. P. C. Z. A., 2018. Linking Cortical and COnnectonal Pathology in Schizophrenia. *Schizophrenia Bulletin*.

Djuwari, K. D. P. M., 2005. *Limitations of ICA for Artefact Removal*. Shanghai, China, IEEE Engineering in Medicine and Biology 27th Annual Conference.

Dvey-Aharon, F. N. P. A. I. N., 2015. Schizophrenia Detection and Classification by Advanced Analys of EEG Recordings Using a Single Electrode Approach. *PLoS ONE*, 10(4).

Echallier, P. F. P. J., 1992. Computer-assisted placement of electrodes on the human head. *Electroencephalography Clinical Neurophysiology*, Issue 82, pp. 160-163.

El-Badri, A. C. M. P. F. I., 2001. Electrophysiological and cognitive function in young euthymic patients with bipolar affective disorder. *Bipolar Disorder*, 3(2), pp. 79-87.

Fitzgibbon, L. T. P. D. W. E. W. J. P. K., 2013. Surface Laplacian of central scalp electrical signals is insensitive to muscle contamination. *IEEE Trans. Biomed*, 60(1), pp. 4-9.

FixXL Ltd., 2018. *EEG Disc Electrode Disposable*. [Online] Available at: <https://www.biofeedback-tech.com/biofeedback-shop/eeg-disc-electrodes> [Accessed 21 February 2019].

Gage, B. B., 2018. *Brodman Area - An overview*. [Online] Available at: <https://www.sciencedirect.com/topics/neuroscience/brodman-area> [Accessed 17 February 2019].

Giannitrapani, K. L., 1974. Schizophrenia and EEG spectral analysis. *Electroencephalography and Clinical Neurophysiology*, Volume 36, pp. 377-386.

Griss, T.-L. H. M. P. S. G., 2002. Characterization of micromachines spiked biopotential electrodes. *IEEE Trans. Blom, ed. ENg.*, Issue 49, pp. 597-604.

Guger, K. G. A. B. E. G., 2012. Comparison of dry and gel based electrodes for P300 brain computer interfaces. *Frontier Neuroscience*.

Hjorth, 1975. An on line transformation of EEG scalp potentials in orthogonal source derivations. *Electroencephalography Clinical Neurophysiology*, Issue 39, pp. 526-530.

Hotelling, 1935. Relations Between Two Sets of Variates. *Biometrika*, Issue 28, pp. 321-377.

Jung, M. S., n.d. *Removing Artifacts from EEG*. [Online] Available at: <https://cnl.salk.edu/~jung/artifact.html> [Accessed 17 February 2019].

Kamarajan, P. A. C. D. P. B., 2016. The use of current source density as electrophysiological correlates in neuropsychiatric disorders: a review of human studies. *International Journal of Psychophysiology*, 97(3), pp. 310-322.

Kam, B. A. O. B. H. W. B. C., 2013. Resting State EEG Power and COherence Abnormalities in bipolar disorder and Schizophrenia. *Journal of Psychiatric Research*, 47(12), pp. 1893-1901.

Kayser, T. C., 2016. Issues and considerations for using the scalp surface Laplacian in EEG/ERP research: A tutorial review. *Int. J. Psychophysiol*, Issue 97(3), pp. 189-209.

Kim, B. A. H. J. R. O. S. O. H. W. B. A. O. B., 2013. Disturbed resting state EEG synchronization in bipolar disorder: A graph-theoretic analysis. *NeuroImage: Clinical*, pp. 414-423.

Lau, G. J. F. D., 2012. How Many Electrodes Are Really Needed for EEG-Based Mobile Brain Imaging. *Journal of Behavioral and Brain Science*, Volume 2, pp. 387-393.

Lera-Miguel, A.-P. S. C. R. F.-V. M. F. L. L. L., 2011. Early onset bipolar disorder: how about visual spatial skills and executive functions?. *Eur. Arch. Psychiatry Clin. Neuroscience*, 261(3), pp. 195-203.

Liao, W. I.-J. C. S.-F. C. J.-Y. L. C.-T., 2011. Design, Fabrication and Experimental Validation of a Novel, Dry-Contact Sensor for Measuring Electroencephalographym, Signals without Skin preparation. *Sensors*, 11(6), pp. 5810-5834.

Ludwig, M. R. L. N. J. M. A. D. K. D., 2009. Using a Common Average Reference to Improve COrtical Neuron Recordings From Microelectrode Arrays. *Journal of Neurophysiology*, 101(3), pp. 1679-1689.

Makeig, B. A. J. T.-P. S. T., 1996. Independent Component Analysis of Electroencephalographic Data. *Advances in Neural information processing systems*, pp. 145-151.

Mammone, L. F. F. M. F., 2012. Automatic Artifact Rejection from Multichannel Scalp EEG by Wavelet ICA. *IEEE Sensors journal*, 12(3), pp. 533-542.

Mansour, B. A. O. N., 2000. Blind Separation of Sources: Methods, Assumption and Applications. *CE Trans. Fundamentals*, E83-A(8), pp. 1498-1512.

McDermid, 2014. *EEG findings specific to mood state in bipolar disorder*. [Online] Available at: <https://www.news-medical.net/news/20140327/EEG-findings-specific-to-mood-state-in-bipolar-disorder.aspx>

[Accessed 17 February 2019].

- Merrin, F. T. F. G., 1989. EEG Coherence in Unmedicated Schizophrenic Patients. *Biology in Psychiatry*, Issue 25, pp. 60-66.
- Michel, M. M. L. G. G. S. S. L. D. P. G., 2004. EEG Source Imaging. *Clinical Neurophysiology*, Issue 115, pp. 2195-2222.
- Muthukumaraswamy, 2013. *High-frequency brain activity and muscle artifacts in MEG/EEG: a review and recommendations*. [Online]
Available at: <https://www.ncbi.nlm.nih.gov/pmc/articles/PMC3625857/>
[Accessed 17 February 2019].
- Nicholson, 1973. Theoretical Analysis of Field Potentials in Anisotropic Ensembles of Neuronal Elements. *IEEE Transactions on Biomedical Engineering*, BME-20(4), pp. 278-288.
- Peters, 2018. *What Is an Electroencephalogram (EEG) ?*. [Online]
Available at: <https://www.verywellhealth.com/what-is-an-eeg-test-and-what-is-it-used-for-3014879>
[Accessed 21 February 2019].
- Pope, K., 2019. *Professor* [Interview] (18 February 2019).
- Saab, B. B. G.-W. M., 2011. *Simultaneous EEG recordings with Dry and Wet Electrodes in Motor-Imagery*, Graz, Austria: Verlag der Technischen Universität Graz.
- SANE Australia, 2017. *Schizophrenia*. [Online]
Available at: <https://www.sane.org/mental-health-and-illness/facts-and-guides/schizophrenia>
[Accessed 17 February 2019].
- Schalk, M. J., 2010. *A Practical Guide to Brain-Computer Interface Research, Data Acquisition, Stimulus Presentation, and Brain Monitoring*. 23 ed. s.l.:Springer.
- Sherlin, 2015. *Comparison of frequency response using different high pass filters*. [Online]
Available at: https://www.researchgate.net/figure/Comparison-of-frequency-response-using-different-high-pass-filters-Solid-line-indicates_fig8_283421753
[Accessed 17 February 2019].
- Sponheim, C. B. I. W. B. M., 1994. Resting EEG in first-episode and chronic schizophrenia. *Psychophysiology*, 31(1).
- Srinivasan, 1999. Methods To Improve the Spatial Resolution of EEG. *International Journal of BioElectroMagnetism*, 1(1), pp. 102-111.
- St.Vincent's Hospital, Melbourne, 2014. *EEG Test*. [Online]
Available at: <https://www.betterhealth.vic.gov.au/health/conditionsandtreatments/eeg-test>
[Accessed 21 February 2019].
- Sullivan, D. S. C. G., 2007. *A Low-Noise, Non Contact EEG/ECG Sensor*. In *Proceedings of the Biomedical Circuits and Systems Conference*. Montreal, QC, BIOCAS, pp. 154-157.

- Teplan, 2002. Fundamentals of EEG Measurement. *Measurement Science Review*, 2(2).
- Thulasidas, G. C. W. J., 2006. Robust Classification of EEG signals for brain-computer interface. *IEEE transactions on Neural Systems and Rehabilitation Engineering*, 14(1), pp. 24-29.
- Towle, B. J. S. D. T. K. G. R. L. D. C. R. F. S. S. J.-P., 1993. The spatial location of EEG electrodes: locating the best-fitting sphere relative to cortical anatomy. *Electroencephalography and Clinical Neurophysiology*, Issue 86, pp. 1-6.
- Tres, B. S., 2014. Visuospatial Processing: A review from basic to current concepts. *Dement Neuropsychology*, 8(2), pp. 175-181.
- Ungureanu, B. C. S. R. L. V., 2004. Independent Component Analysis Applied in Biomedical Signal Processing. *Measurement Science Review*, 4(2).
- Vergult, D. C. W. P. A. V. B. D. P. V. H. S. V. P. W., 2007. Improving the Interpretation of Ictal Scalp EEG: BSS-CCA Algorithm for Muscle Artifact Removal. *Epilepsia*, 48(5).
- Villamar, V. M. B. M. D. A., 2013. Technique and Considerations in the Use of 4x1 Ring High-definition Transcranial Direct Current Stimulation (HD-tDCS). *Journal of Visualized Experiments*, 77(77).
- Vrocher III, L. M., 2017. *Electroencephalography*. [Online] Available at: https://www.emedicinehealth.com/electroencephalography_eeg/article_em.htm#electroencephalography_eeg_introduction [Accessed 21 February 2019].
- Weatherspoon, 2017. *EEG (Electroencephalogram)*. [Online] Available at: <https://www.healthline.com/health/eeg> [Accessed 21 February 2019].
- Wikimedia, 2011. *Brodmann area 6 lateral*. [Online] Available at: https://commons.wikimedia.org/wiki/File:Brodmann_area_6_lateral.jpg [Accessed 17 February 2019].
- Wycoff, S. L. F. N. D. D., 2015. Validation of a wireless dry electrode system for electroencephalography. *Journal of NeuroEngineering and Rehabilitation*, 12(95).
- Xing, W. P. G. X. L. Z. W. F. M. G. Z. H. G. Q. C. G., 2018. *A High-Speed SSVEP-Based BCI Using Dry EEG Electrodes*. [Online] Available at: <https://www.nature.com/articles/s41598-018-32283-8> [Accessed 17 February 2019].

9. Appendix

9.1. Appendix A

Matlab code used for data analysis. Code written by Professor Kenneth J. Pope, with a few minor edits by Roshan

F. Coelho

9.1.1. Loading the data

```
fpath = 'R:\CSE-EEG\Projects\tCRE\Data';
subject = 'Subject1';
allfiles =
{'tCRE_Baseline_EC.xdf','tCRE_Baseline_EO.xdf','tCRE_AuditoryMMN.xdf','tCRE_Muscle.xd
f','tCRE_MotorImag.xdf'};
alltasks = {'EyesClosed','EyesOpen','AudMMN','Muscle','MotorImag'};
clear d
tasks = {'EyesClosed','EyesOpen','Muscle'};
tcodes = {{'40','41'},{'30','31'},{'50','60'}};
discard_bad_channels = false;

% CPz is the reference, others are bad channels
switch subject
    case 'Subject1'
        chantodiscard =
{'CPz','TP7','F8','F10','FT9','FT7','FC3','FC1','P6','P8','PO9','PO9','FTT8h','FTT10h
','TTP7h','CCP5h'};
        case { 'Subject2', 'Subject3', 'Subject4', 'Subject5', 'Subject6', ...
              'Subject7', 'Subject8', 'Subject9', 'Subject10', ...
              'Subject14', 'Subject15', 'Subject16', 'Subject17', ...
              'Subject18', 'Subject19', 'Subject20'}
            chantodiscard = { 'CPz'};
        otherwise
            error( 'Unknown subject' );
end

% load data for each task
d = eeg3.eeg.alloc( 1, length( tasks));
for ti = 1:length(tasks)

    % work out which file to load from
    fi = find(strcmp(tasks{ti},alltasks));

    % load the data
    fprintf('load task %s from file %s\n', tasks{ti}, allfiles{fi})
    d(ti) = eeg3.eeg.load(fullfile(fpath,subject,allfiles{fi}));

    % remove bad channels
    if discard_bad_channels
        d( ti) = d( ti).discardchans( chantodiscard);
    end

    % Correcting a mis-typed channel label
    ind = find( strcmp( 'tFP1', d( ti).chan.getlabels));
    if ~isempty( ind)
        d( ti).chan( ind).label = 'tFp1';
    end

end
```

9.1.2. Find the tCRE electrodes

```
clabels = d(1).chan.getlabels;
itCRE = strncmp('t',clabels,1);

tdt = dt.selectchan(itCRE);
edt = dt.selectchan(~itCRE);

for ti = 1:length(tasks)
    for ci = 1:length(tdt(1).chan)
        tdt(ti).chan(ci).label = strrep(tdt(ti).chan(ci).label,'t','');
    end
    for ci = 1:length(edt(1).chan)
        edt(ti).chan(ci).label = strrep(edt(ti).chan(ci).label,'e','');
    end
    tdt(ti) = addlocation( tdt( ti));
    edt( ti) = addlocation( edt( ti));
end
```

9.1.3. Extract task specific data

```
dt = eeg3.eeg.alloc( 1, length( tasks));
for ti = 1:length(tasks)

    dtend = max( d( ti).timebase);
    if any( [ d( ti).event.offset] > dtend)
        for ei = 1:numel( d( ti).event)
            d( ti).event( ei).offset = min( dtend, ...
                d( ti).event( ei).offset);
        end
    end

    temp = d(ti).eventslice(tcodes{ti}{1},tcodes{ti}{2},[0 0]);
    if iscell( temp)
        dt(ti) = [temp{:}];
    elseif isa( temp, 'eeg3.eeg')
        dt(ti) = temp;
    else
        error( 'Unknown class after eventslicing');
    end
end
```

9.1.4. Separating the EEG and the tCRE EEG electrodes

```
clabels = d(1).chan.getlabels;
itCRE = strncmp('t',clabels,1);

tdt = dt.selectchan(itCRE);
edt = dt.selectchan(~itCRE);

for ti = 1:length(tasks)
    for ci = 1:length(tdt(1).chan)
        tdt(ti).chan(ci).label = strrep(tdt(ti).chan(ci).label,'t','');
    end
    for ci = 1:length(edt(1).chan)
        edt(ti).chan(ci).label = strrep(edt(ti).chan(ci).label,'e','');
    end
    tdt(ti) = addlocation( tdt( ti));
    edt( ti) = addlocation( edt( ti));
end
```

9.1.5. Calculate the Spectra

```
% do a CAR
cedt = edt.car;

% calculate spectra
tst = tdt.pwelch;
est = edt.pwelch;
cest = cedt.pwelch;

% Channel Choice
switch subject
    % we used tCRE electrodes
    case { 'Subject1', 'Subject2', 'Subject6', 'Subject7', 'Subject8', ...
           'Subject9', 'Subject16', 'Subject17', 'Subject18', 'Subject20' }
        tchans = tst(1).chan.getlabels;
        legendtext = { 'Laplacian EC', 'Laplacian EO', 'Laplacian Jaw Clench', ...
                       'tCRE EC', 'tCRE EO', 'tCRE Jaw Clench', ...
                       };
    % we didn't use tCRE electrodes
    case { 'Subject3', 'Subject4', 'Subject5', 'Subject10', 'Subject14', ...
           'Subject15', 'Subject19' }
        tchans = est(1).chan.getlabels;
        legendtext = { 'Laplacian EC', 'Laplacian EO', 'Laplacian Jaw Clench', ...
                       'EC', 'EO', 'Jaw Clench', 'CAR EC', 'CAR EO', 'CAR Jaw Clench' };
end

% Montage
m = eeg3.util.getmontage( tchans);
for i = 1:numel( m)
    m( i).x = m( i).x * 2 - 1;
    m( i).y = m( i).y * 2 - 1;
end
```

9.1.6. Berger Effect

```
% definitions
clims = [ -1 1];
Bfr = [ 8 10];
topo_opts = { 'colorbar', false, 'clim', clims, 'normalise', false, 'montage', m};

% calculate relative and average over alpha range
Berger = [ cest( 1).relative( cest( 2)), tst( 1).relative( tst( 2))];
Berger = Berger.selectfreq( Bfr( 1), Bfr( 2)).meanfreq;

% draw the figure
figure;
if numel( Berger( 1).discardchans( tchans)) > 1
    subplot( 1, 3, 1);
    Berger( 1).discardchans( tchans).plottopography( topo_opts{ :});
    title( 'Berger effect : EEG');
end
if numel( Berger( 1).selectchan( tchans).data) > 1
    subplot( 1, 3, 2);
    Berger( 1).selectchan( tchans).plottopography( topo_opts{ :});
    title( 'Berger effect : emulated EEG');
end
if numel( Berger( 2).data) > 1
    subplot( 1, 3, 3);
    Berger( 2).plottopography( topo_opts{ :});
    title( 'Berger effect : tCRE');
end
```

9.1.7. Laplacian of EEG from selected electrodes

```
% check the CSD toolbox is available
if ~exist( 'ExtractMontage', 'file') == 2
    addpath( genpath( 'V:\EEG\Matlab\CSDtoolbox'));
end

% calculate the Laplacian on the eeg channels (including emulated tCRE)
ldt = edt.csdtoolbox_scd;
% l2dt = kjp_laplacian( edt.selectchan( 1:108));
lst = ldt.pwelch;
l2dt = cedt.csdtoolbox_scd;
```

9.1.8. Display Spectra

```
switch subject
% tCRE
case { 'Subject1', 'Subject2', 'Subject6', 'Subject7', 'Subject8', ...
       'Subject9', 'Subject16', 'Subject17', 'Subject18', 'Subject20'}
    tchans = tst(1).chan.getlabels;
    spectoshow = [ lst.selectchan( tchans), tst];
    legendtext = { 'Laplacian EC', 'Laplacian EO', 'Laplacian Jaw Clench', ...
                  'tCRE EC', 'tCRE EO', 'tCRE Jaw Clench', ...
                  };

% no tCRE
case { 'Subject3', 'Subject4', 'Subject5', 'Subject10', 'Subject14', ...
       'Subject15', 'Subject19'}
    tchans = est(1).chan.getlabels;
    spectoshow = [ lst.selectchan( tchans), est.selectchan( tchans),
cest.selectchan( tchans)];
    legendtext = { 'Laplacian EC', 'Laplacian EO', 'Laplacian Jaw Clench', ...
                  'EC', 'EO', 'Jaw Clench', 'CAR EC', 'CAR EO', 'CAR Jaw Clench'};
end

spectoshow.plotmontage( 'xlim', [ 0 60], 'LineWidth', 2.5);
legend( legendtext);
set((gcf, 'Units', 'Normalized', 'Position', [ 0.1 0.1 0.8 0.8]));
tightfig

% individual channels
chanstoshow = { 'Cz', 'Pz'};
for i = 1:numel( chanstoshow)
    figure
    spectoshow.selectchan( chanstoshow{ i}).plot( 'xlim', [ 0 60], 'LineWidth', 2.5);
    legend( legendtext);
    title( chanstoshow{ i});
end
hl = findobj( gca, 'Type', 'Line');
set( hl, 'LineWidth', 2.5);
%
```

9.1.9. Topographies of Muscle, Relative Muscle between Laplacian of EEG and electrode EEG

```
% definitions
clims = 5 * [-1 1];
mfr = [ 52 98];
topo_opts = { 'colorbar', false, 'clim', clims, 'normalise', false, 'montage', m};

switch subject

%tCRE ELECTRODES
    case { 'Subject1', 'Subject2', 'Subject6', 'Subject7', 'Subject8', ...
           'Subject9', 'Subject16', 'Subject17', 'Subject18', 'Subject20'}
        muscle = [ cest( 3).relative( cest( 2)), tst( 3).relative( tst( 2))];
muscle = muscle.selectfreq( mfr( 1), mfr( 2)).meanfreq;
% draw the figure for relative muscle between tCREs and hardware laplacian
figure(1)
clf;
if numel( muscle( 1).discardchans( tchans)) > 1
    subplot( 1, 3, 1);
    muscle( 1).discardchans( tchans).plottopography( topo_opts{ :});
    title( 'relative muscle : EEG');
end
if numel( muscle( 1).selectchan( tchans).data) > 1
    subplot( 1, 3, 2);
    muscle( 1).selectchan( tchans).plottopography( topo_opts{ :});
    title( 'relative muscle: emulated EEG');
end
if numel( muscle( 2).data) > 1
    subplot( 1, 3, 3);
    muscle( 2).plottopography( topo_opts{ :}, 'colorbar', true);
    title( 'relative muscle : tCRE');
end
% draw the berger effect comparing tCREs and hardware laplacian
figure(2)
clf;
muscle( 1).selectchan( tchans).relative( muscle( 2)).plottopography( topo_opts{ :},
'colorbar', true);
title( 'muscle in EEG relative to muscle in tCRE');

%NON-tCRE ELECTRODES
    case { 'Subject3', 'Subject4', 'Subject5', 'Subject10', 'Subject14', ...
           'Subject15', 'Subject19'}
% calculate relative and average over muscle range
muscle = [ cest( 3).relative( cest( 2)), lst( 3).relative( lst( 2))];
muscle = muscle.selectfreq( mfr( 1), mfr( 2)).meanfreq;
% draw the figure for non-tCRE electrodes relative to software laplacian
figure
if numel( muscle( 1).discardchans( tchans)) > 1
    subplot( 1, 3, 1);
    muscle( 1).discardchans( tchans).plottopography( topo_opts{ :});
    title( 'relative muscle : EEG');
end
if numel( muscle( 1).selectchan( tchans).data) > 1
    subplot( 1, 3, 2);
    muscle( 1).selectchan( tchans).plottopography( topo_opts{ :});
    title( 'relative muscle: software Laplacian of EEG');
end
if numel( muscle( 2).data) > 1
    subplot( 1, 3, 3);
    muscle( 2).plottopography( topo_opts{ :}, 'colorbar', true);
    title( 'relative muscle : EEG');
end
% draw the berger effect comparing non-tCRE EEG with laplacian version
figure
muscle( 1).selectchan( tchans).relative( muscle( 2)).plottopography( topo_opts{ :},
'colorbar', true);
title( 'muscle in software laplacian EEG relative to muscle in electrode');
end
```

9.2. Appendix B

A version of the EEG cap used for the experiments is given below. Not all positions shown in the cap were used for the experiments (TP9 and TP10).

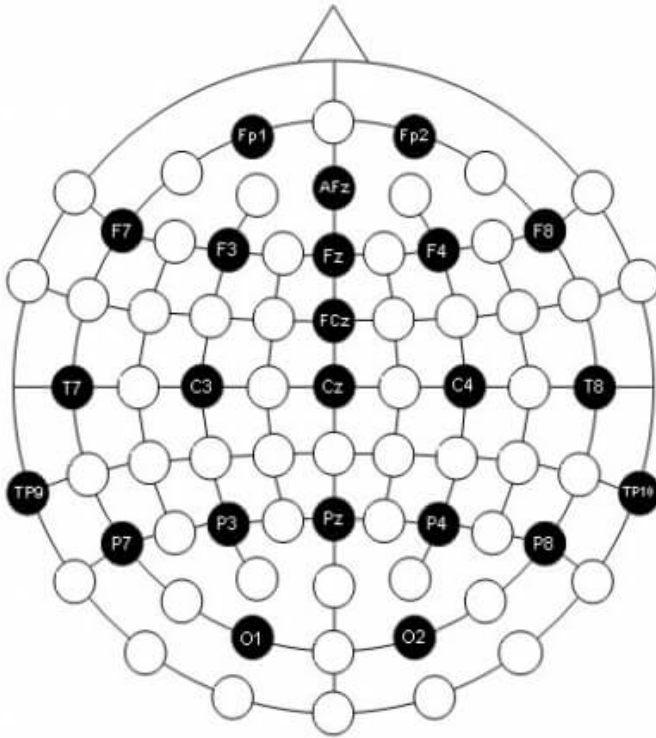


Figure 123. Figure shows the electrode locations on the head using EasyCap in a 10-10 system ((American Clinical Neurophysiology Society, 2006)). Most of these locations were used for experiments. TP9 and TP10 were considered too peripheral for the tests. (Access: <http://www.fieldtriptoolbox.org/assets/img/template/layout/easycapm25.png>)

The following are graphs of interest for individual experiments. They are labelled by their position on the EEG cap used on the head. In the case of tCRE electrodes legend is given by,

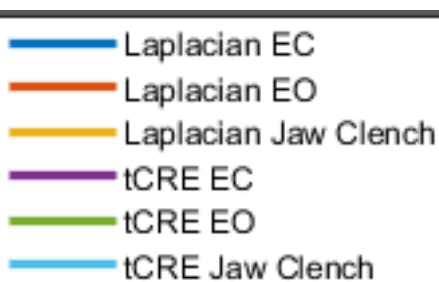


Figure 124. Figure shows legend for tCRE electrodes EEG spectra graphs

In the case of dry electrodes being used, the legend is given by,



Figure 125. Figure shows legend for non-tCRE electrodes EEG spectra graphs

9.2.1. 20 tCRE electrodes with 108 passive wet electrodes

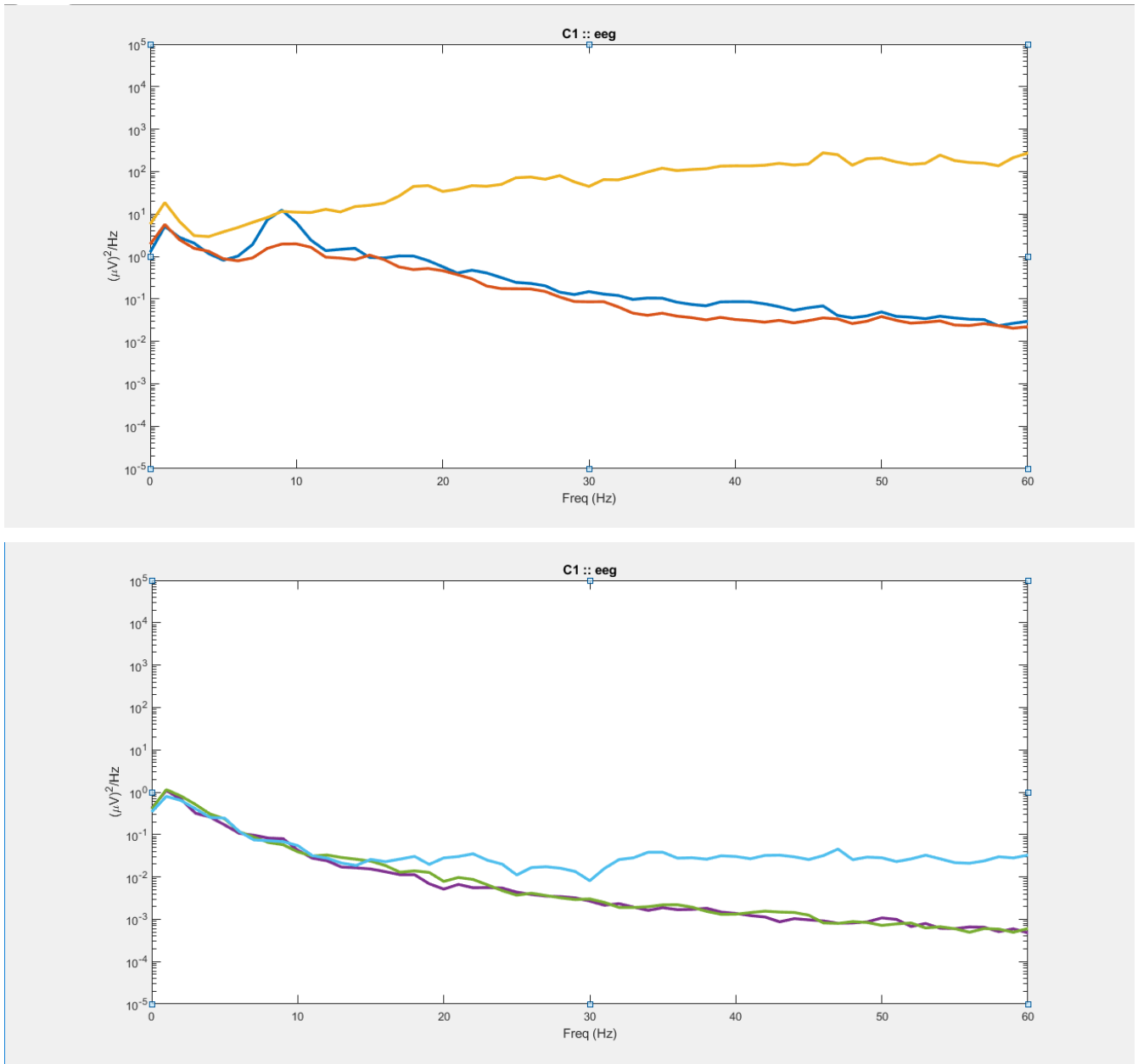


Figure 126. Graph shows electrode location C1. (top) shows software laplacian of tCRE EEG. (bottom) shows tCRE EEG

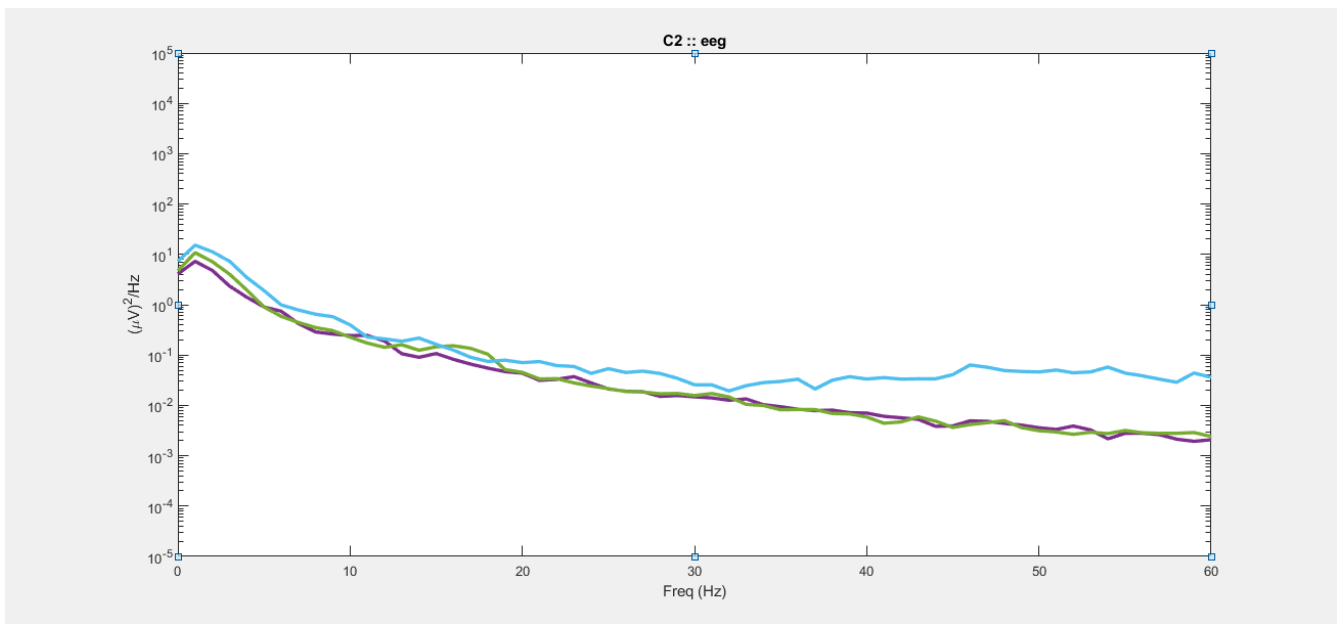
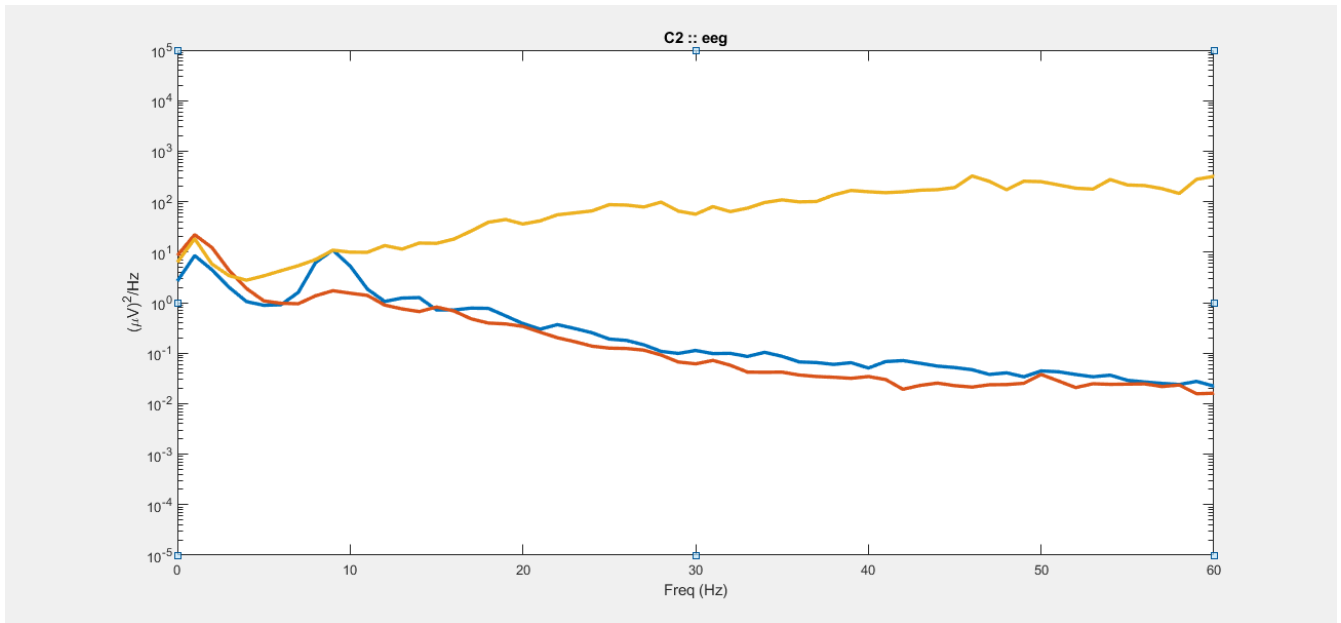


Figure 127. Graph shows electrode location C2. (top) shows software laplacian of tCRE EEG. (bottom) shows tCRE EEG

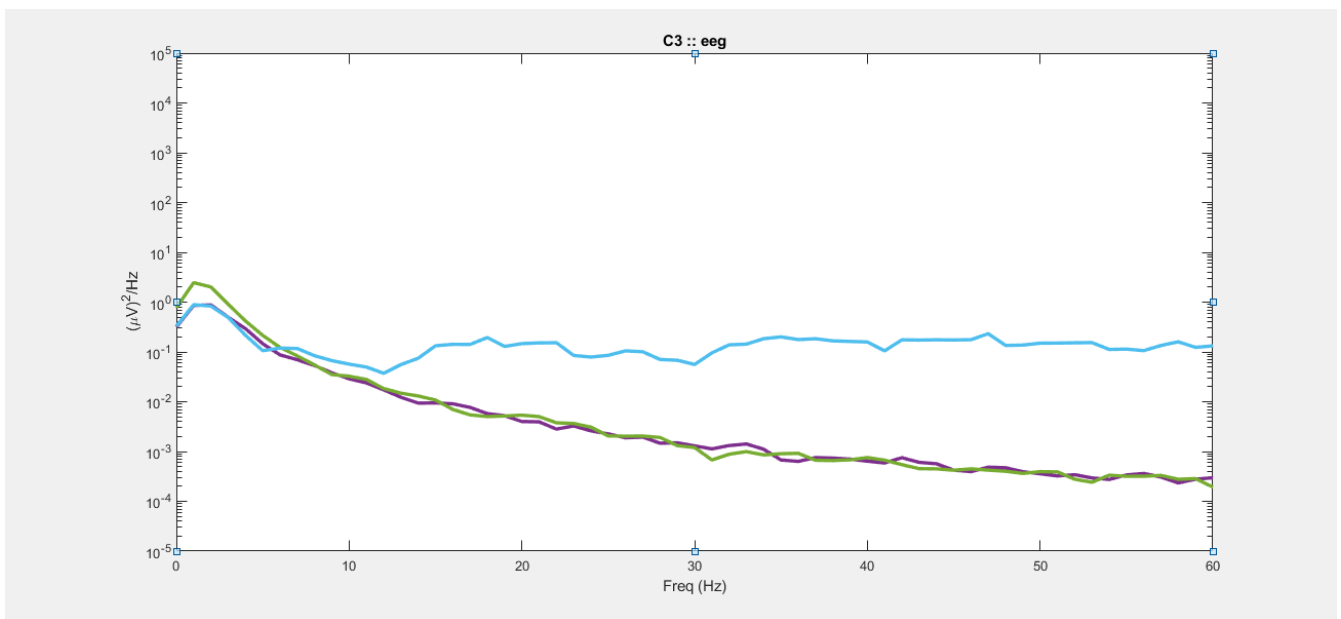
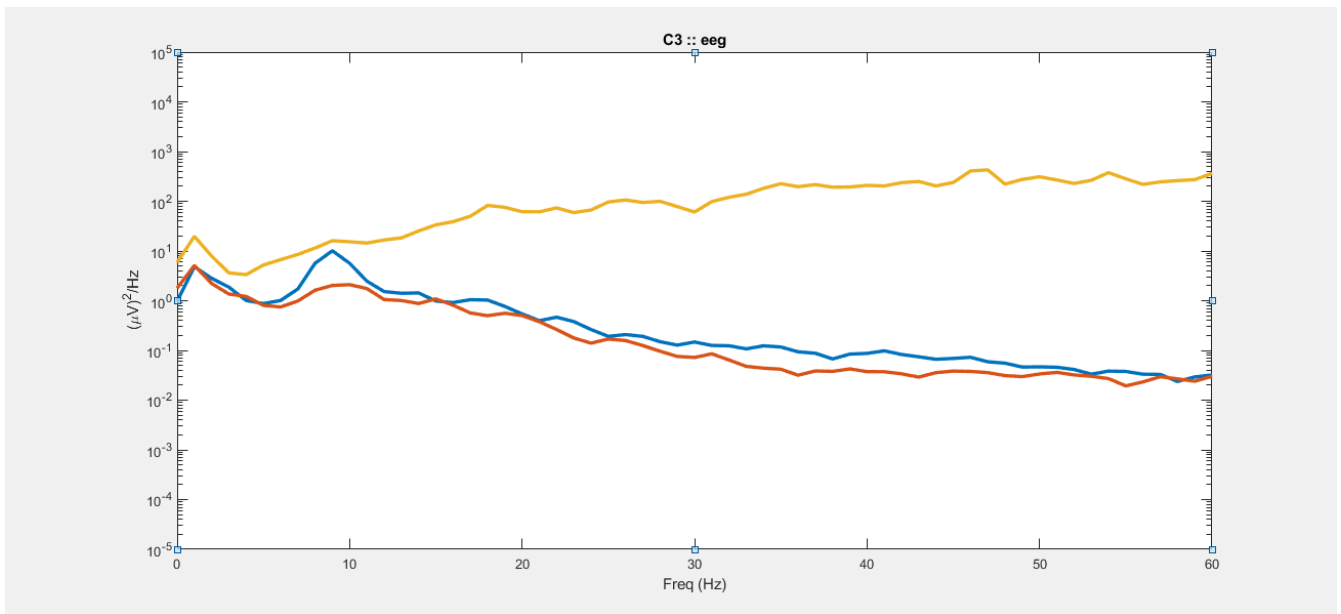


Figure 128. Graph shows electrode location C3. (top) shows software laplacian of tCRE EEG. (bottom) shows tCRE EEG

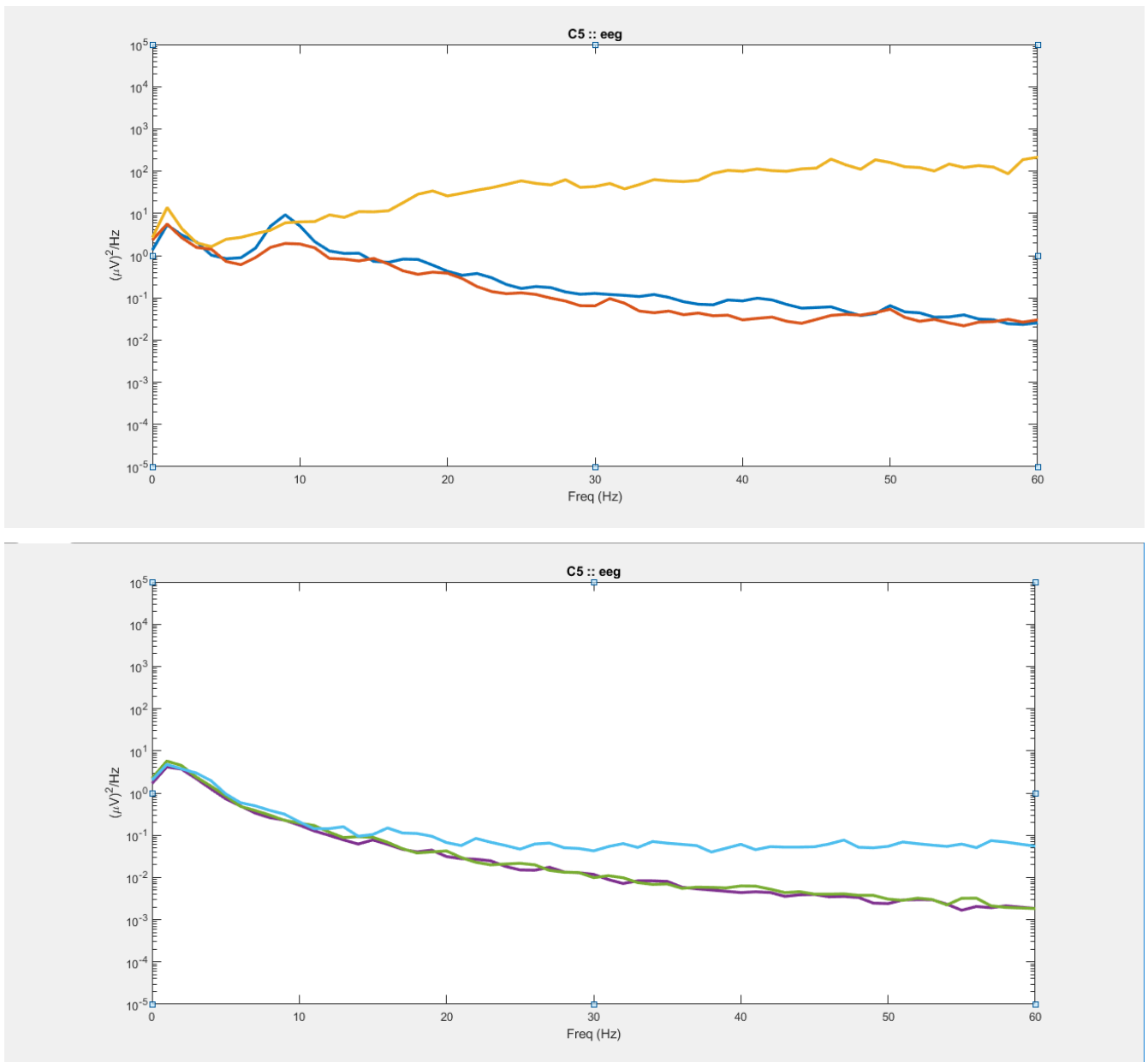


Figure 129. Graph shows electrode location C5. (top) shows software laplacian of tCRE EEG. (bottom) shows tCRE EEG

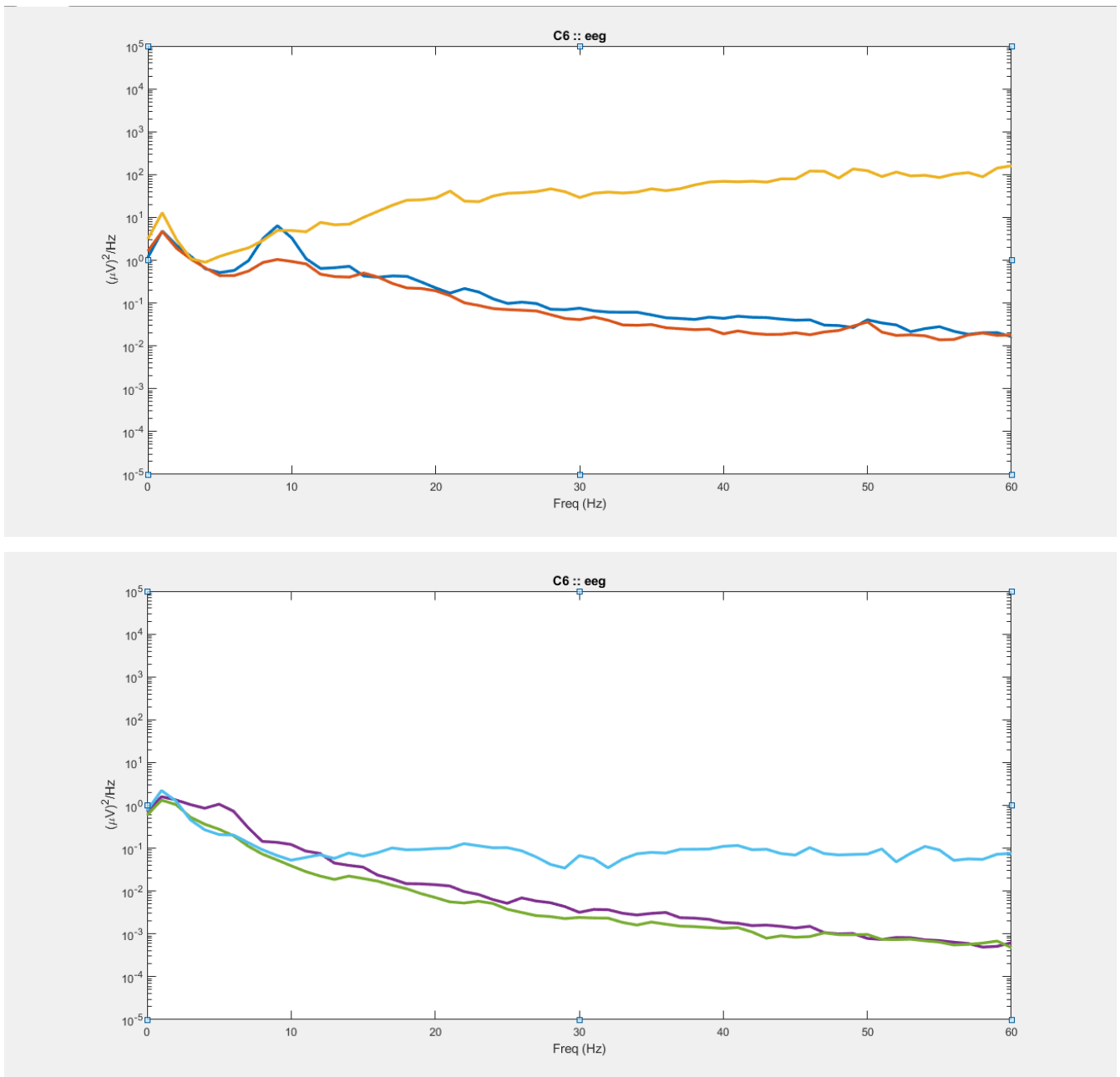


Figure 130. Graph shows electrode location C6. (top) shows software laplacian of tCRE EEG. (bottom) shows tCRE EEG

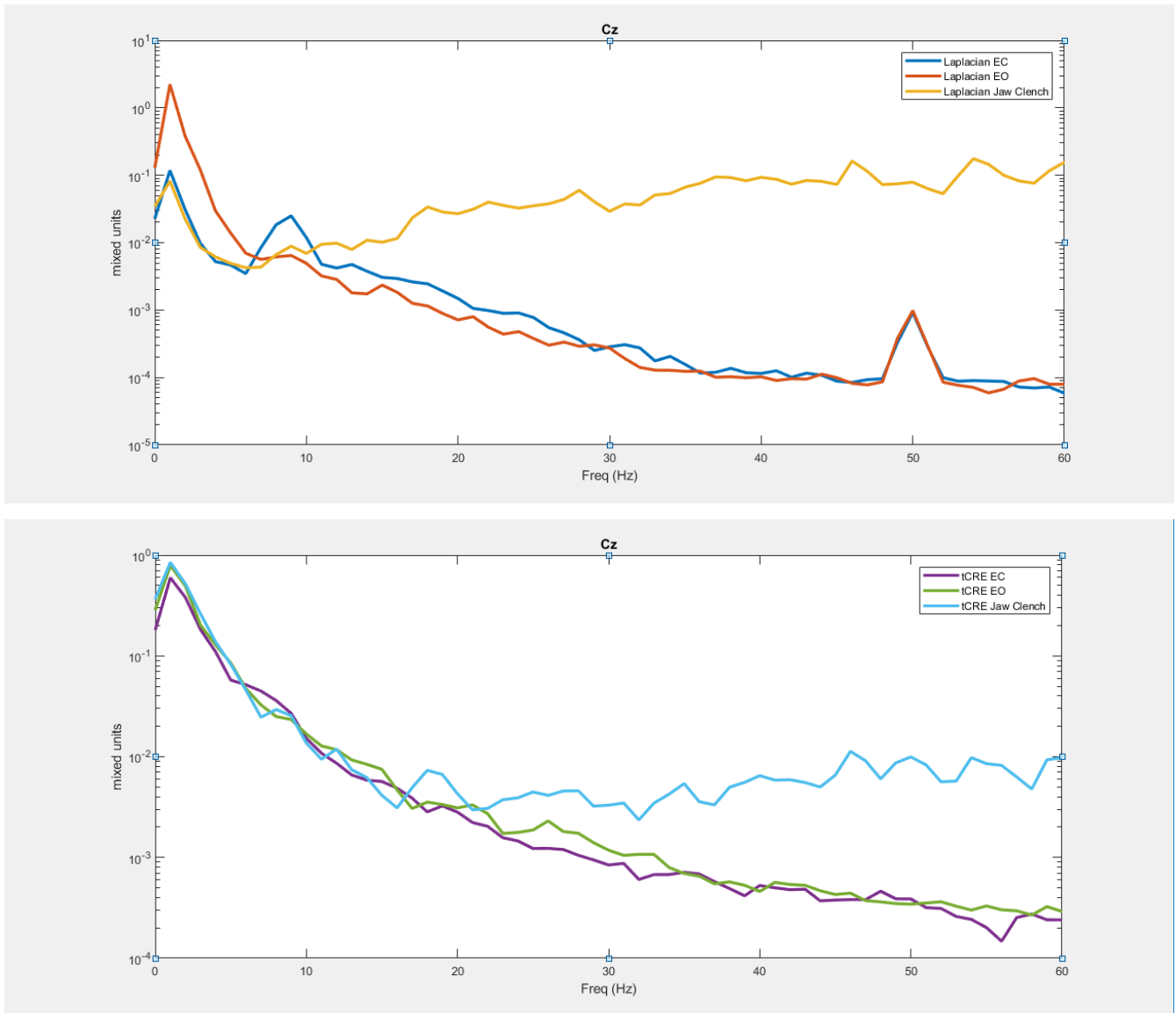


Figure 131. Graph shows electrode location Cz. (top) shows software laplacian of tCRE EEG. (bottom) shows tCRE EEG

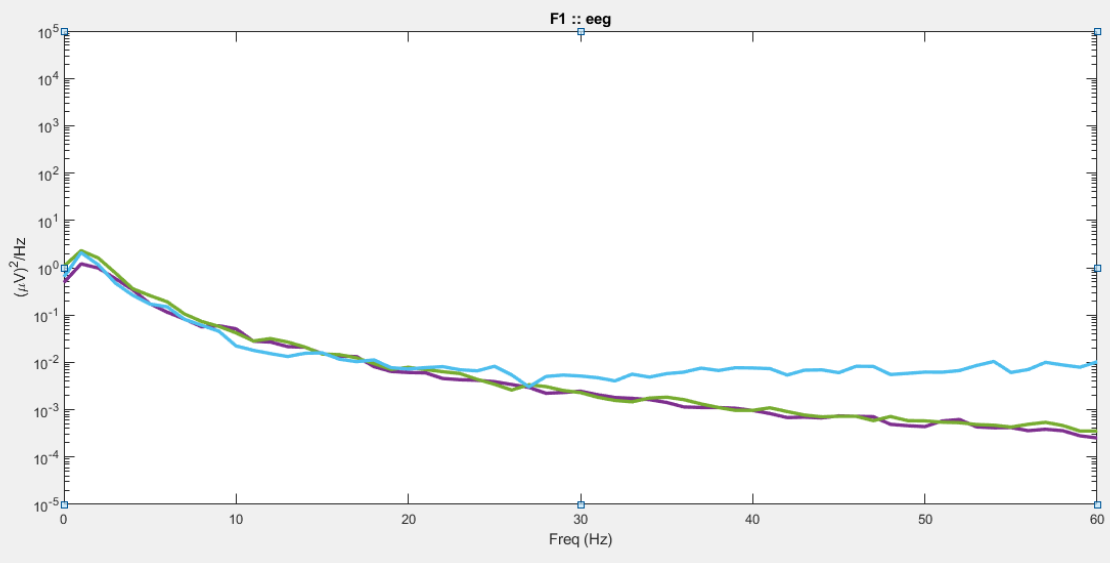
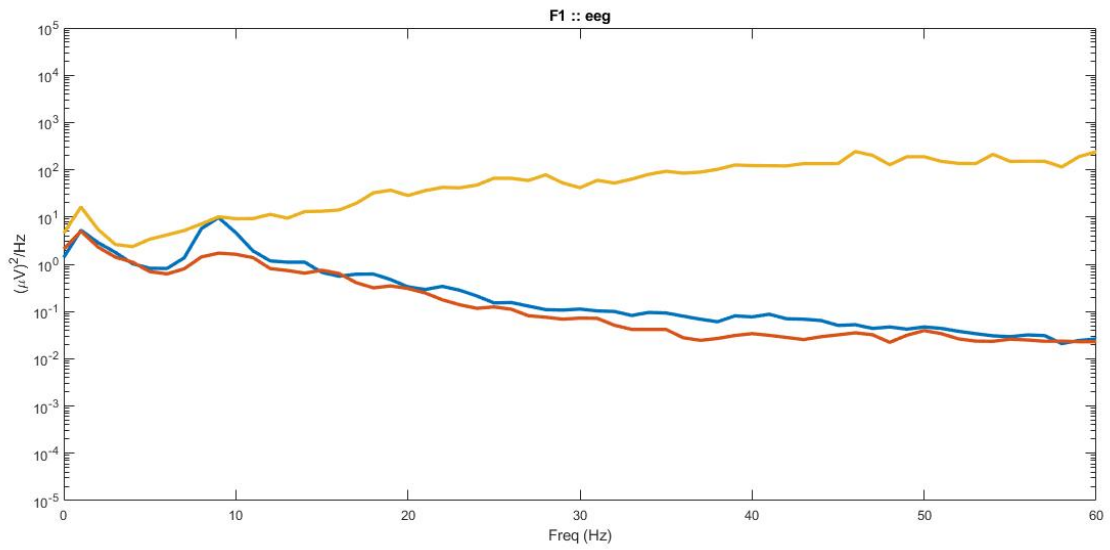


Figure 132. Graph shows electrode location F1. (top) shows software laplacian of tCRE EEG. (bottom) shows tCRE EEG

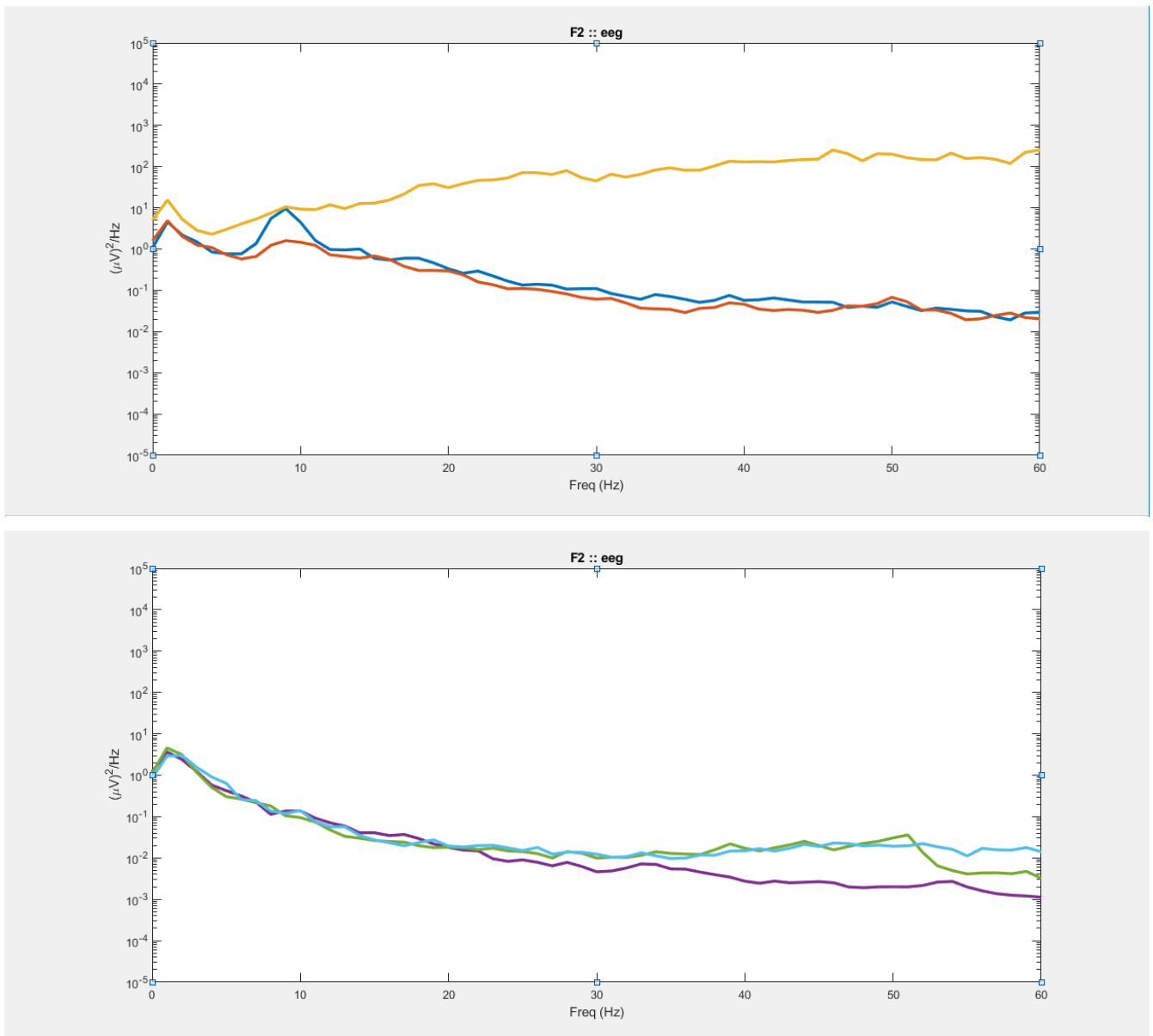


Figure 133. Graph shows electrode location F2. (top) shows software laplacian of tCRE EEG. (bottom) shows tCRE EEG

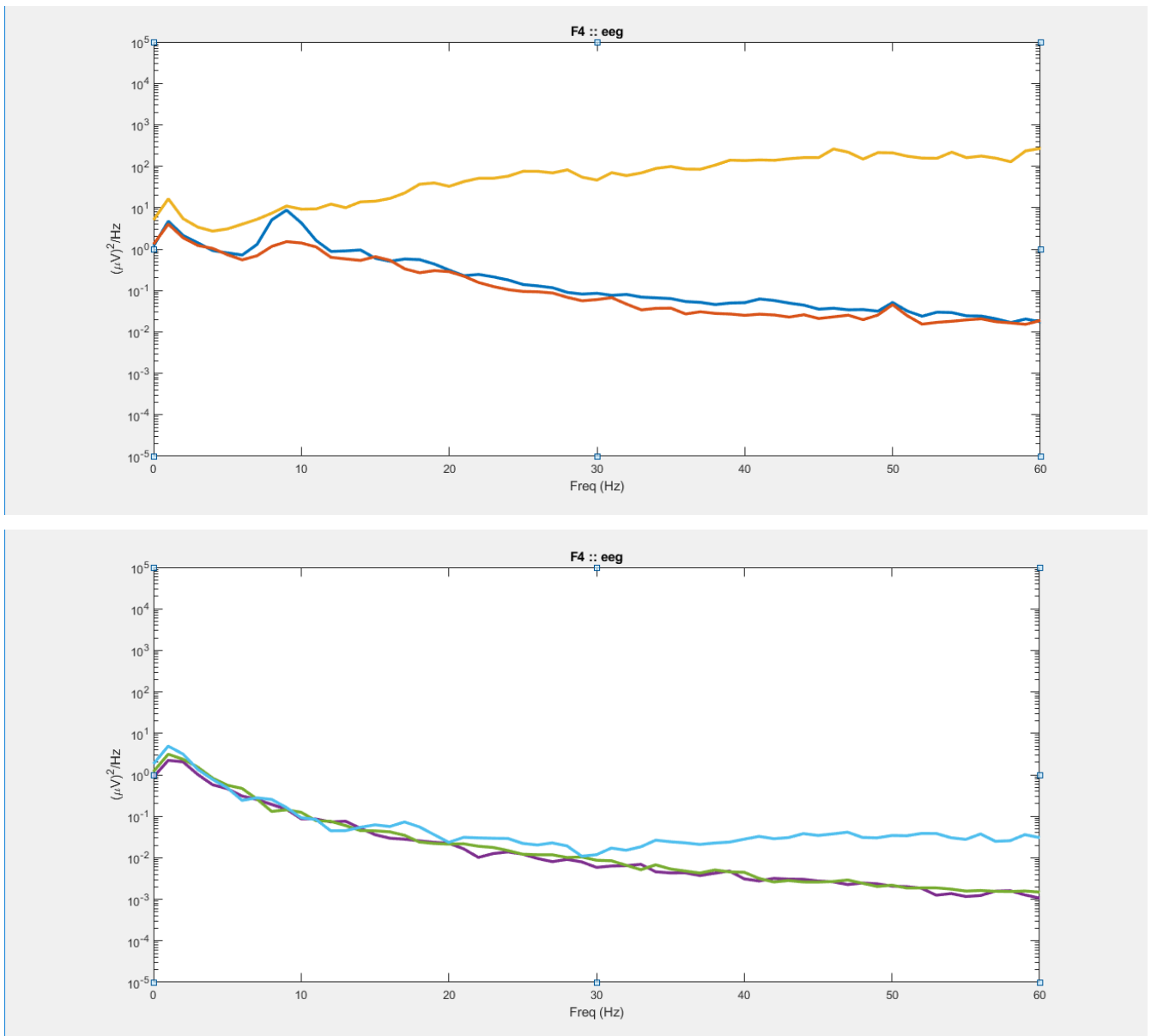


Figure 134. Graph shows electrode location F4. (top) shows software laplacian of tCRE EEG. (bottom) shows tCRE EEG

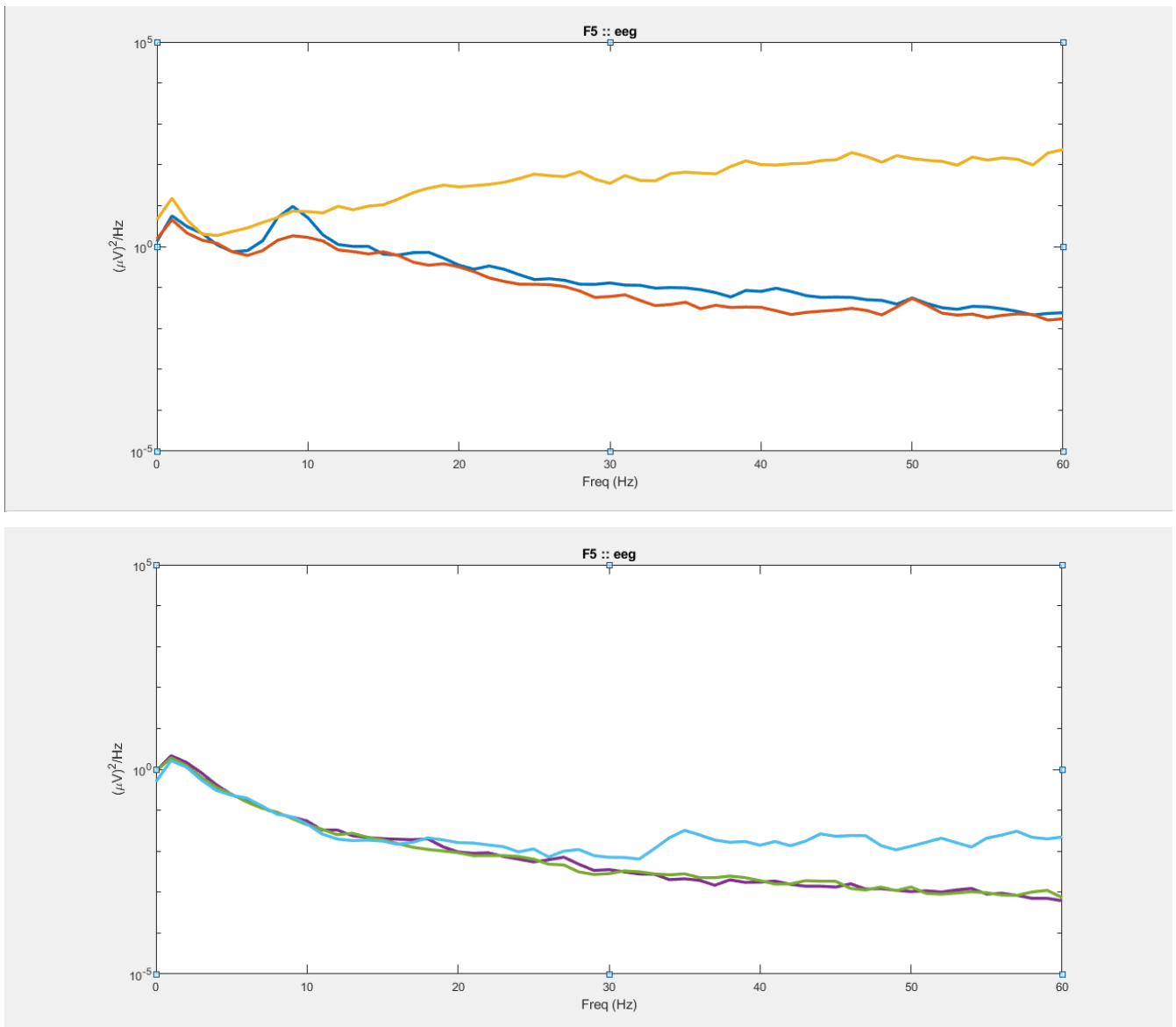


Figure 135. Graph shows electrode location F5. (top) shows software laplacian of tCRE EEG. (bottom) shows tCRE EEG

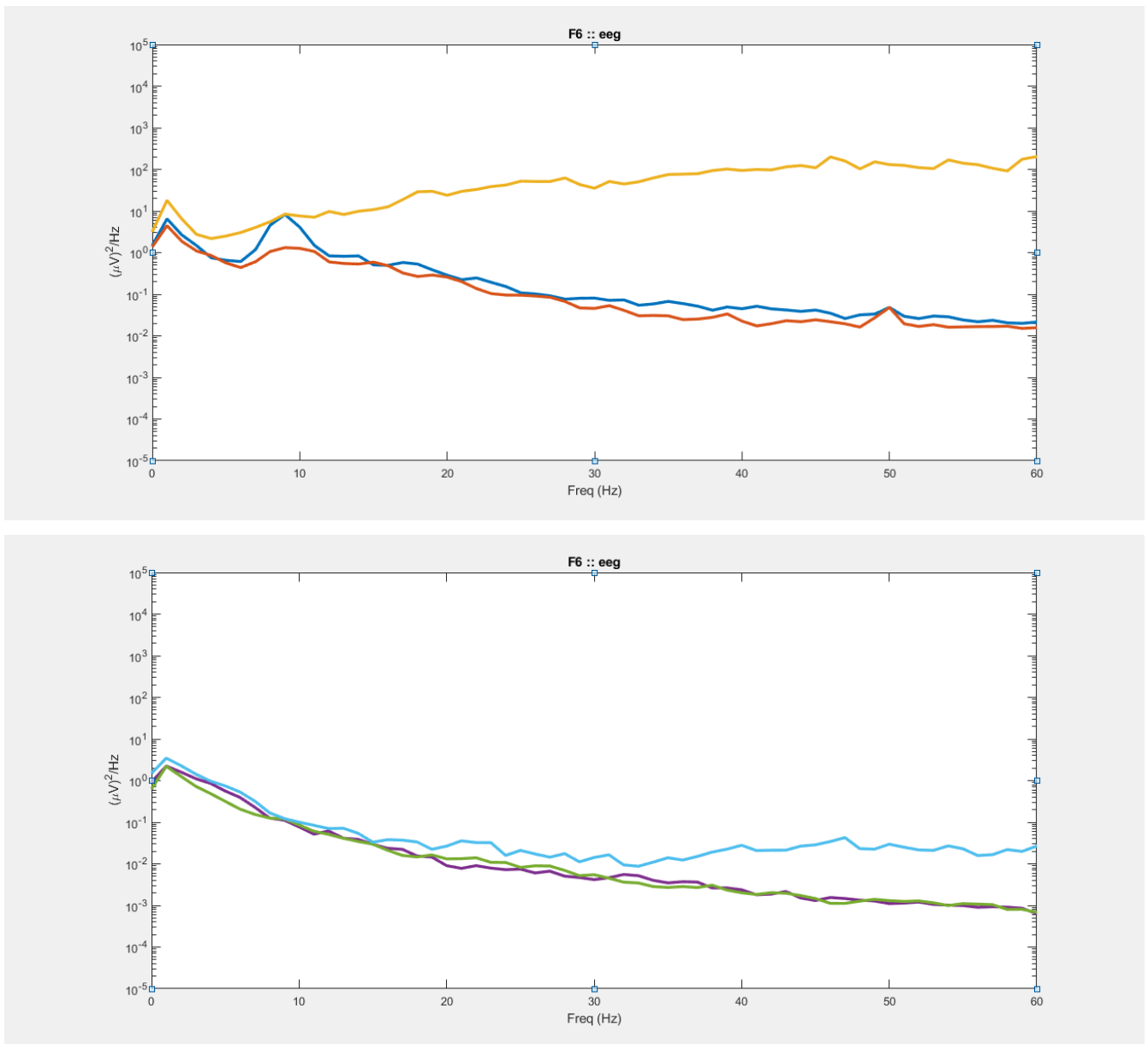


Figure 136. Graph shows electrode location F6. (top) shows software laplacian of tCRE EEG. (bottom) shows tCRE EEG

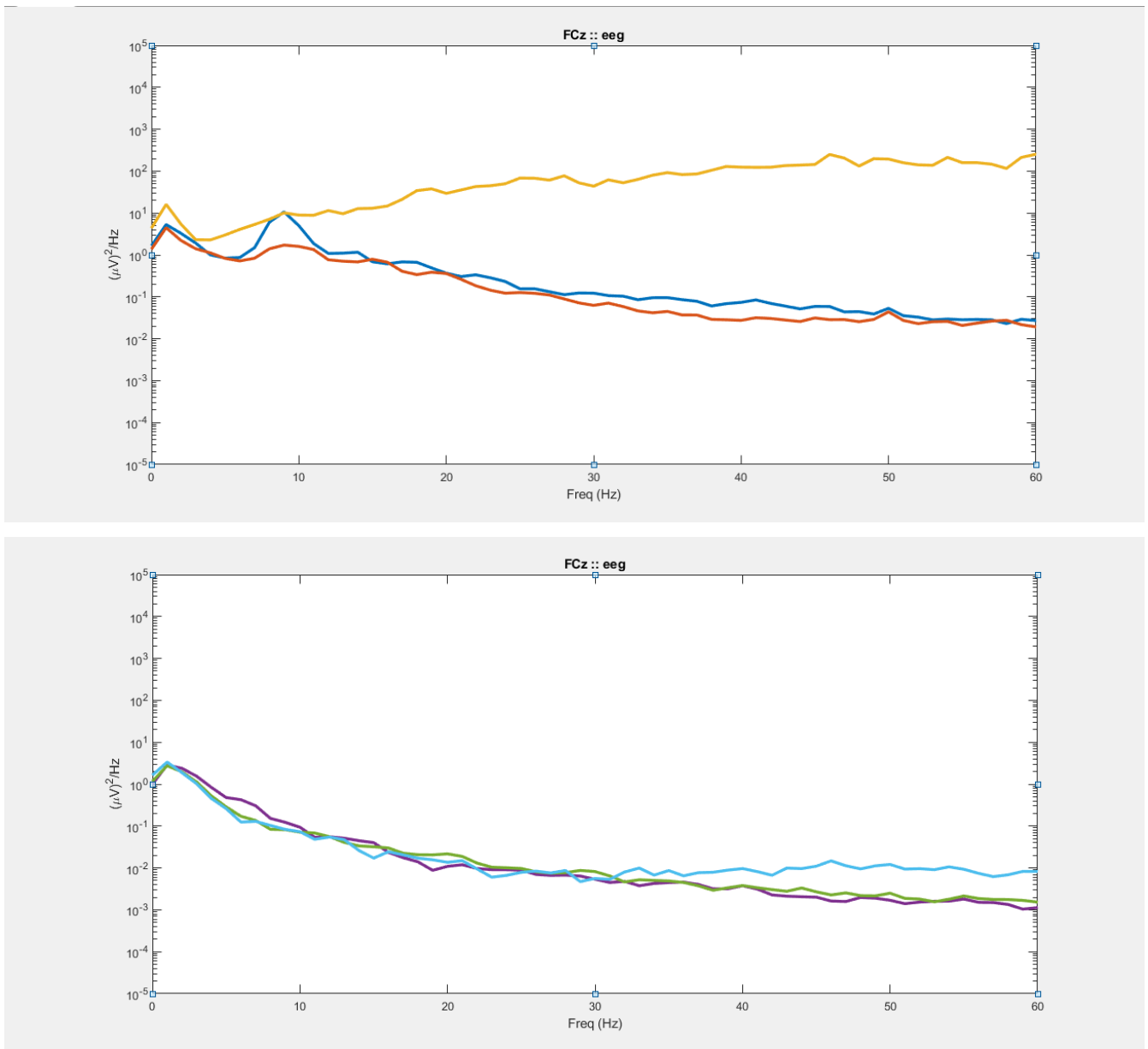


Figure 137. Graph shows electrode location FCz. (top) shows software laplacian of tCRE EEG. (bottom) shows tCRE EEG

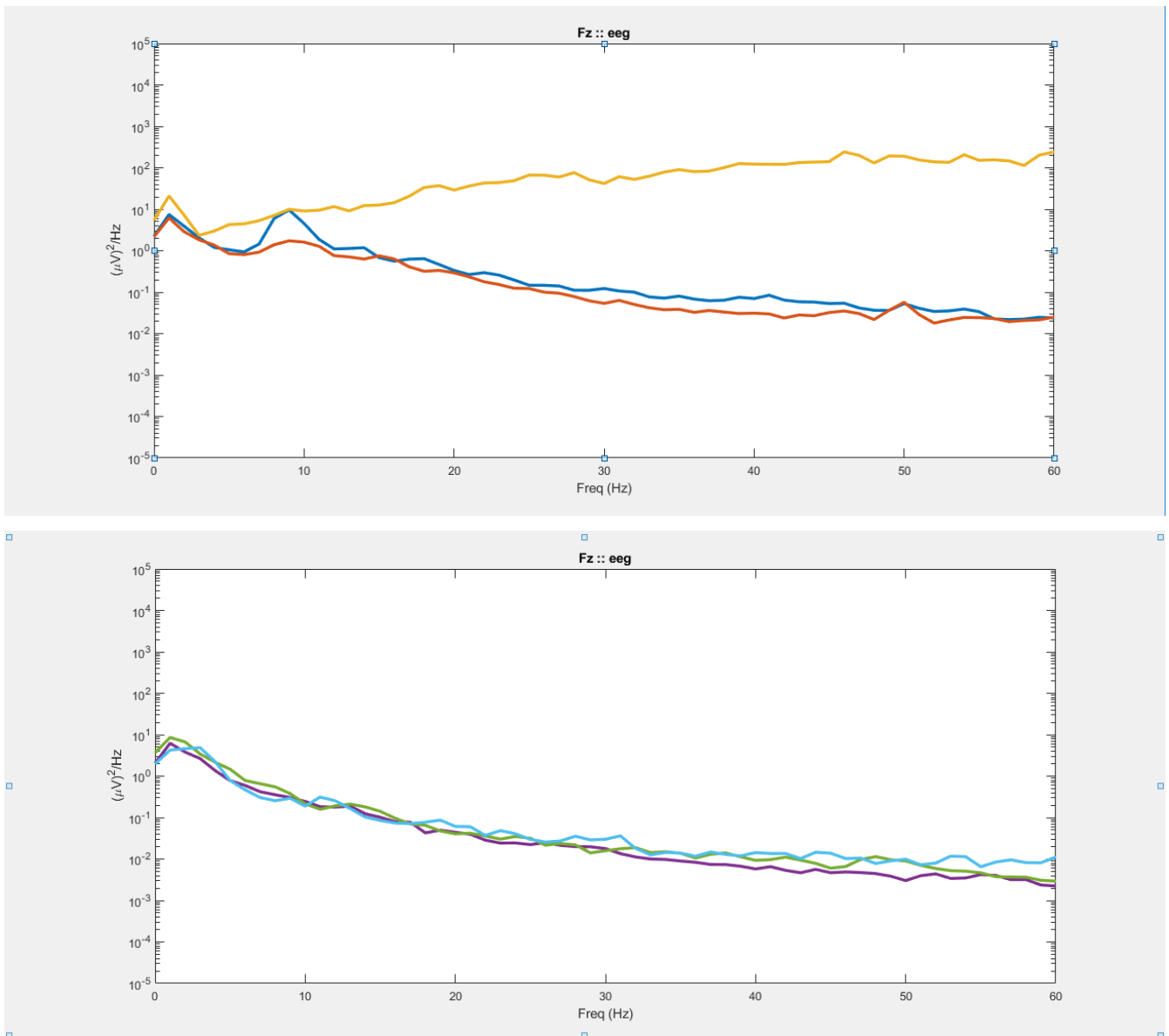


Figure 138. Graph shows electrode location Fz. (top) shows software laplacian of tCRE EEG. (bottom) shows tCRE EEG

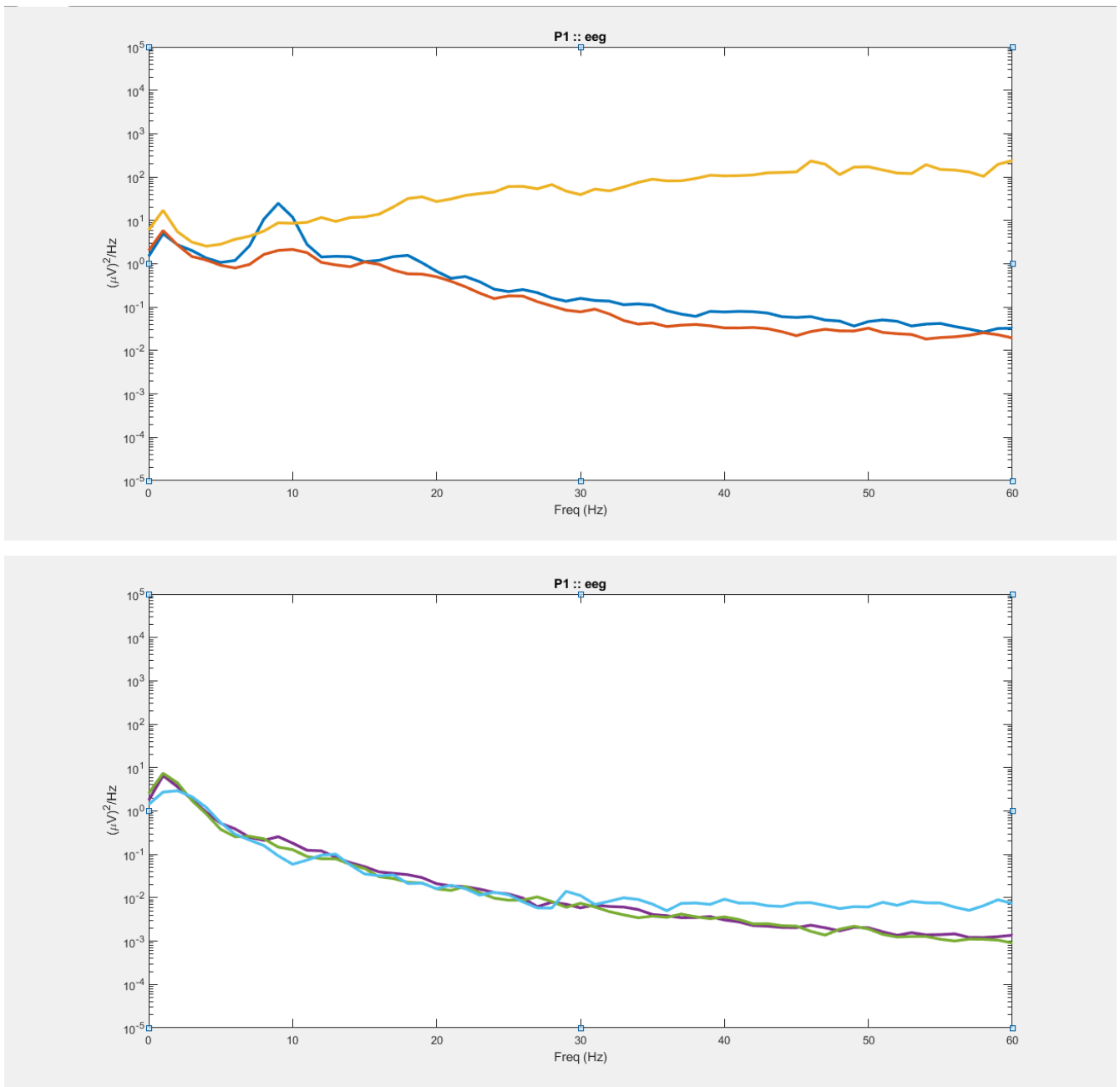


Figure 139. Graph shows electrode location P1. (top) shows software laplacian of tCRE EEG. (bottom) shows tCRE EEG

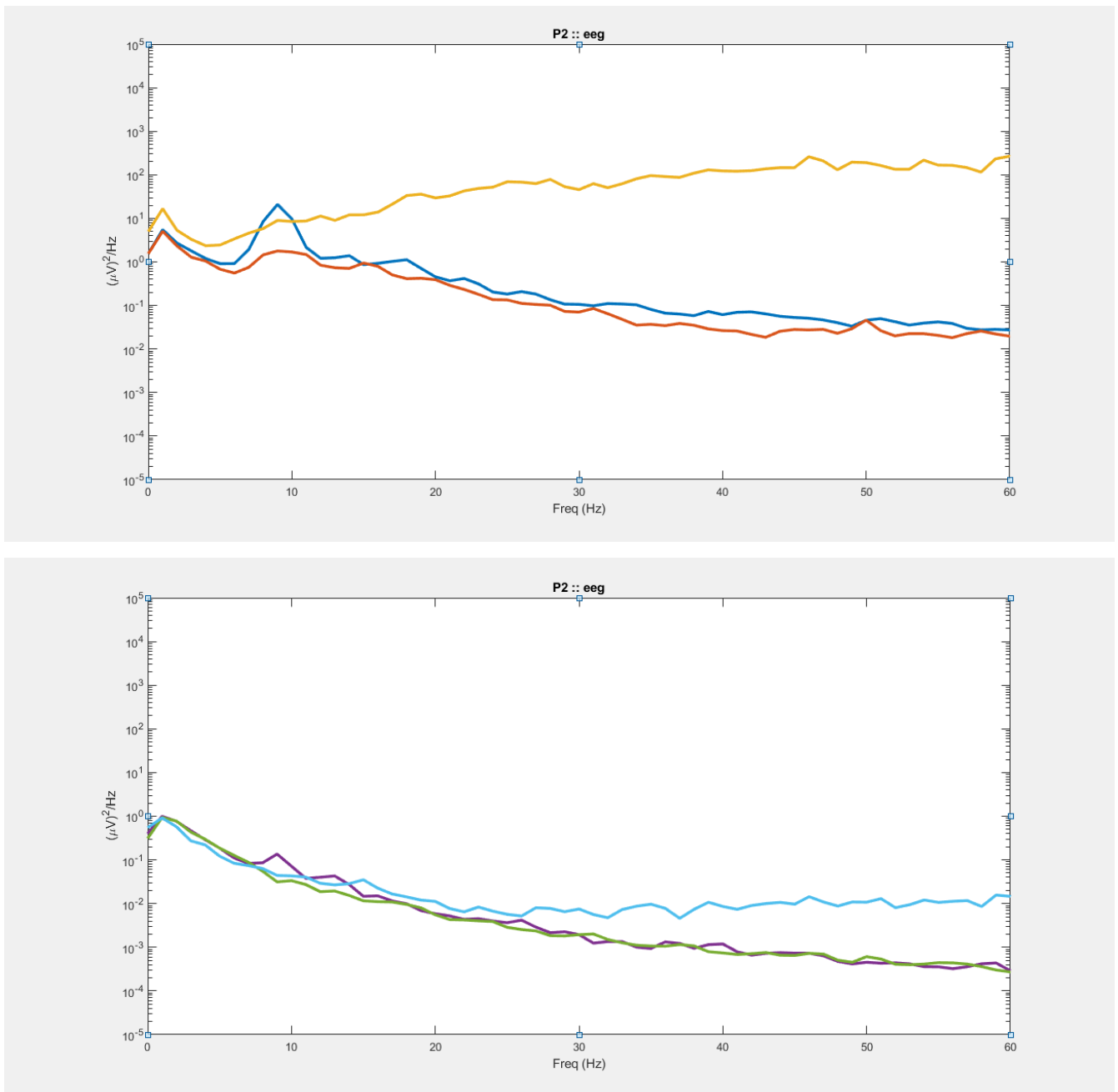


Figure 140. Graph shows electrode location P2. (top) shows software laplacian of tCRE EEG. (bottom) shows tCRE EEG

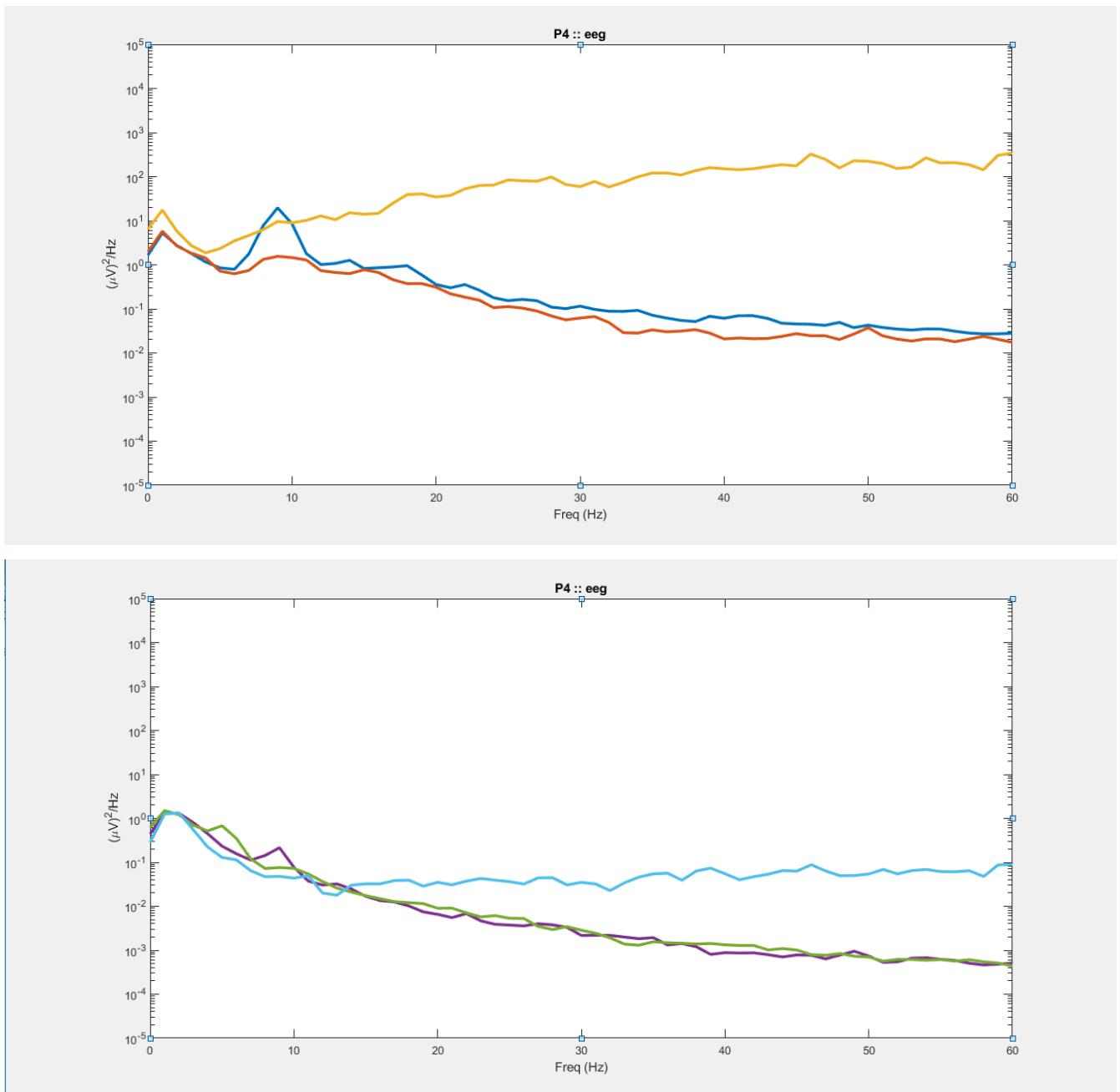


Figure 141. Graph shows electrode location P4. (top) shows software laplacian of tCRE EEG. (bottom) shows tCRE EEG

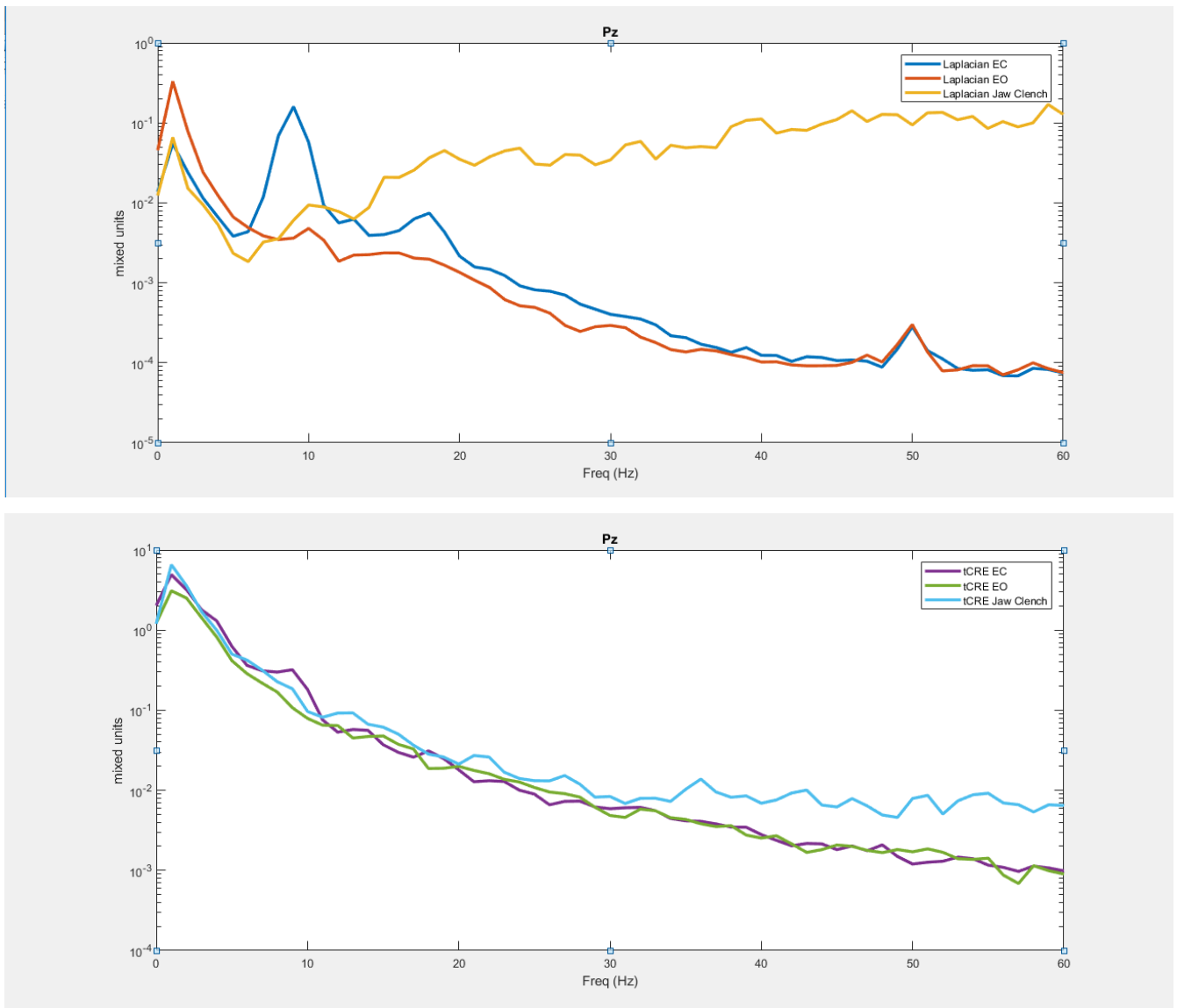


Figure 142. Graph shows electrode location Pz. (top) shows software laplacian of tCRE EEG. (bottom) shows tCRE EEG

9.2.2. tCRE electrodes periphery test (9 central + 11 peripheral electrodes)

9.2.2.1. tCRE electrode periphery test on subject with thin, wispy hair

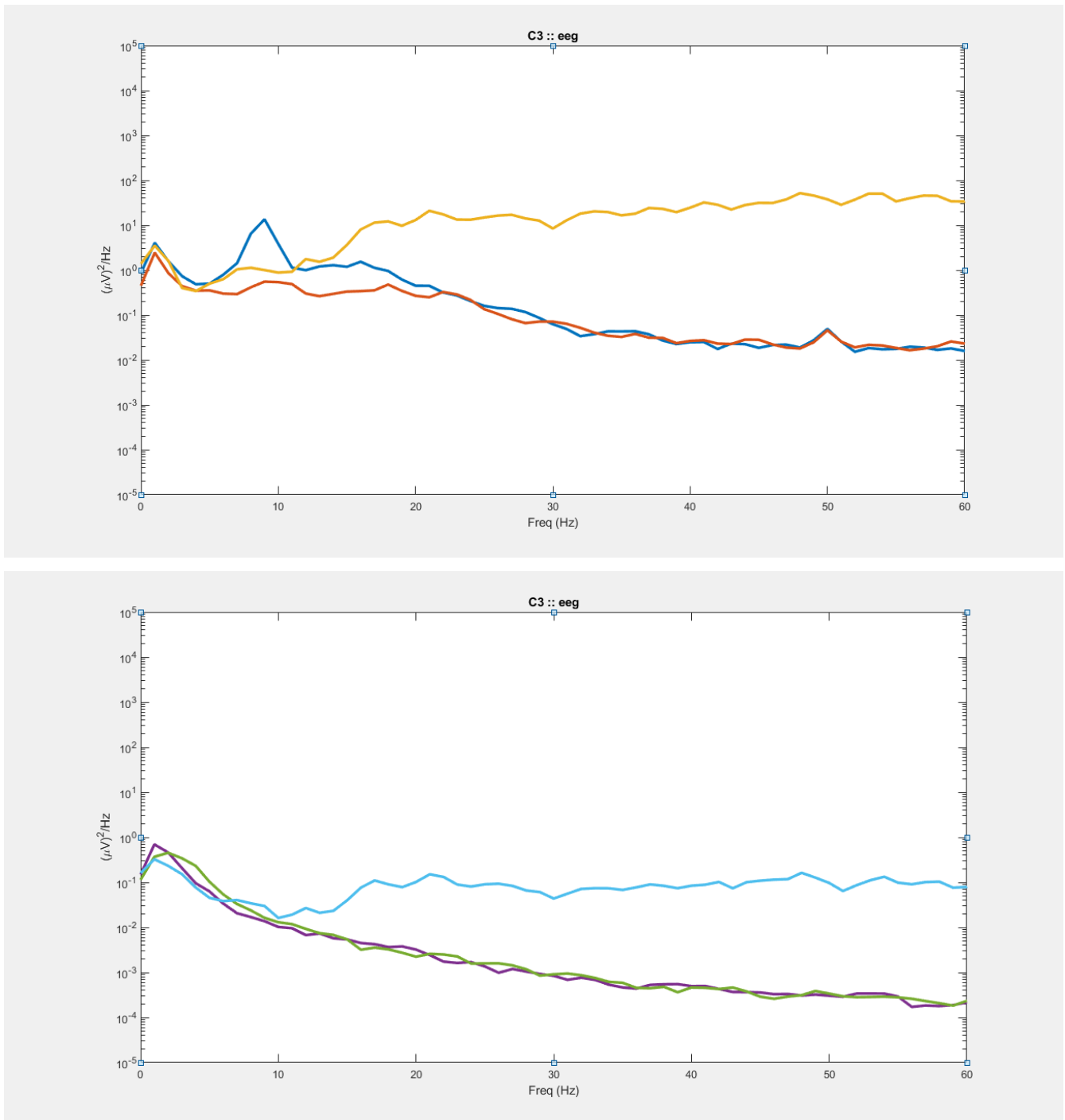


Figure 143. Graph shows electrode location C3. (top) shows software laplacian of tCRE EEG. (bottom) shows tCRE EEG

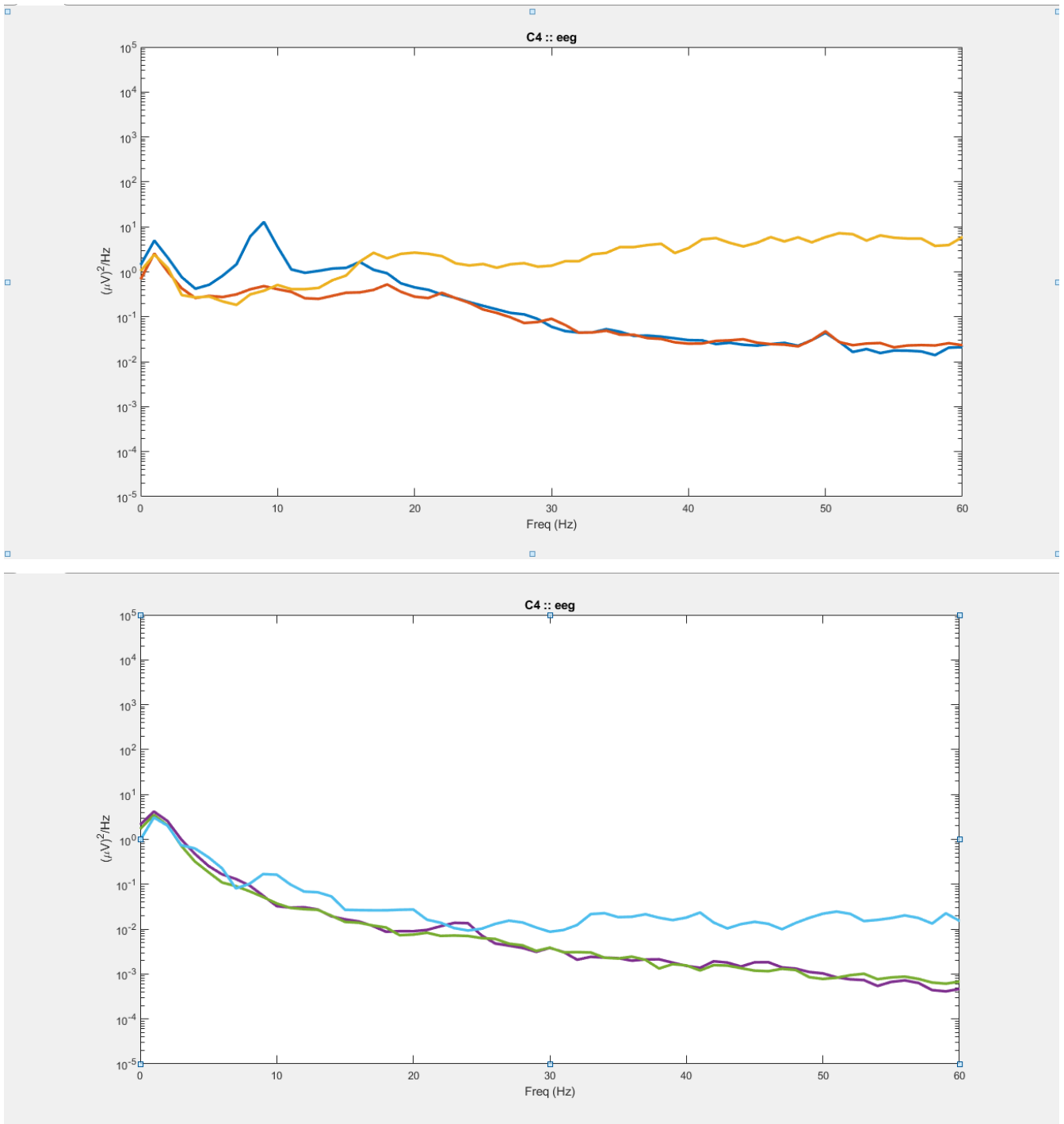


Figure 144. Graph shows electrode location C4. (top) shows software laplacian of tCRE EEG. (bottom) shows tCRE EEG

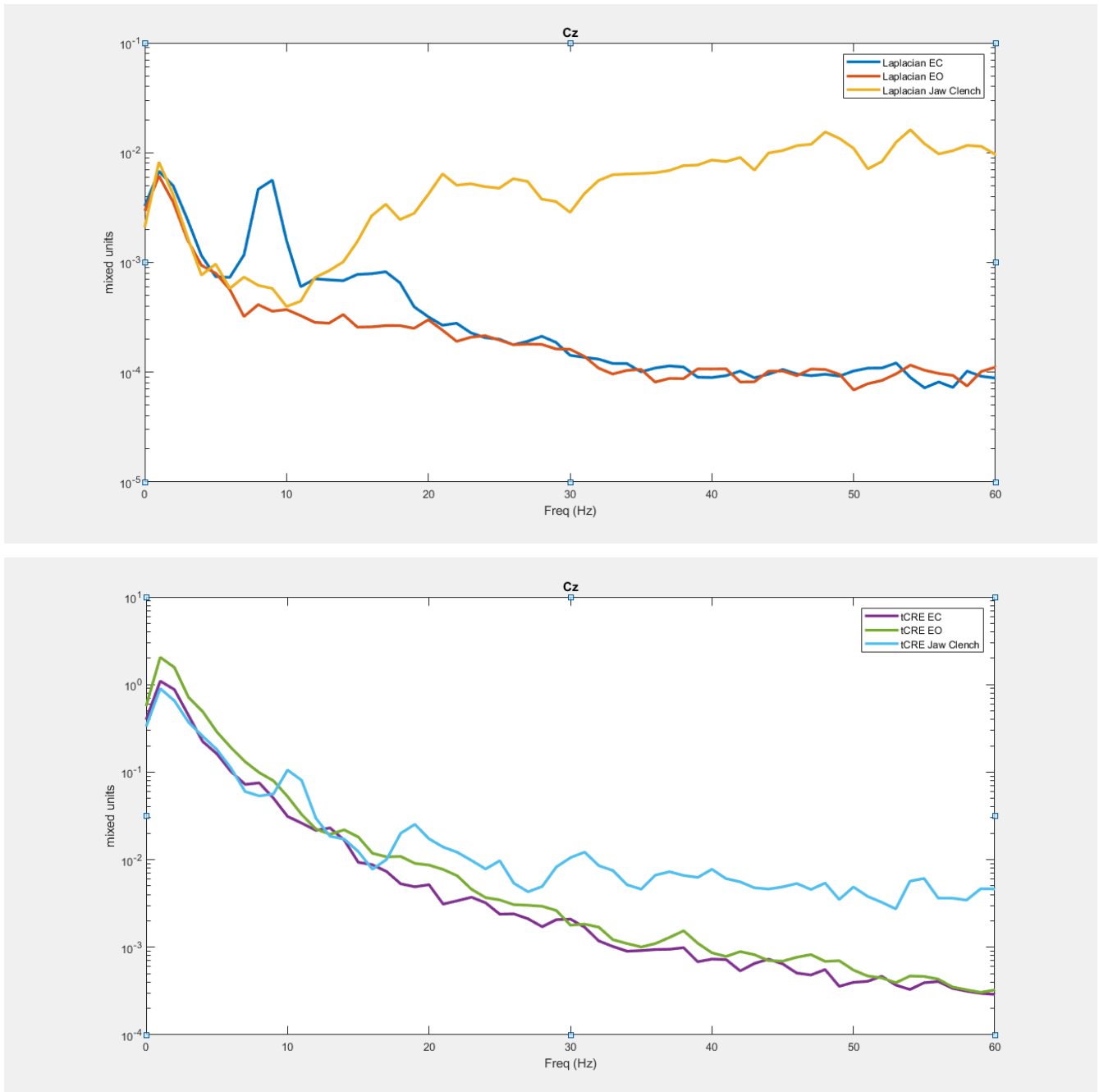


Figure 145. Graph shows electrode location Cz. (top) shows software laplacian of tCRE EEG. (bottom) shows tCRE EEG

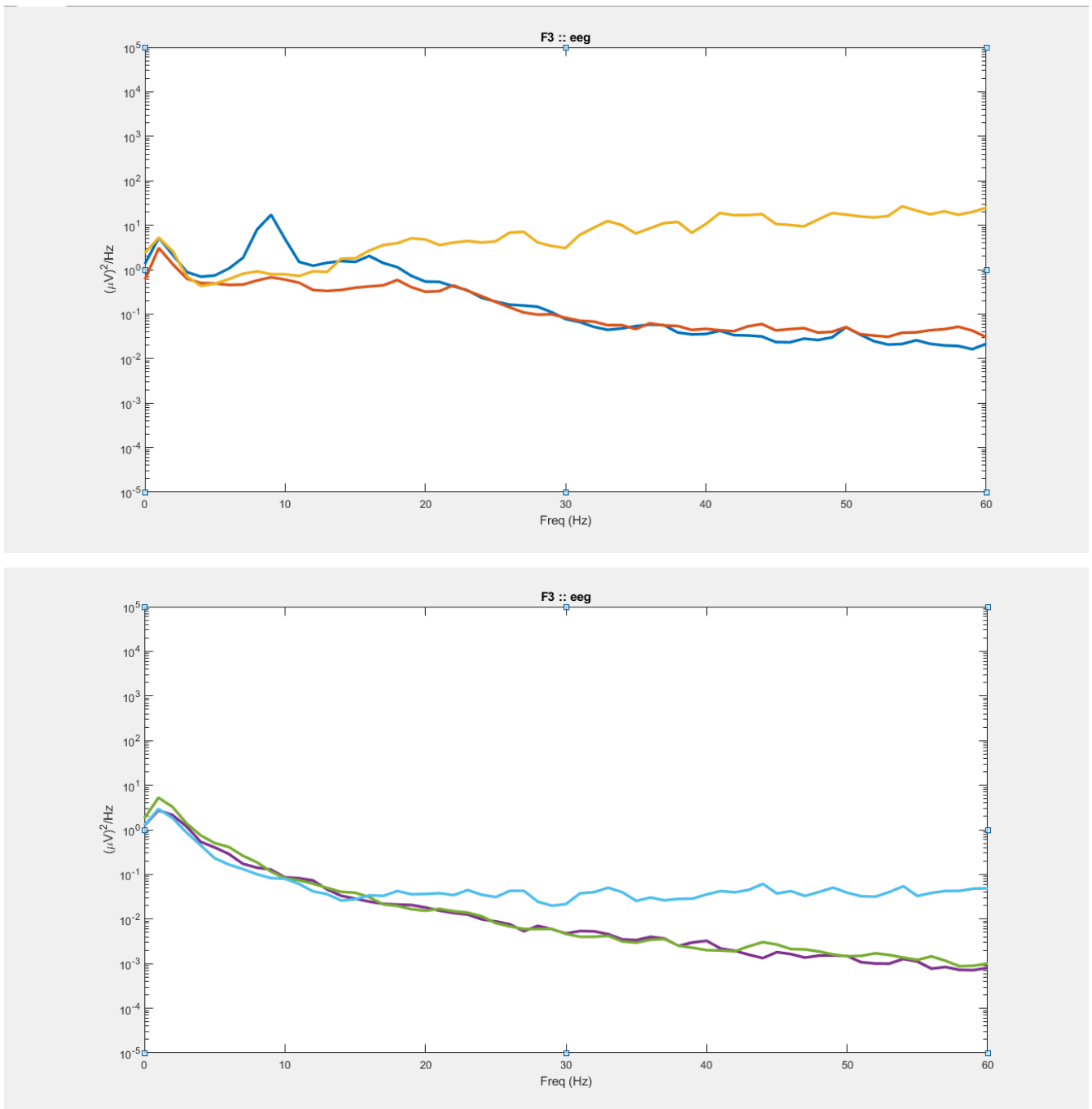


Figure 146. Graph shows electrode location F3. (top) shows software laplacian of tCRE EEG. (bottom) shows tCRE EEG

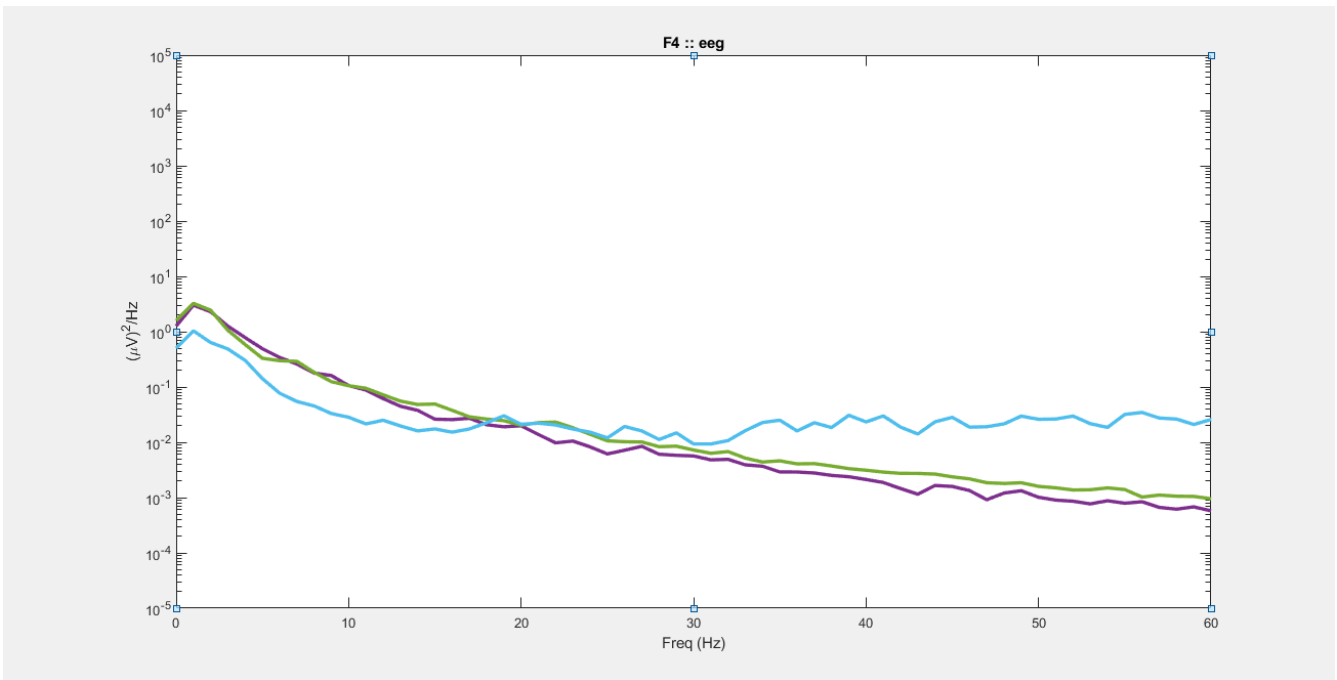
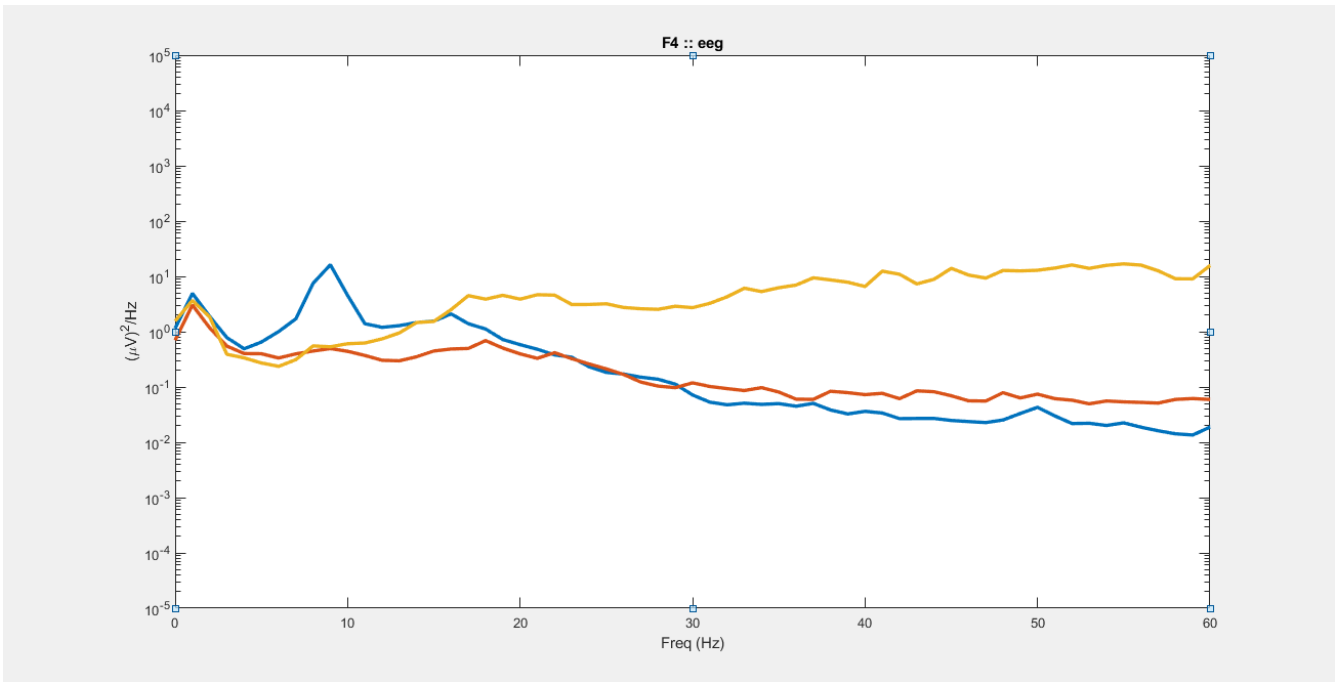


Figure 147. Graph shows electrode location F4. (top) shows software laplacian of tCRE EEG. (bottom) shows tCRE EEG

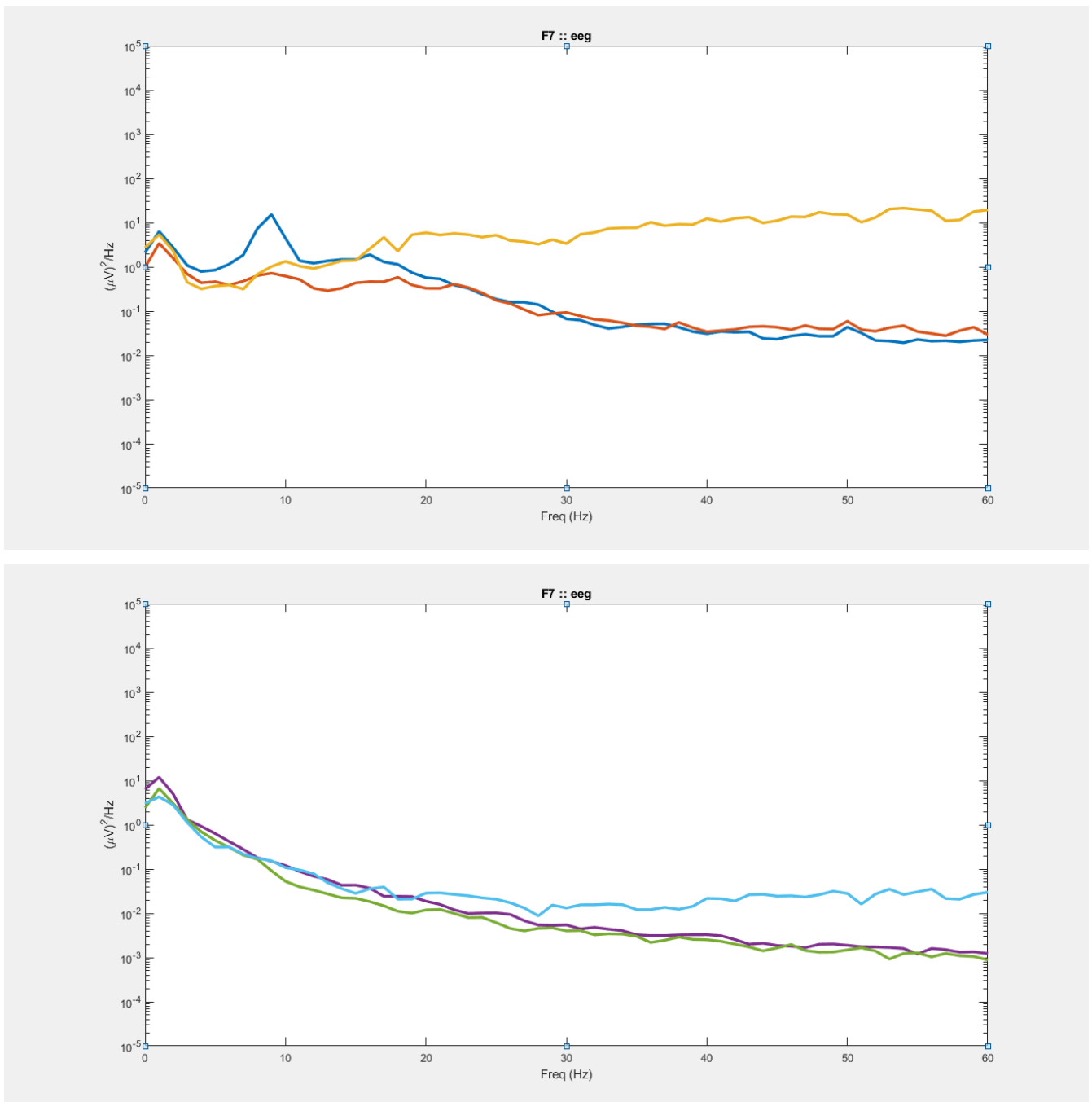


Figure 148. Graph shows electrode location F7. (top) shows software laplacian of tCRE EEG. (bottom) shows tCRE EEG

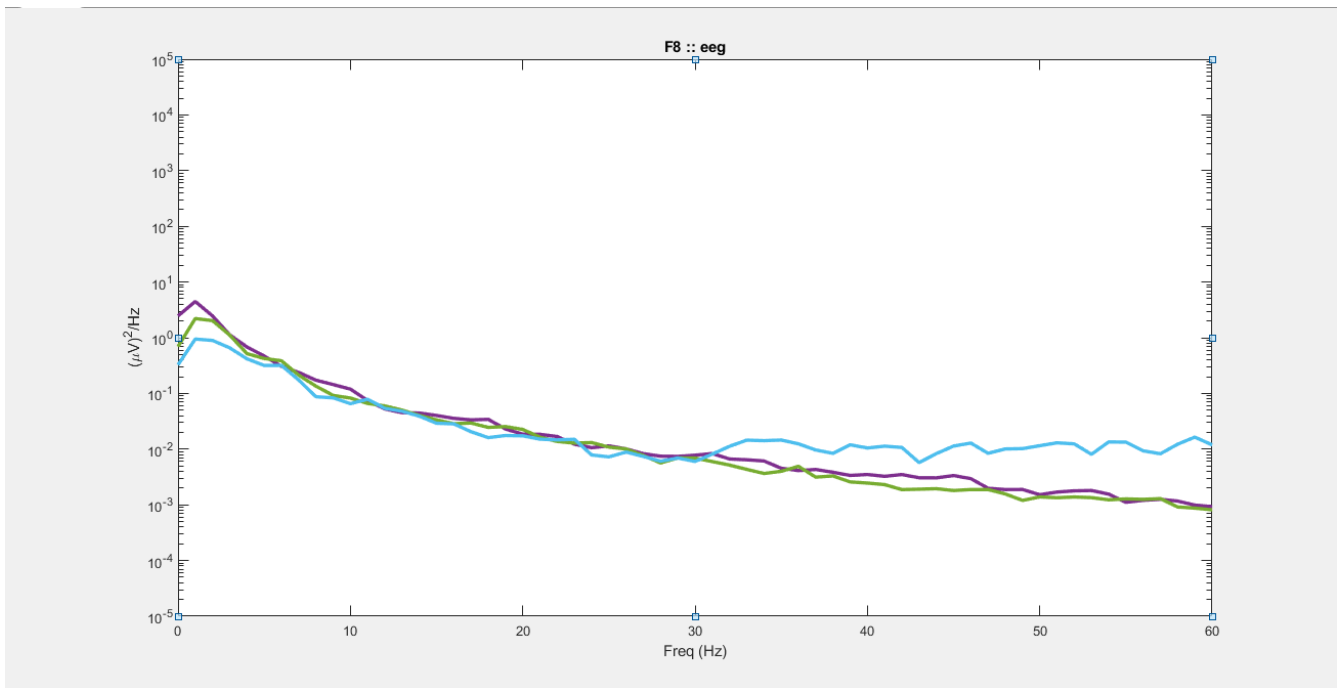
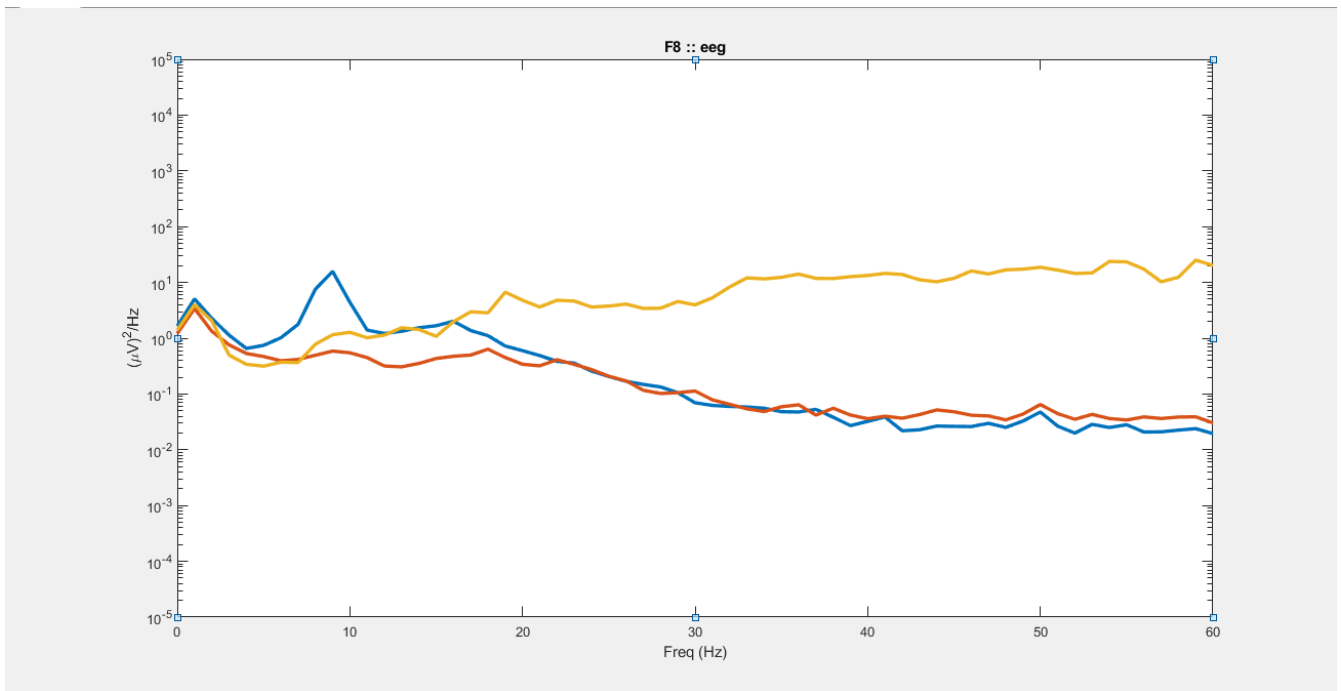


Figure 149. Graph shows electrode location F8. (top) shows software laplacian of tCRE EEG. (bottom) shows tCRE EEG

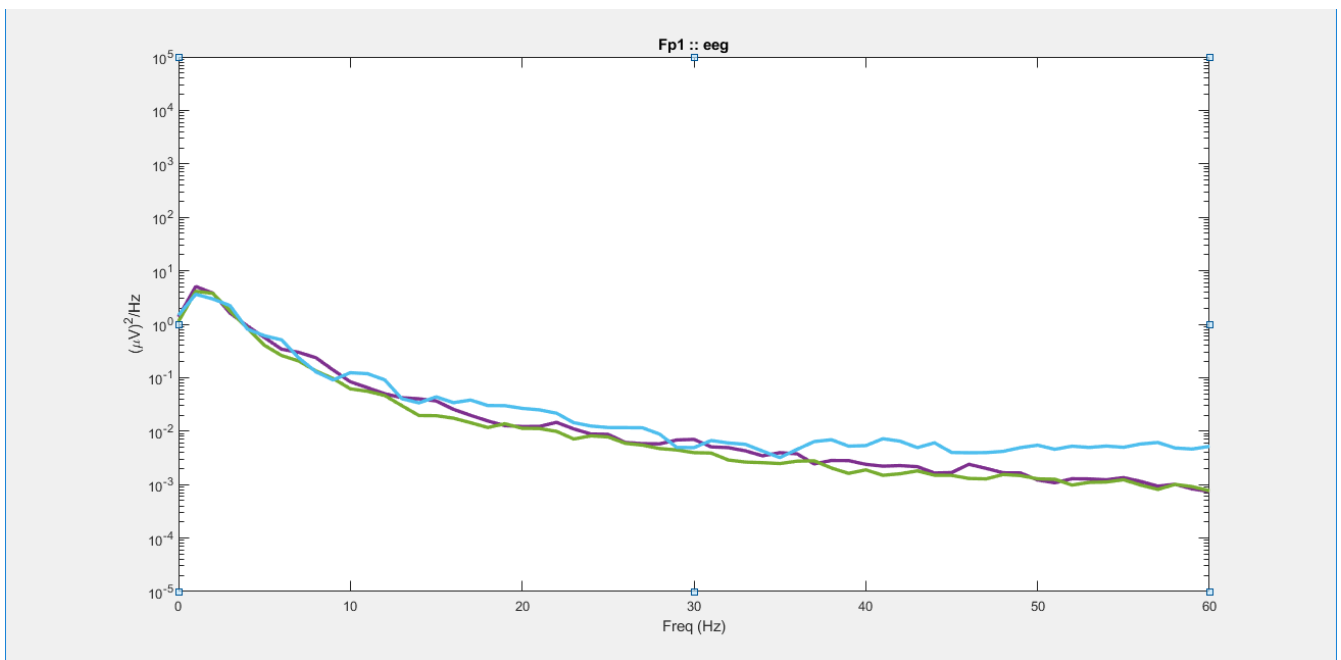
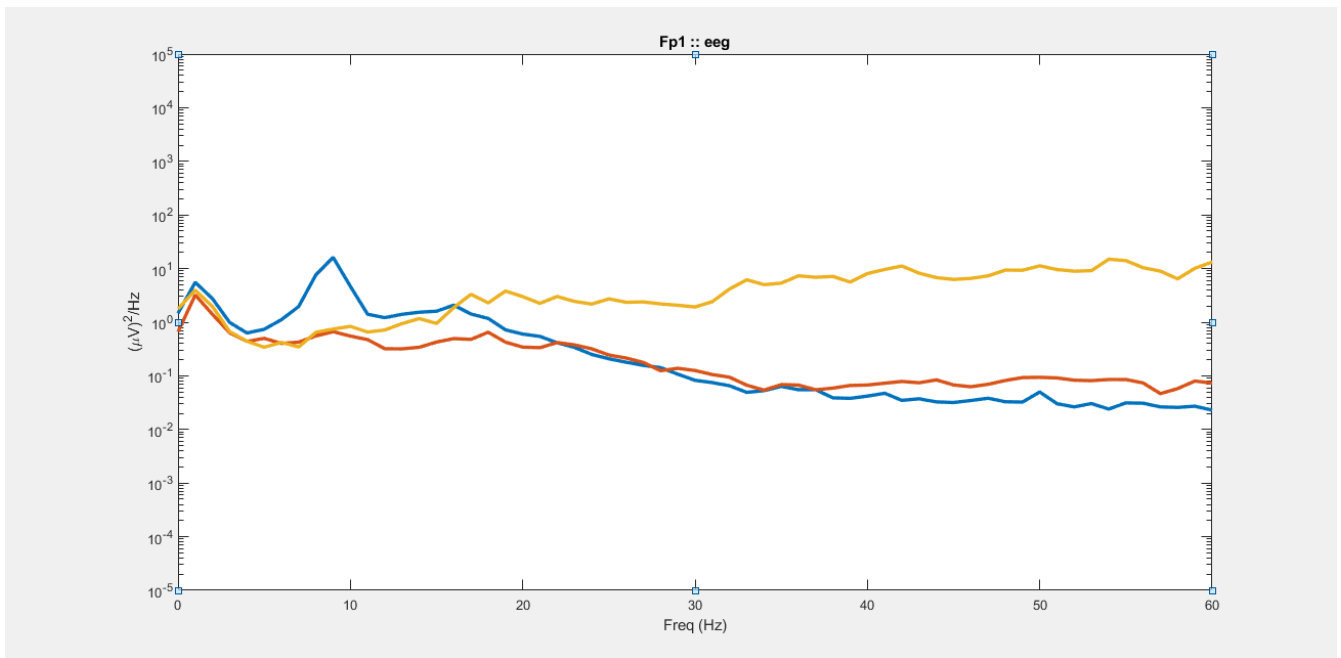


Figure 150. Graph shows electrode location Fp1. (top) shows software laplacian of tCRE EEG. (bottom) shows tCRE EEG

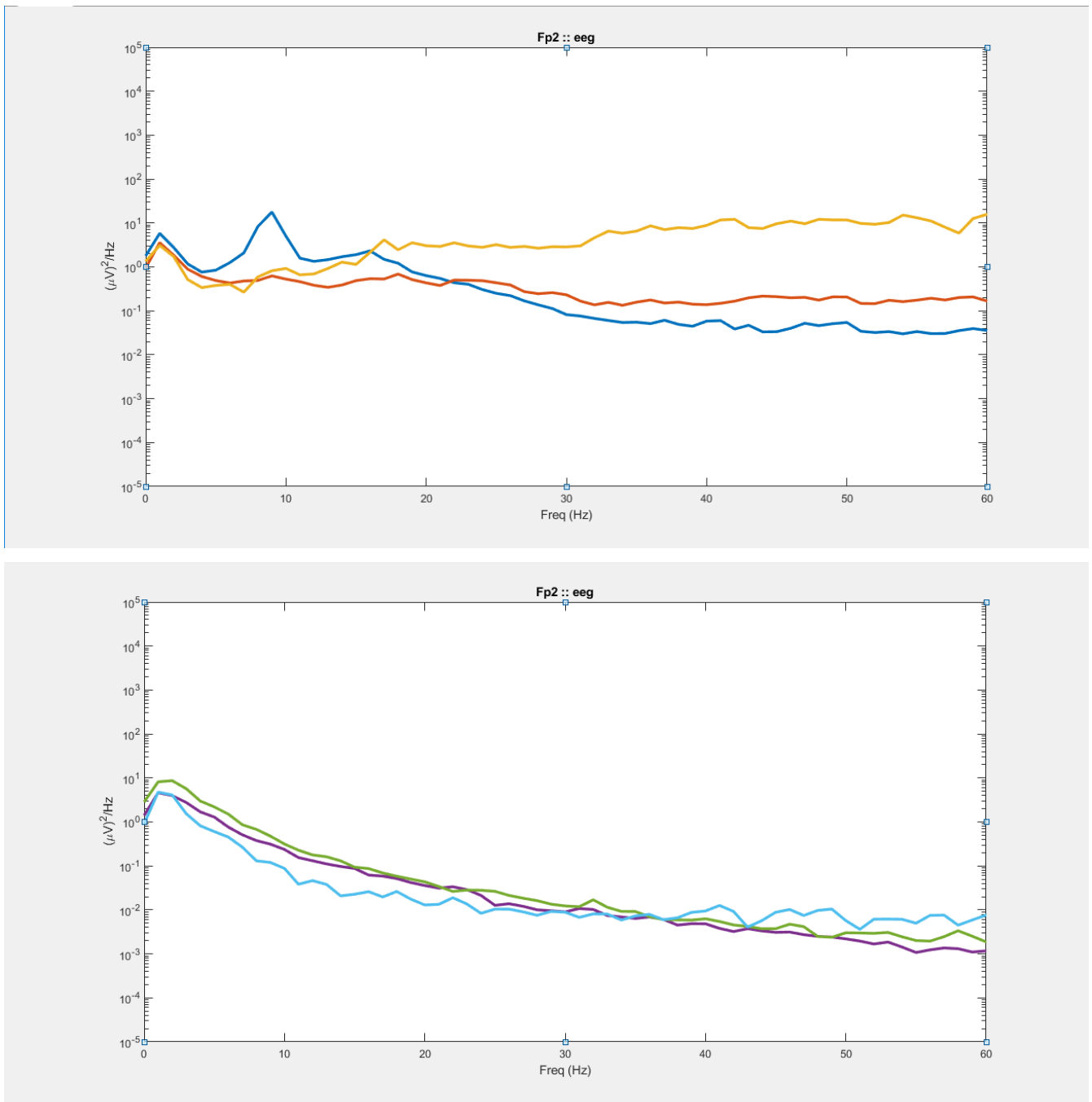


Figure 151. Graph shows electrode location Fp2. (top) shows software laplacian of tCRE EEG. (bottom) shows tCRE EEG

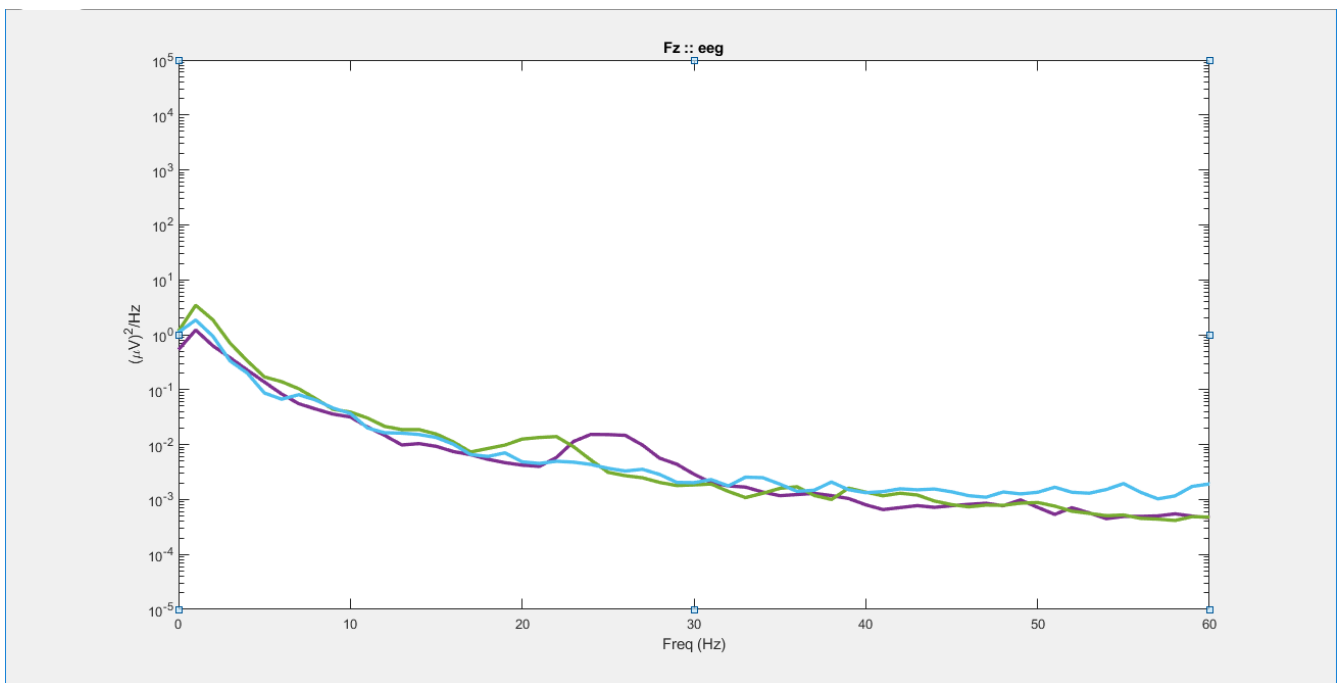
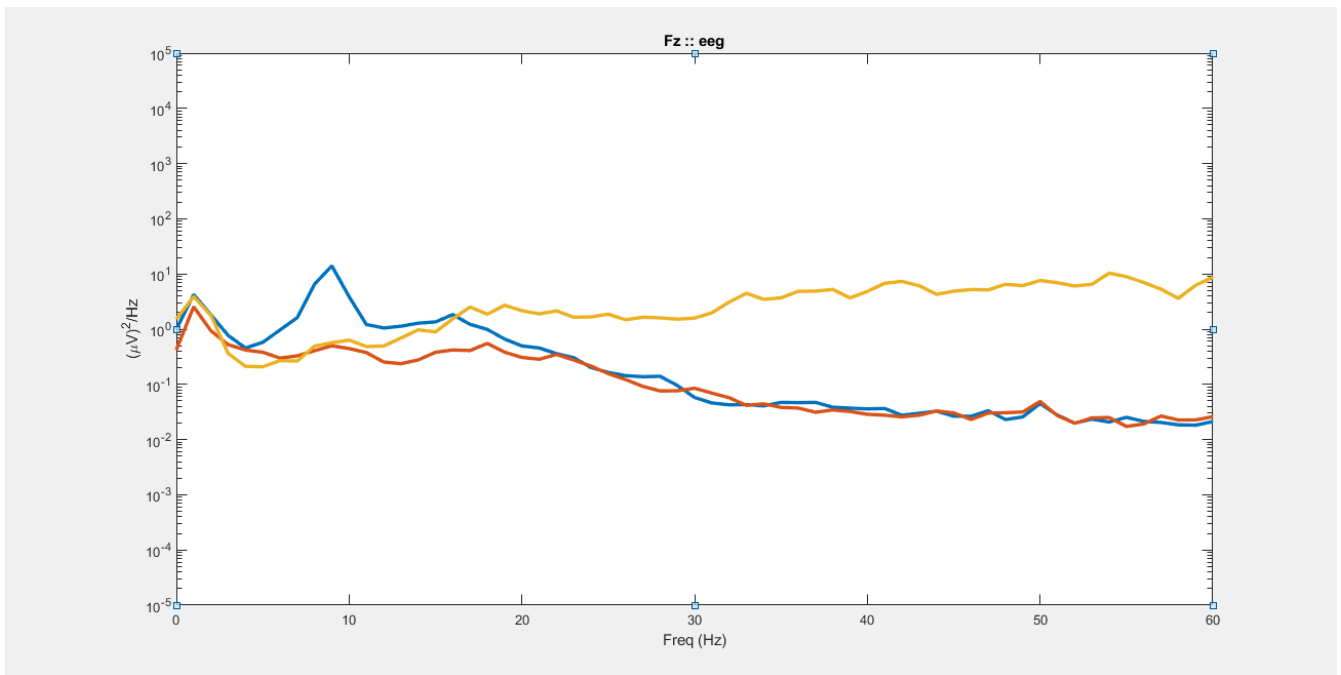


Figure 152. Graph shows electrode location Fz. (top) shows software laplacian of tCRE EEG. (bottom) shows tCRE EEG

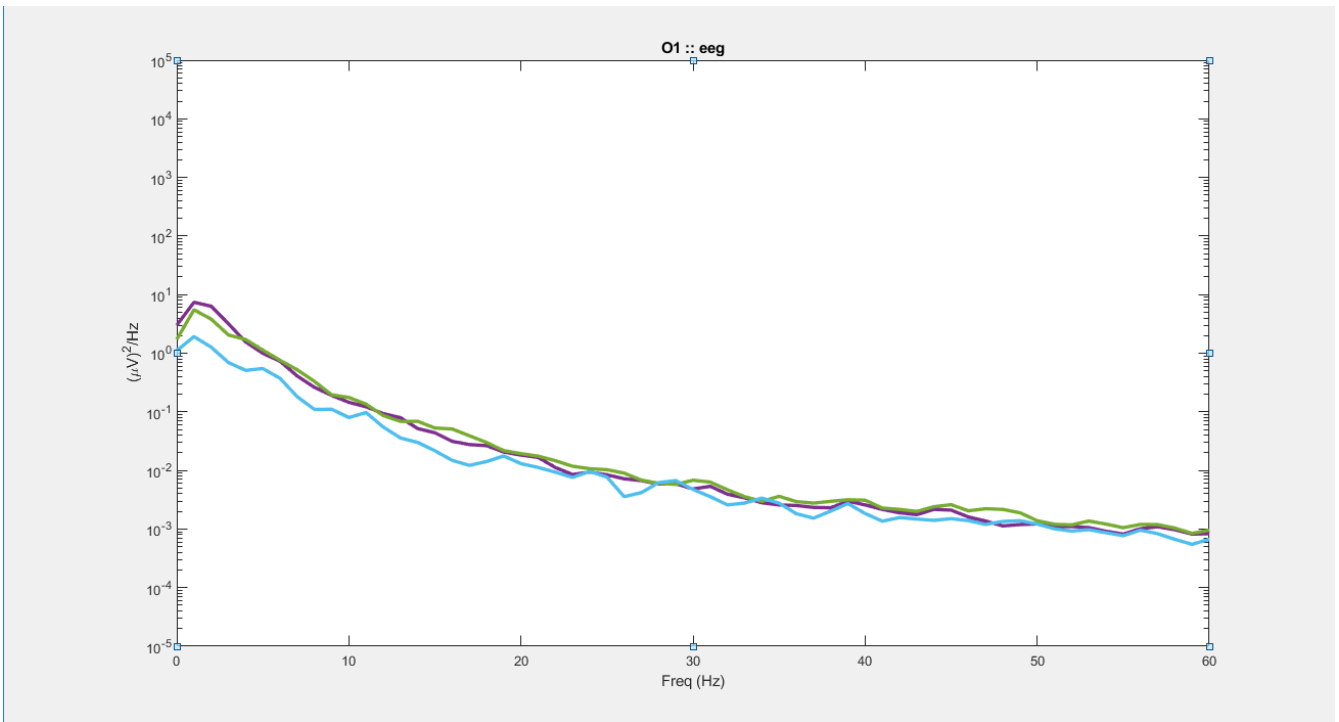
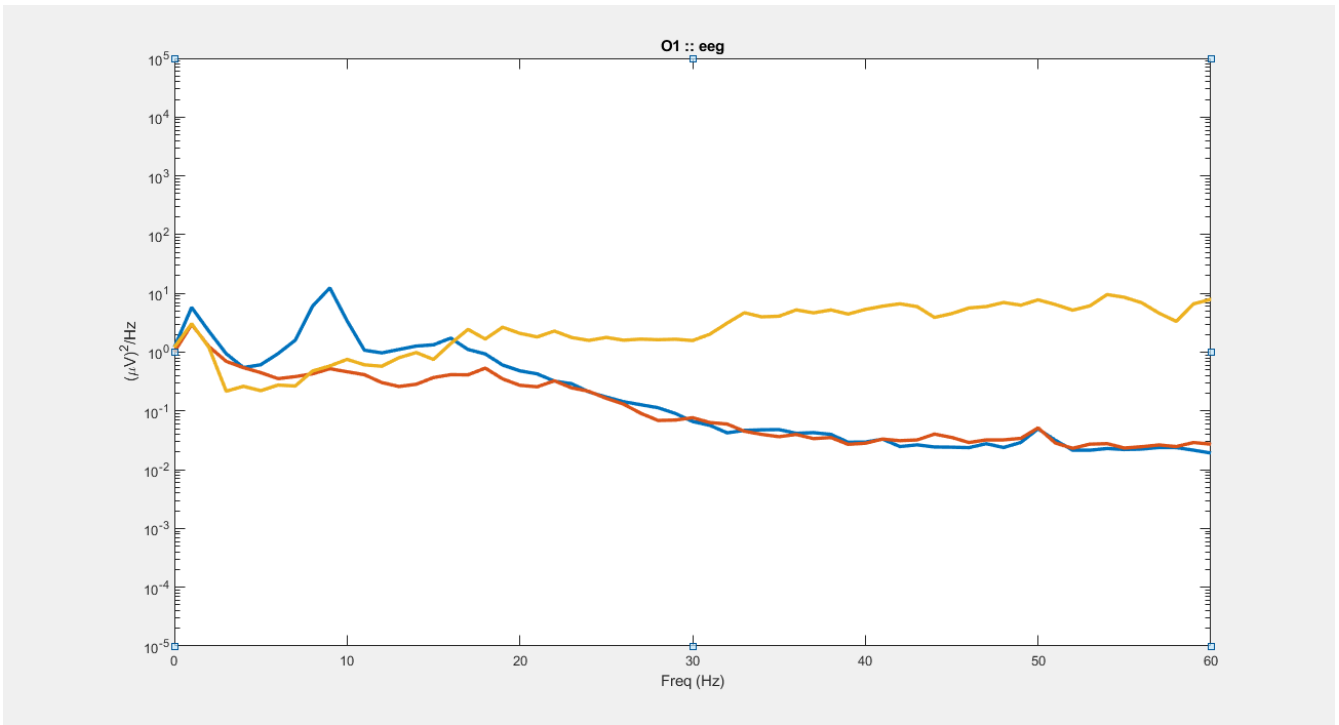


Figure 153. Graph shows electrode location O1. (top) shows software laplacian of tCRE EEG. (bottom) shows tCRE EEG

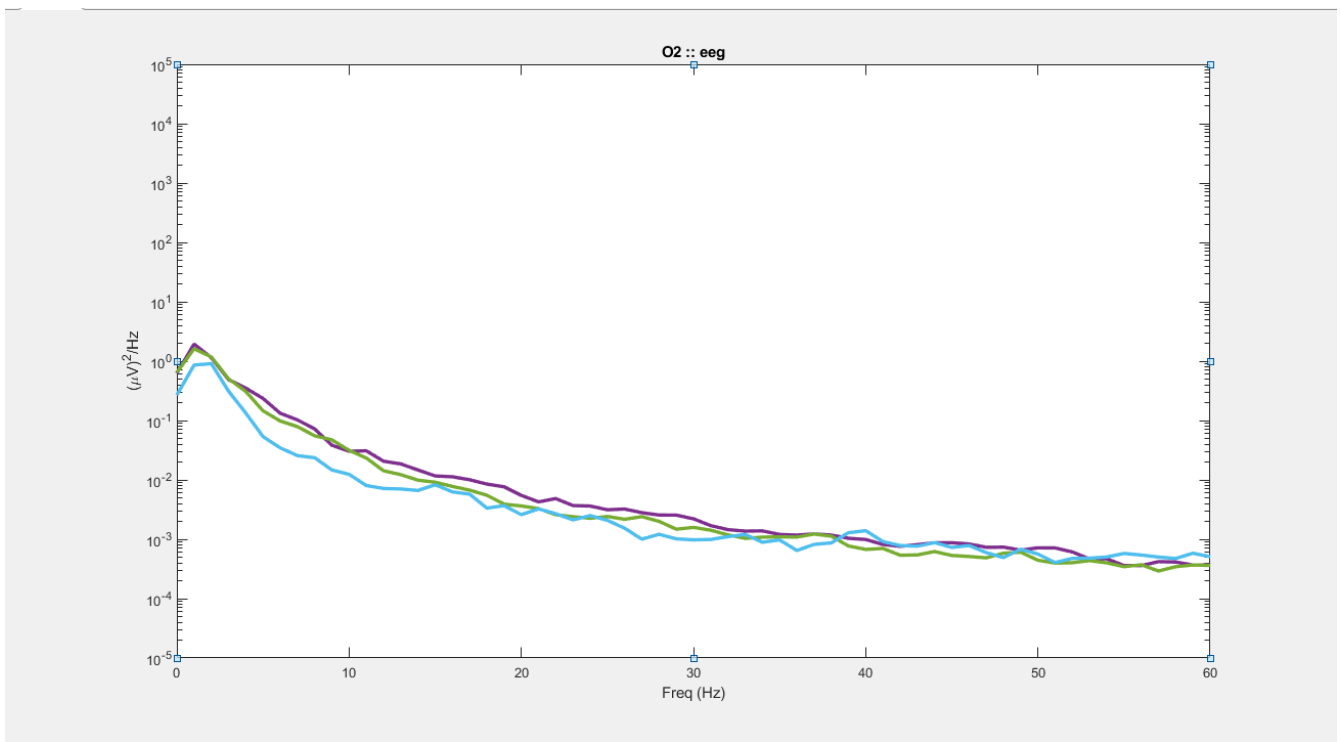
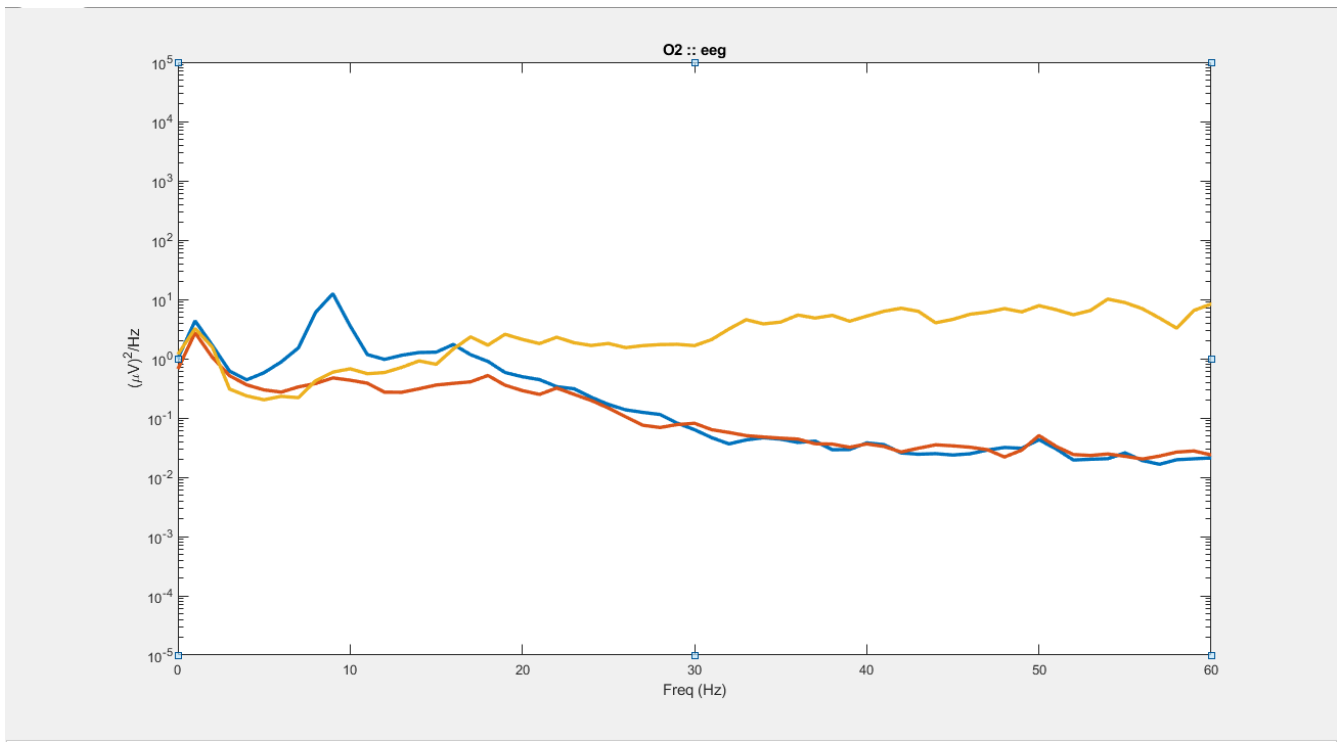


Figure 154. Graph shows electrode location O2. (top) shows software laplacian of tCRE EEG. (bottom) shows tCRE EEG

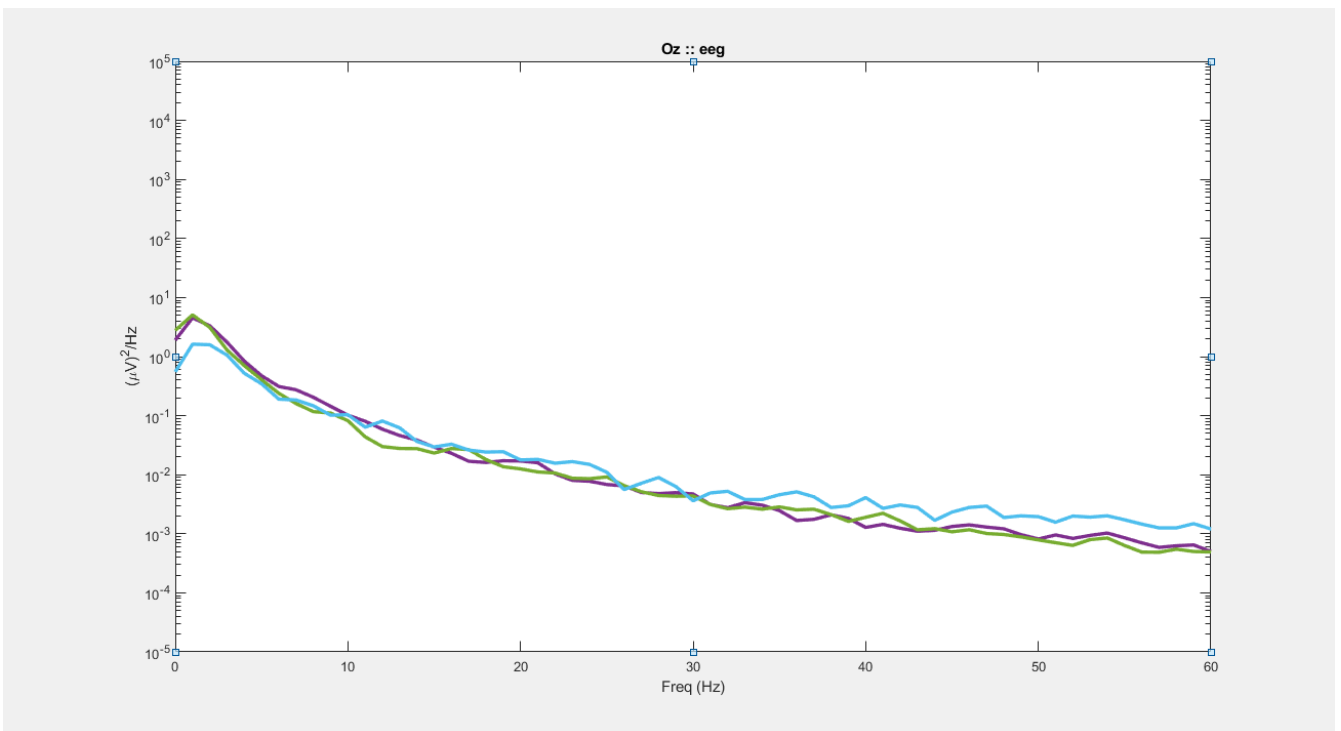
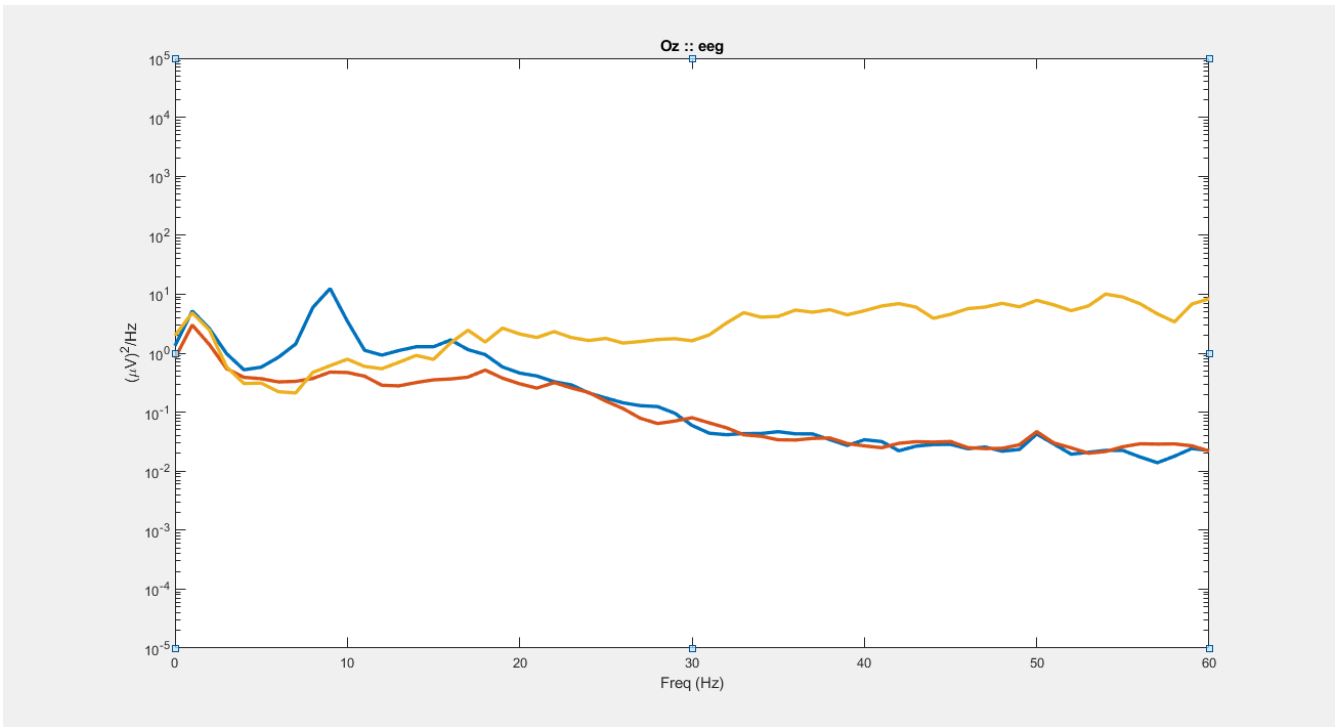


Figure 155. Graph shows electrode location Oz. (top) shows software laplacian of tCRE EEG. (bottom) shows tCRE EEG

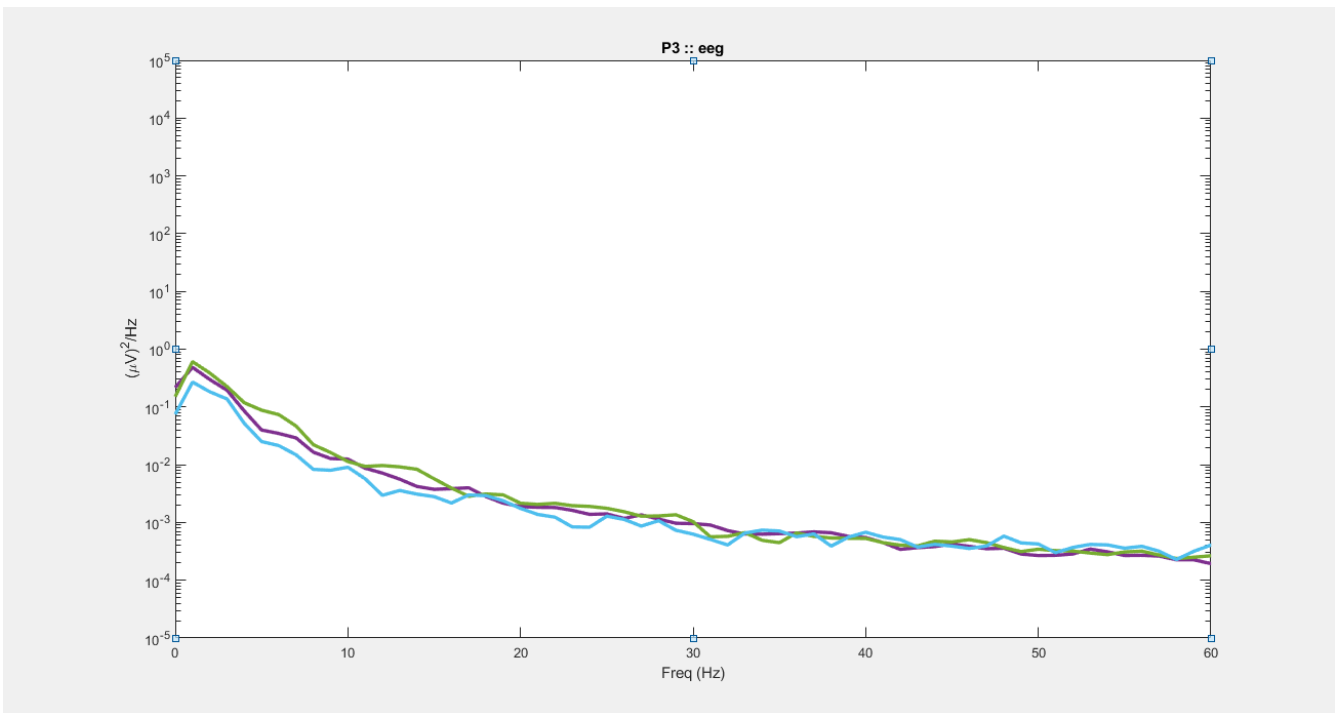
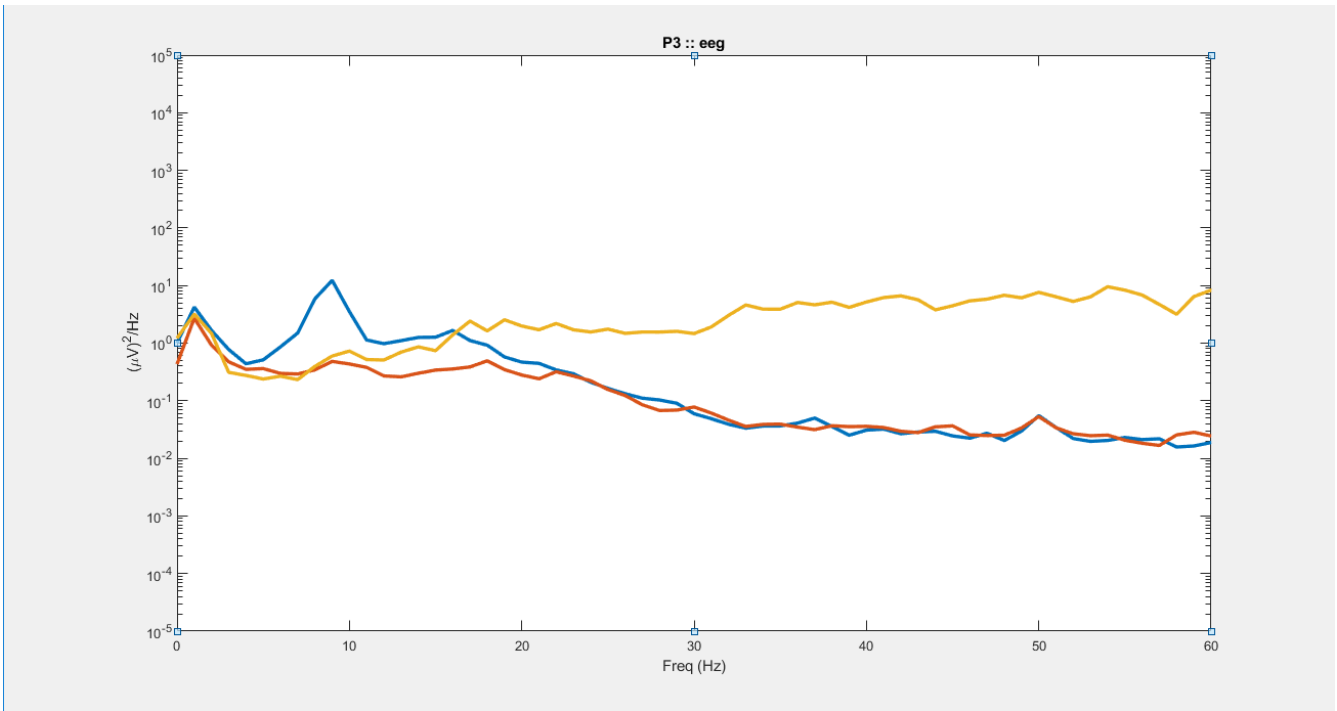


Figure 156. Graph shows electrode location P3. (top) shows software laplacian of tCRE EEG. (bottom) shows tCRE EEG

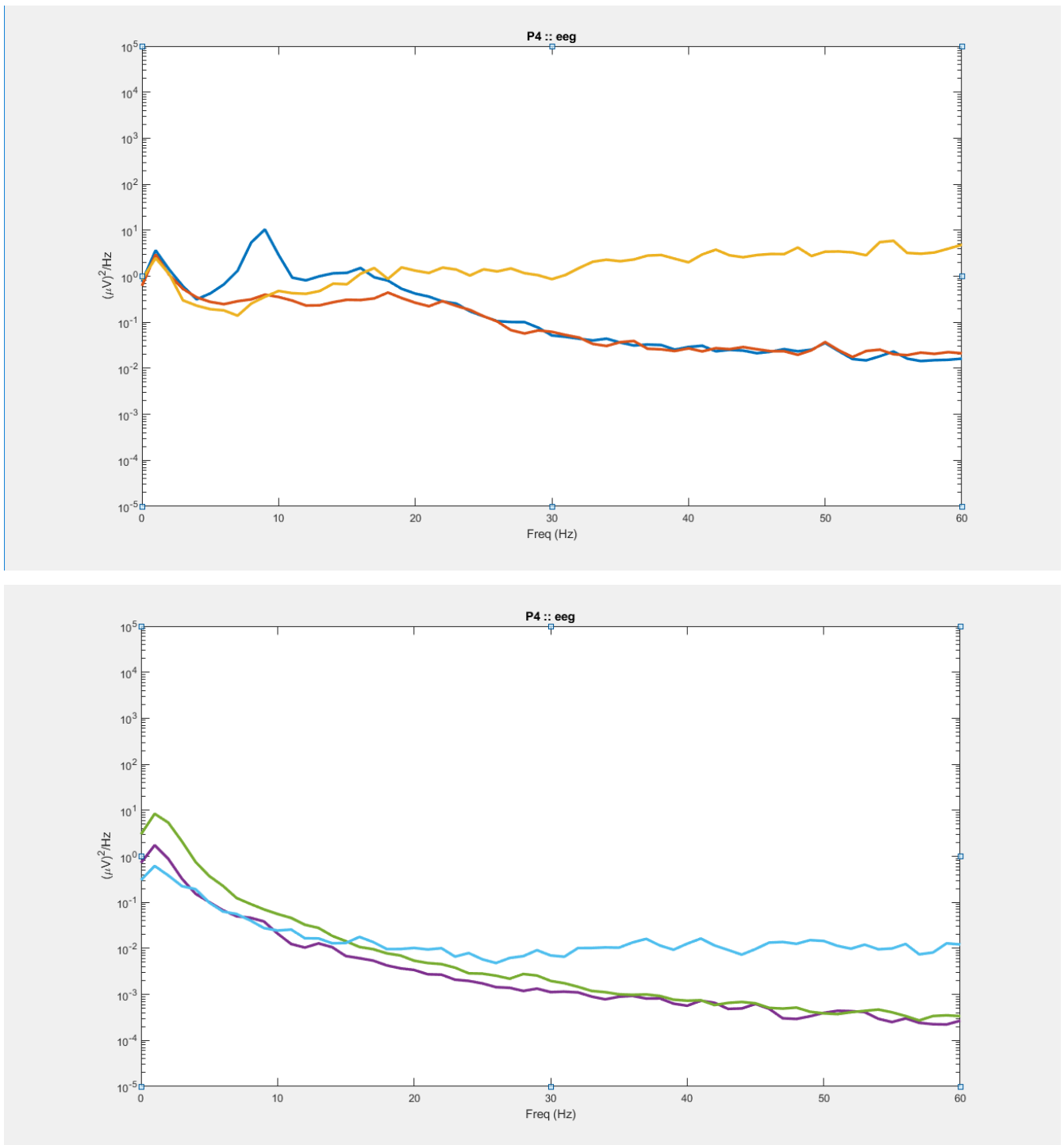


Figure 157. Graph shows electrode location P4. (top) shows software laplacian of tCRE EEG. (bottom) shows tCRE EEG

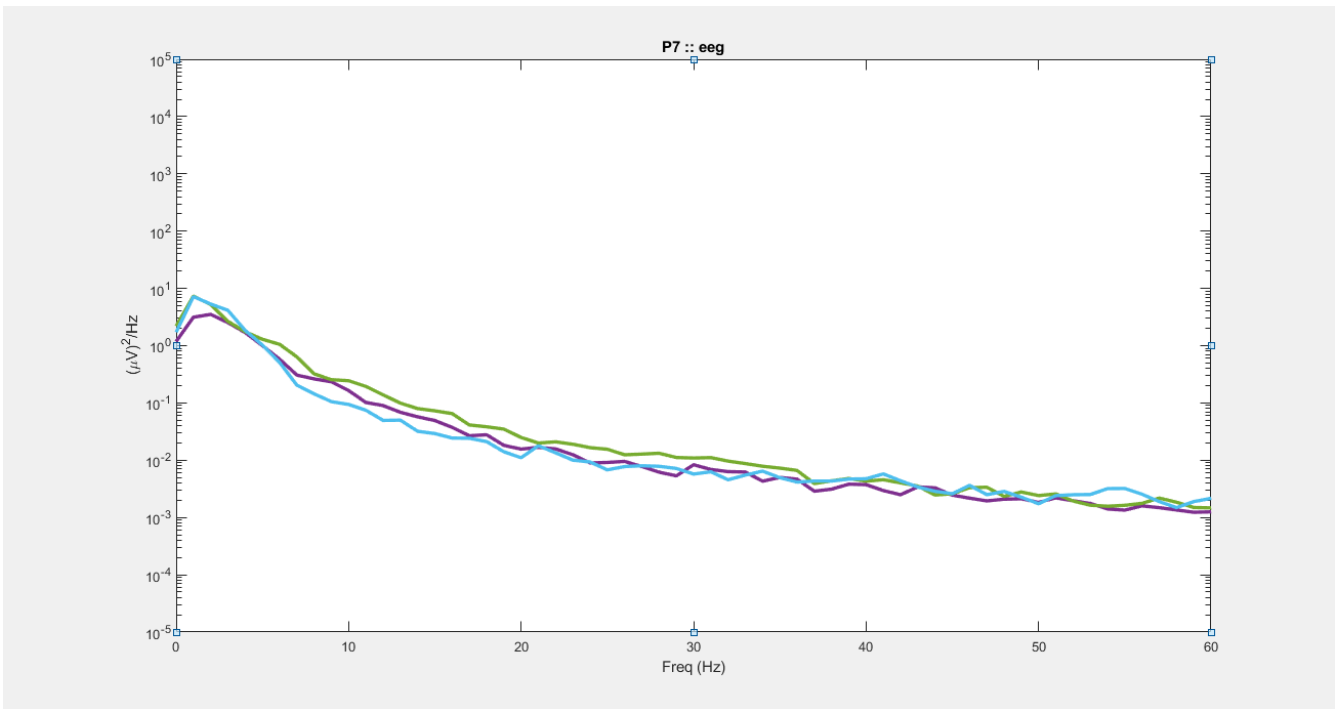
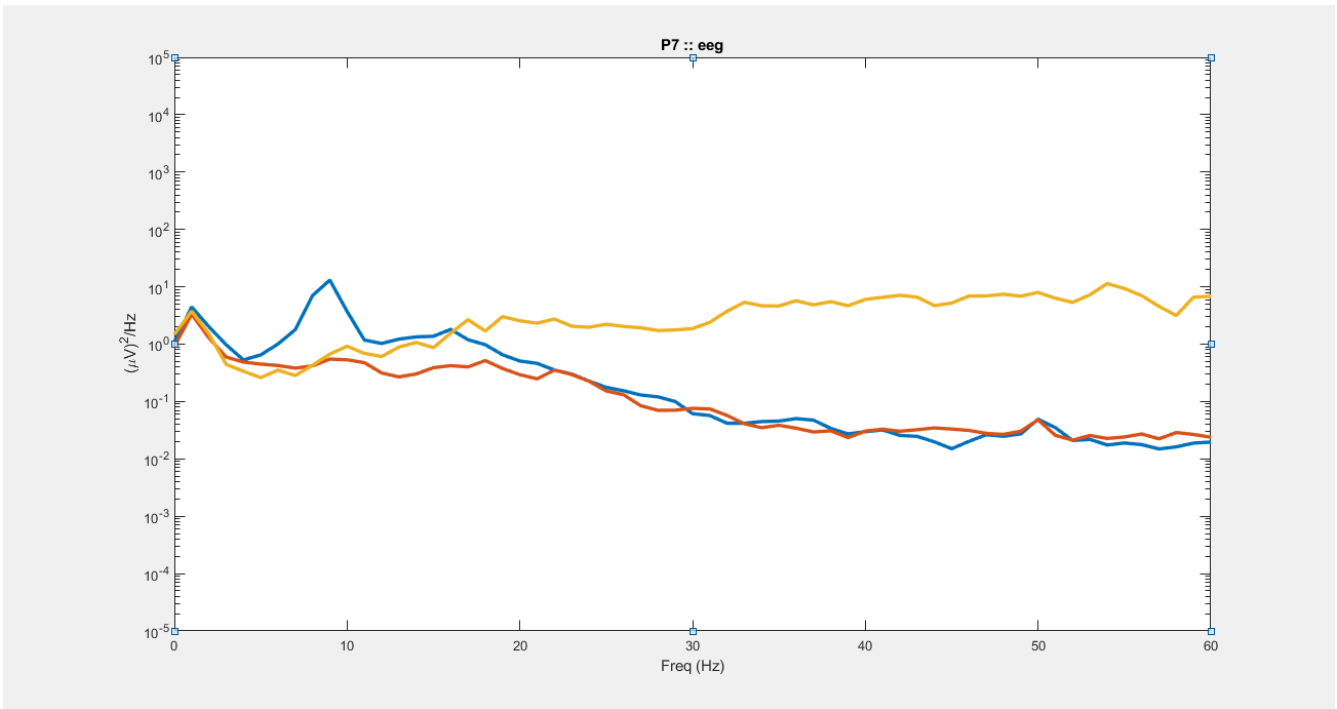


Figure 158. Graph shows electrode location P7. (top) shows software laplacian of tCRE EEG. (bottom) shows tCRE EEG

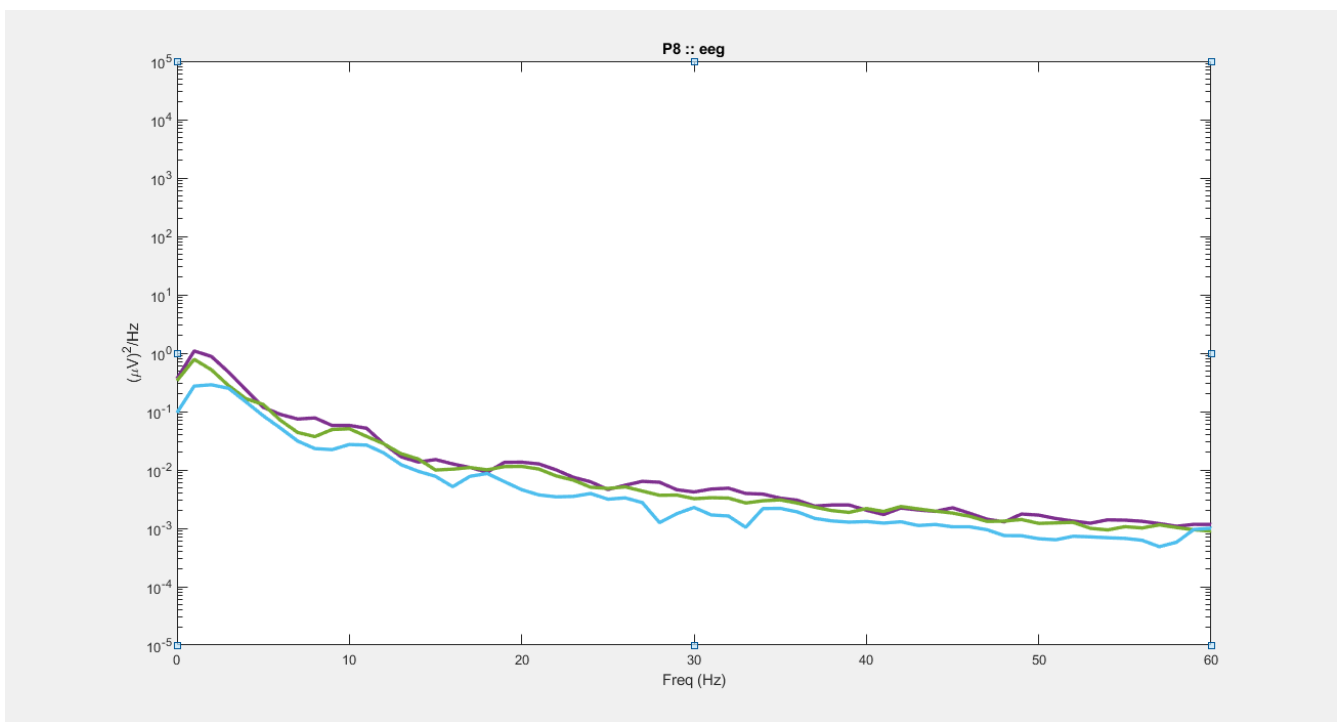
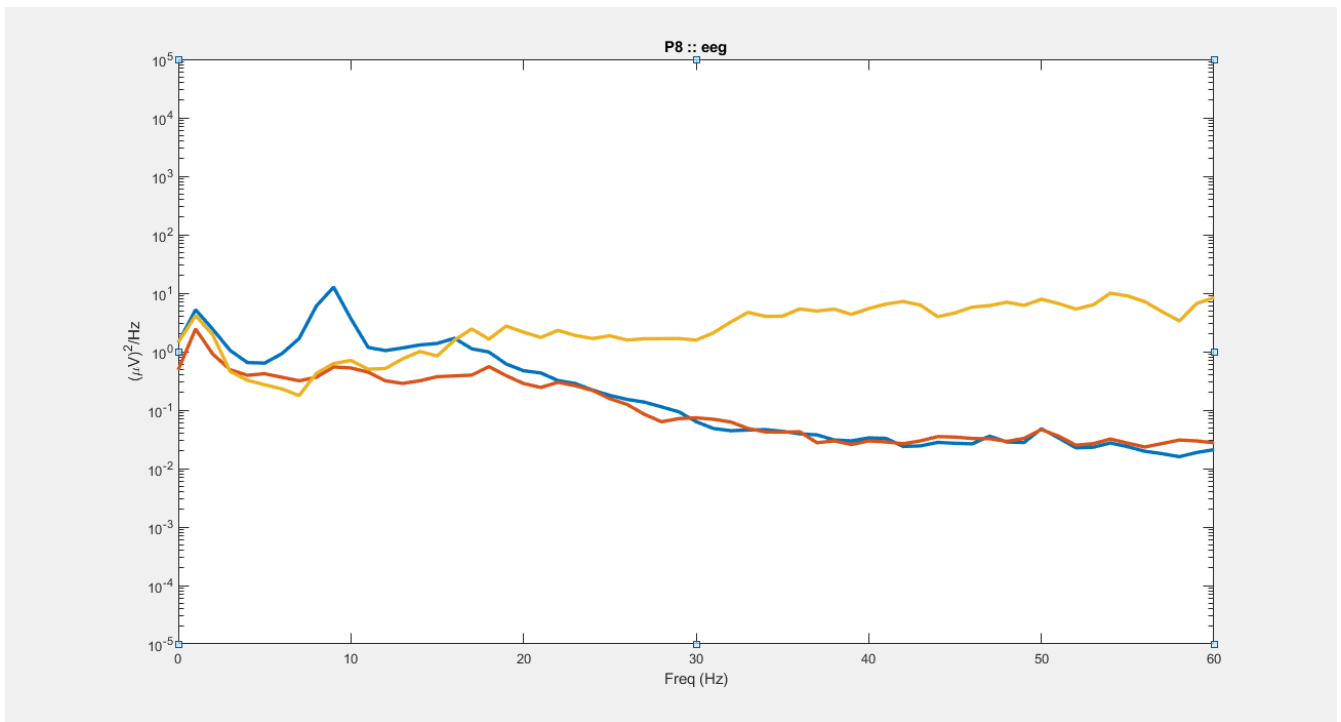


Figure 159. Graph shows electrode location P8. (top) shows software laplacian of tCRE EEG. (bottom) shows tCRE EEG

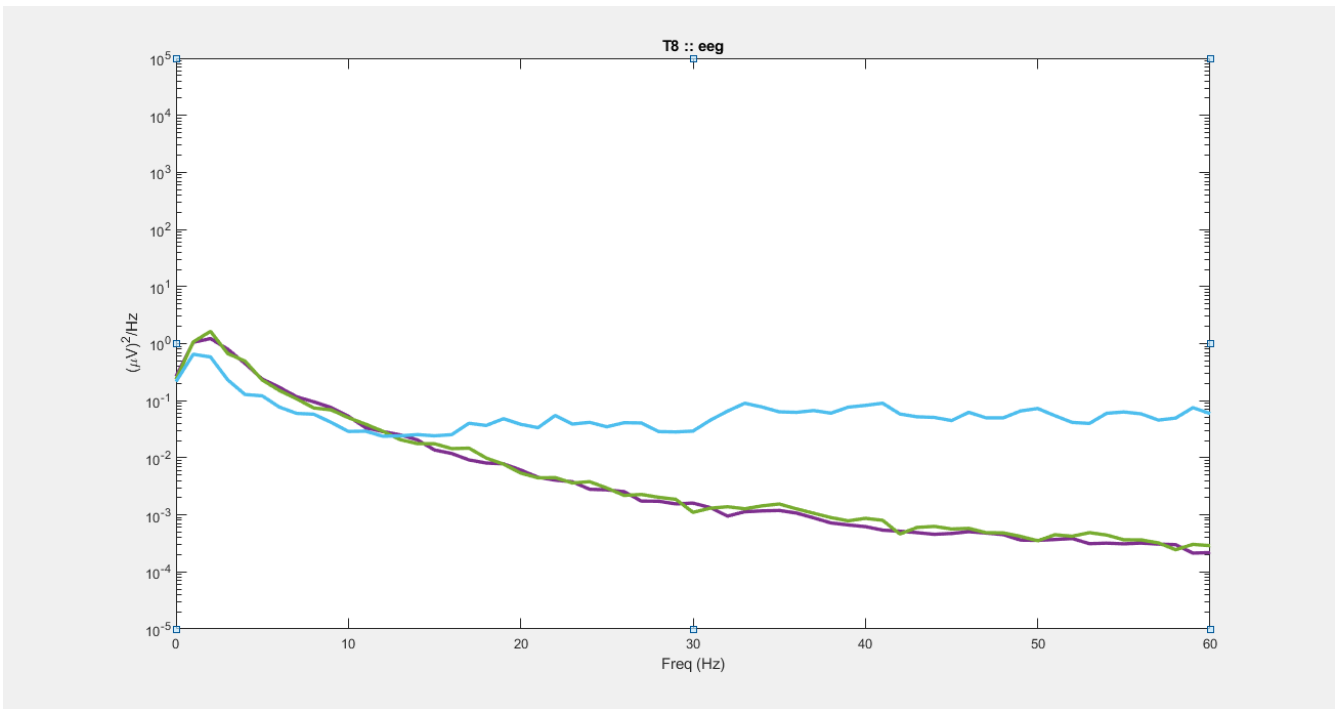
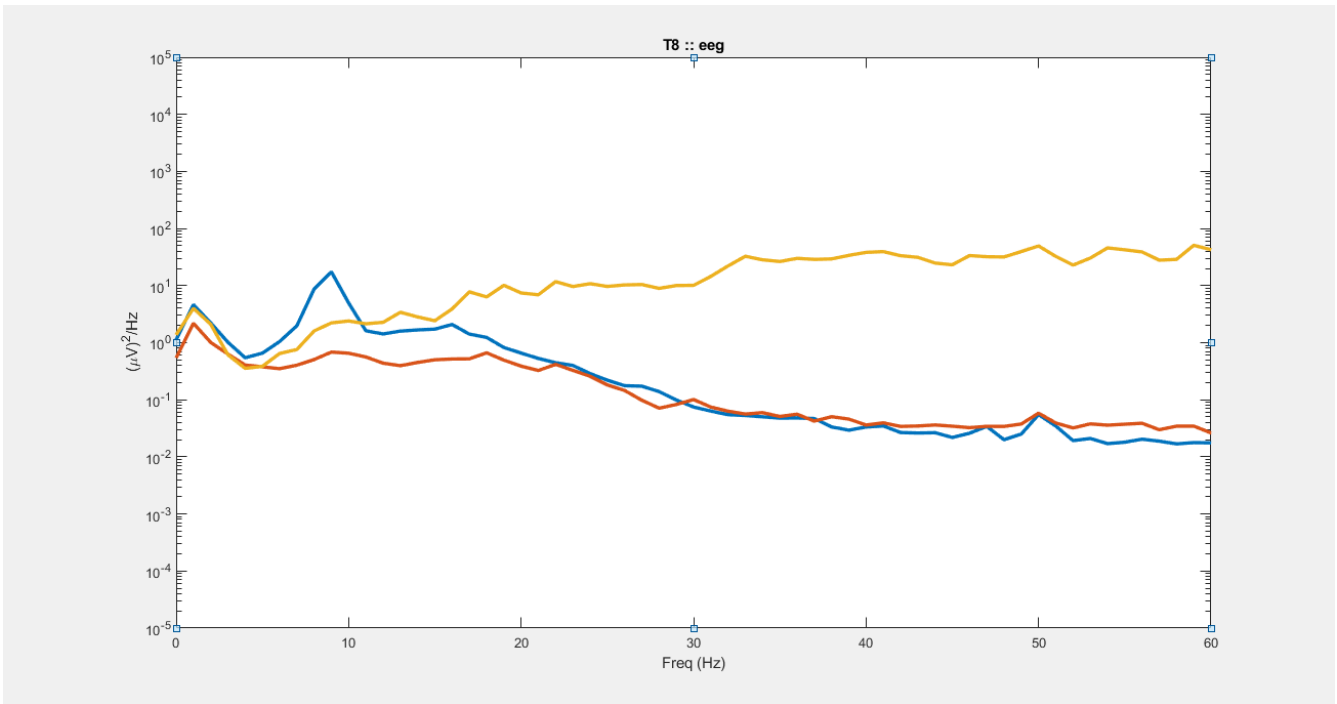


Figure 160. Graph shows electrode location T8. (top) shows software laplacian of tCRE EEG. (bottom) shows tCRE EEG

9.2.2.2. *tCRE electrode periphery test on subject with short, stiff curly hair*

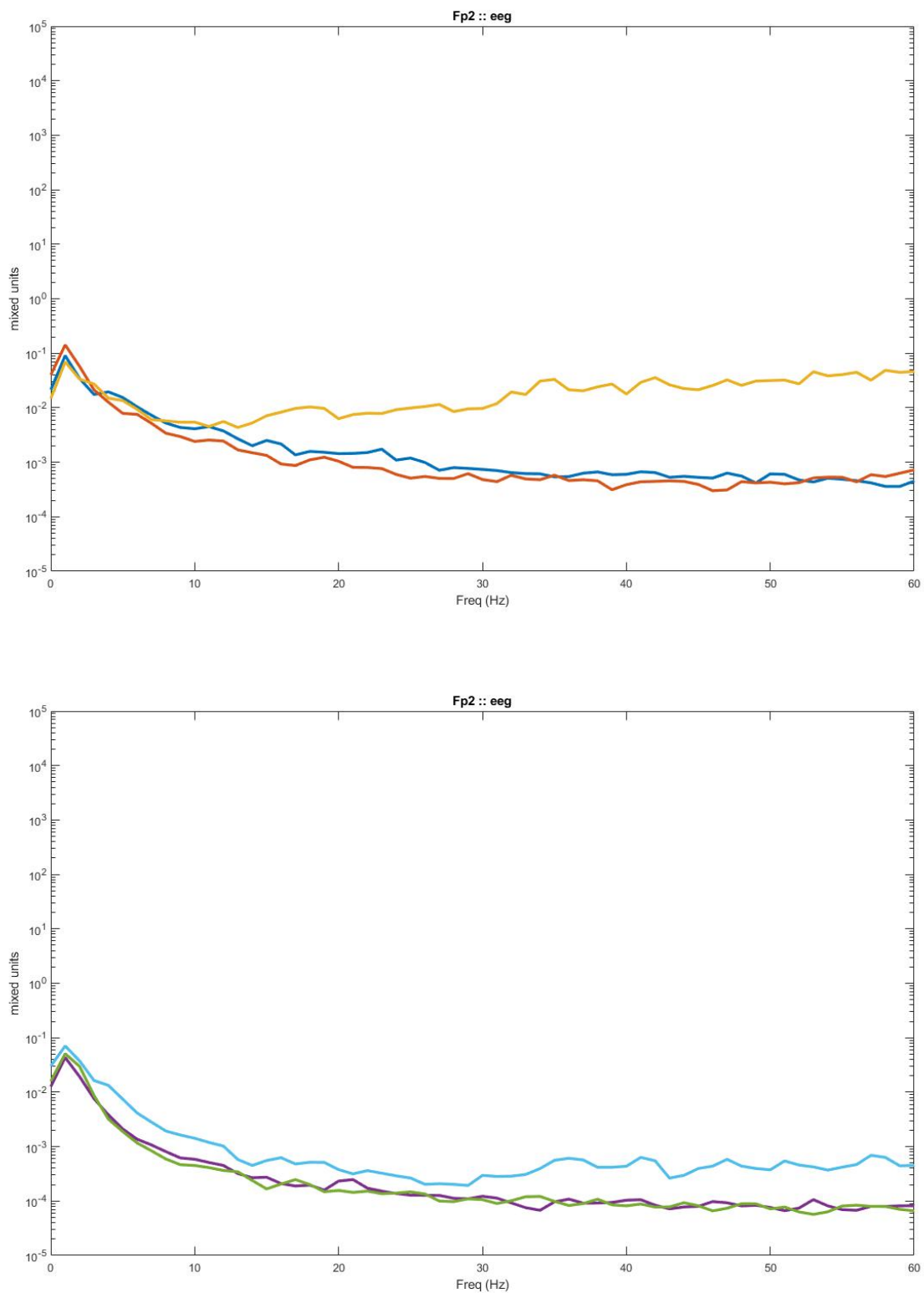


Figure 161. Graph shows electrode location Fp2. (top) shows software laplacian of tCRE EEG. (bottom) shows tCRE EEG

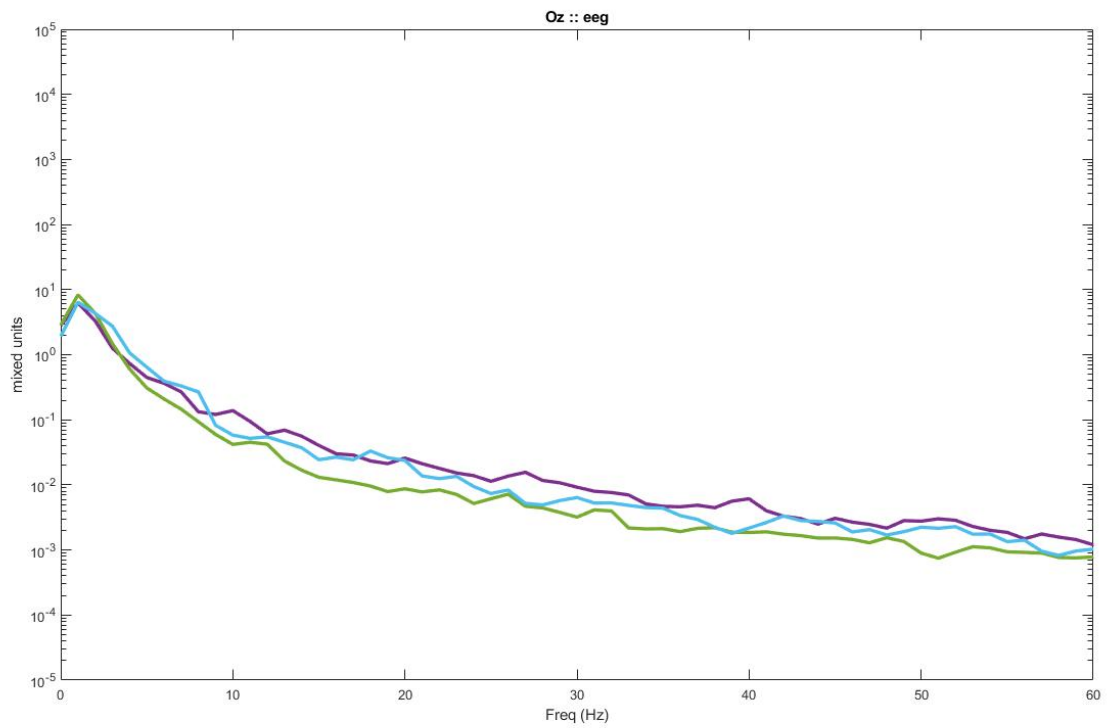
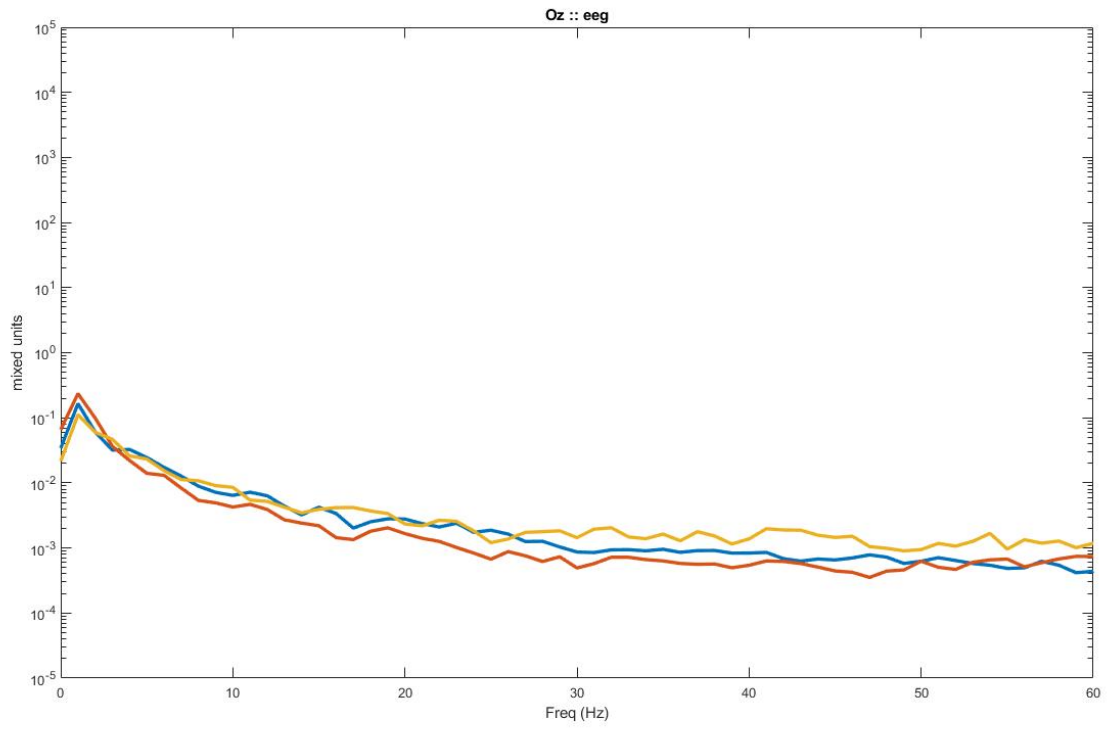


Figure 162. Graph shows electrode location Oz. (top) shows software laplacian of tCRE EEG. (bottom) shows tCRE EEG

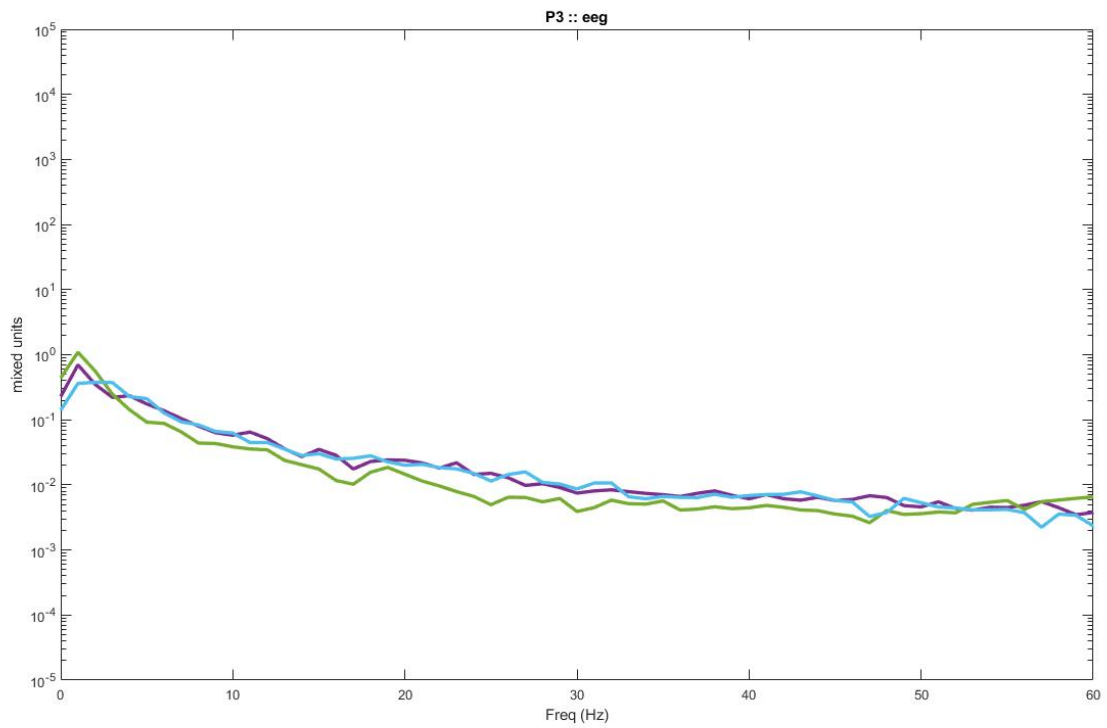
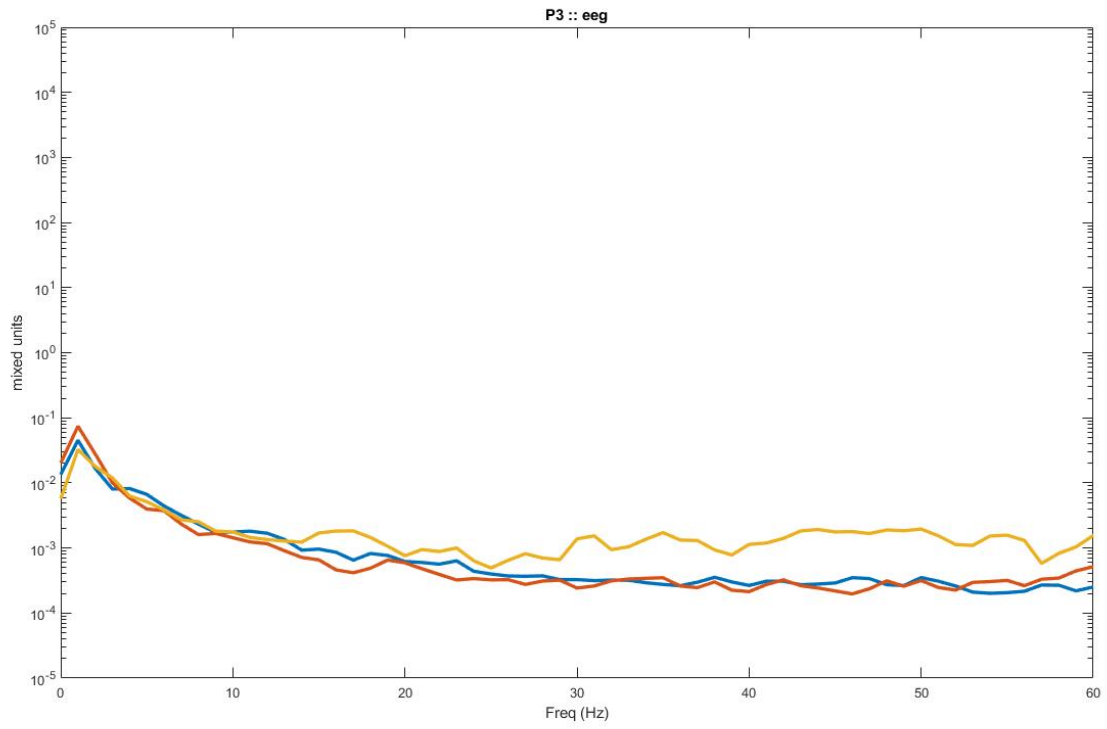


Figure 163. Graph shows electrode location P3. (top) shows software laplacian of tCRE EEG. (bottom) shows tCRE EEG

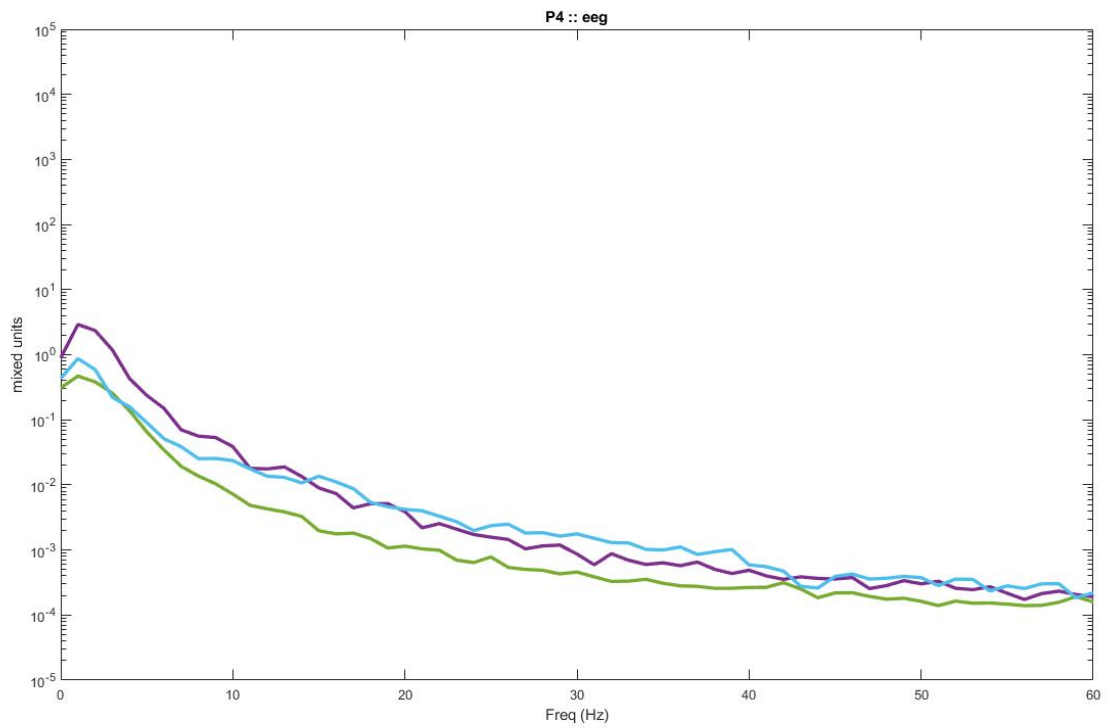
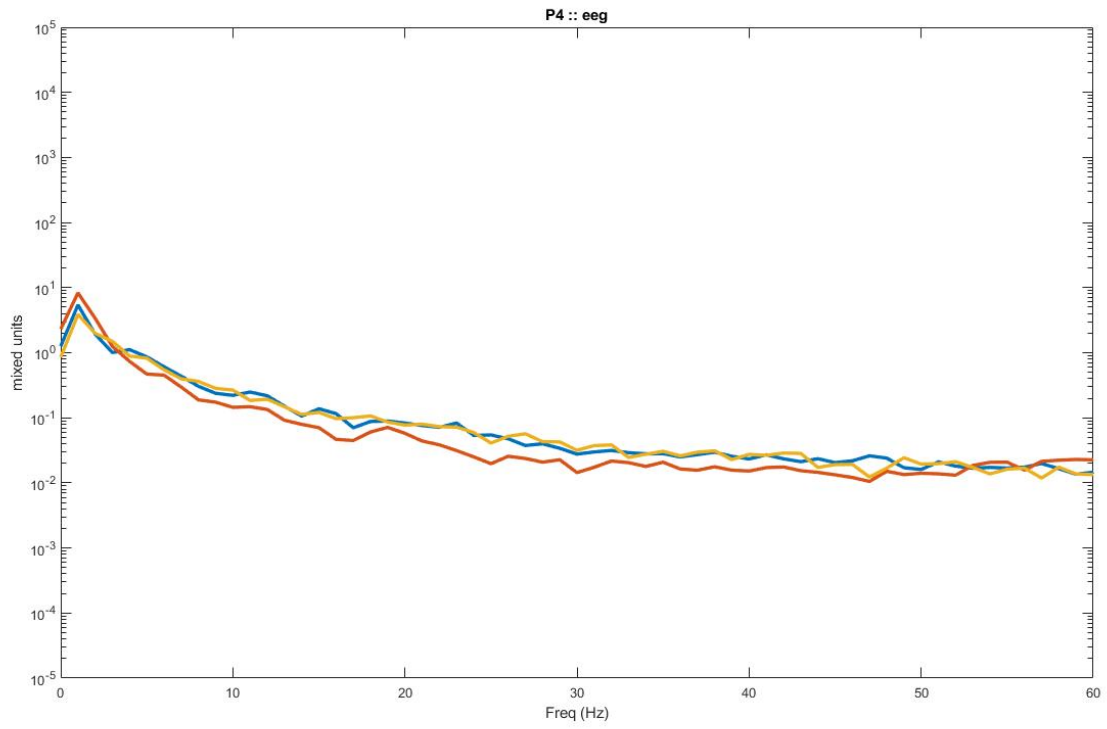


Figure 164. Graph shows electrode location P4. (top) shows software laplacian of tCRE EEG. (bottom) shows tCRE EEG

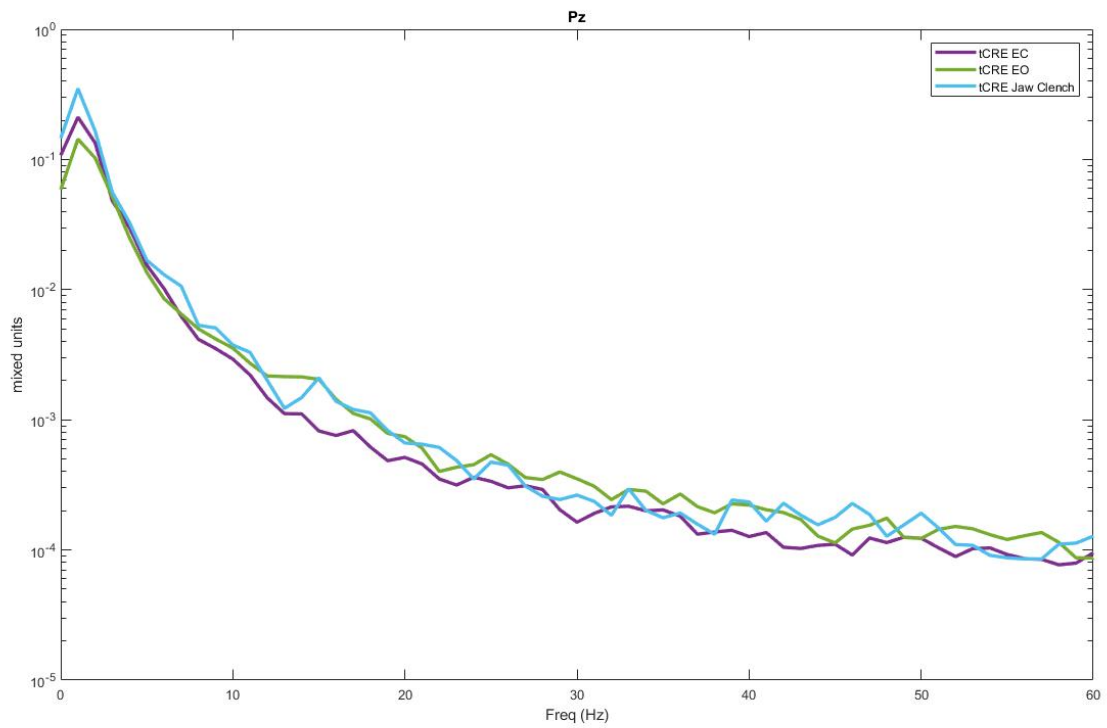
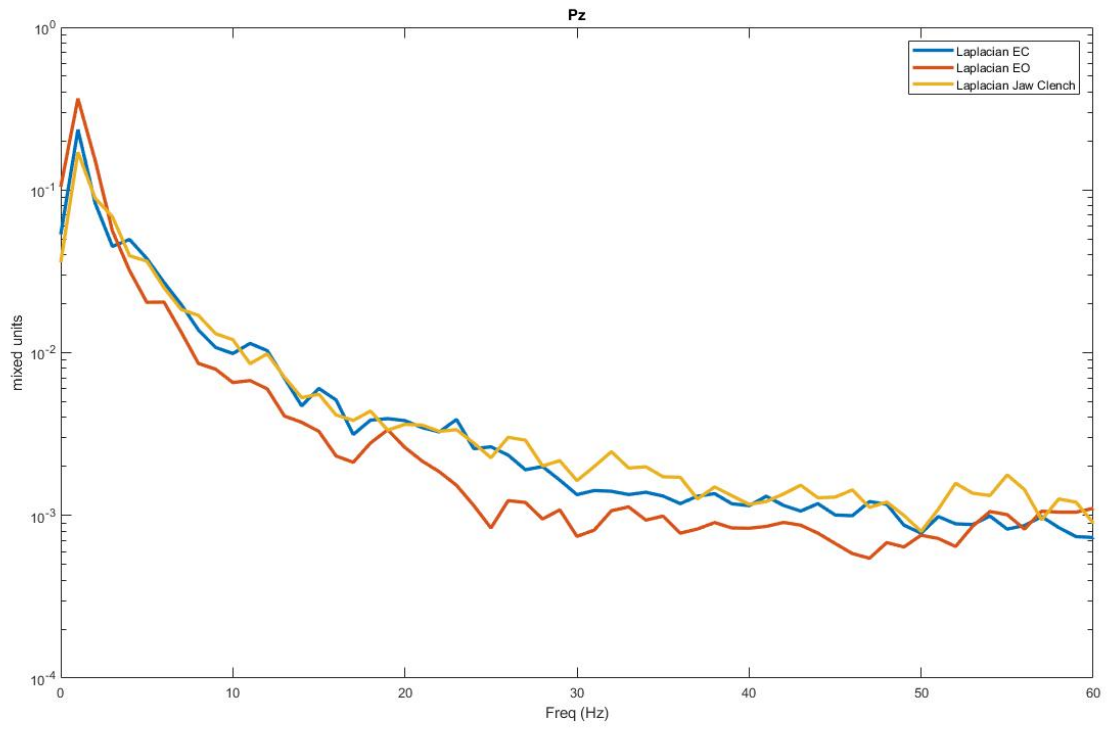


Figure 165. Graph shows electrode location Pz. (top) shows software laplacian of tCRE EEG. (bottom) shows tCRE EEG

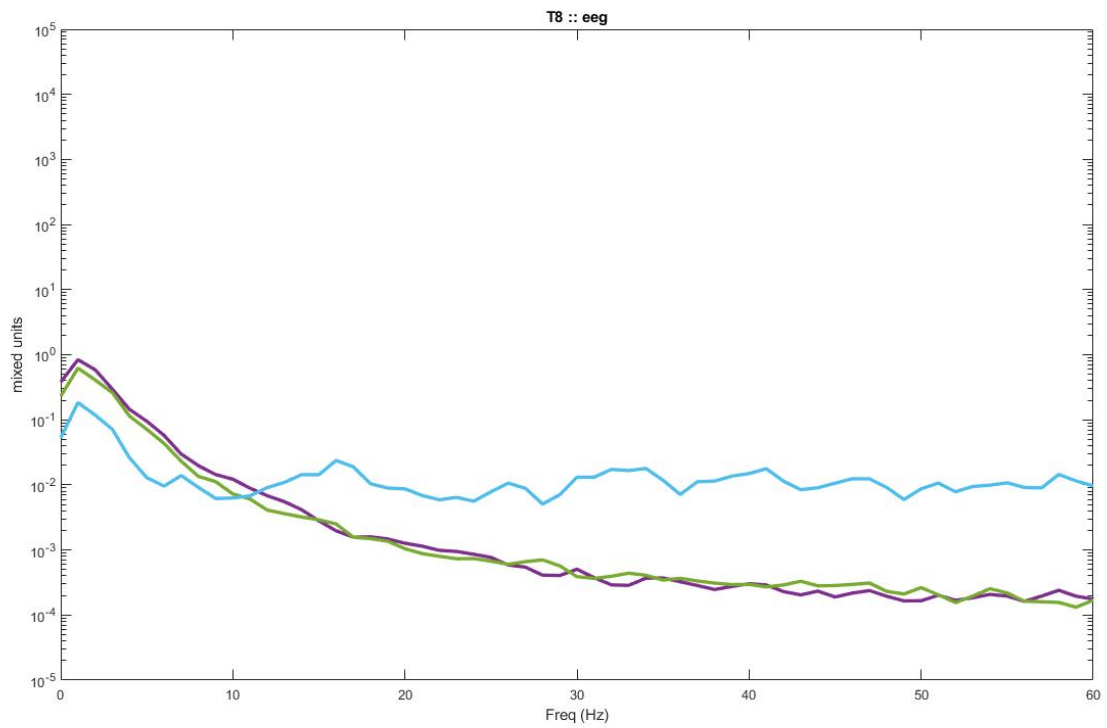
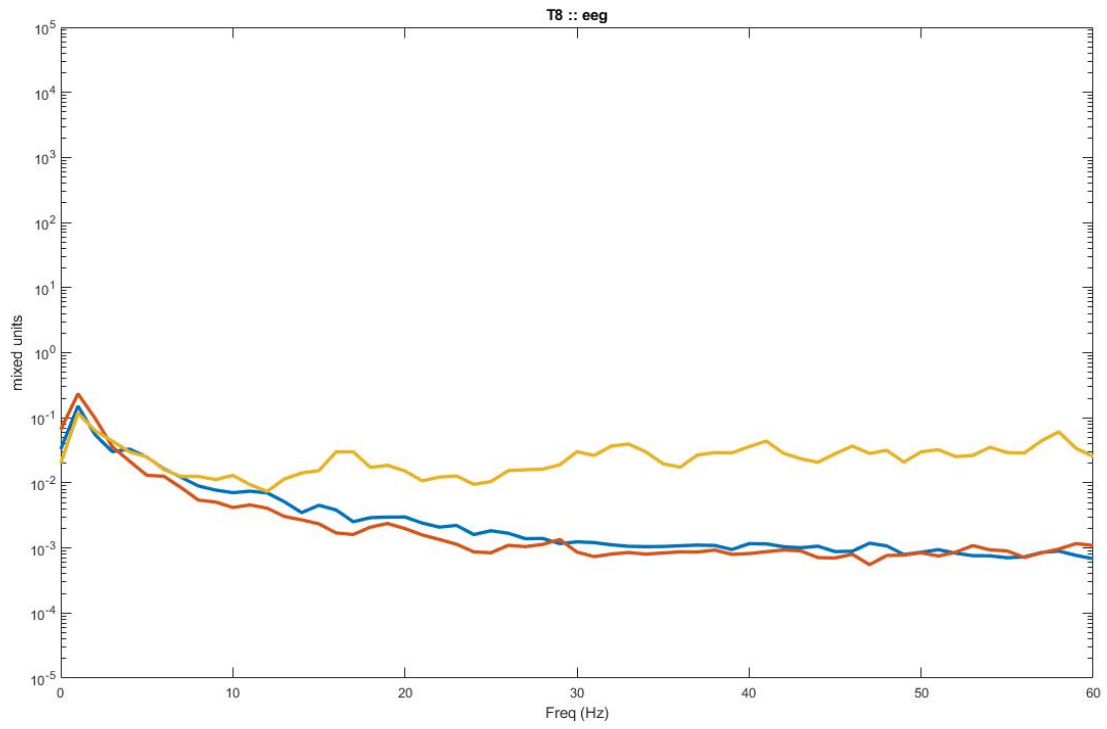


Figure 166. Graph shows electrode location T8. (top) shows software laplacian of tCRE EEG. (bottom) shows tCRE EEG

9.2.3. 20 tCRE electrodes used 'dry' in the cap

9.2.3.1. 20 tCRE electrodes used 'dry' in cap on subject with thick hair

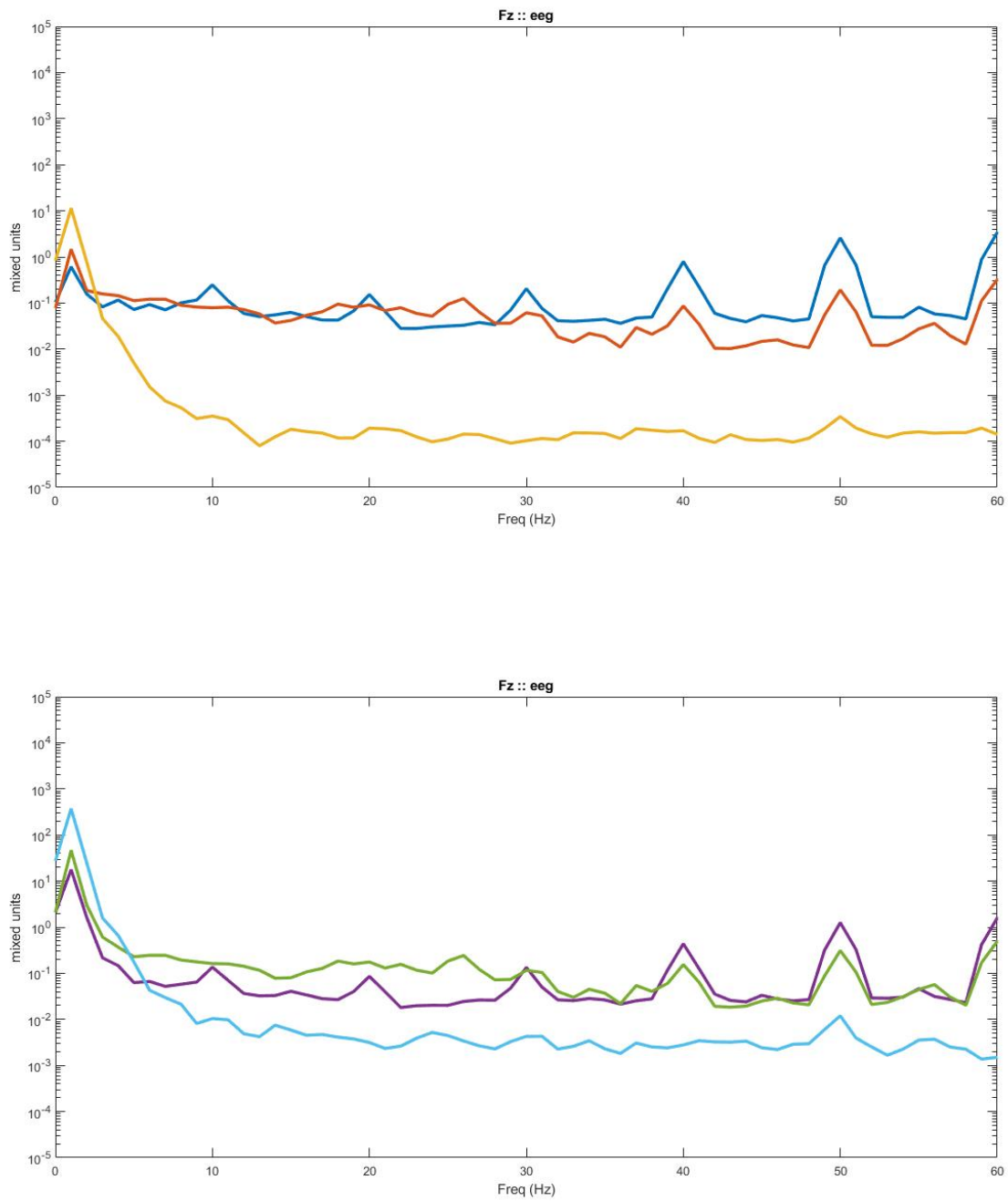


Figure 167. Graph shows electrode location Fz. (top) shows software laplacian of tCRE EEG. (bottom) shows tCRE EEG

9.2.3.2. 20 tCRE electrodes used 'dry' in cap on subject with short, stiff curly hair

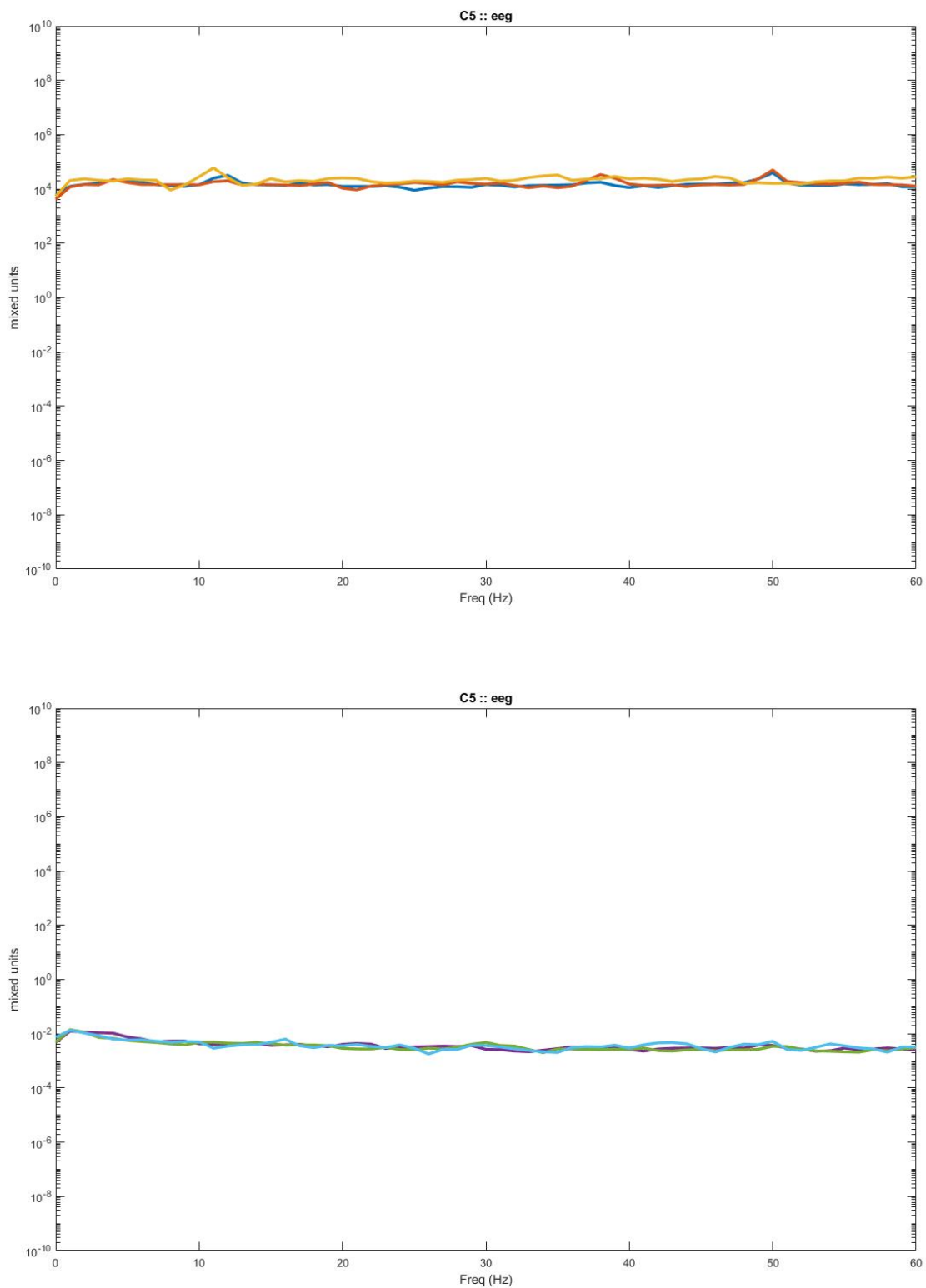


Figure 168. Graph shows electrode location C5. (top) shows software laplacian of tCRE EEG. (bottom) shows tCRE EEG

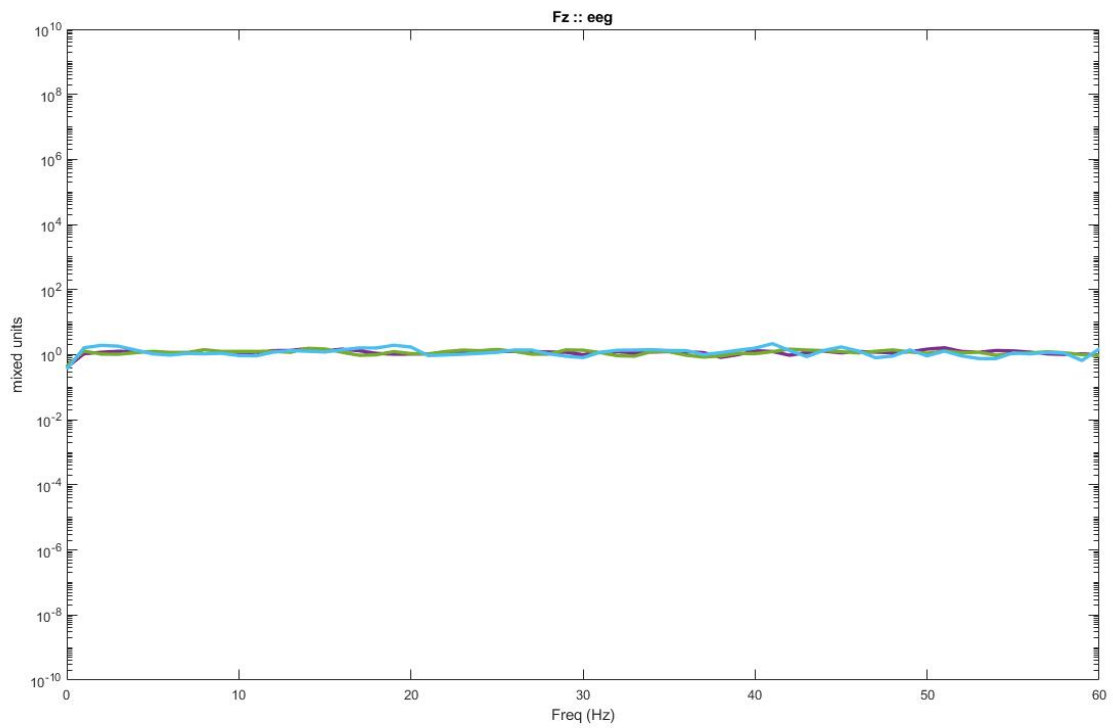
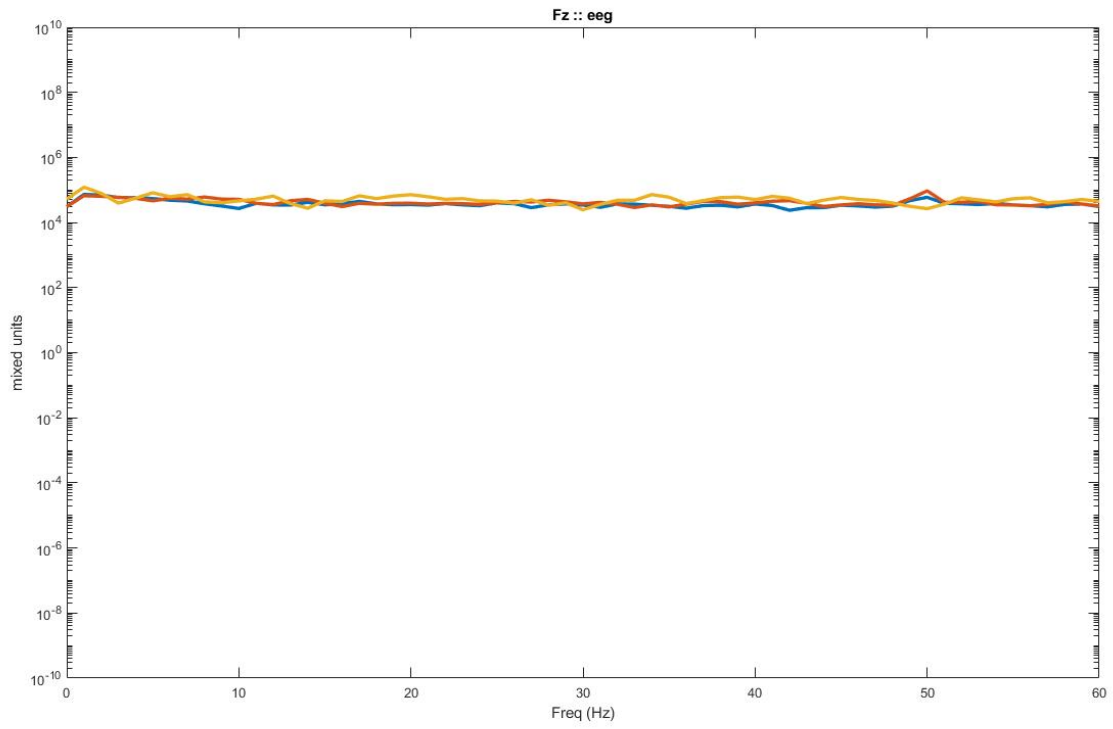


Figure 169. Graph shows electrode location Pz. (top) shows software laplacian of tCRE EEG. (bottom) shows tCRE EEG

9.2.4. 20 tCRE electrodes used 'dry' under the cap

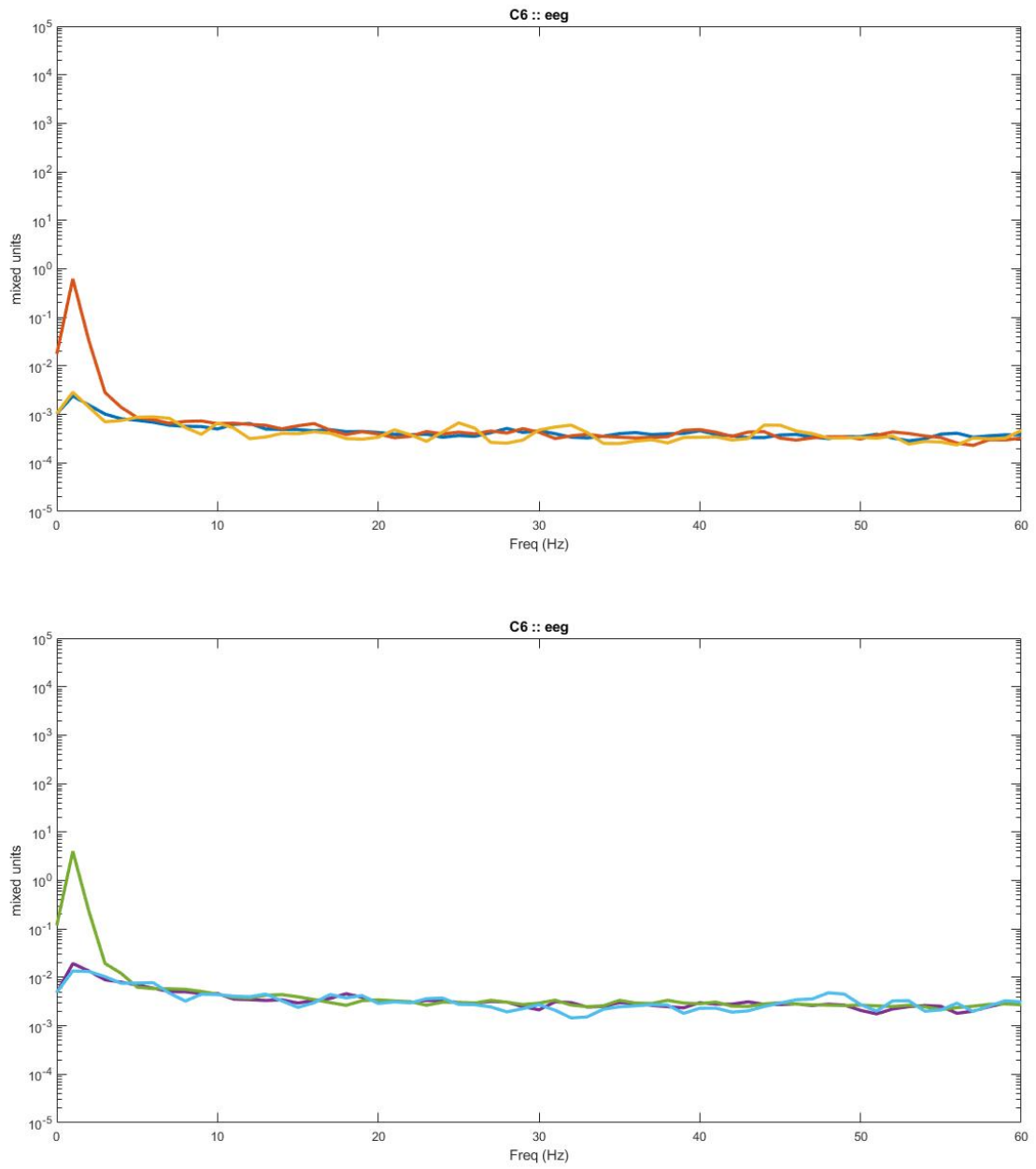


Figure 170. Graph shows electrode location C6. (top) shows software laplacian of tCRE EEG. (bottom) shows tCRE EEG

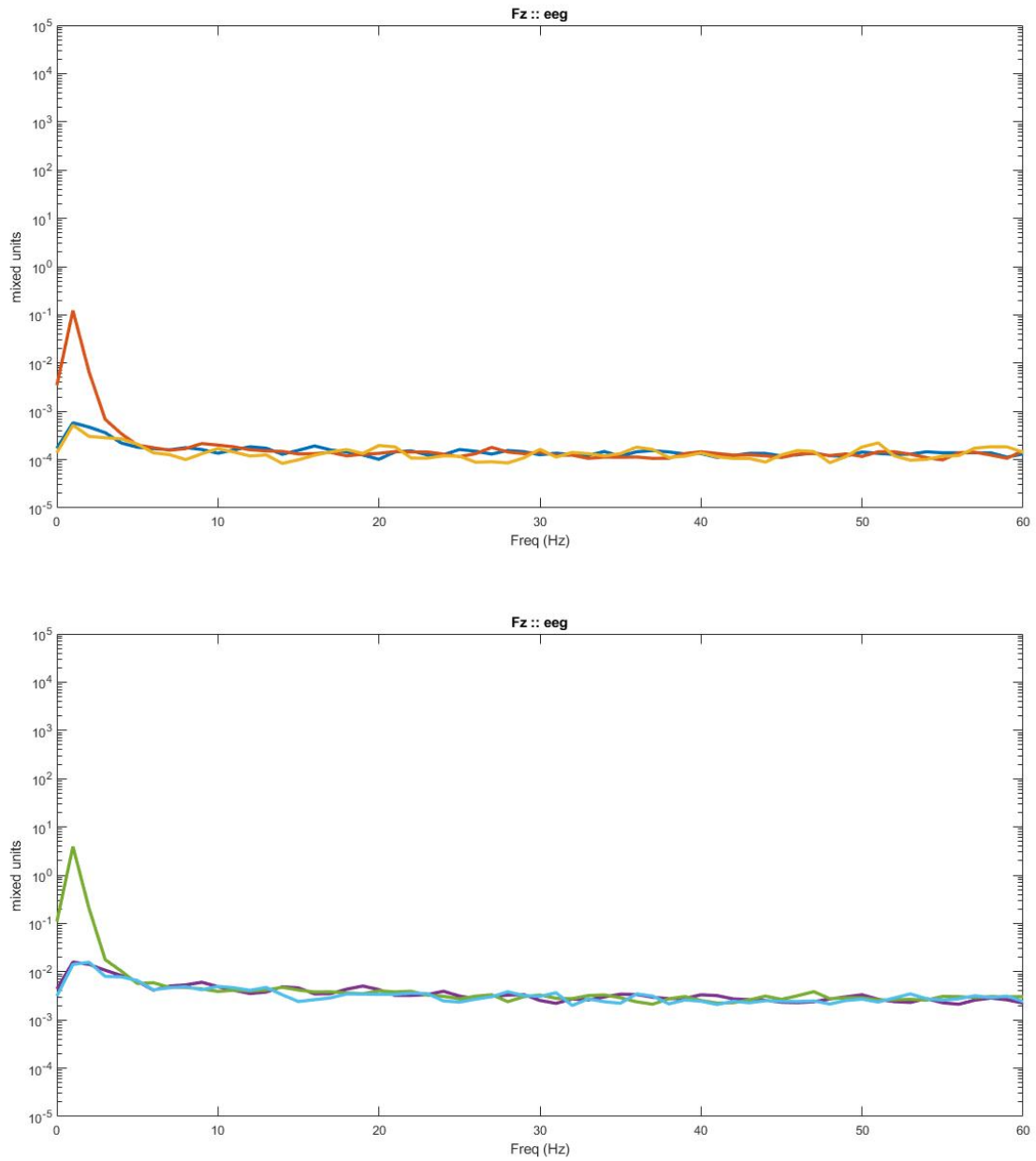


Figure 171. Graph shows electrode location Fz. (top) shows software laplacian of tCRE EEG. (bottom) shows tCRE EEG

9.2.5. 20 tCRE electrodes used in cap with saline filled foam in the cap

9.2.5.1. 20 tCRE electrodes used in cap with saline filled foam in cap used on subject with thin, wispy hair

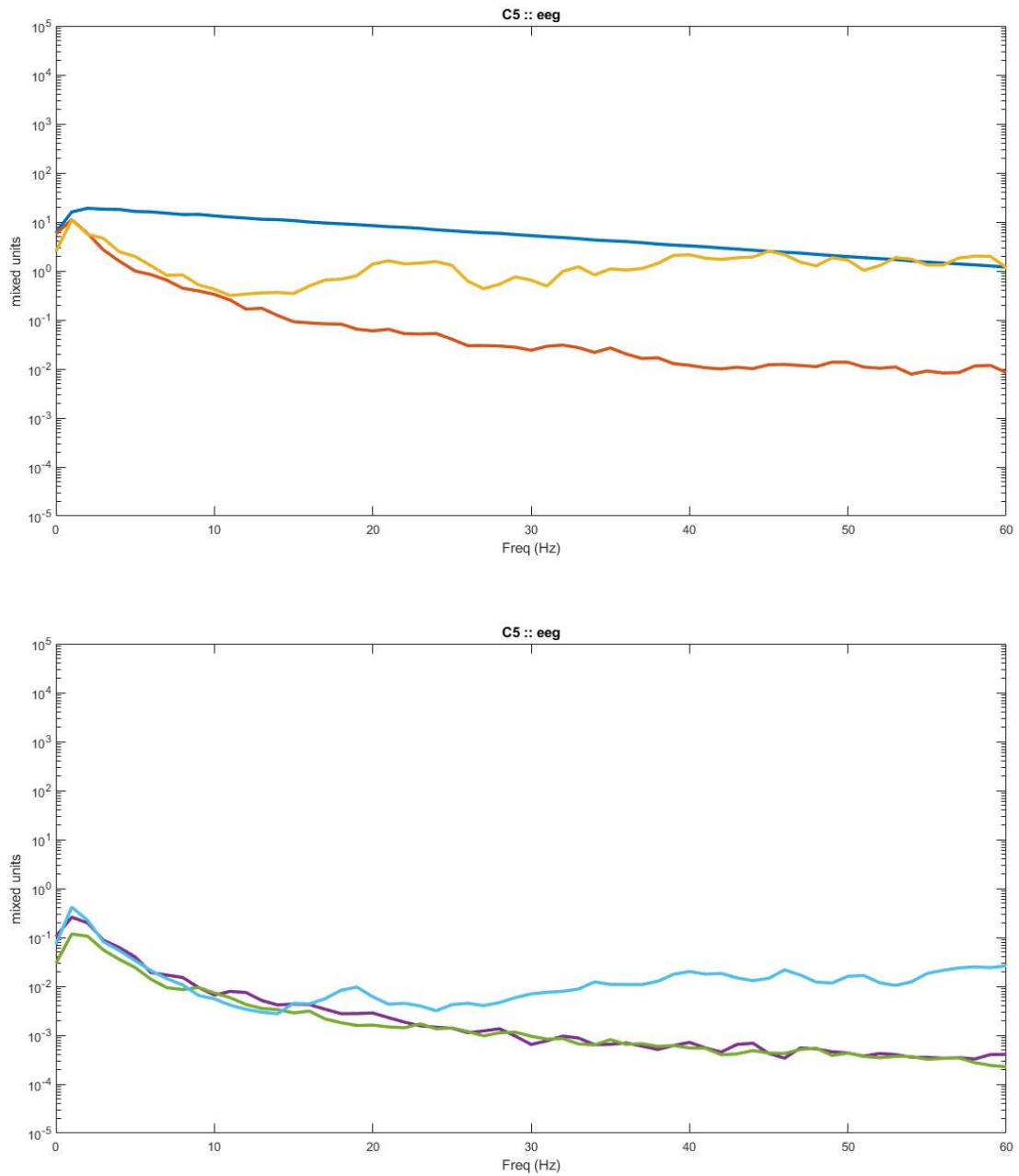


Figure 172. Graph shows electrode location C5. (top) shows software laplacian of tCRE EEG. (bottom) shows tCRE EEG

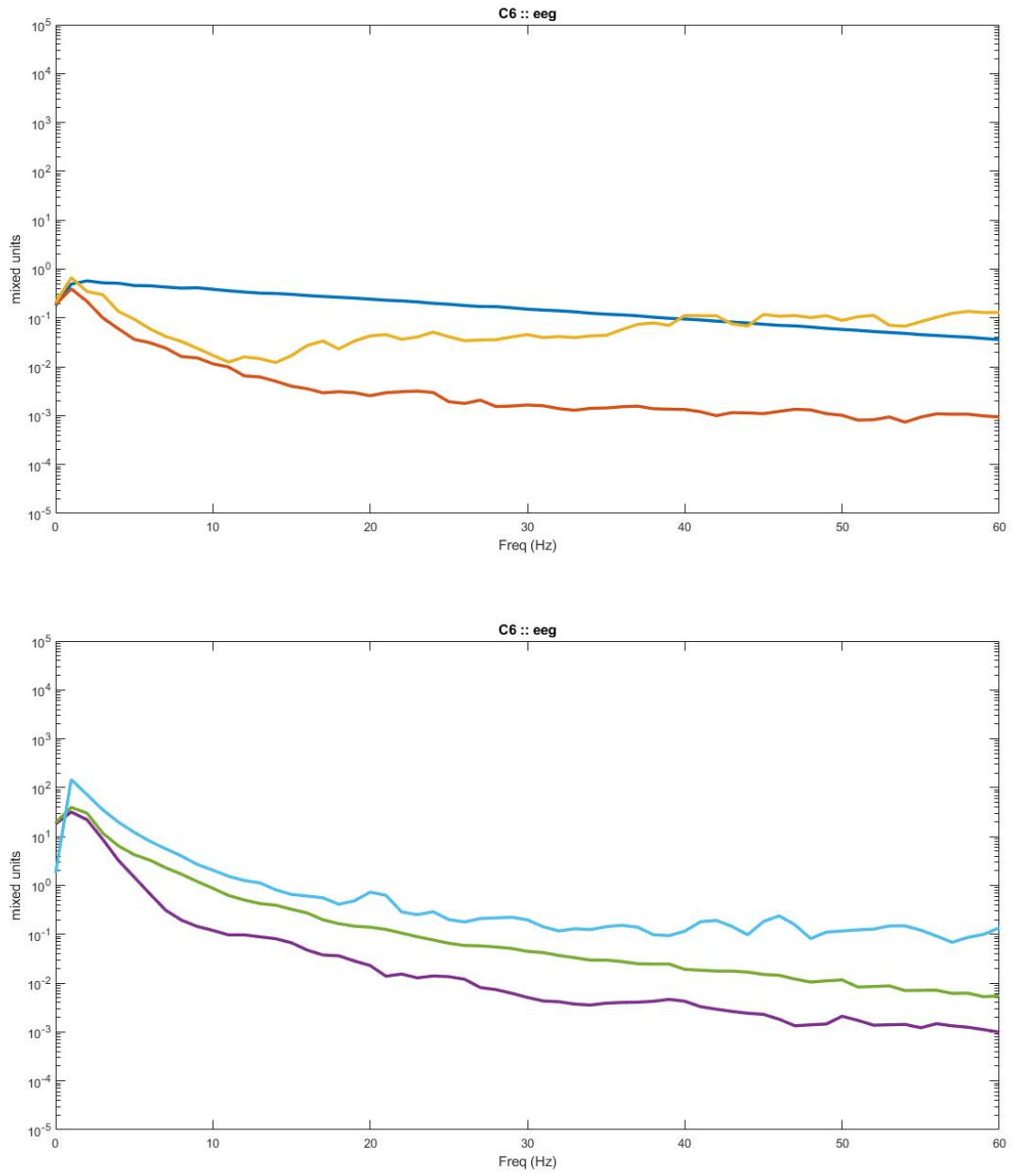


Figure 173. Graph shows electrode location C6. (top) shows software laplacian of tCRE EEG. (bottom) shows tCRE EEG

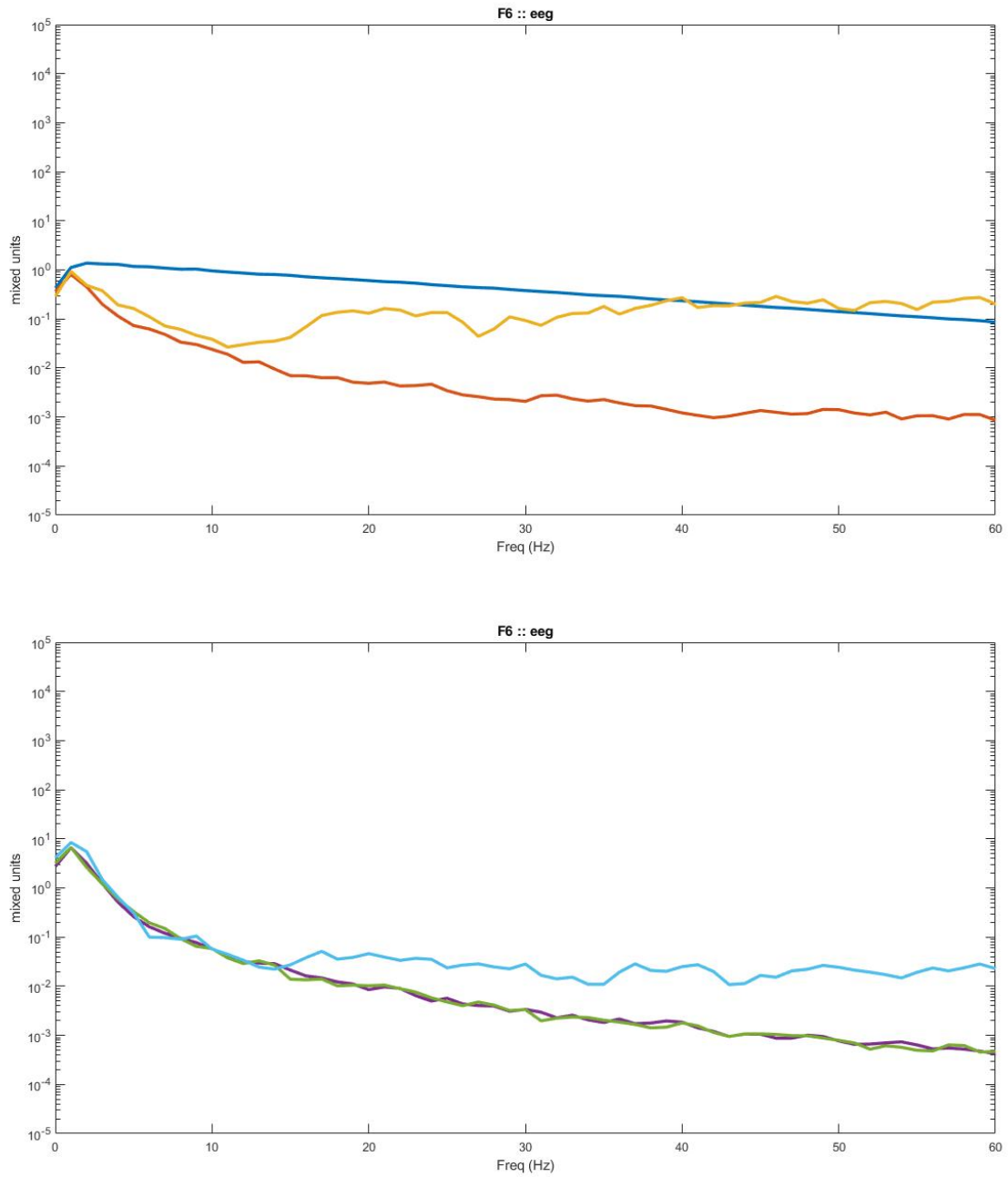


Figure 174. Graph shows electrode location F6. (top) shows software laplacian of tCRE EEG. (bottom) shows tCRE EEG

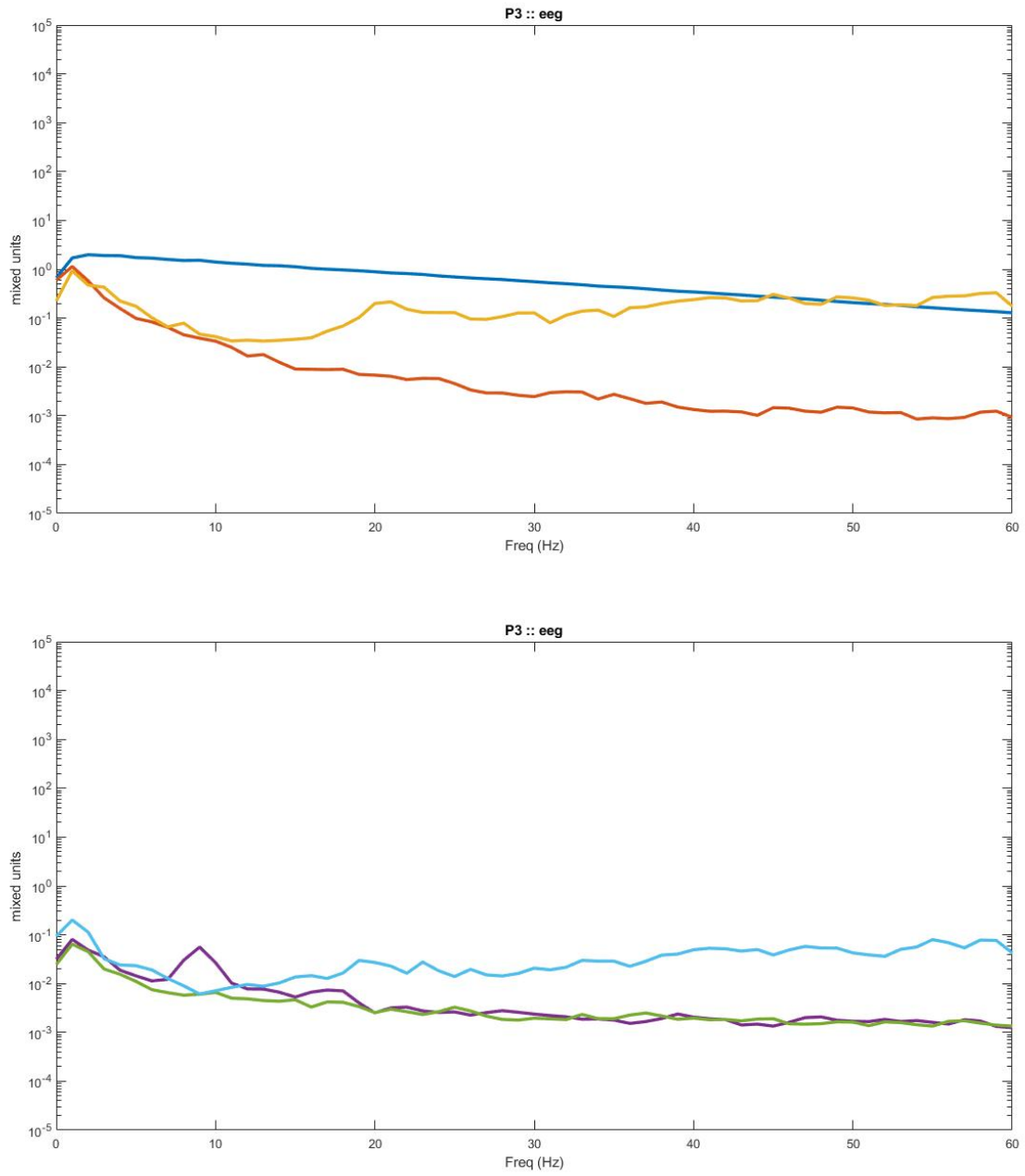


Figure 175. Graph shows electrode location P3. (top) shows software laplacian of tCRE EEG. (bottom) shows tCRE EEG

9.2.5.2. 20 tCRE electrodes used in cap with saline filled foam cap on subject with thick hair

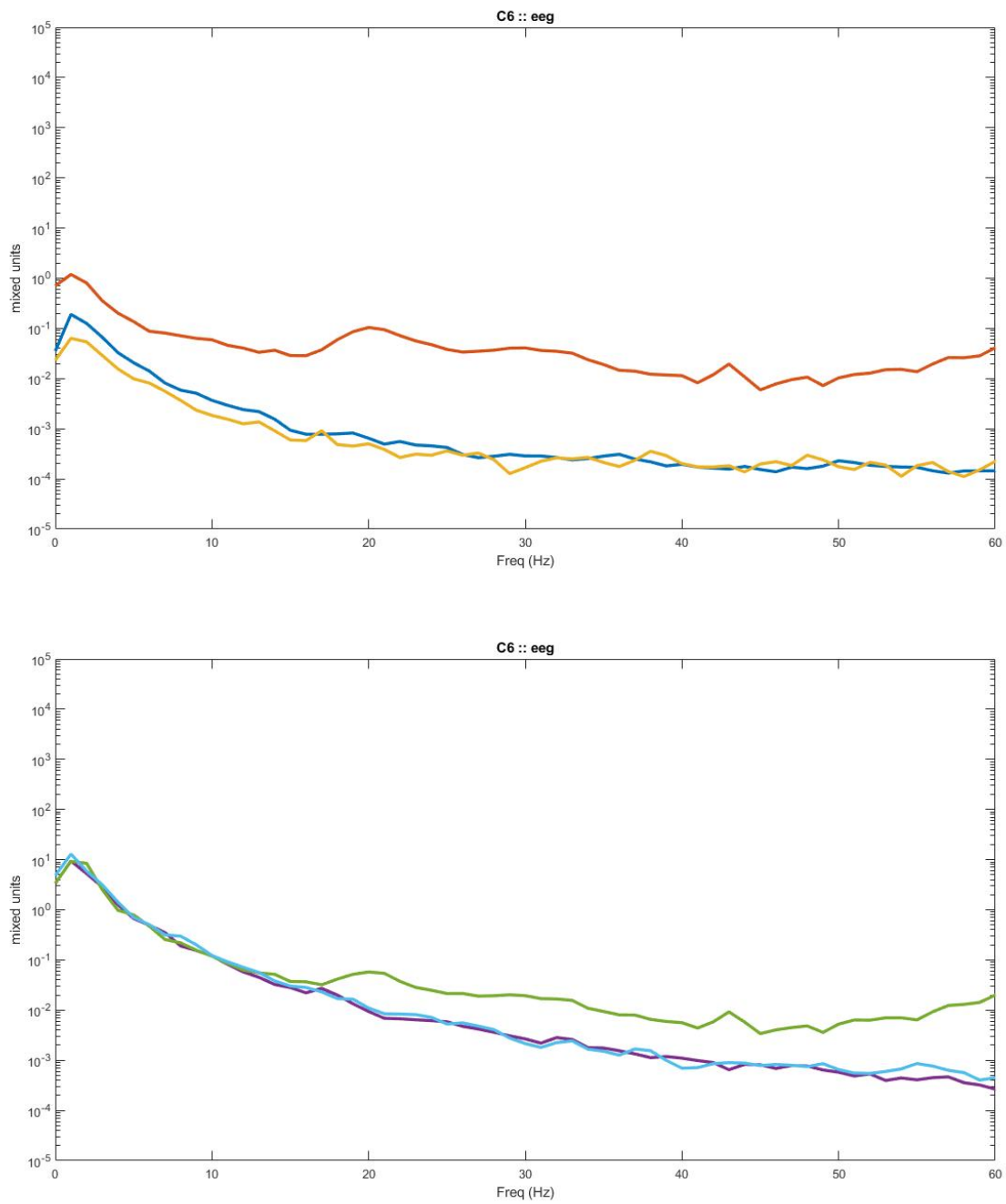


Figure 176. Graph shows electrode location C6. (top) shows software Laplacian of tCRE EEG. (bottom) shows tCRE EEG

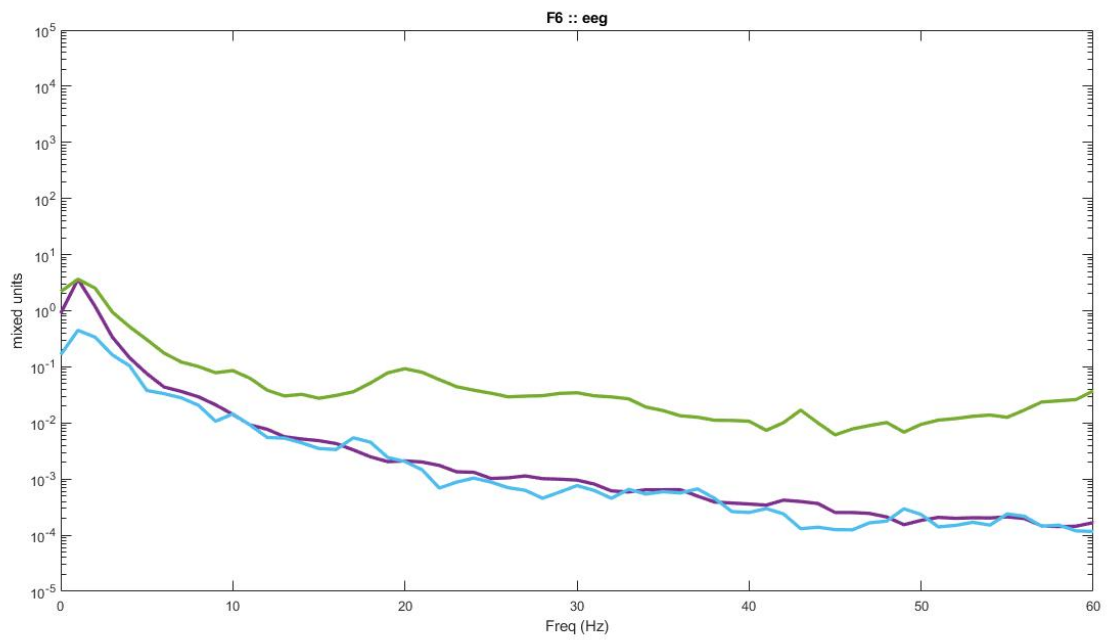
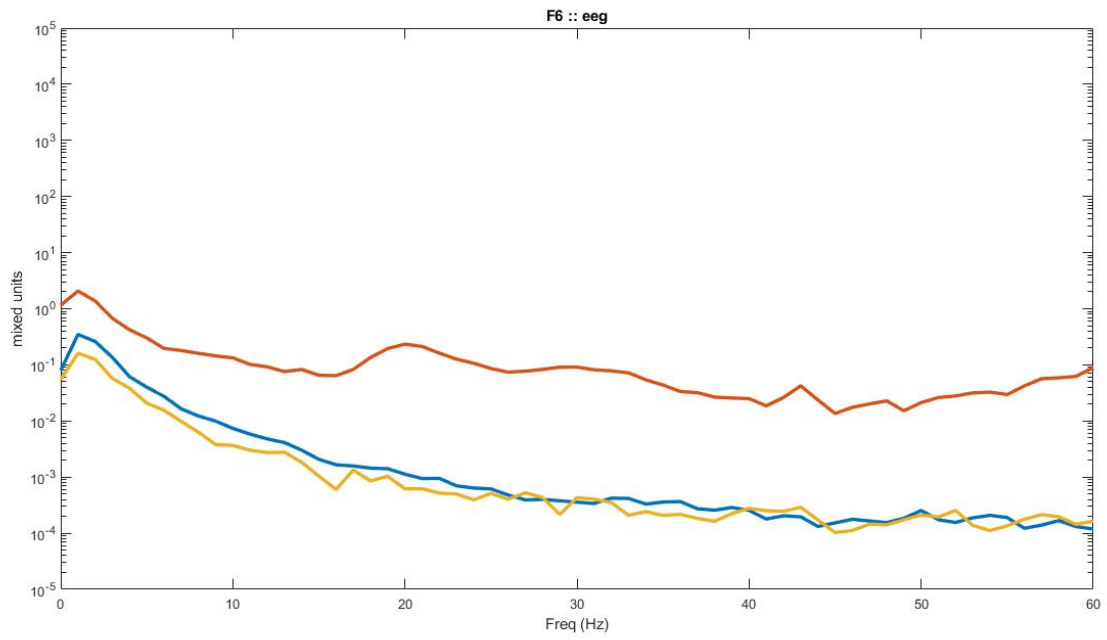


Figure 177. Graph shows electrode location F6. (top) shows software laplacian of tCRE EEG. (bottom) shows tCRE EEG

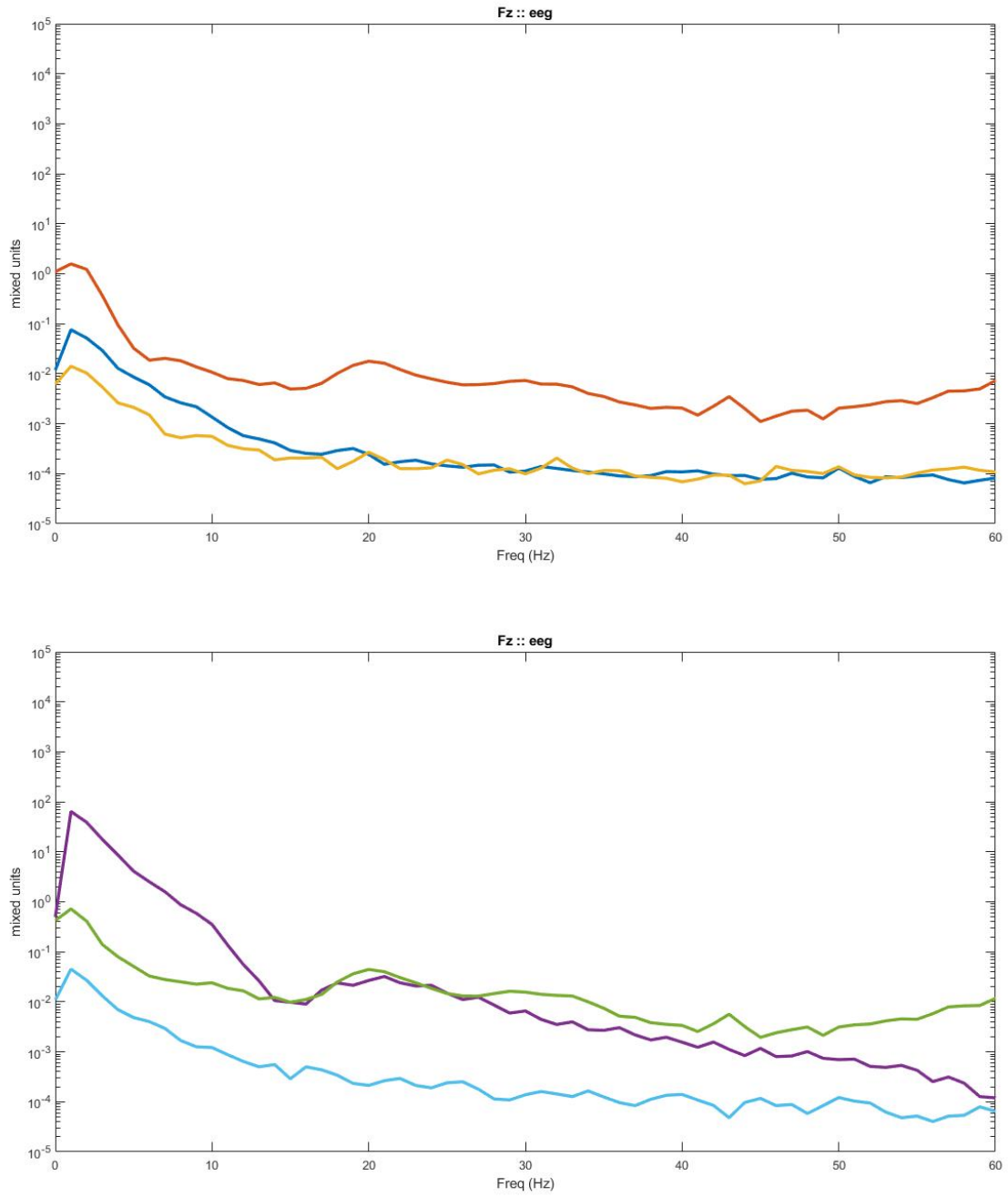


Figure 178. Graph shows electrode location Fz1. (top) shows software laplacian of tCRE EEG. (bottom) shows tCRE EEG

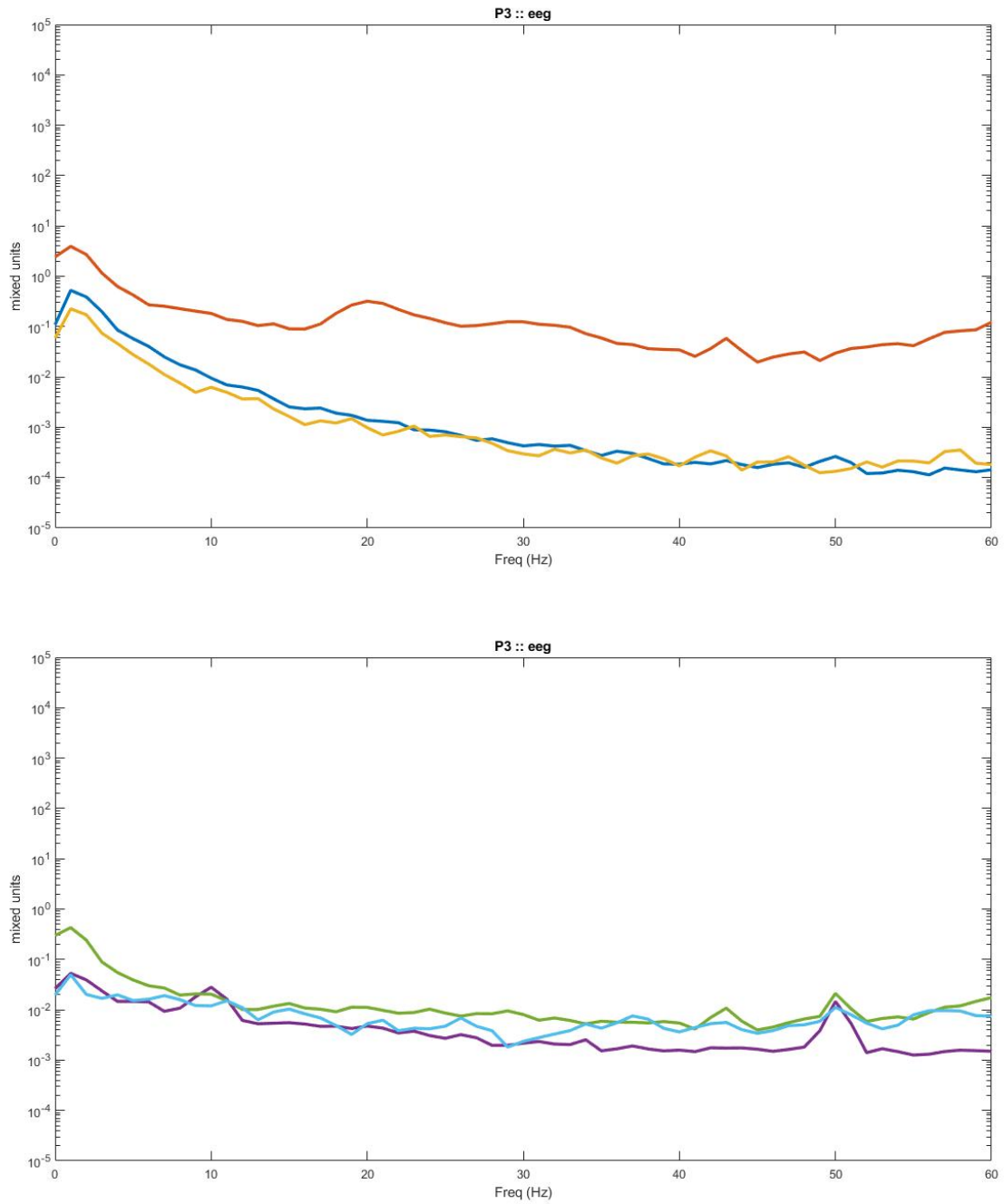


Figure 179. Graph shows electrode location P3. (top) shows software laplacian of tCRE EEG. (bottom) shows tCRE EEG

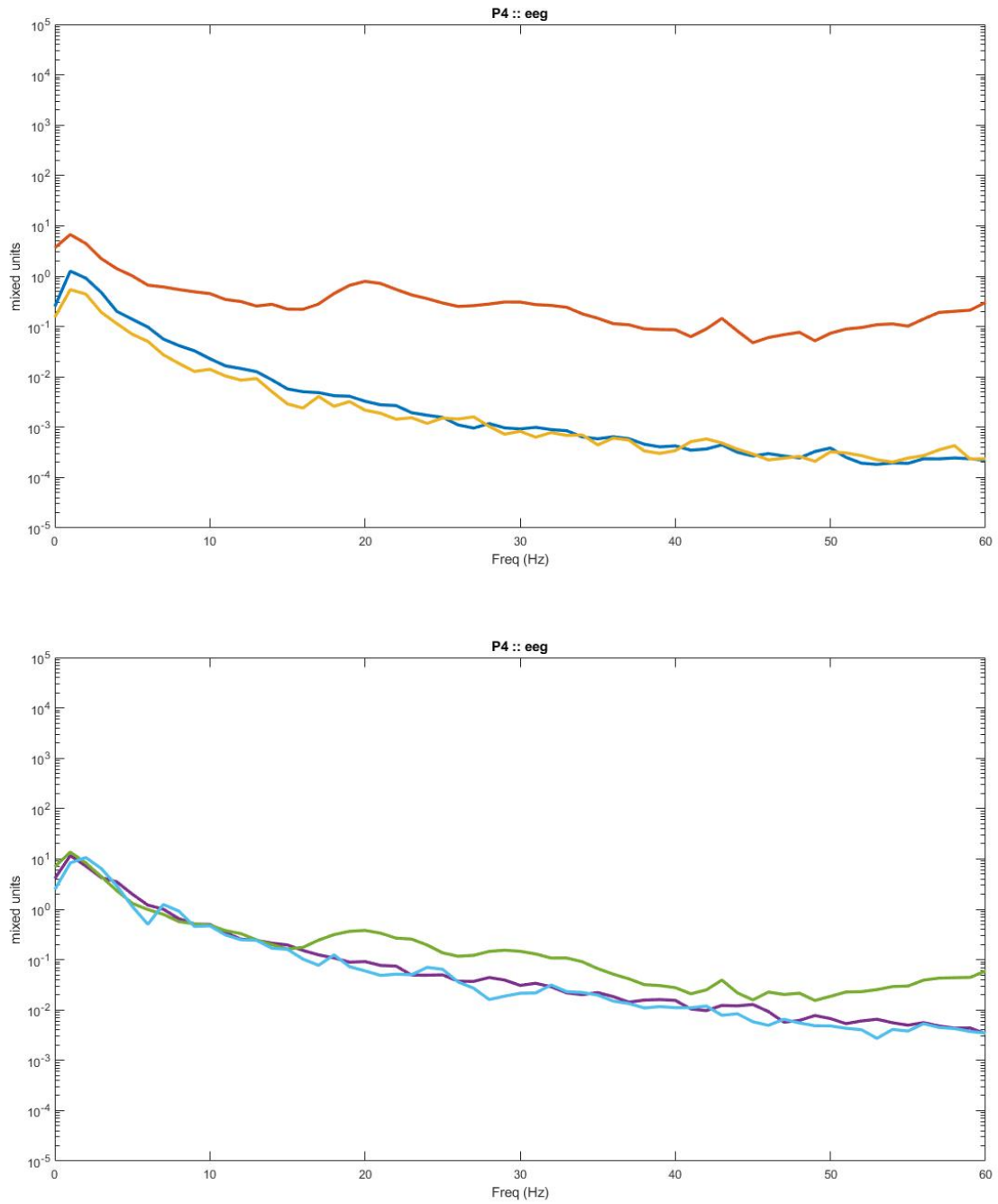


Figure 180. Graph shows electrode location P4. (top) shows software laplacian of tCRE EEG. (bottom) shows tCRE EEG

9.2.6. 20 tCRE electrodes used in cap with foam cap underneath

9.2.6.1. 20 tCRE electrodes used in cap with foam cap underneath on subject with thick hair

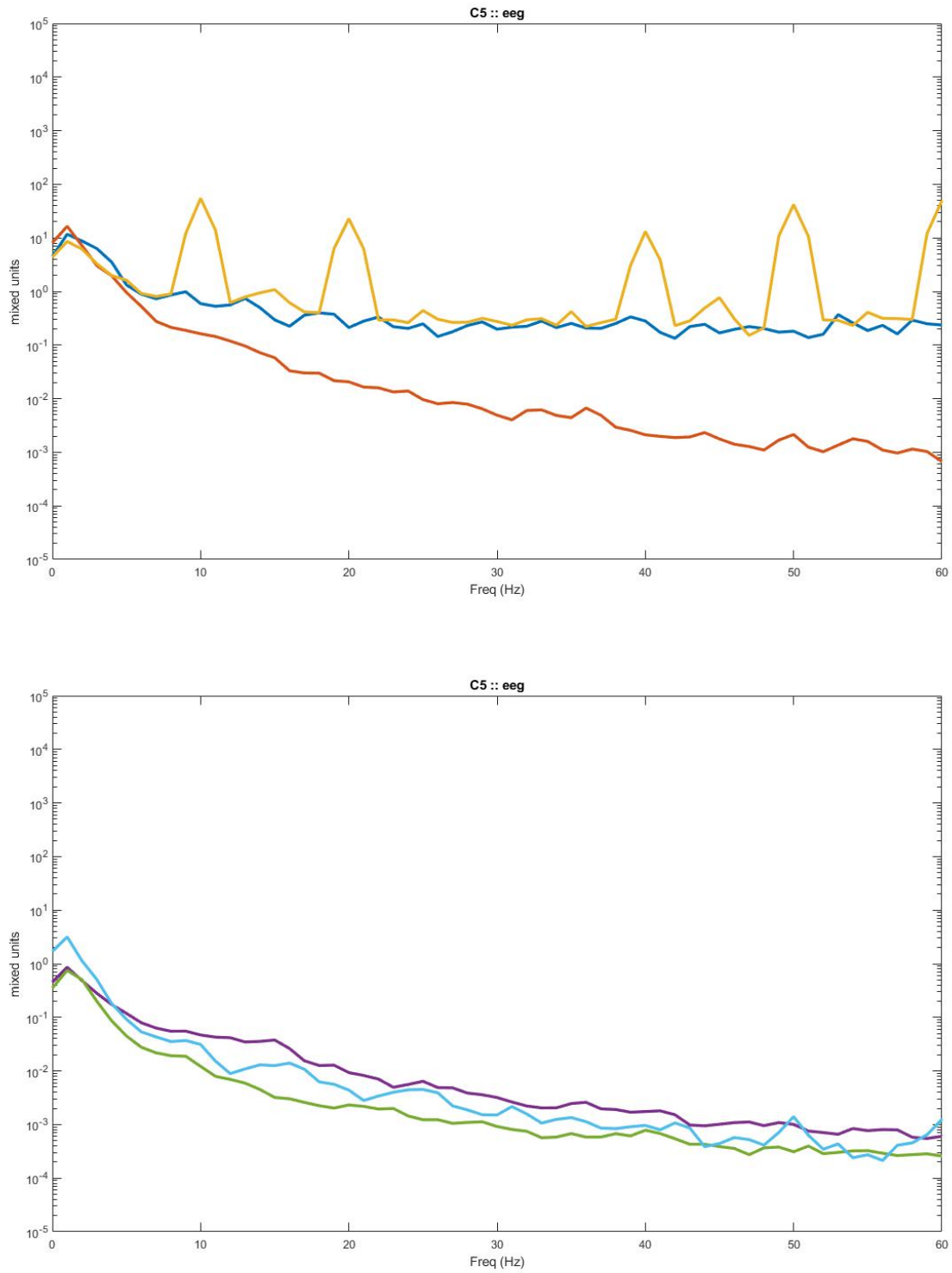


Figure 181. Graph shows electrode location C5. (top) shows software laplacian of tCRE EEG. (bottom) shows tCRE EEG

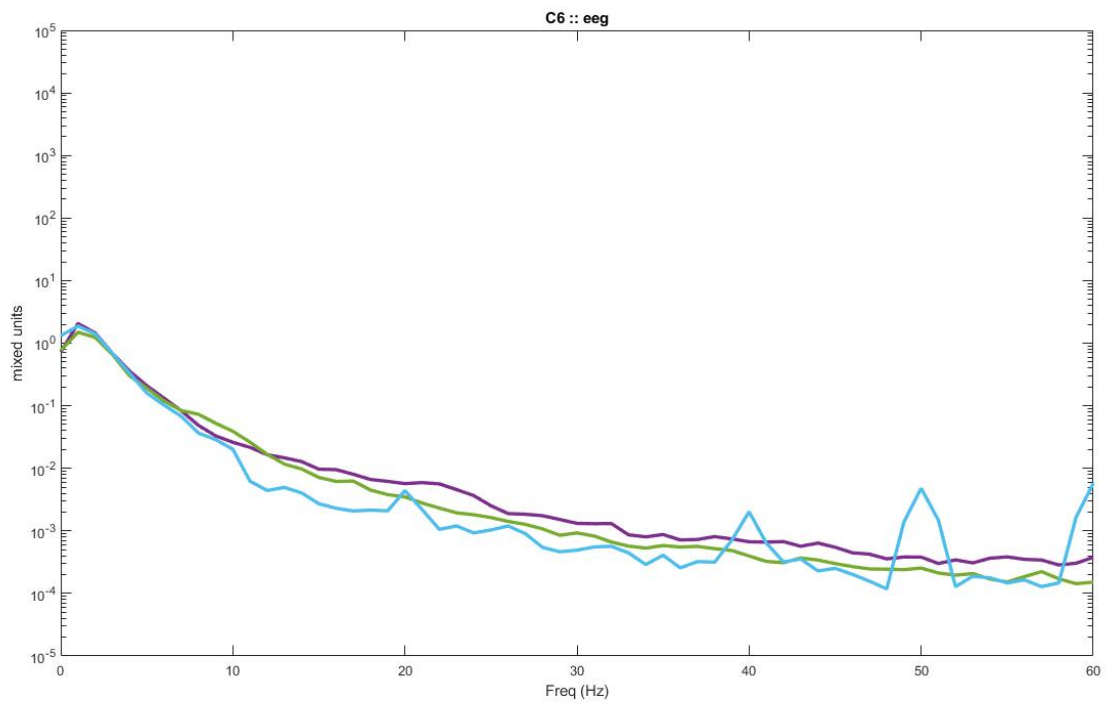
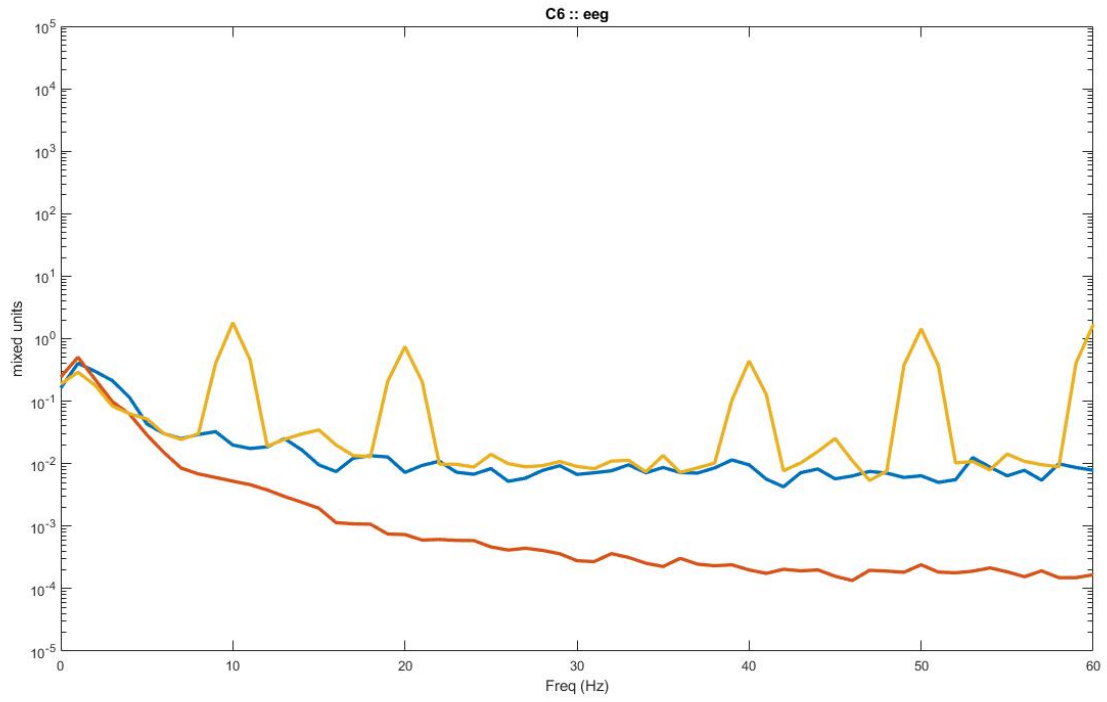


Figure 182. Graph shows electrode location C6. (top) shows software laplacian of tCRE EEG. (bottom) shows tCRE EEG

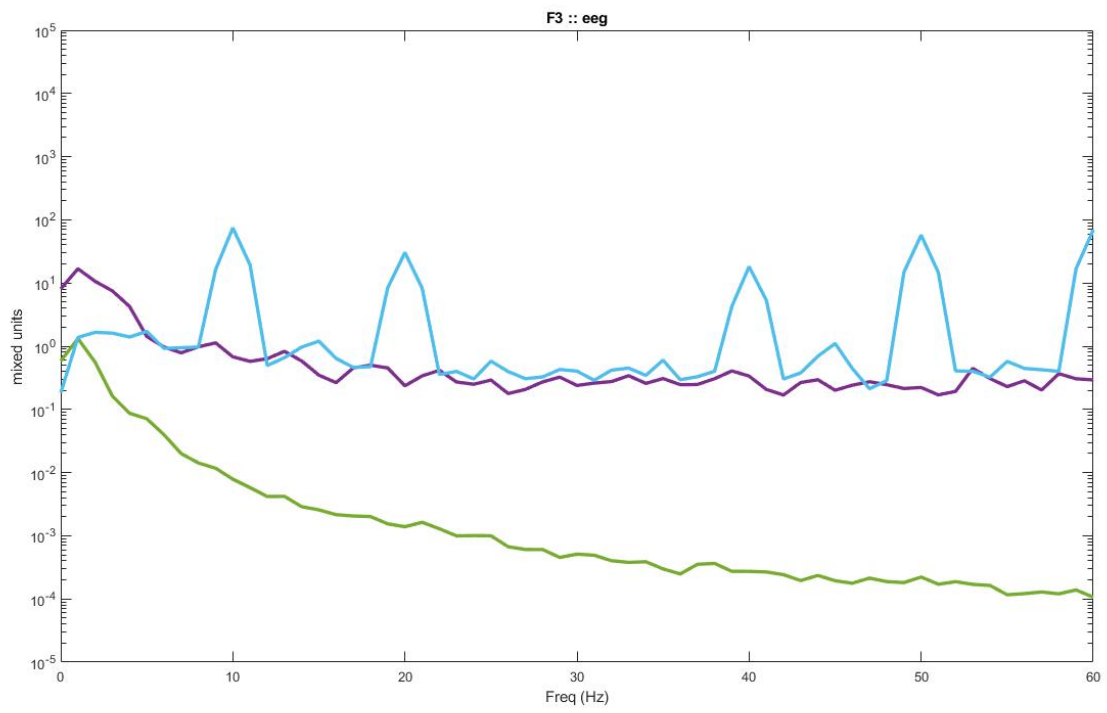
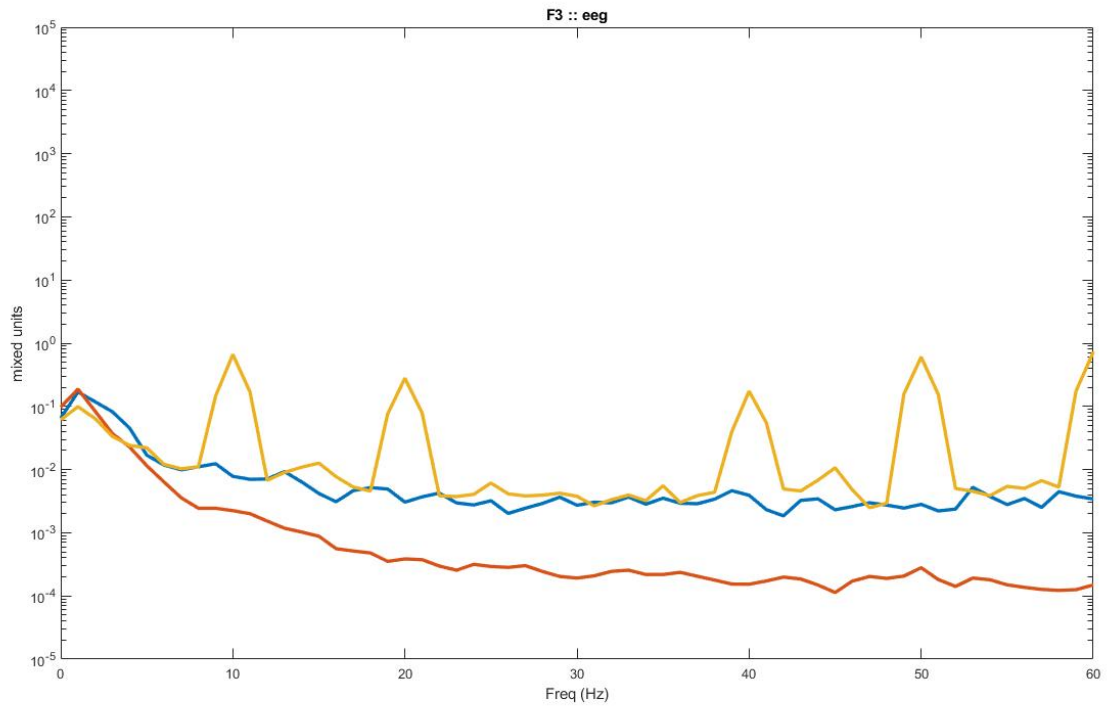


Figure 183. Graph shows electrode location F3. (top) shows software laplacian of tCRE EEG. (bottom) shows tCRE EEG

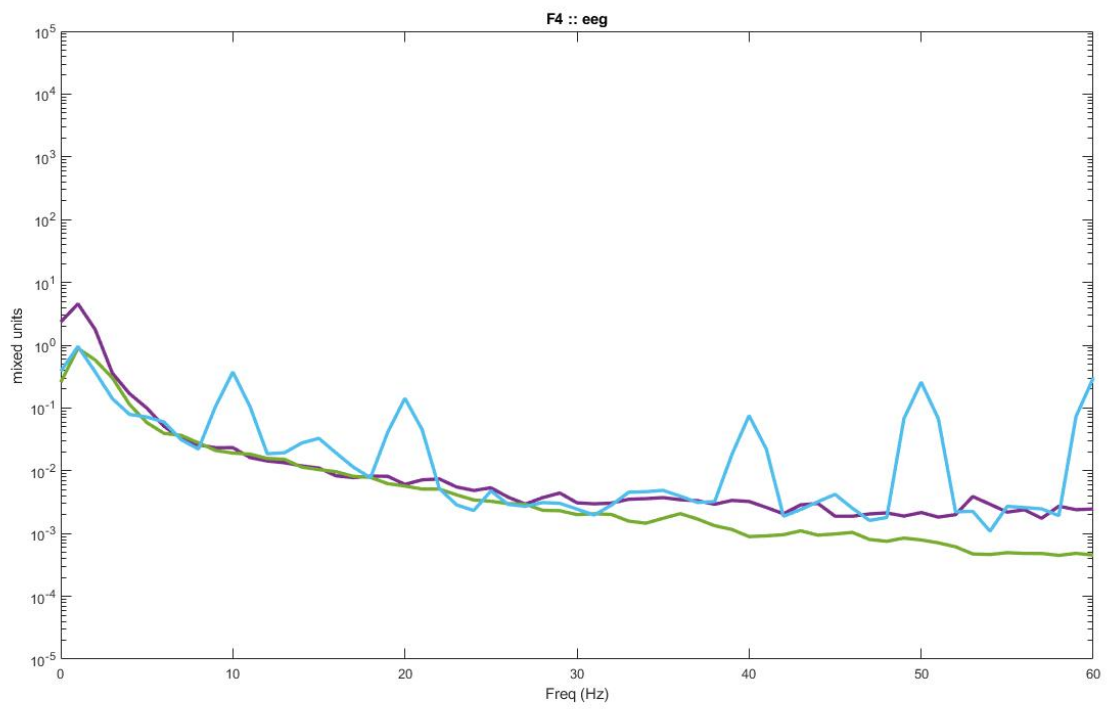
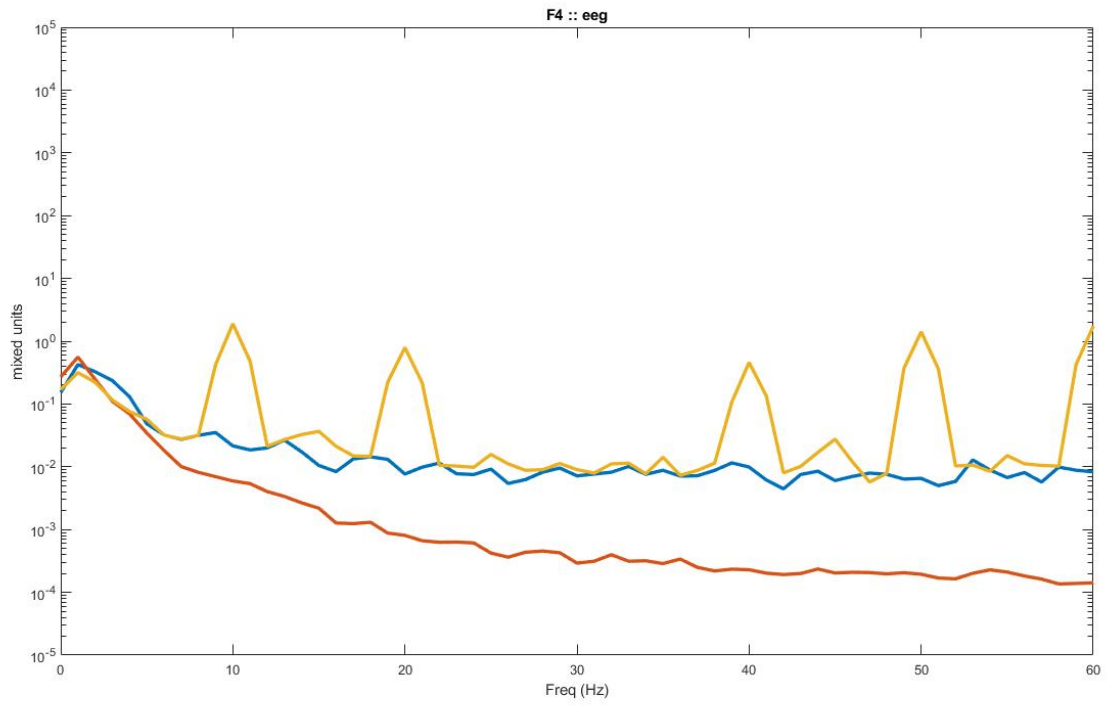


Figure 184. Graph shows electrode location F4. (top) shows software laplacian of tCRE EEG. (bottom) shows tCRE EEG

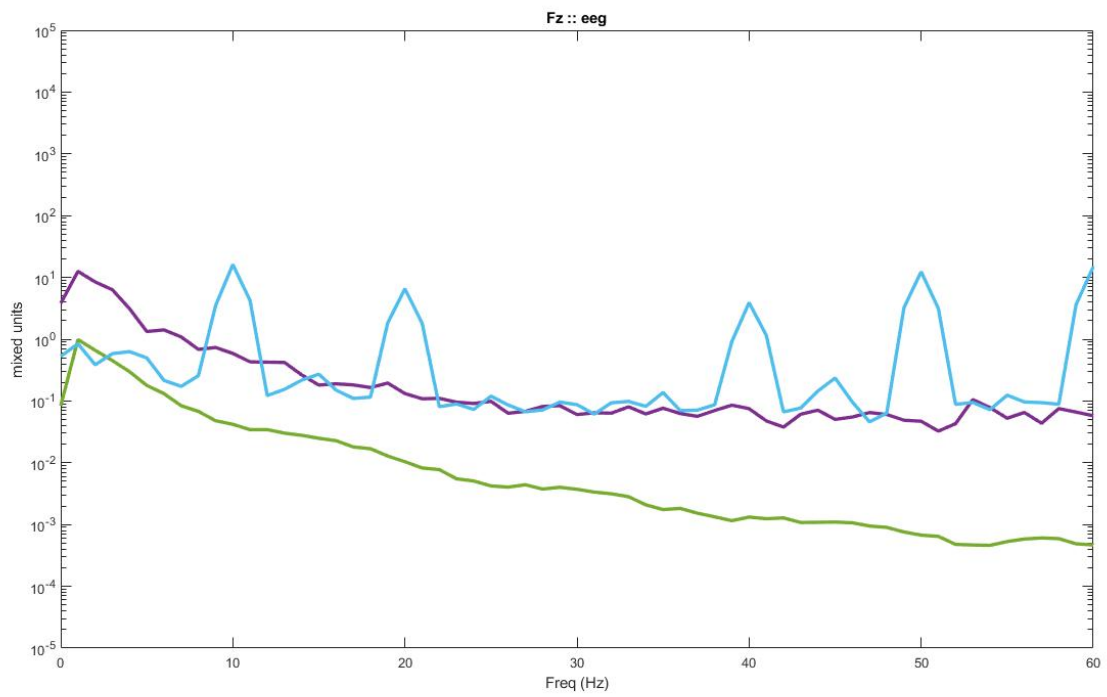
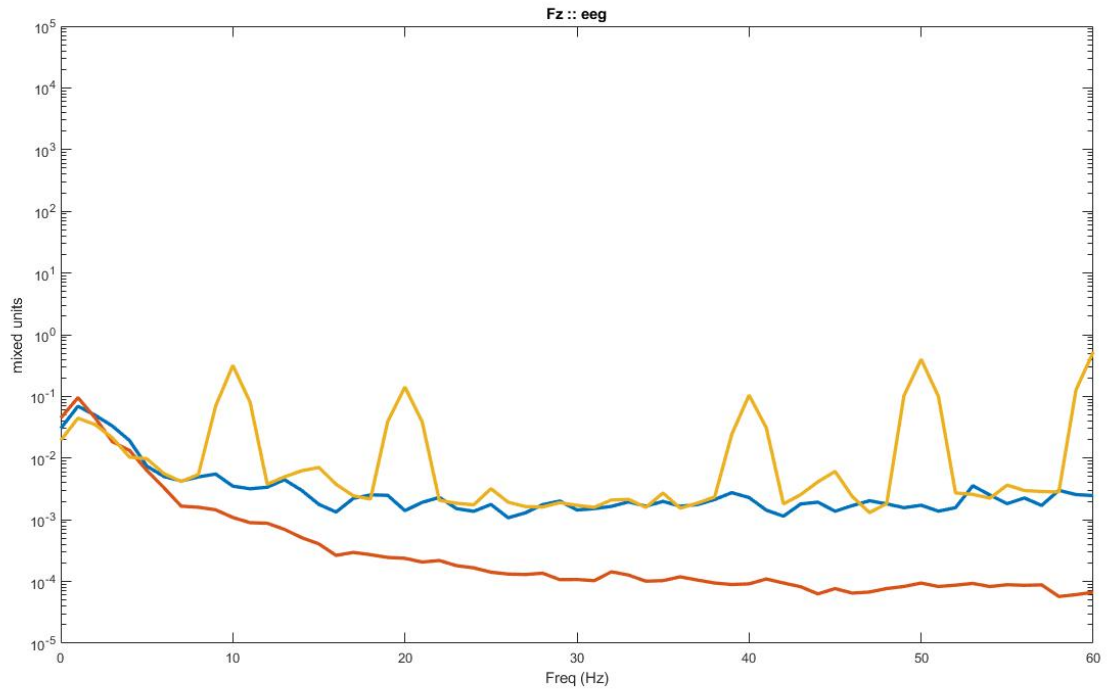


Figure 185. Graph shows electrode location Fz. (top) shows software laplacian of tCRE EEG. (bottom) shows tCRE EEG

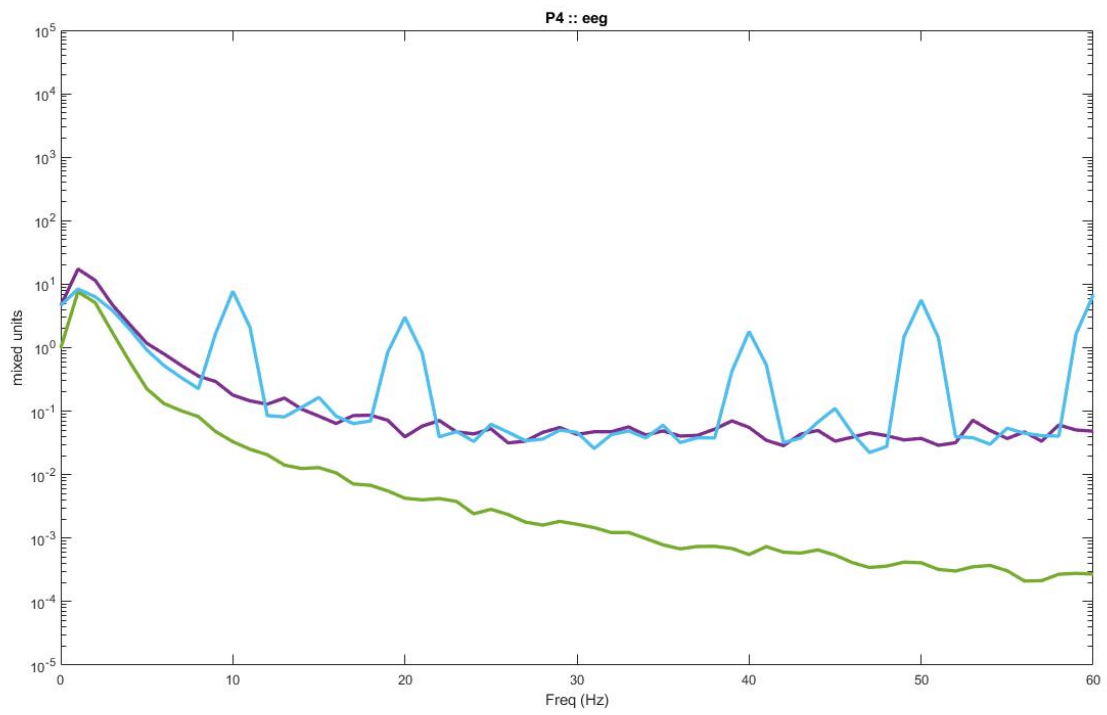
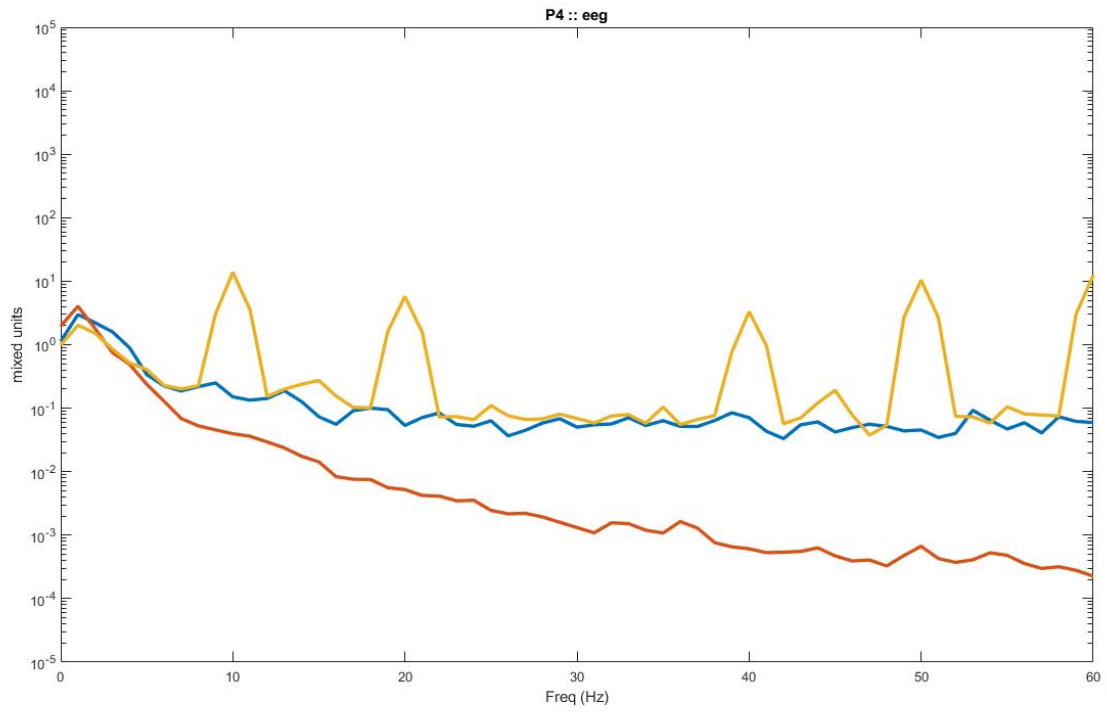


Figure 186. Graph shows electrode location P4. (top) shows software laplacian of tCRE EEG. (bottom) shows tCRE EEG

9.2.6.2. 20 tCRE electrodes with foam cap used on subject with short, stiff curly hair

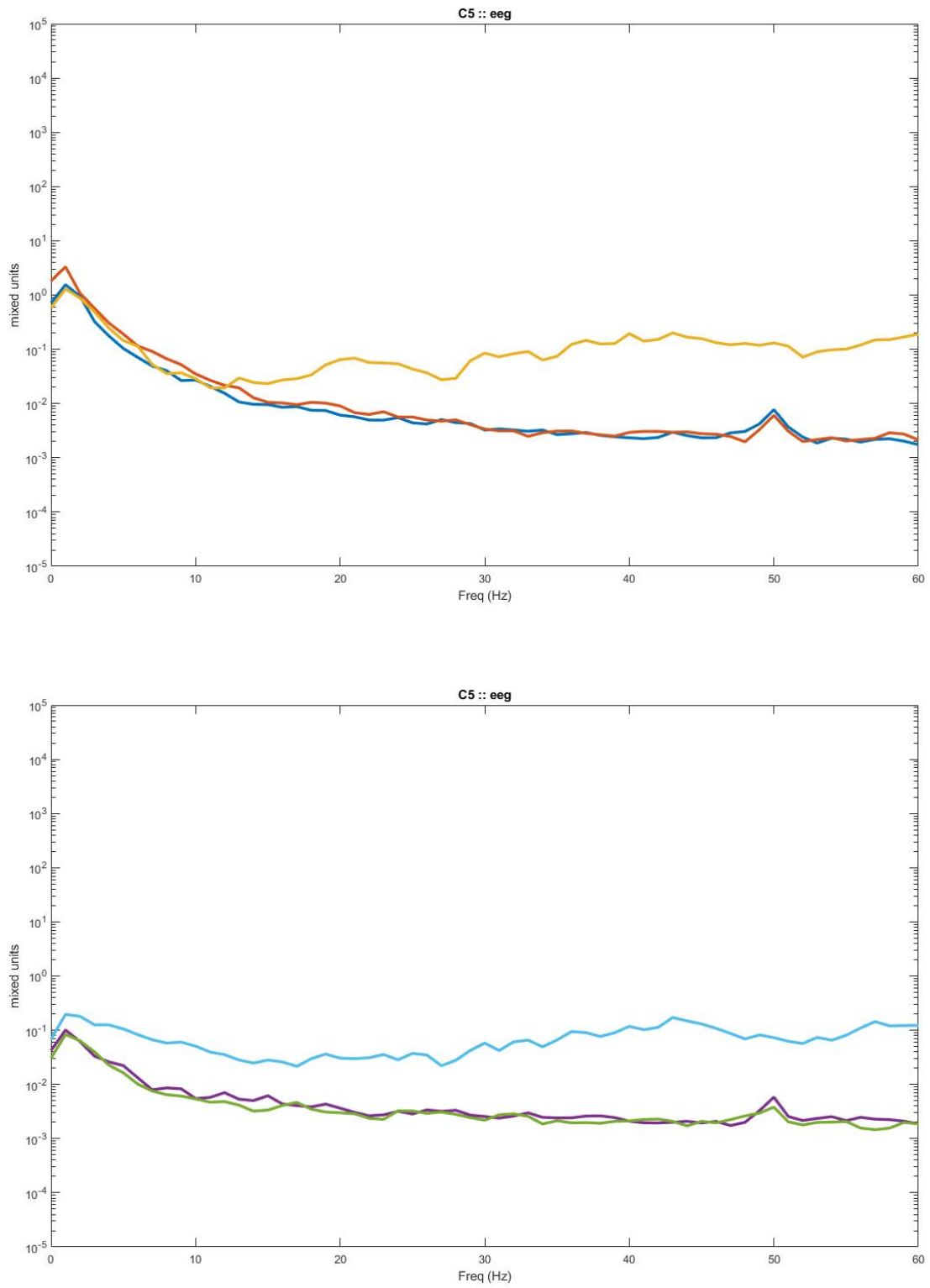


Figure 187. Graph shows electrode location C5. (top) shows software laplacian of tCRE EEG. (bottom) shows tCRE EEG

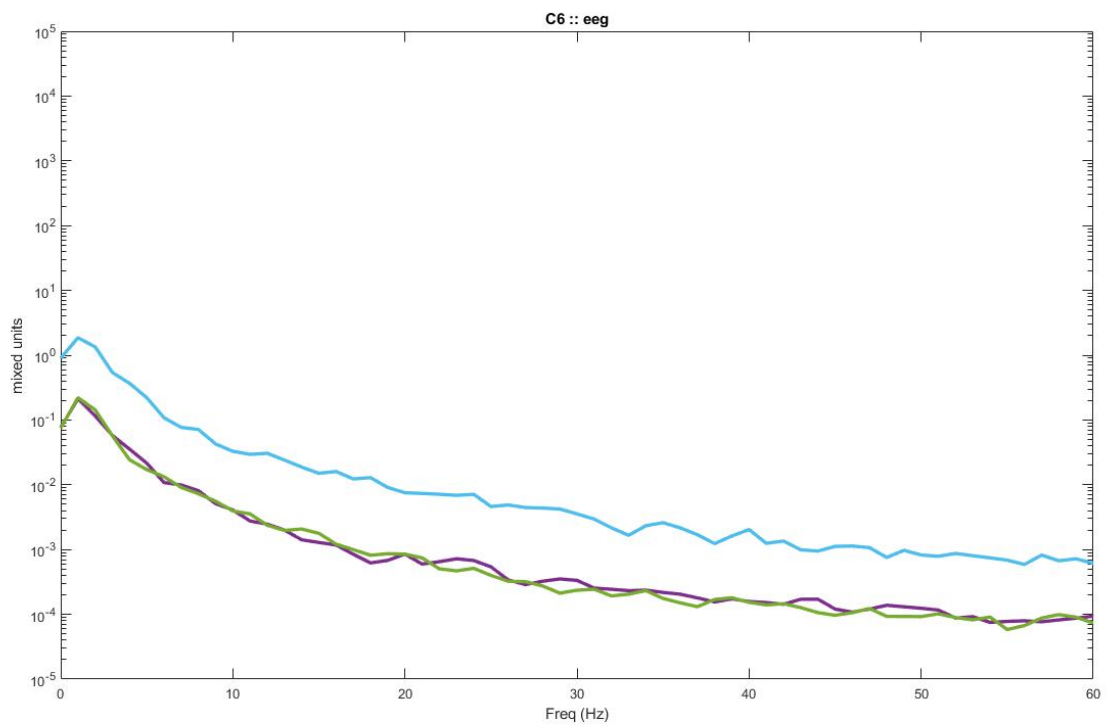
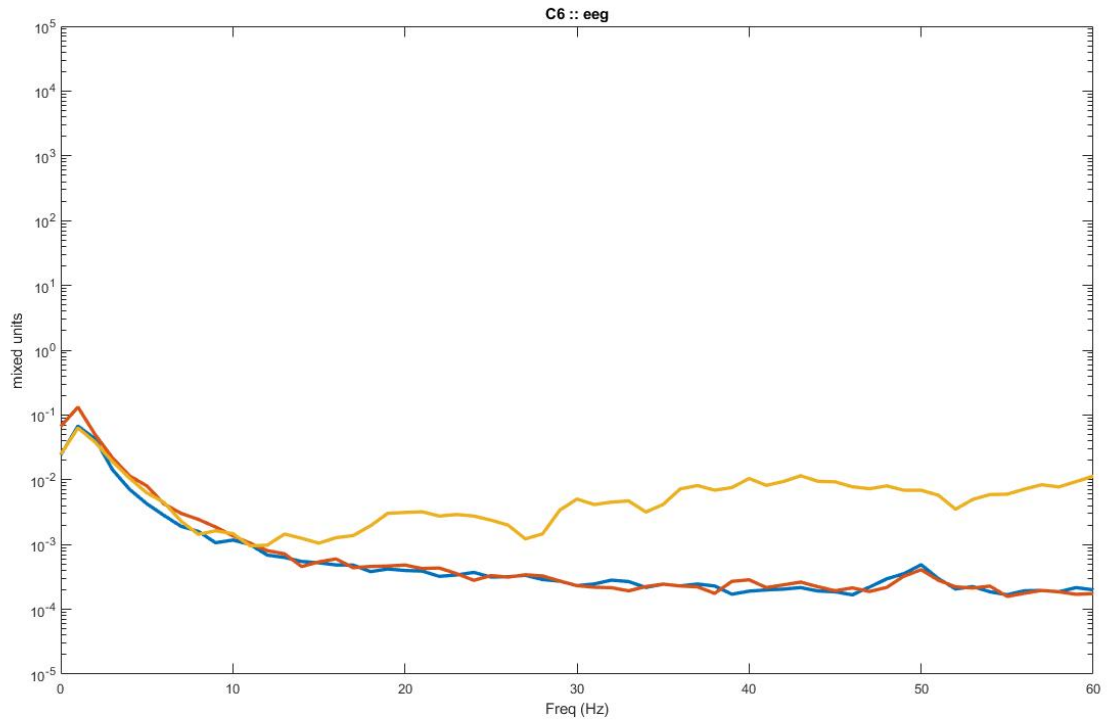


Figure 188. Graph shows electrode location C6. (top) shows software laplacian of tCRE EEG. (bottom) shows tCRE EEG

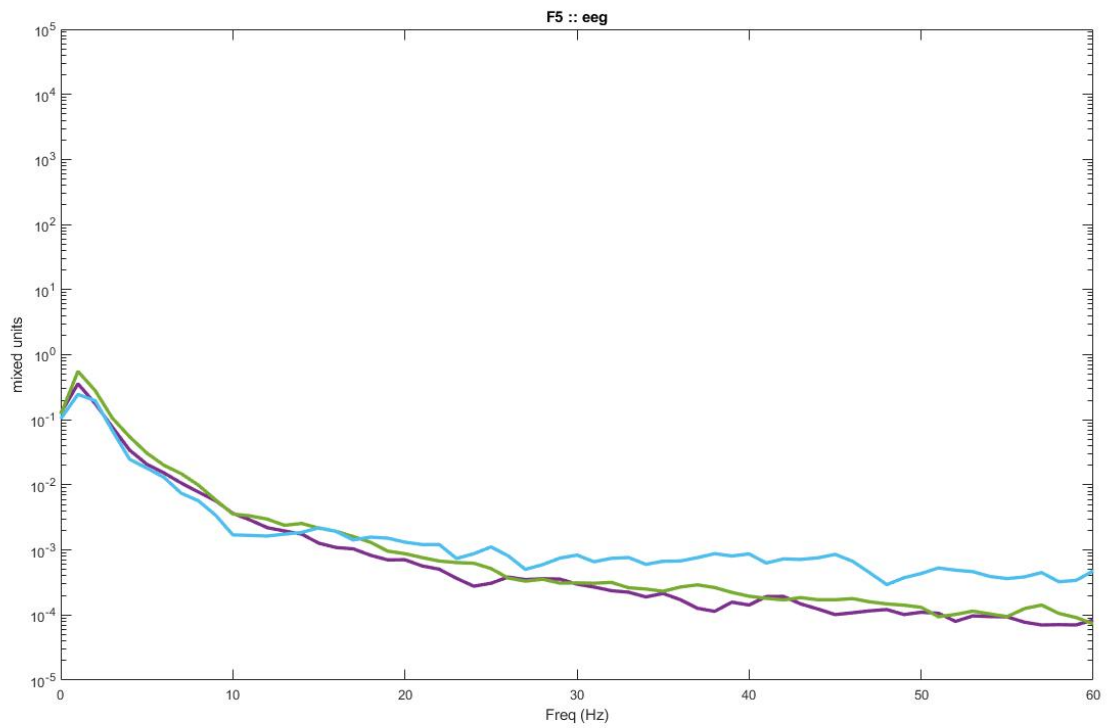
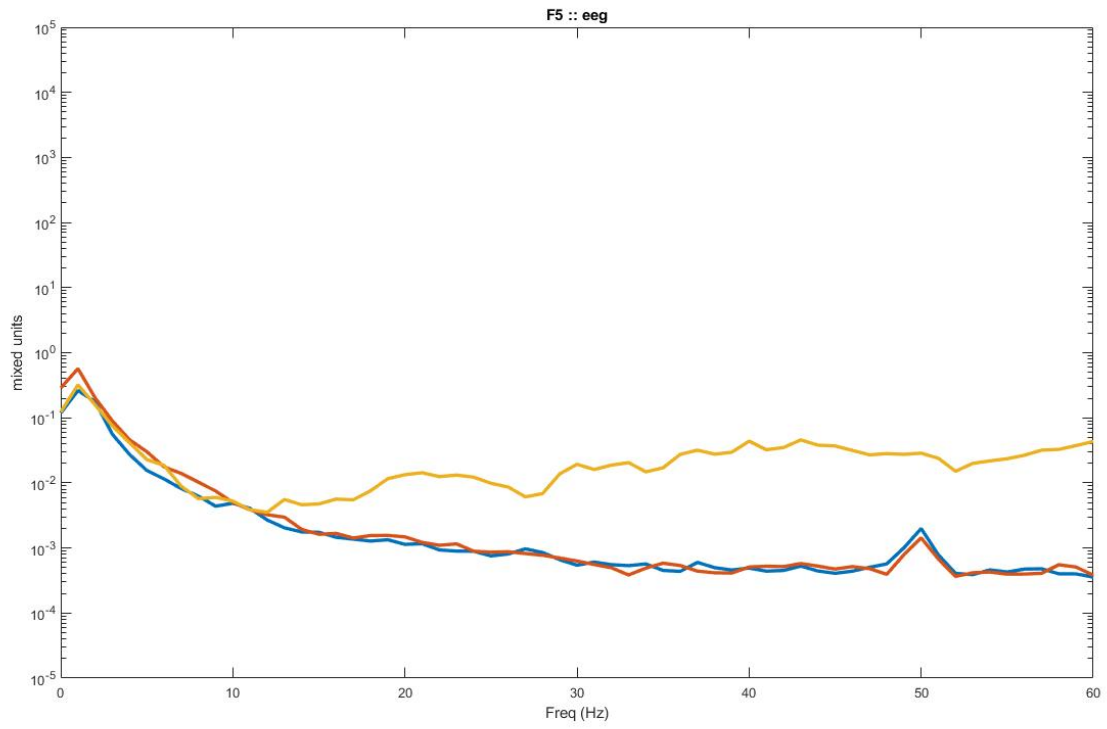


Figure 189. Graph shows electrode location F5. (top) shows software laplacian of tCRE EEG. (bottom) shows tCRE EEG

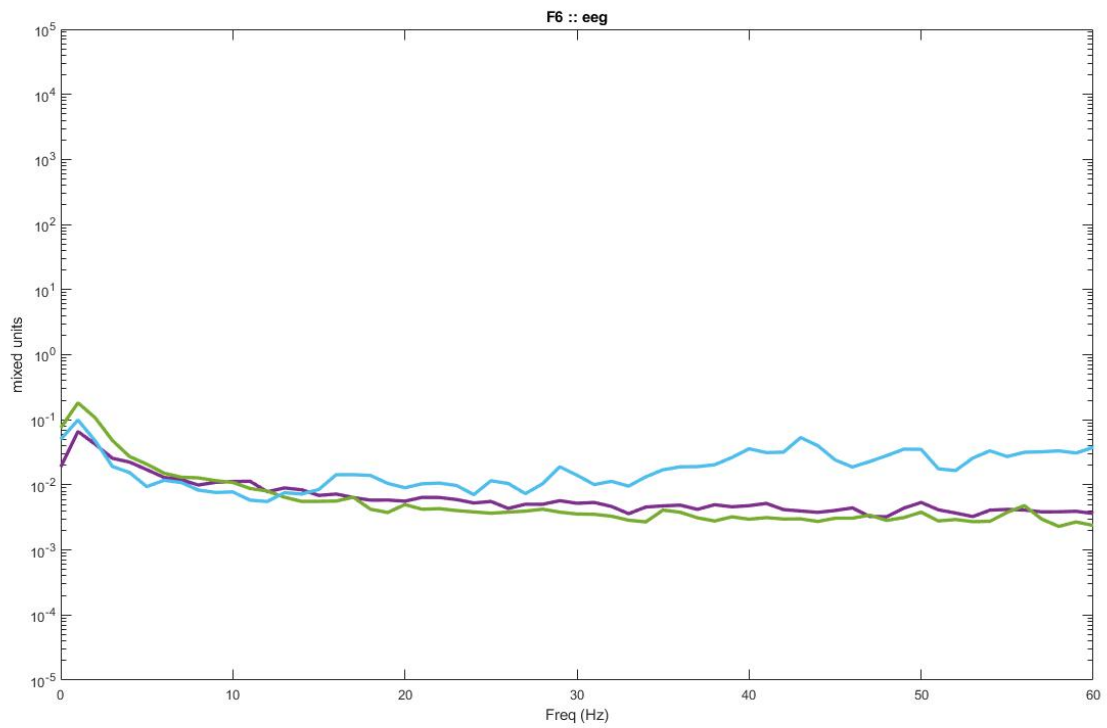
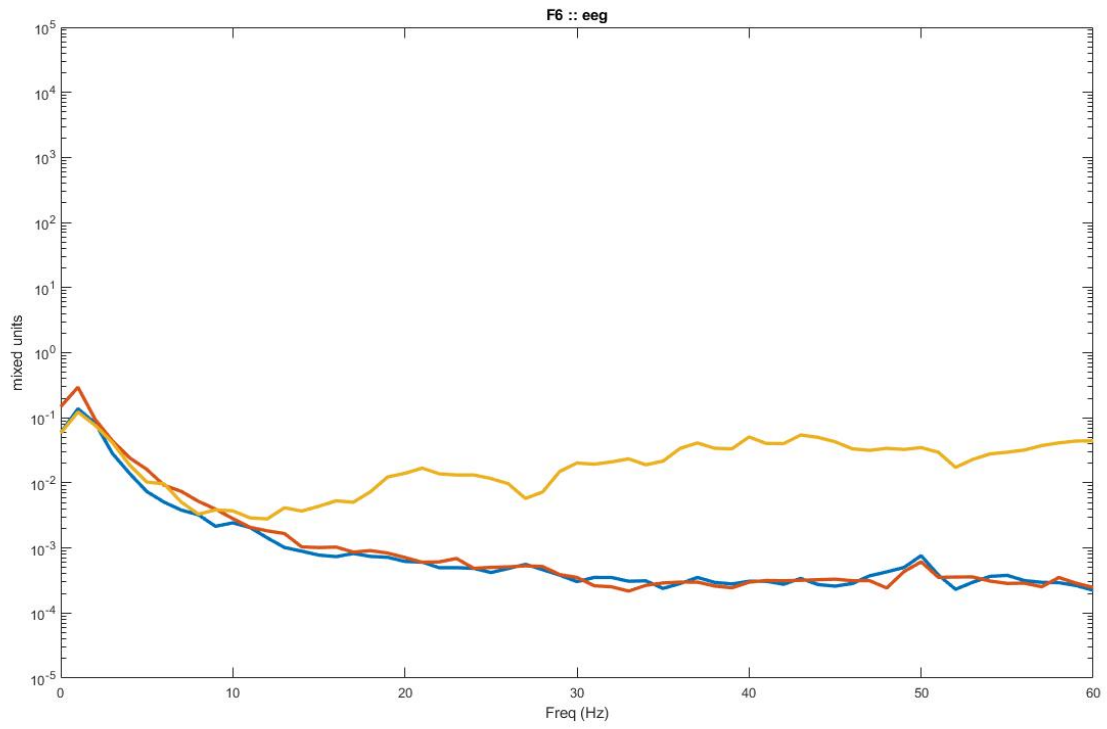


Figure 190. Graph shows electrode location F6. (top) shows software laplacian of tCRE EEG. (bottom) shows tCRE EEG

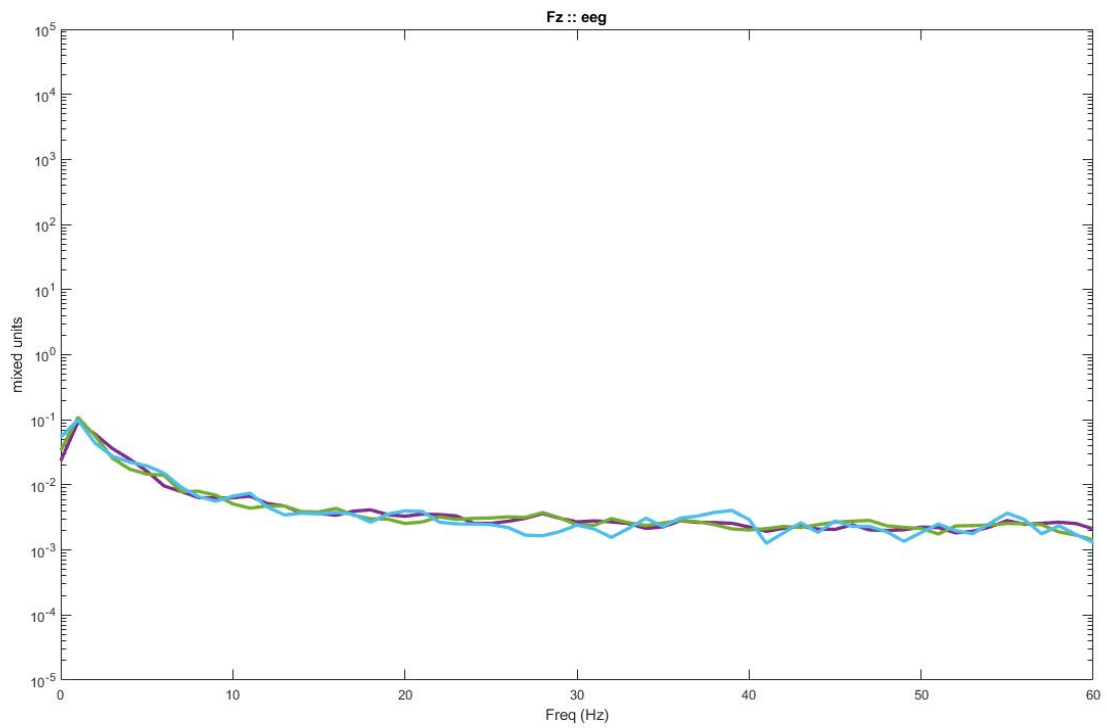
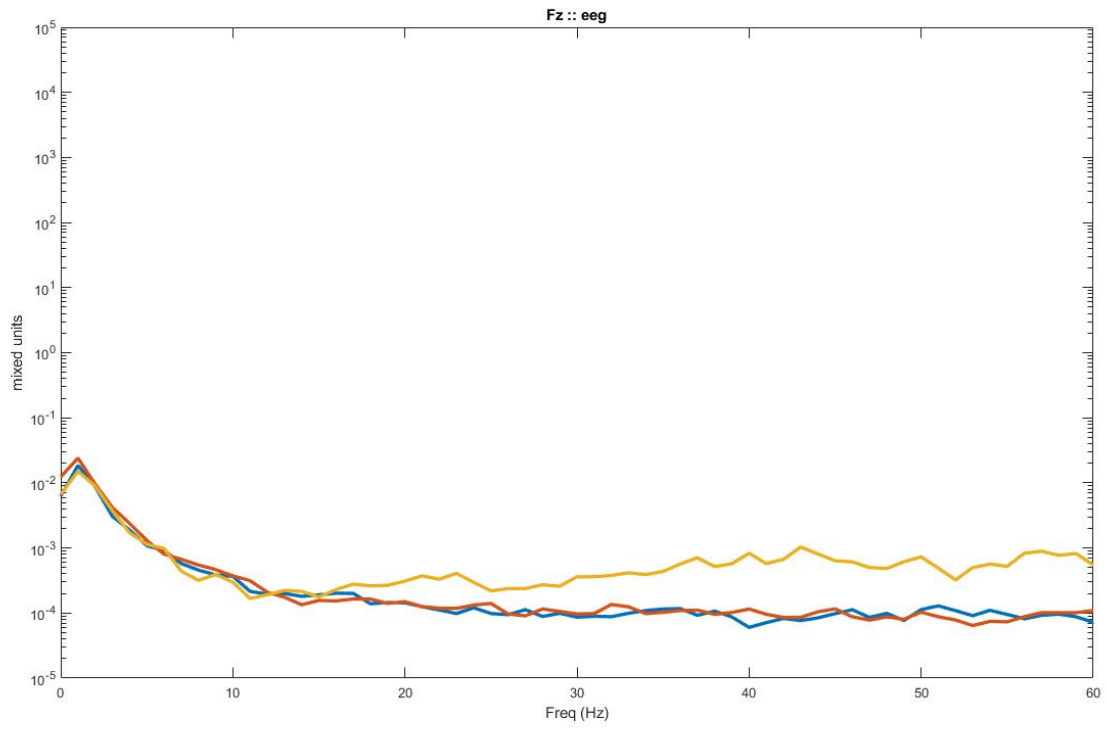


Figure 191. Graph shows electrode location Fz. (top) shows software laplacian of tCRE EEG. (bottom) shows tCRE EEG

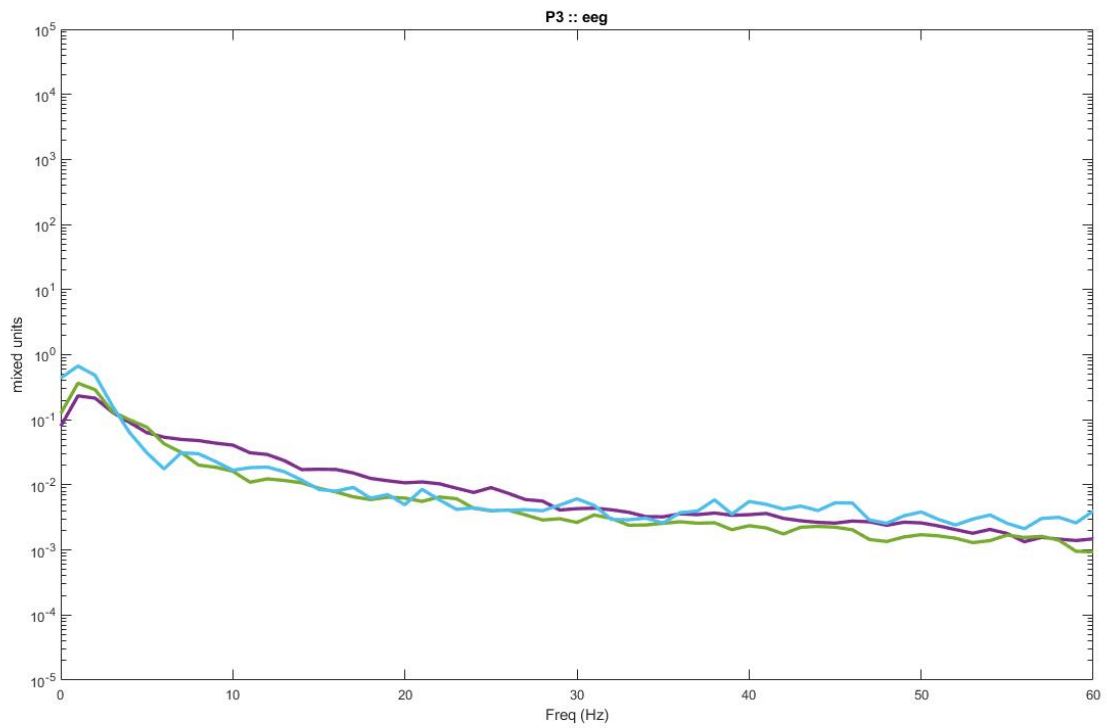
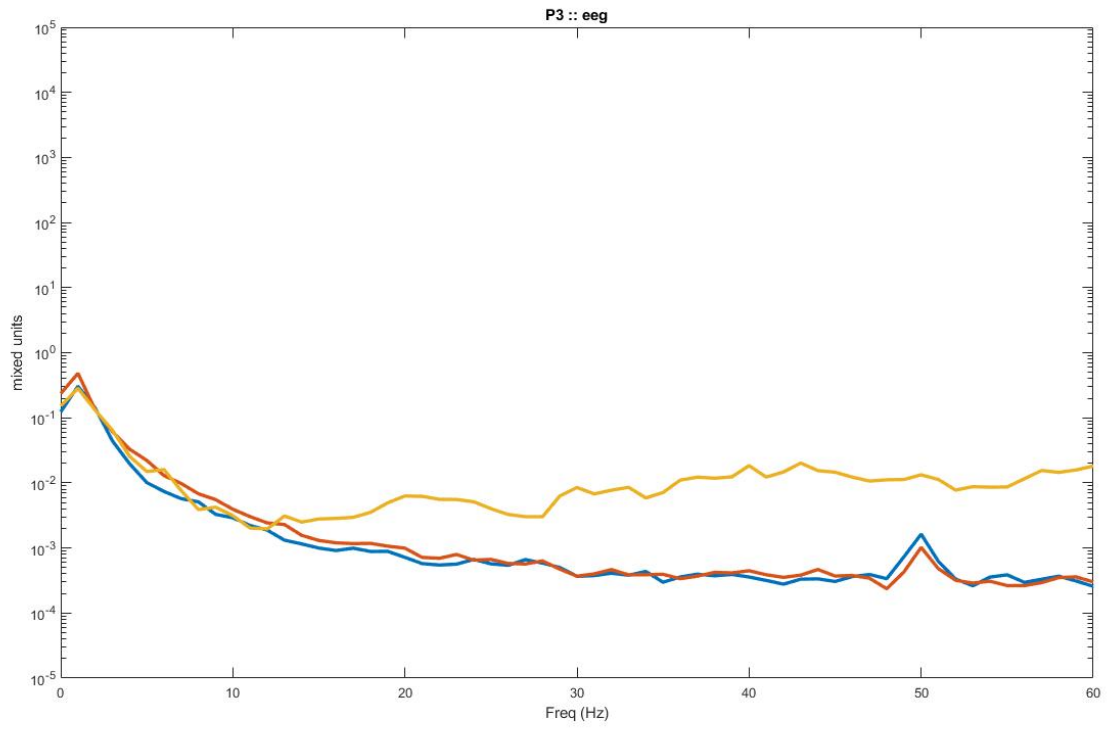


Figure 192. Graph shows electrode location P3. (top) shows software laplacian of tCRE EEG. (bottom) shows tCRE EEG

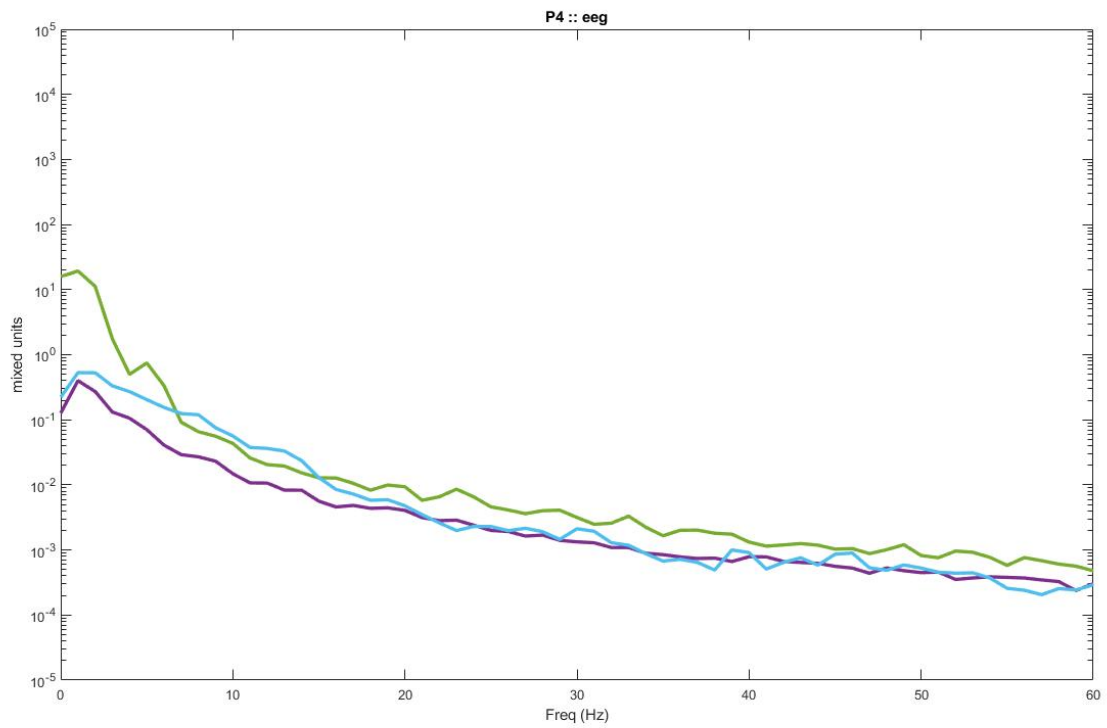
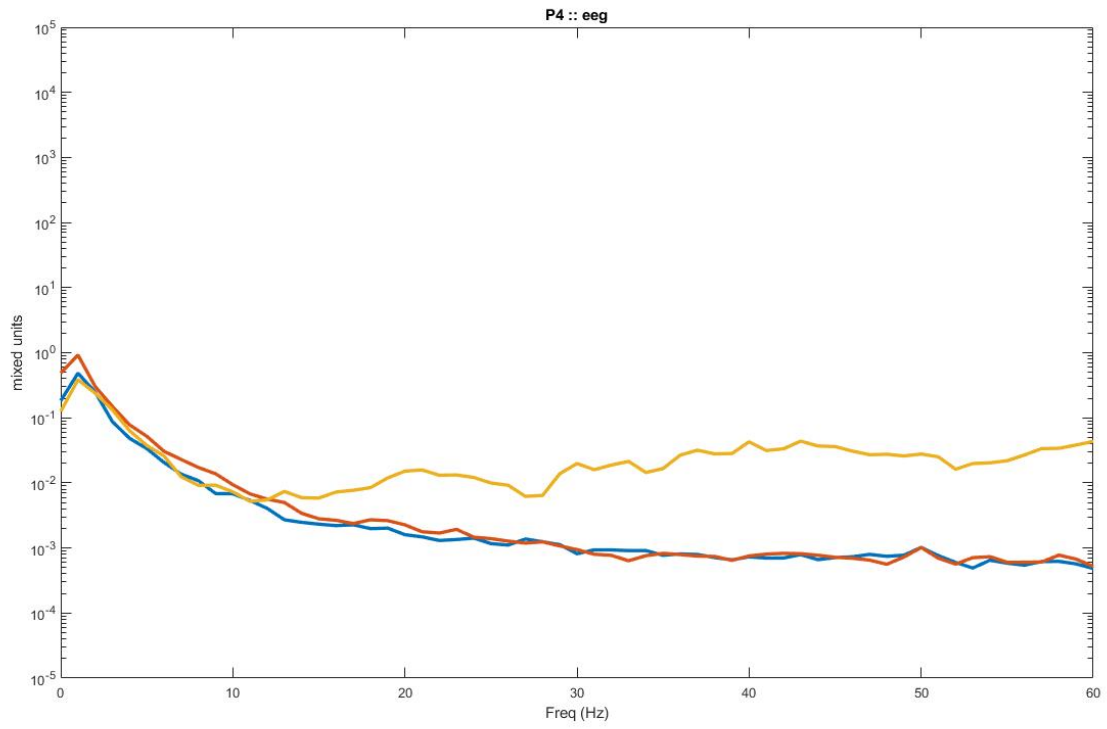


Figure 193. Graph shows electrode location P4. (top) shows software laplacian of tCRE EEG. (bottom) shows tCRE EEG

9.2.7. 20 ring electrodes used 'dry' in the cap

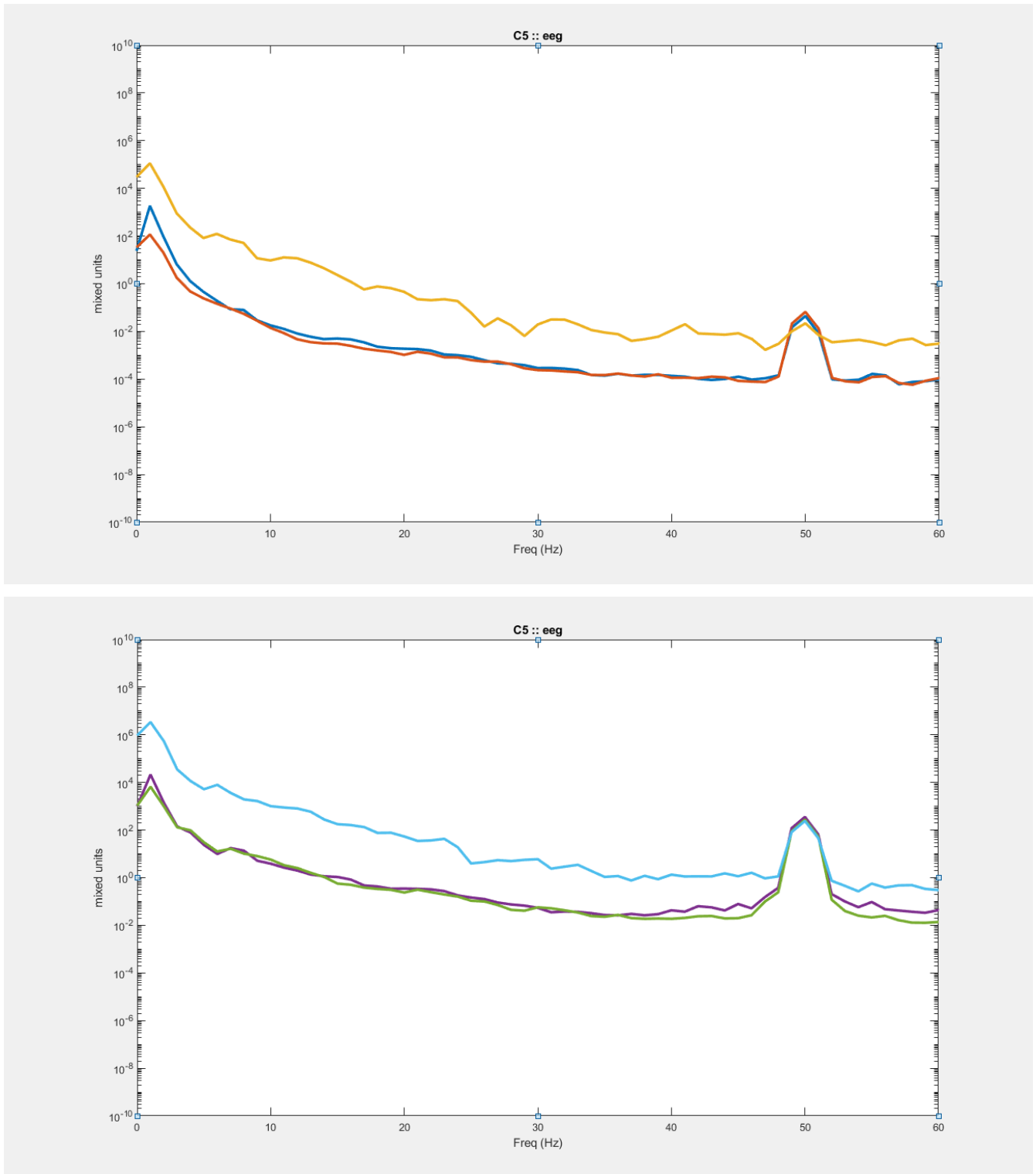


Figure 194. Graph shows electrode location C5. (top) shows software laplacian of electrode EEG. (bottom) shows electrode EEG

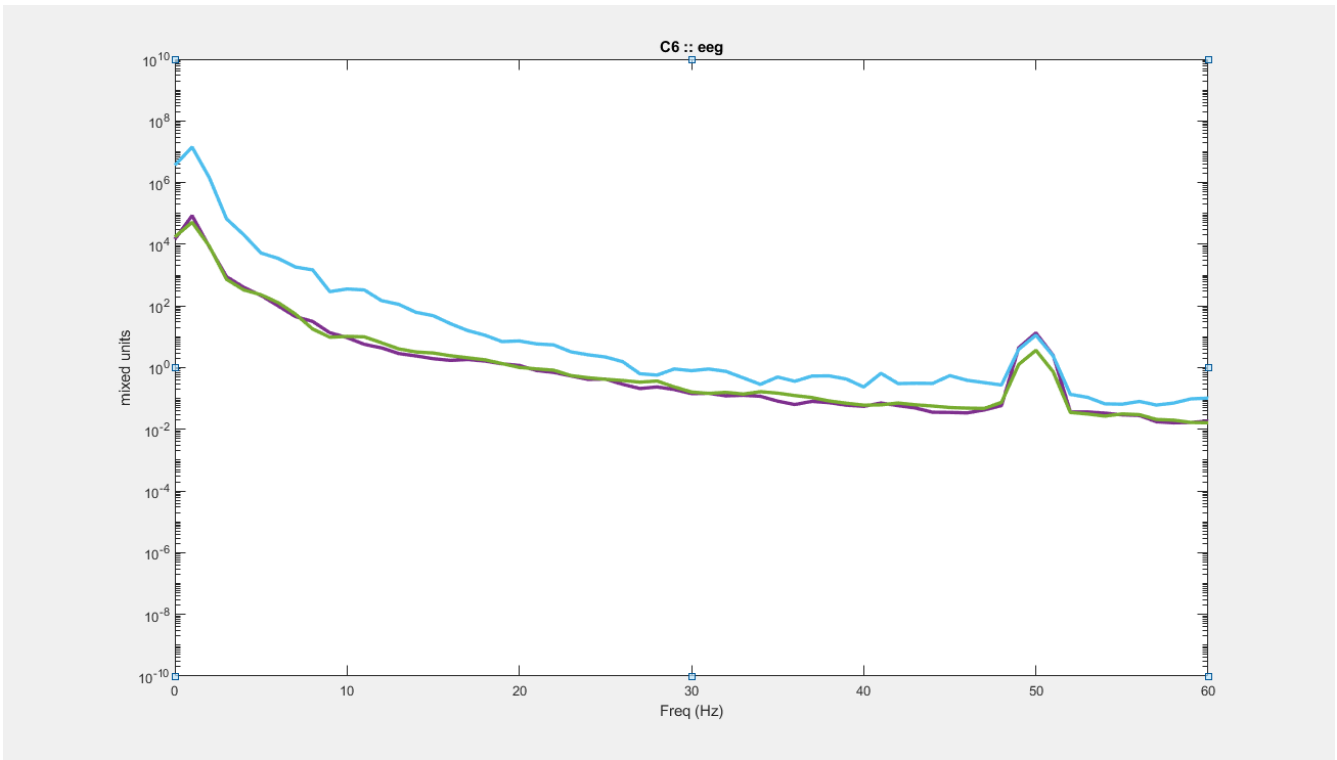
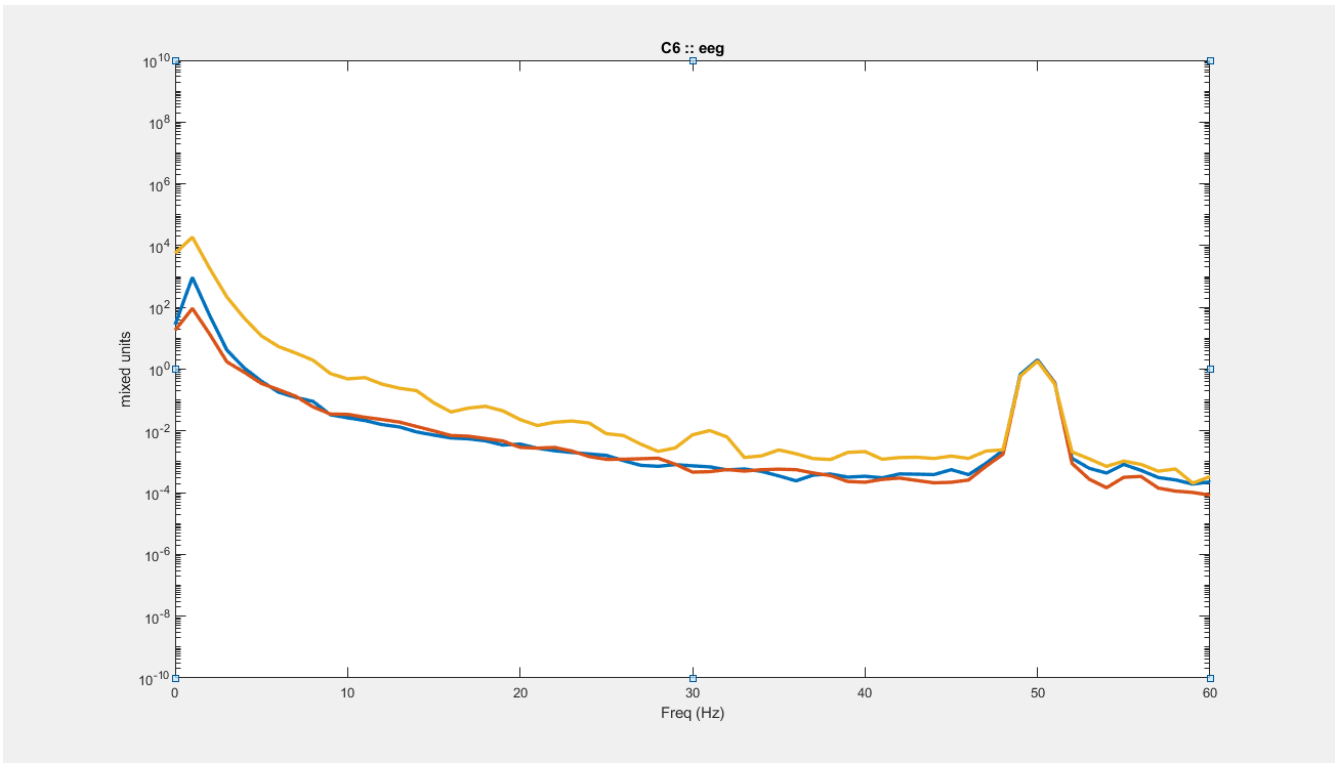


Figure 195. Graph shows electrode location C6. (top) shows software laplacian of electrode EEG. (bottom) shows electrode EEG

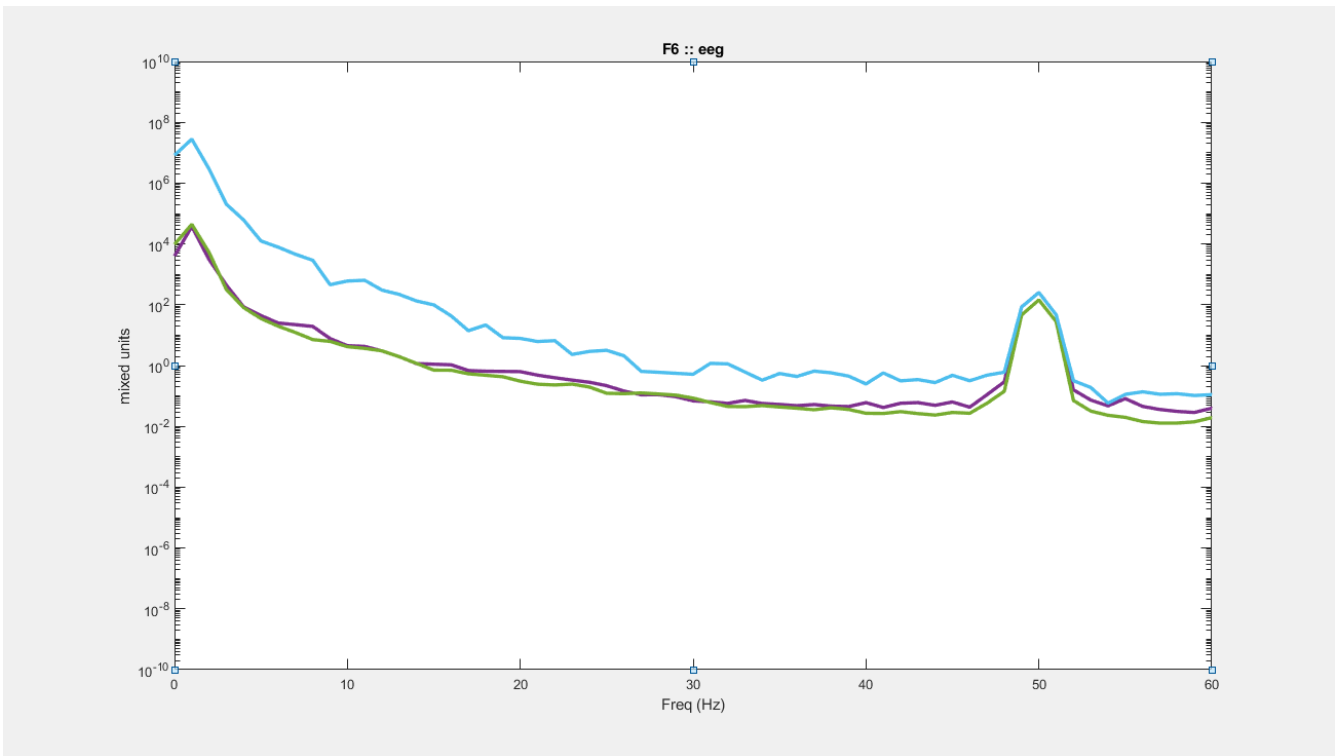
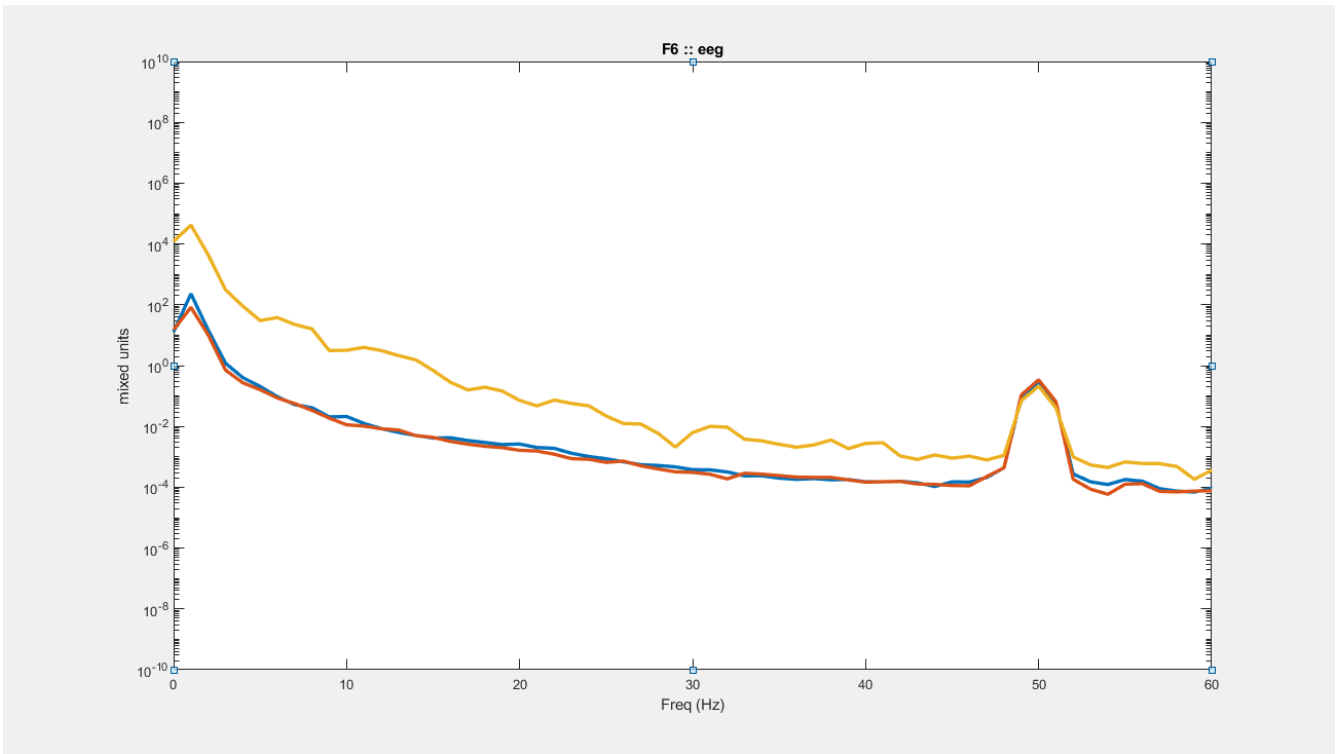


Figure 196. Graph shows electrode location F61. (top) shows software Laplacian of electrode EEG. (bottom) shows electrode EEG

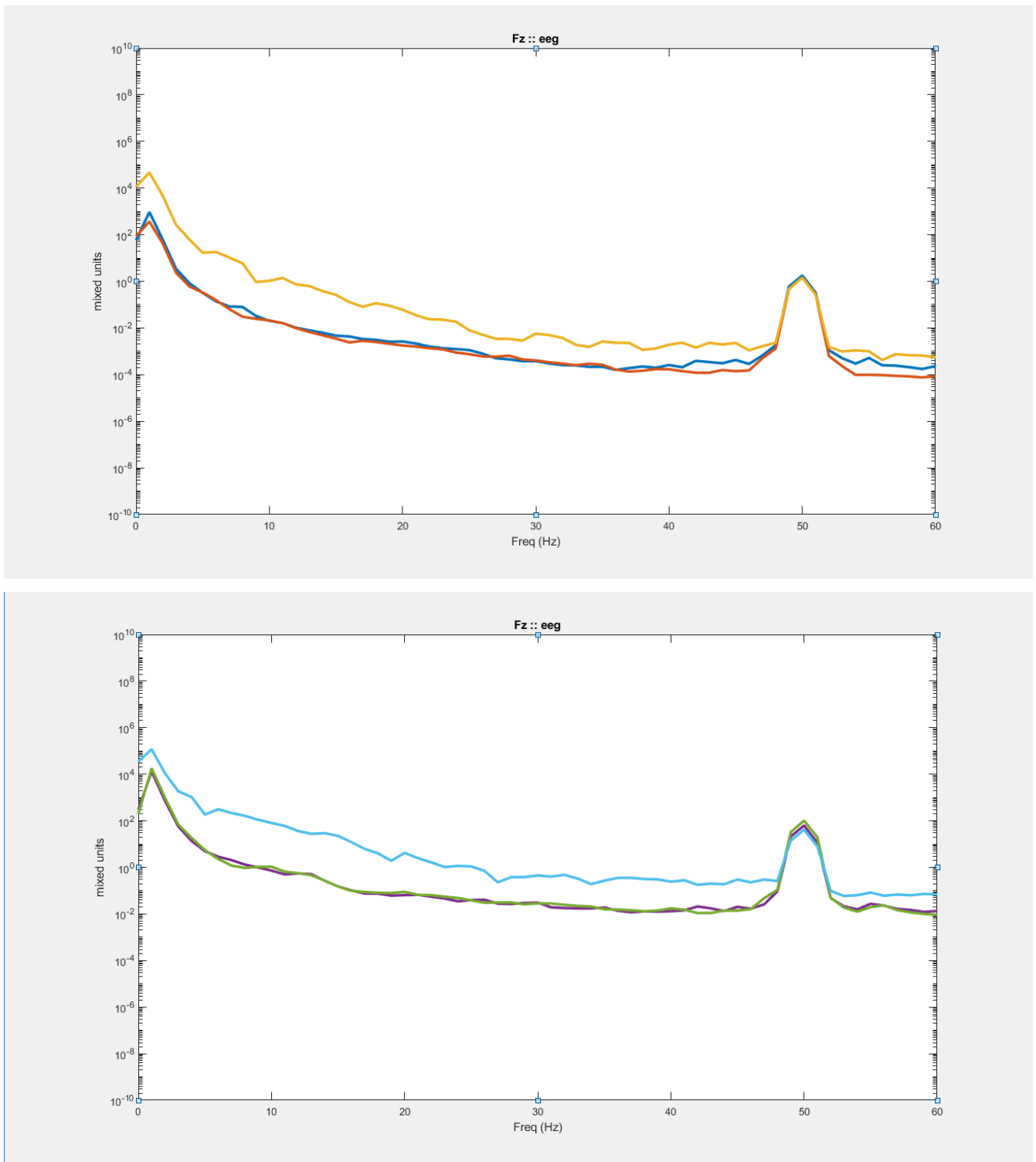


Figure 197. Graph shows electrode location Fz. (top) shows software laplacian of electrode EEG. (bottom) shows electrode EEG

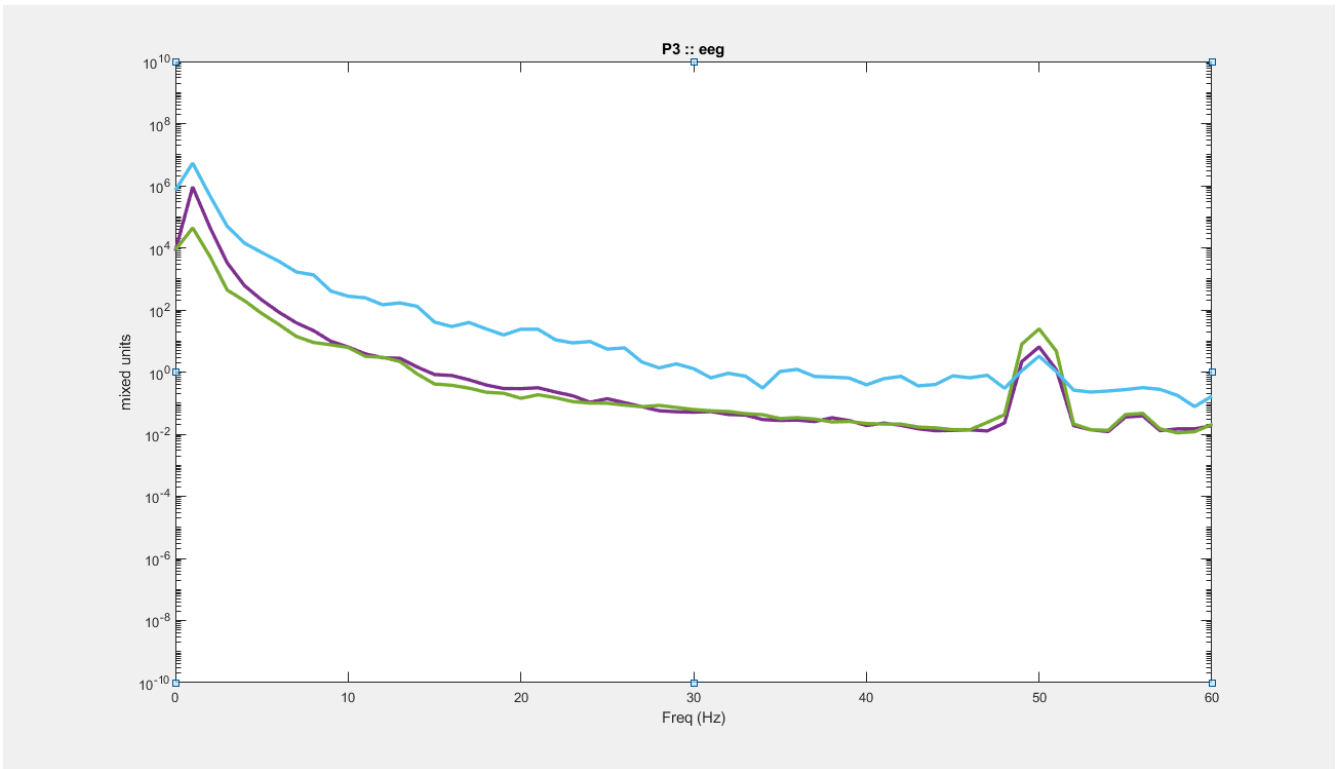
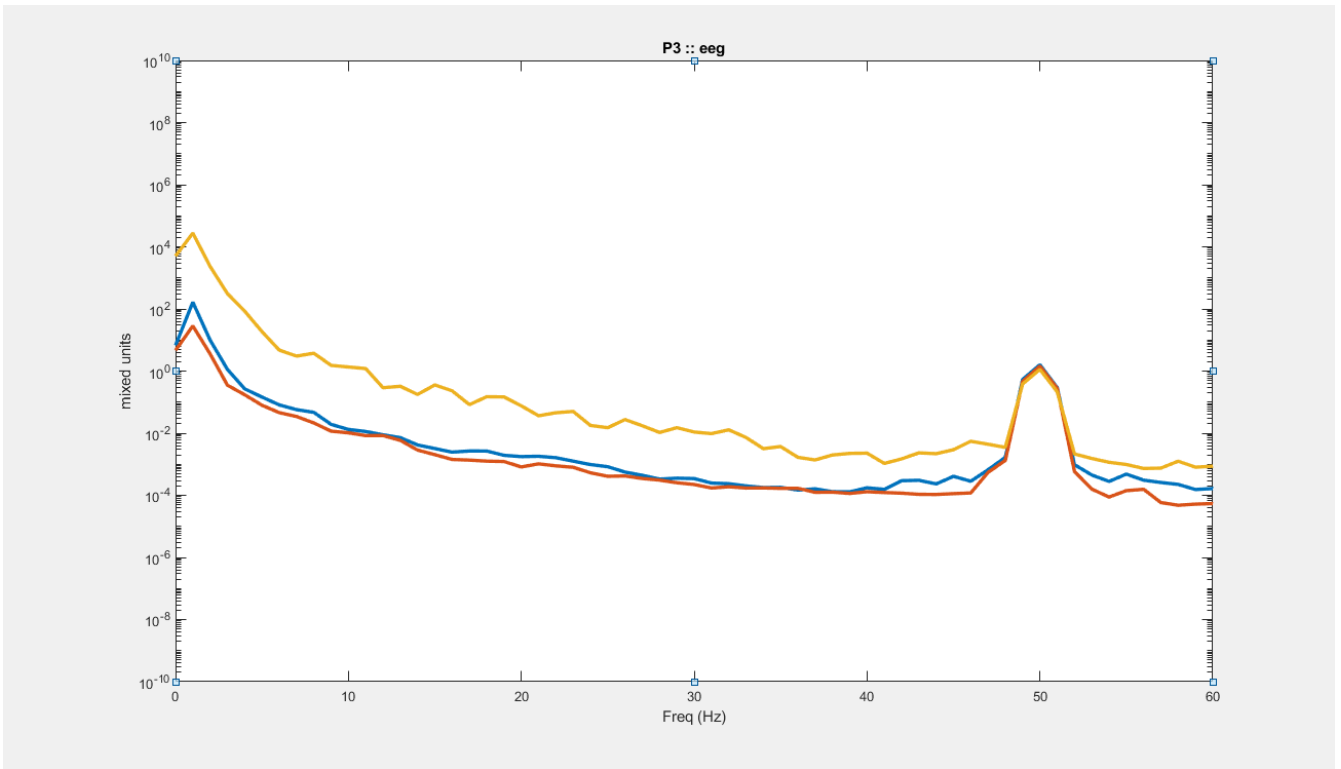


Figure 198. Graph shows electrode location P3. (top) shows software laplacian of electrode EEG. (bottom) shows electrode EEG

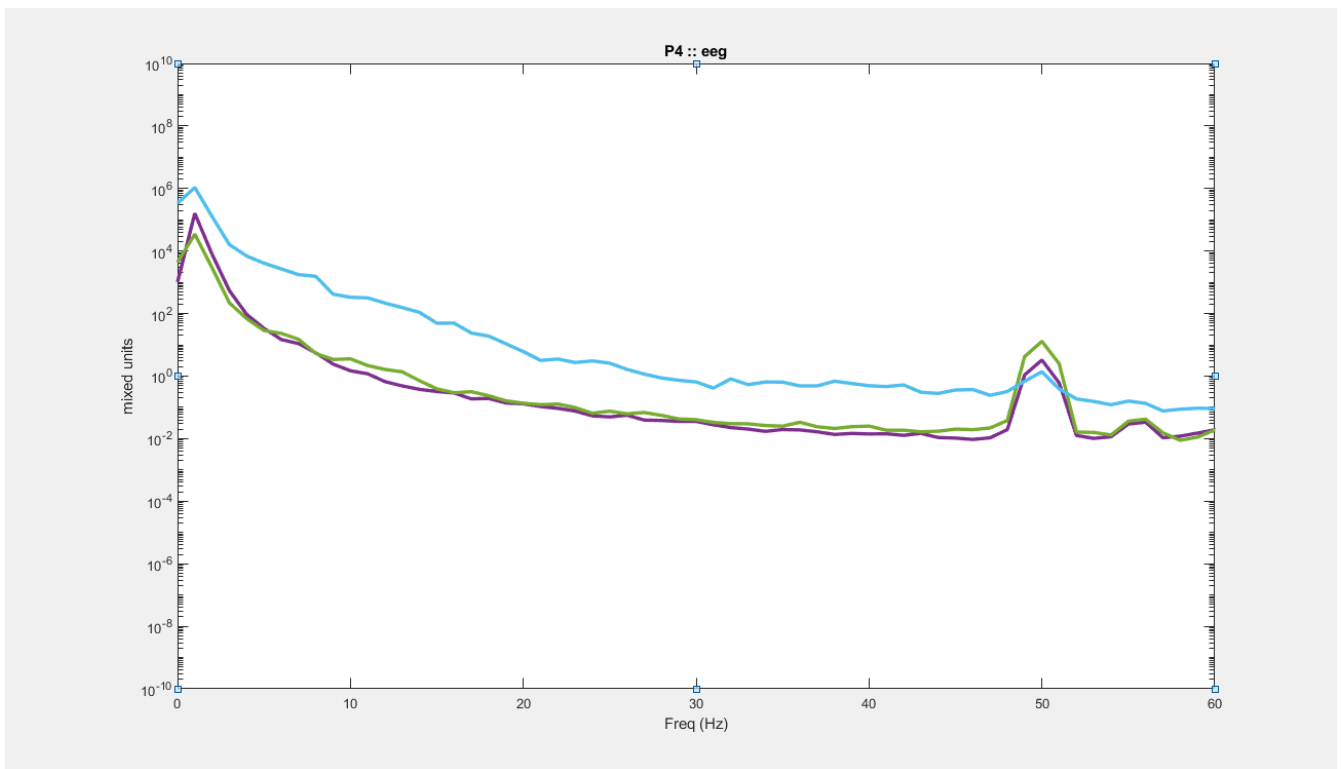
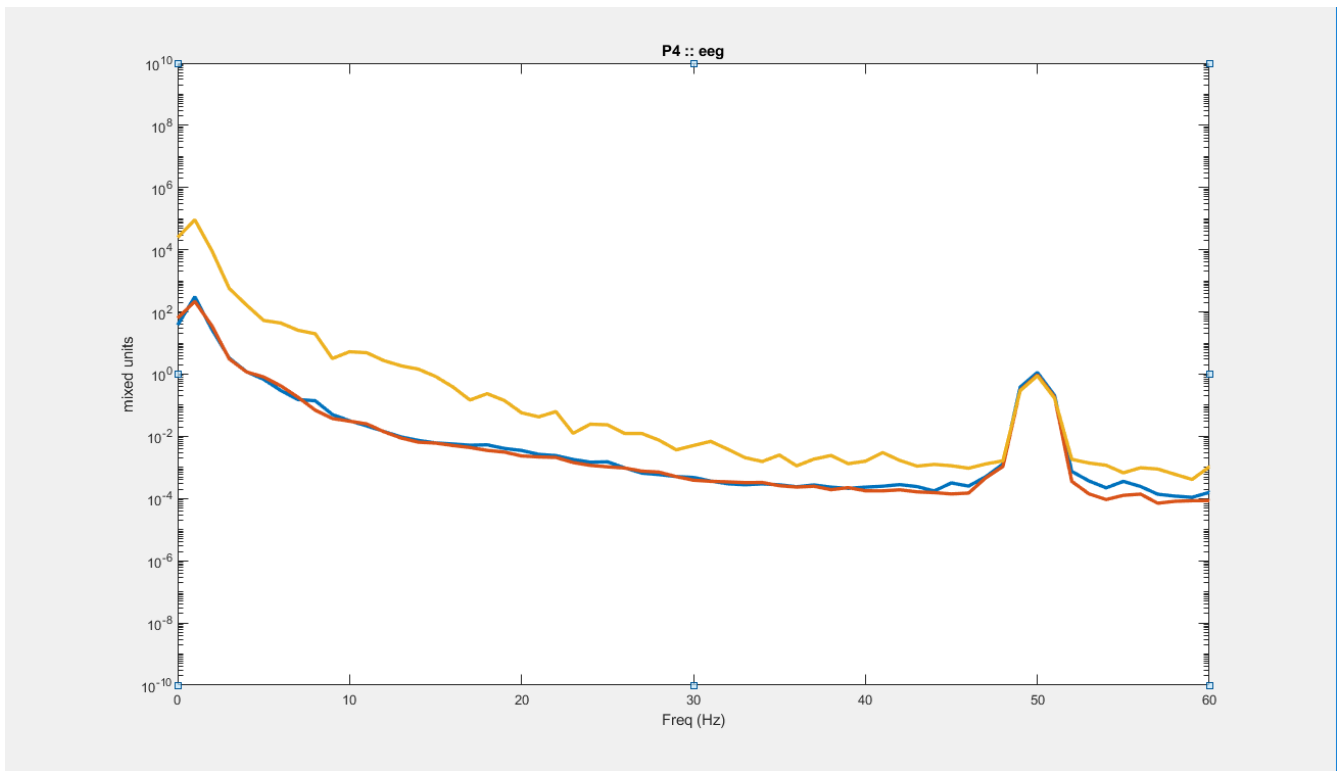


Figure 199. Graph shows electrode location P4. (top) shows software laplacian of electrode EEG. (bottom) shows electrode EEG

9.2.8. 8 SAHARA electrodes used dry in the cap

9.2.8.1. SAHARA electrodes used on subject with thick hair

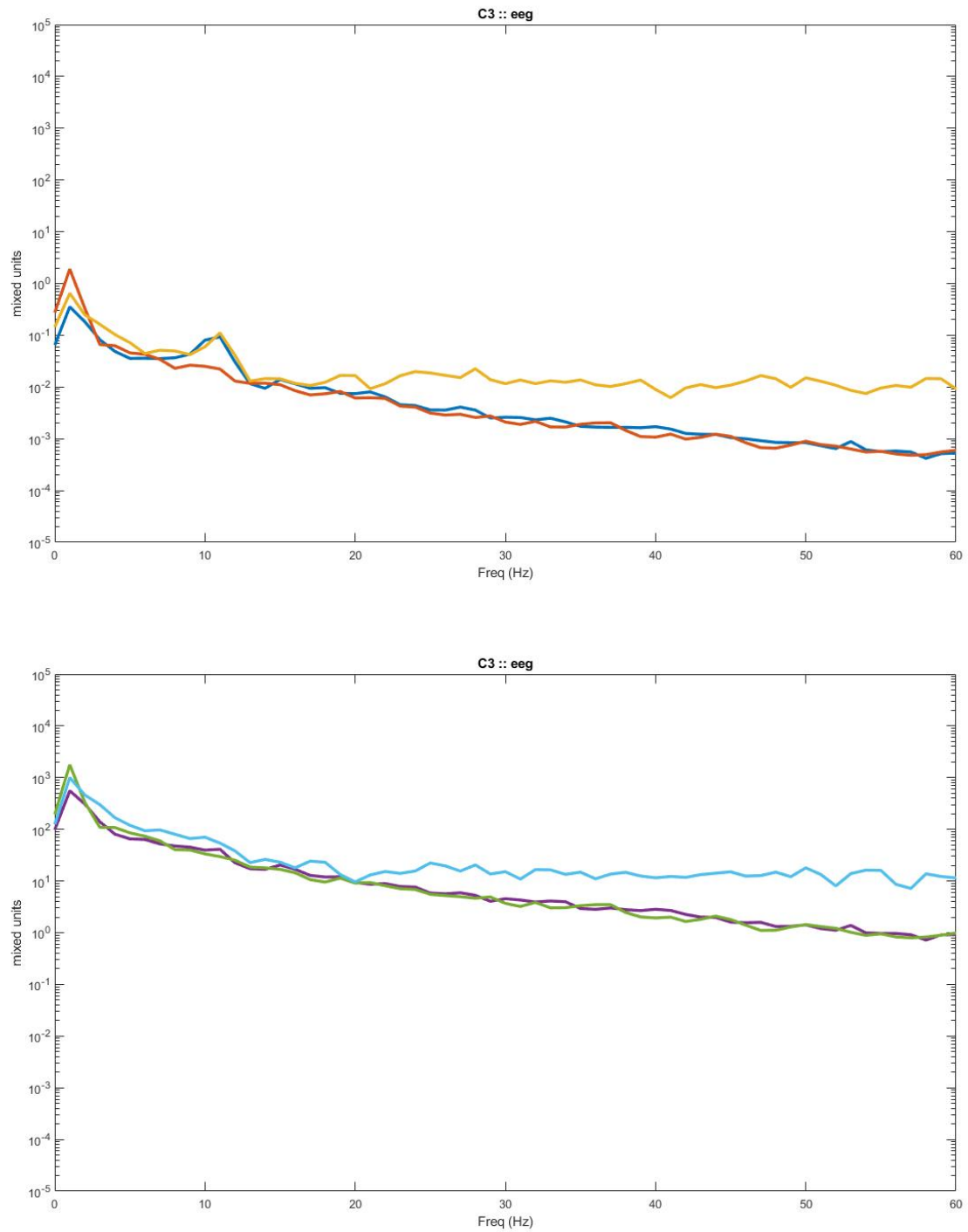


Figure 200. Graph shows electrode location C3. (top) shows software laplacian of electrode EEG. (bottom) shows electrode EEG

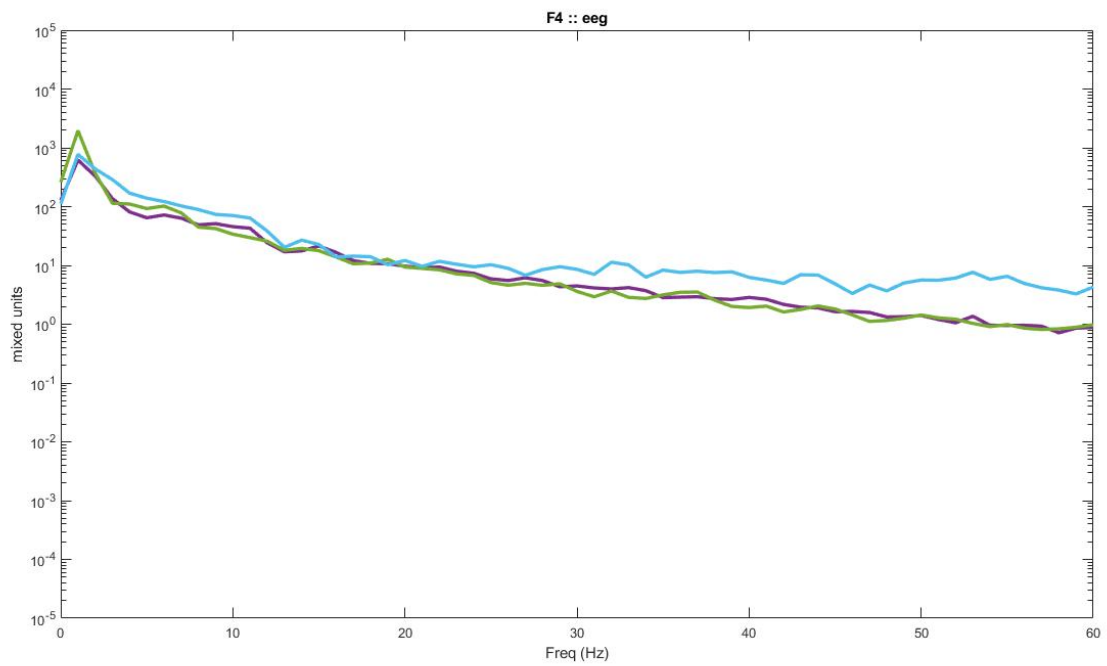
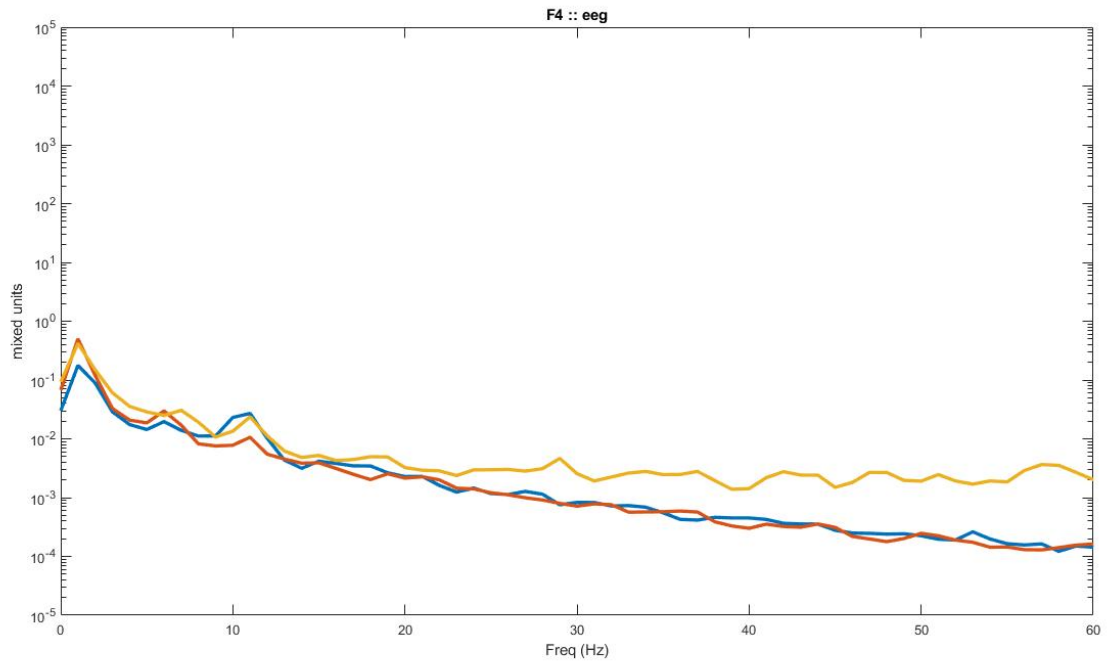


Figure 201. Graph shows electrode location F4. (top) shows software laplacian of electrode EEG. (bottom) shows electrode EEG

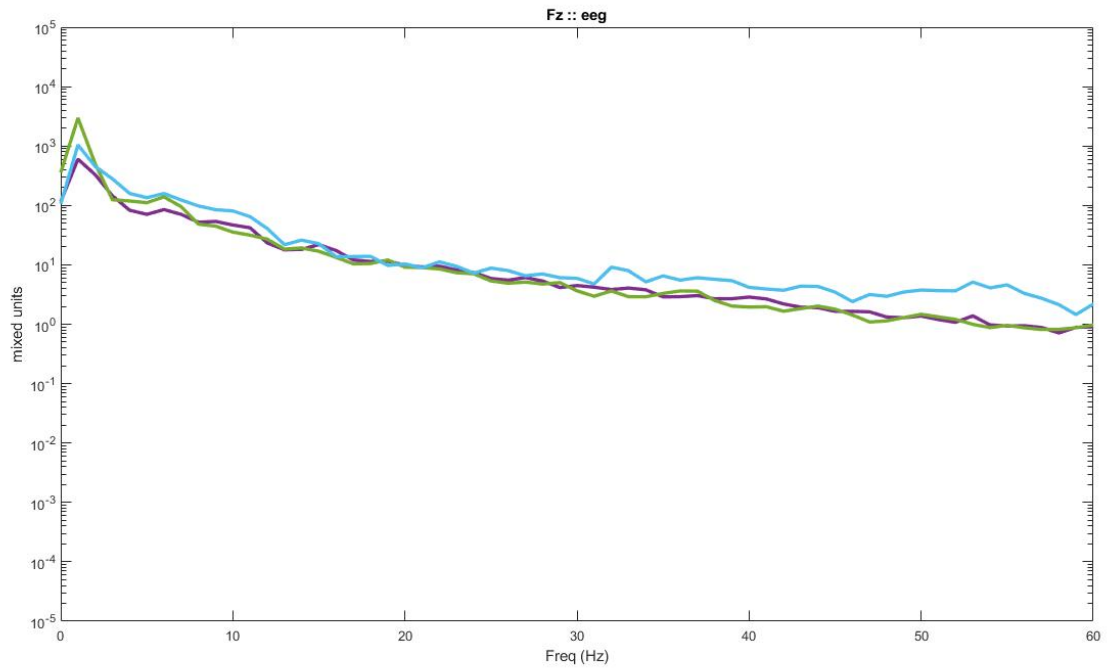
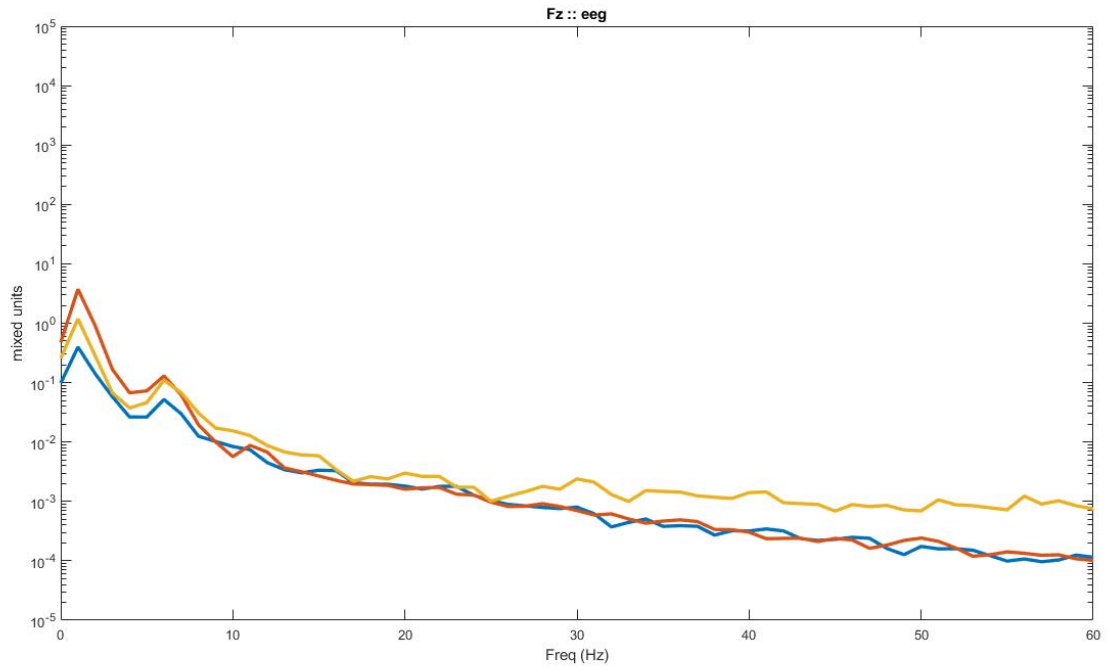


Figure 202. Graph shows electrode location Fz. (top) shows software laplacian of electrode EEG. (bottom) shows electrode EEG

9.2.8.2. SAHARA electrodes used dry on subject with short, stiff curly hair

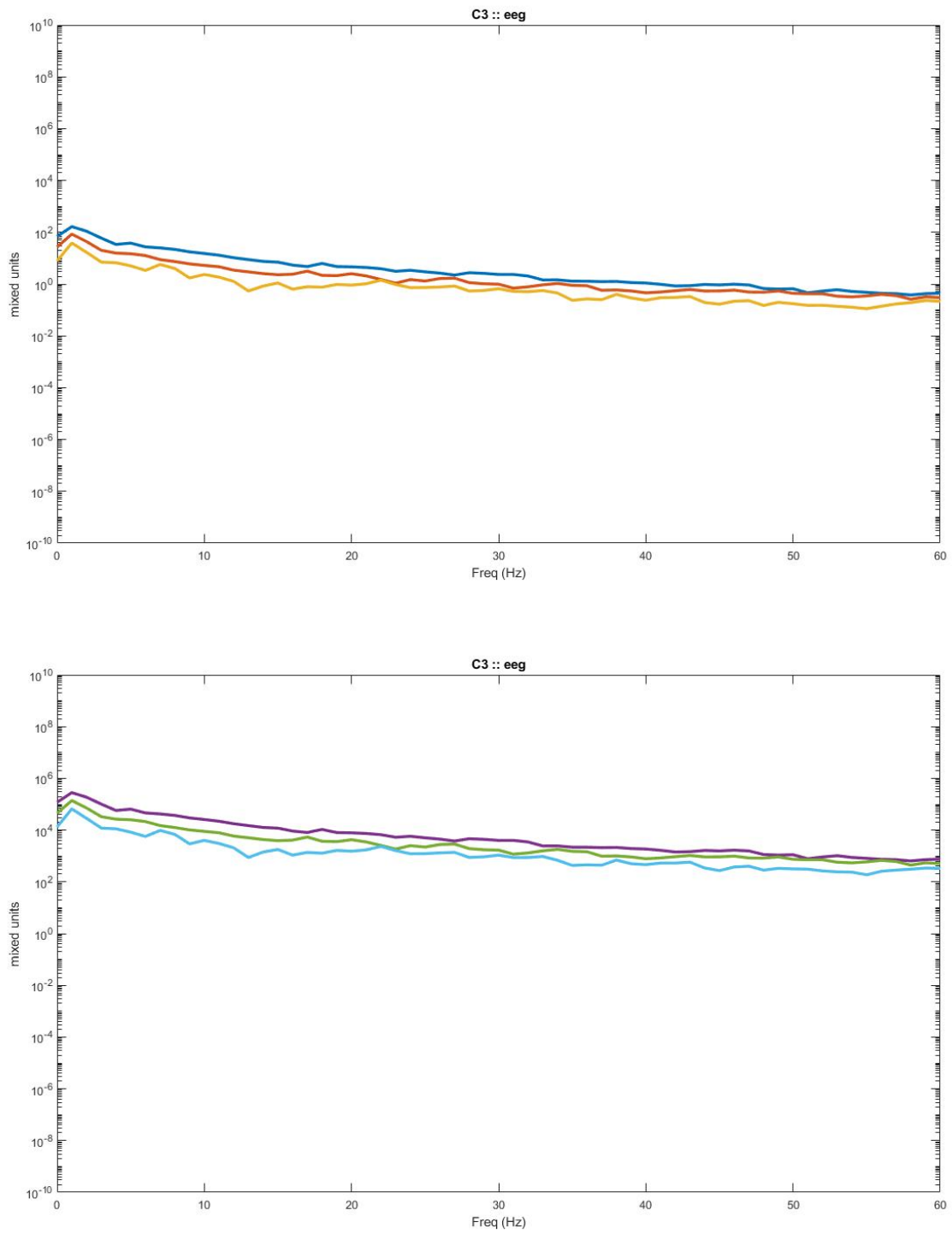


Figure 203. Graph shows electrode location C3. (top) shows software laplacian of electrode EEG. (bottom) shows electrode EEG

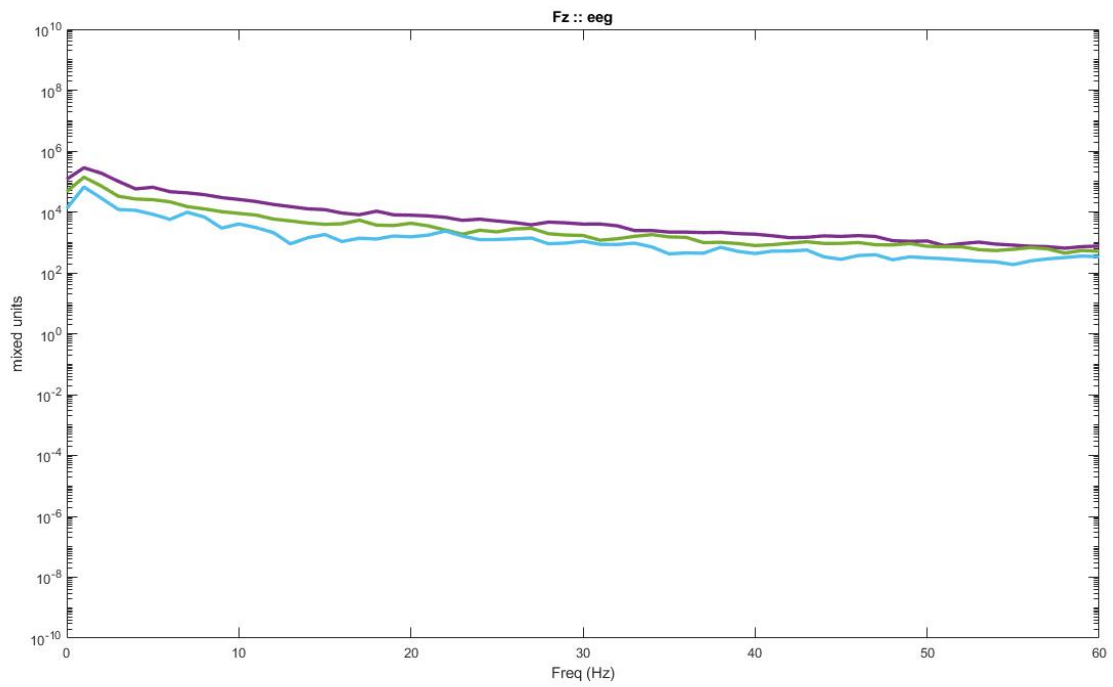
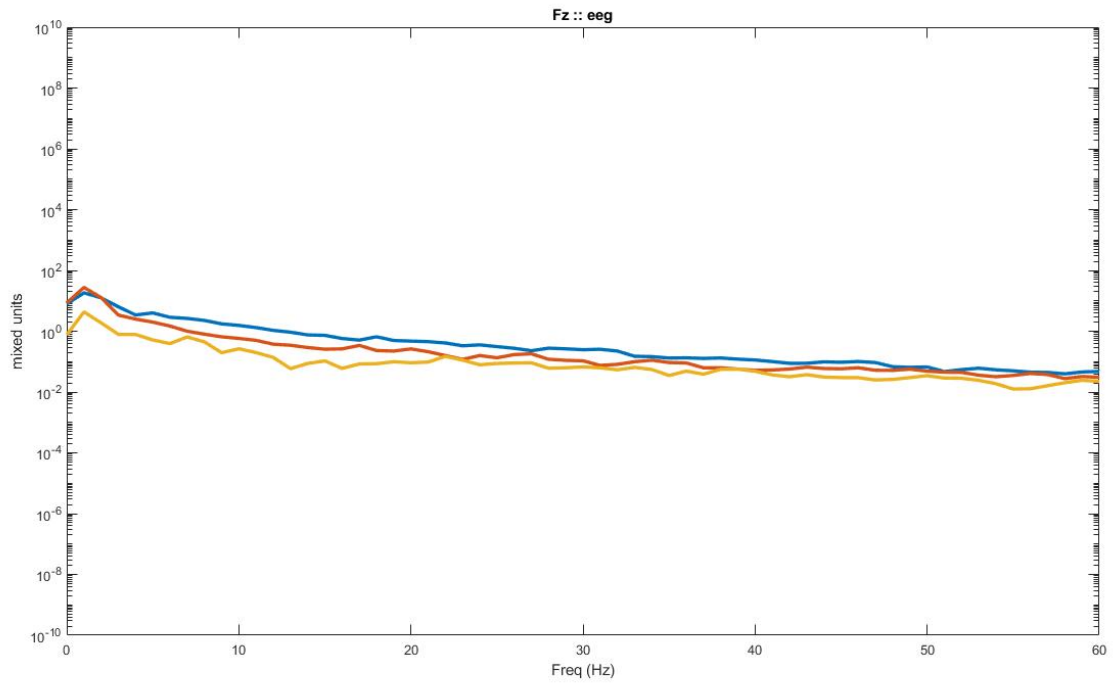


Figure 204. Graph shows electrode location Fz. (top) shows software laplacian of electrode EEG. (bottom) shows electrode EEG

9.2.9. 5mm dry comb electrodes used with ring electrodes in cap

9.2.9.1. Dry comb electrodes with ring electrodes used on subject with thick hair with lights on

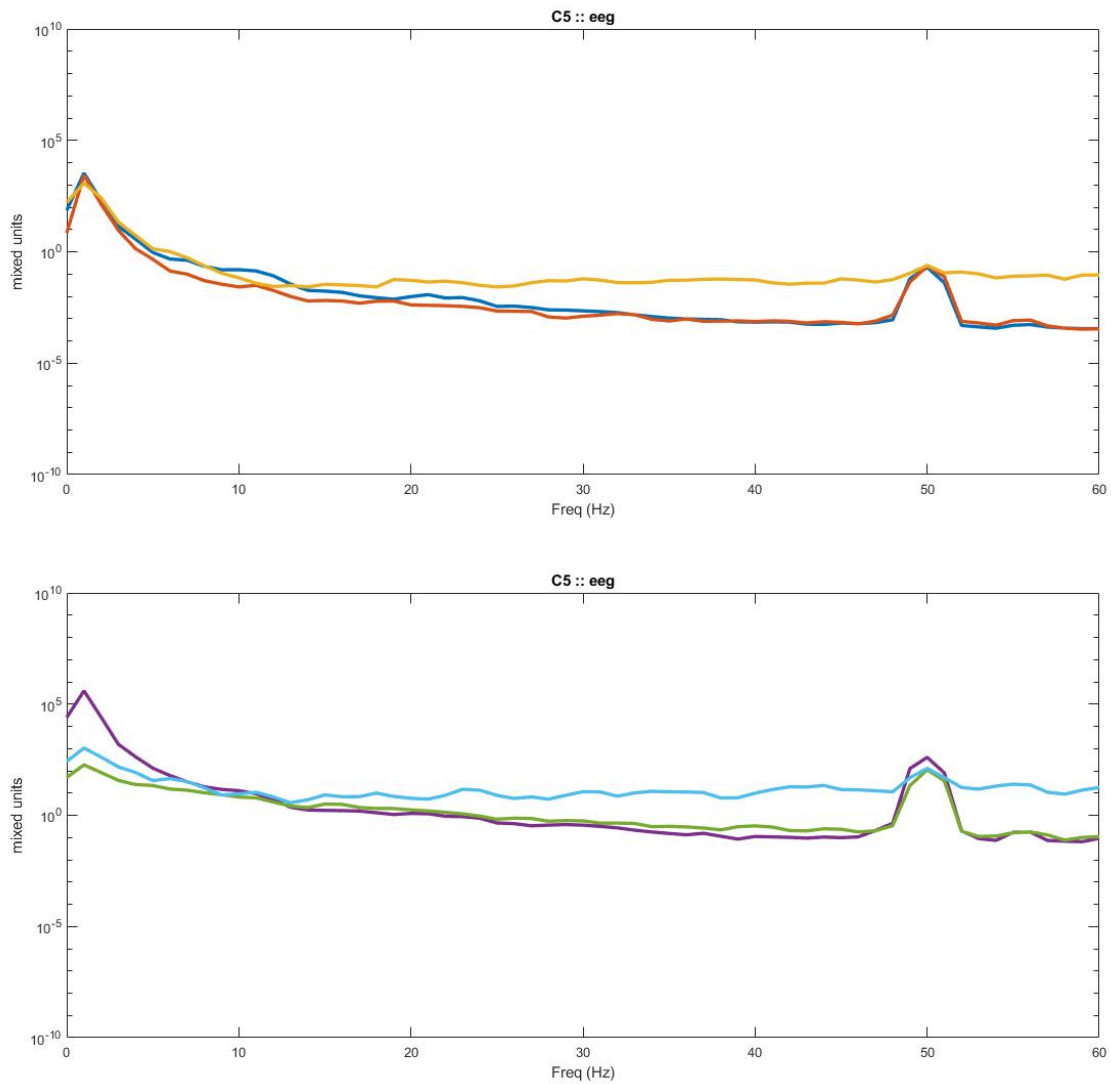


Figure 205. Graph shows electrode location C5. (top) shows software laplacian of electrode EEG. (bottom) shows electrode EEG

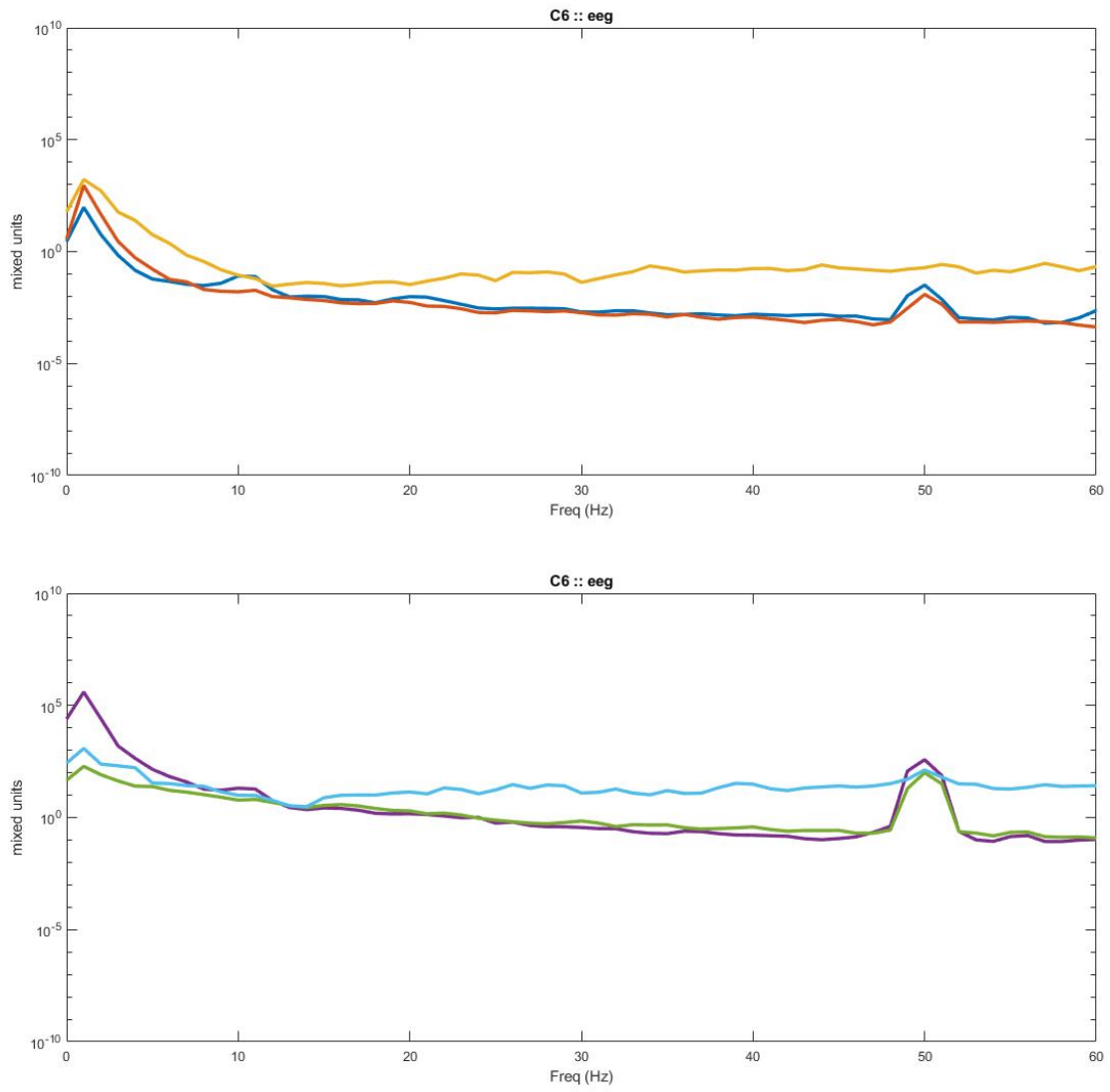


Figure 206. Graph shows electrode location C6. (top) shows software laplacian of electrode EEG. (bottom) shows electrode EEG

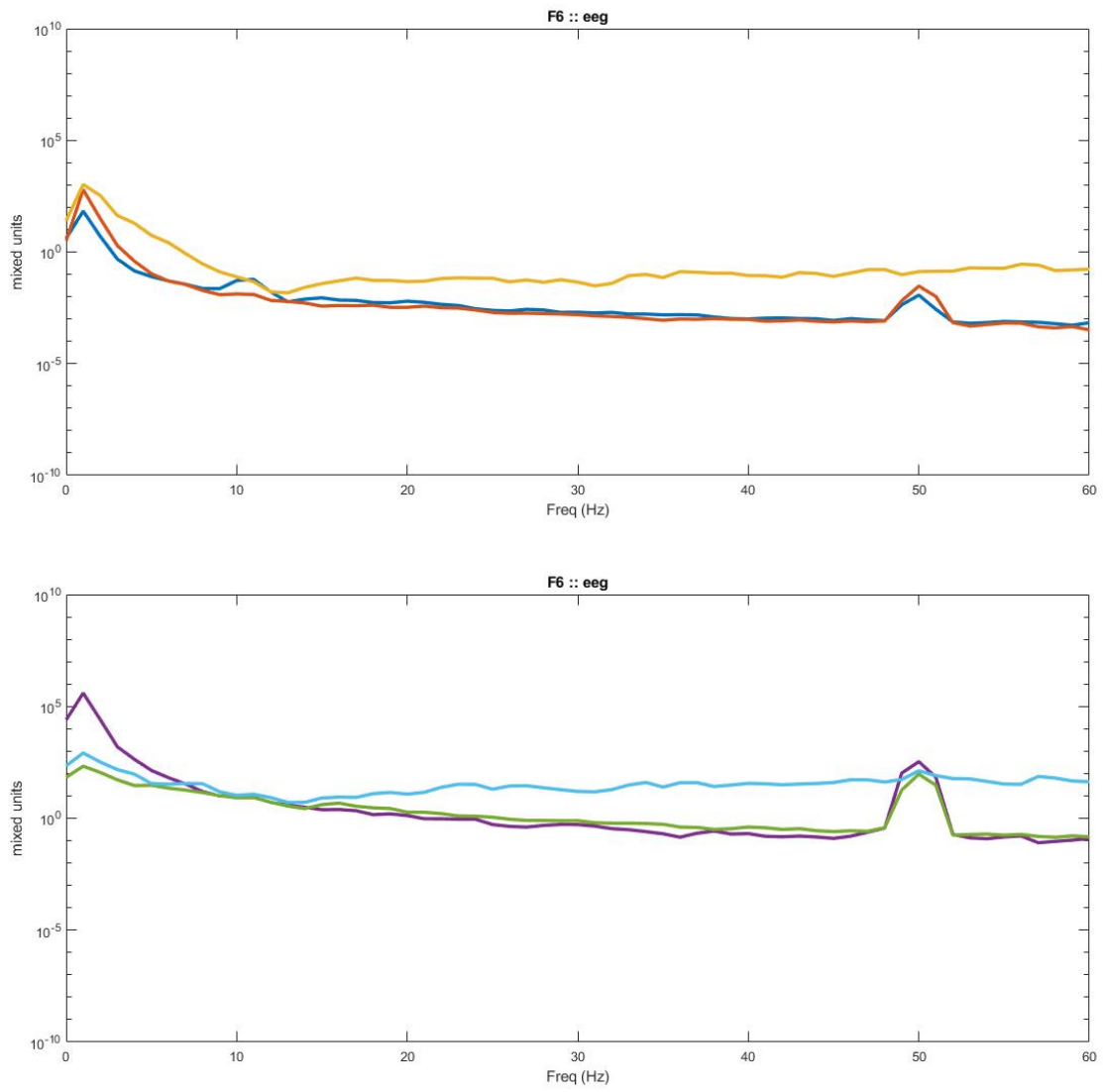


Figure 207. Graph shows electrode location F6. (top) shows software laplacian of electrode EEG. (bottom) shows electrode EEG

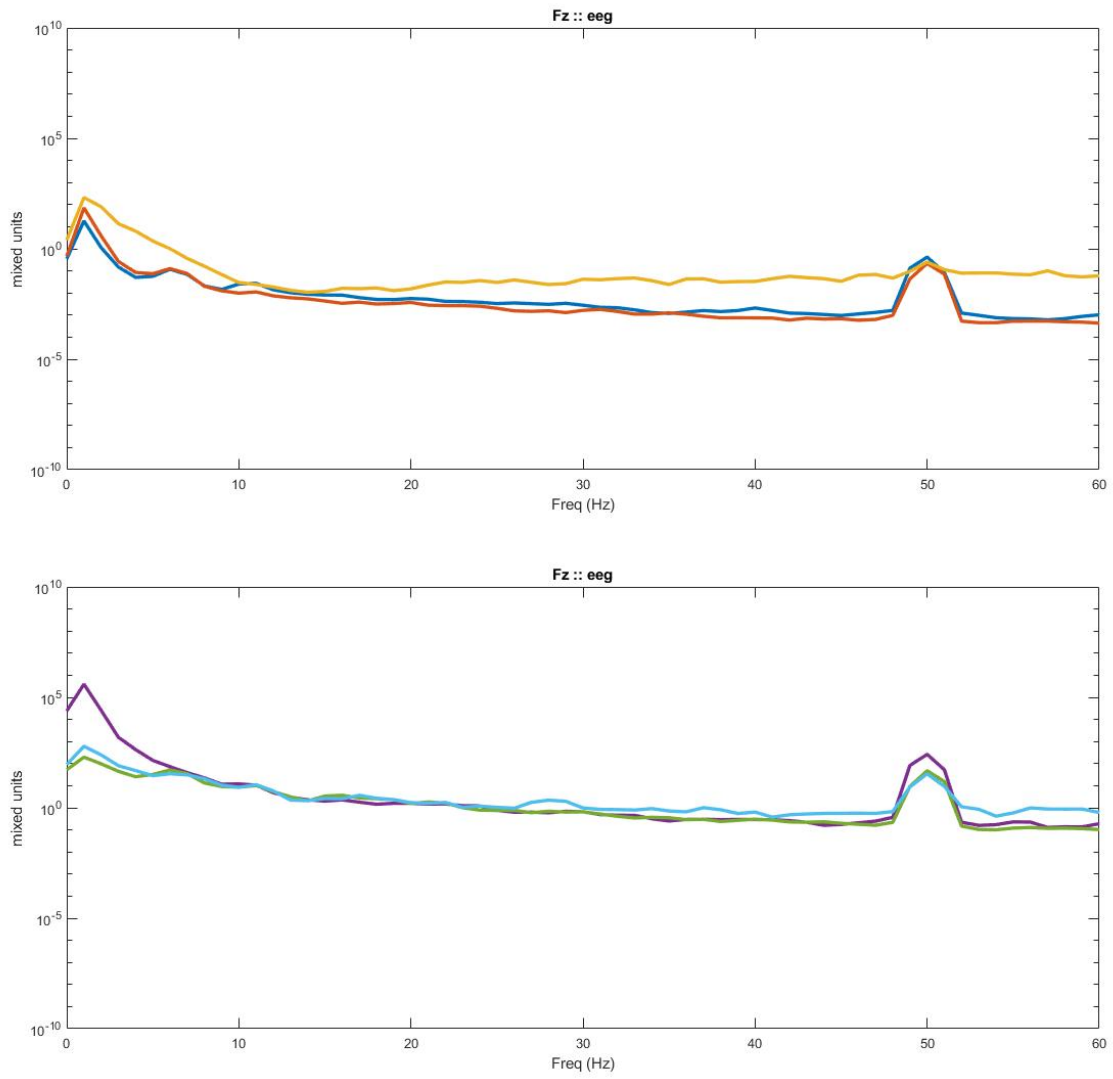


Figure 208. Graph shows electrode location Fz. (top) shows software laplacian of electrode EEG. (bottom) shows electrode EEG

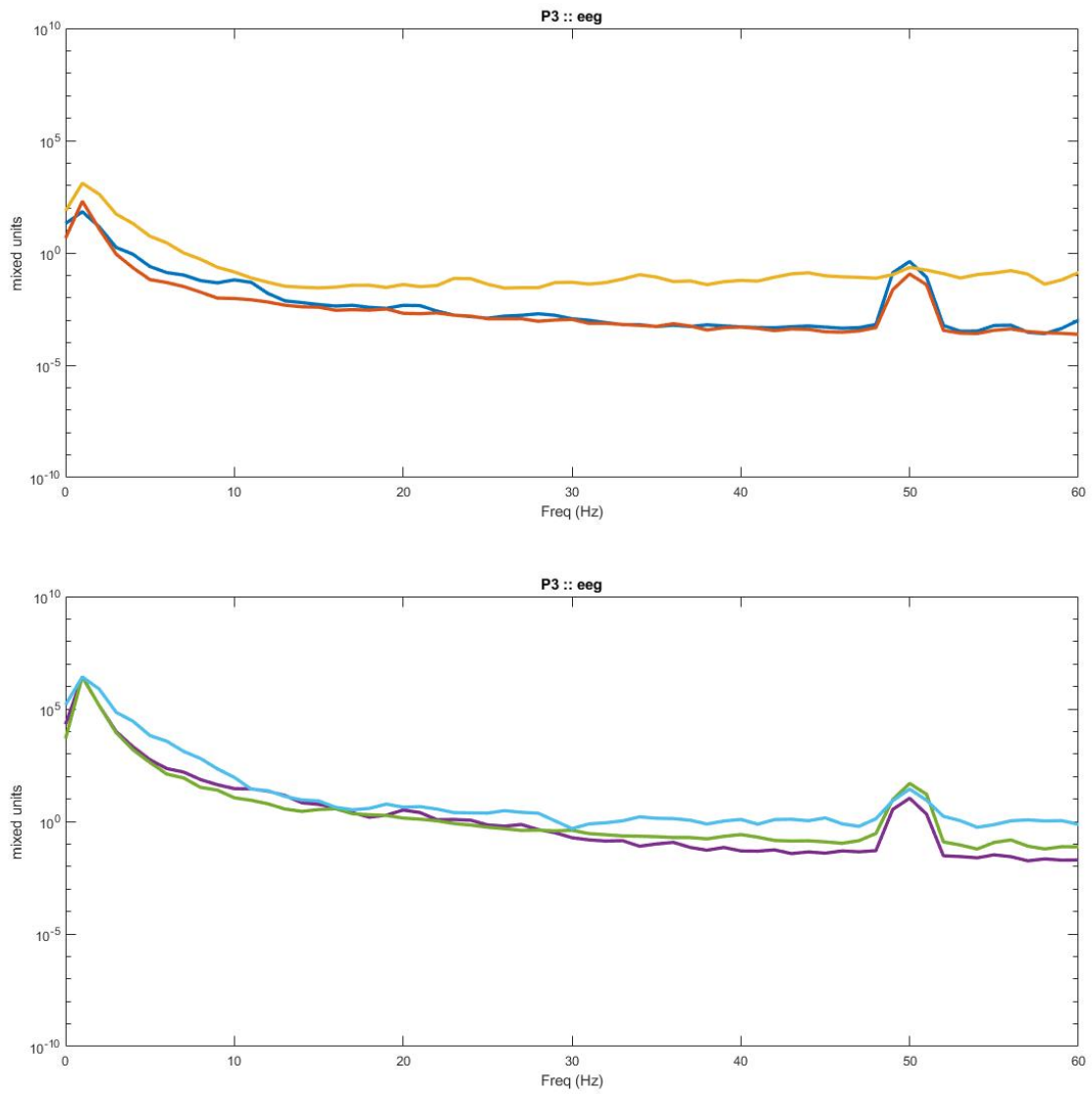


Figure 209. Graph shows electrode location P3. (top) shows software laplacian of electrode EEG. (bottom) shows electrode EEG

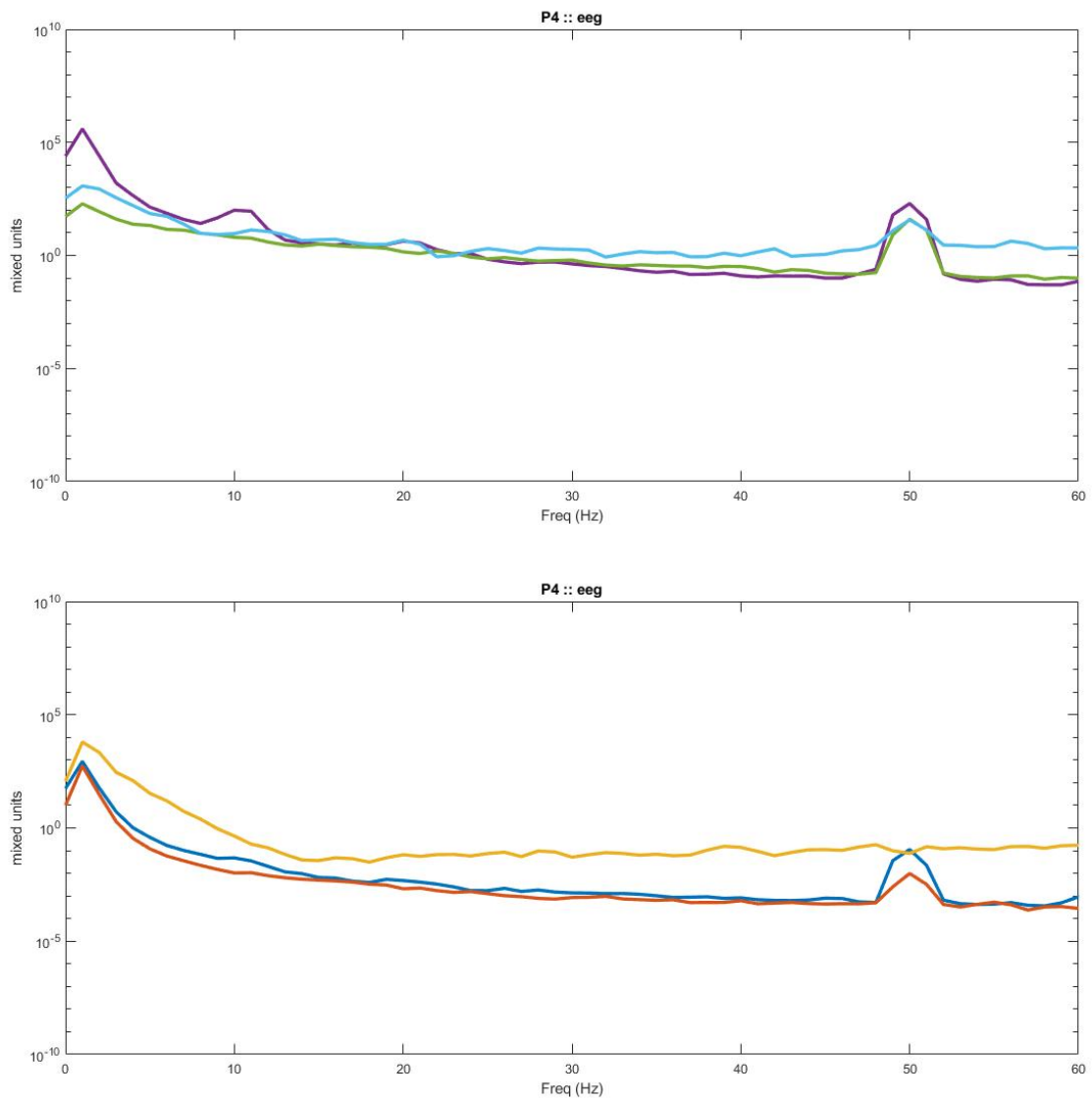


Figure 210. Graph shows electrode location P4. (top) shows software laplacian of electrode EEG. (bottom) shows electrode EEG

9.2.9.2. Dry comb electrodes with ring electrodes used on subject with thick hair with lights off

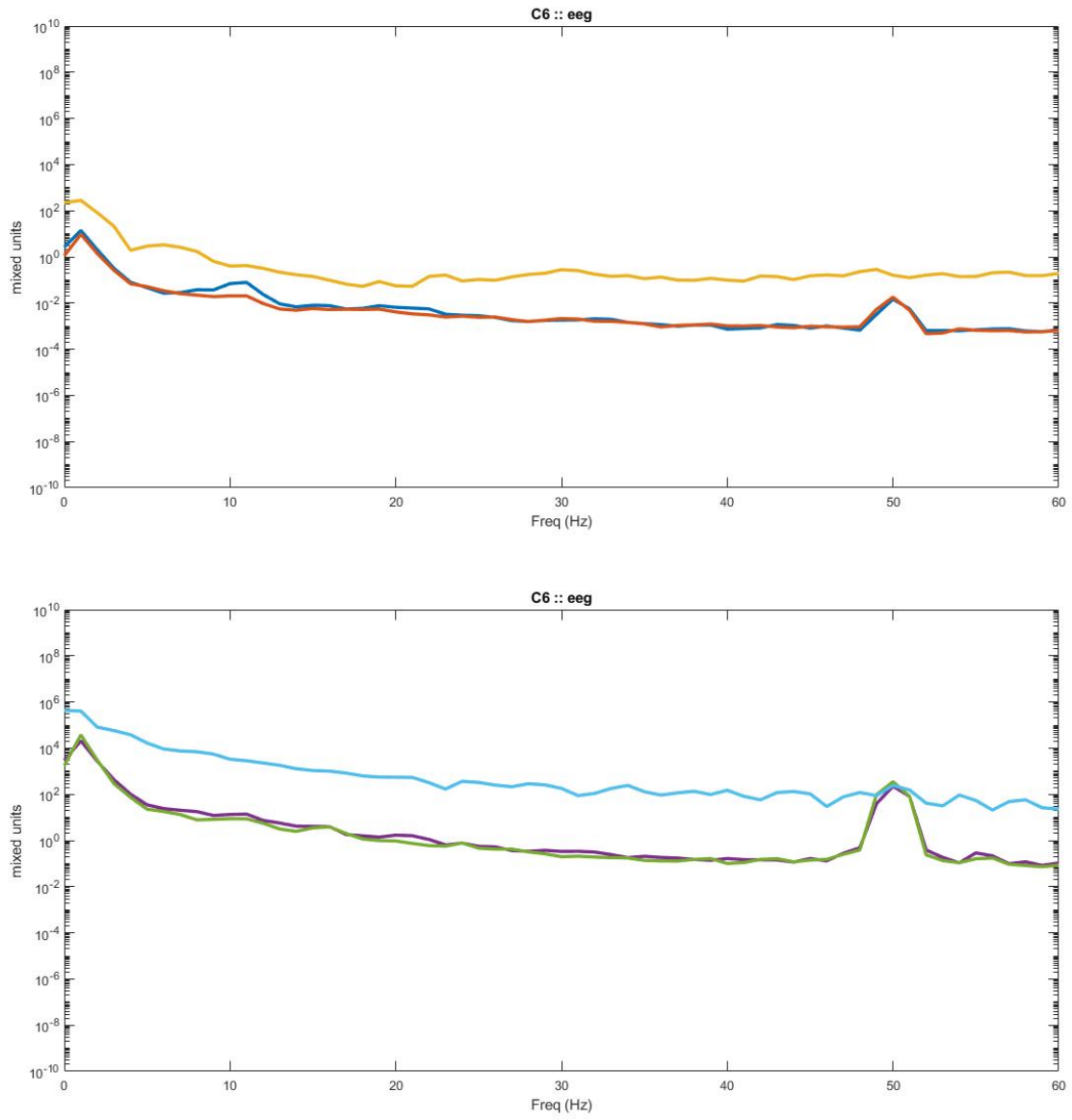


Figure 211. Graph shows electrode location C6. (top) shows software laplacian of electrode EEG. (bottom) shows electrode EEG

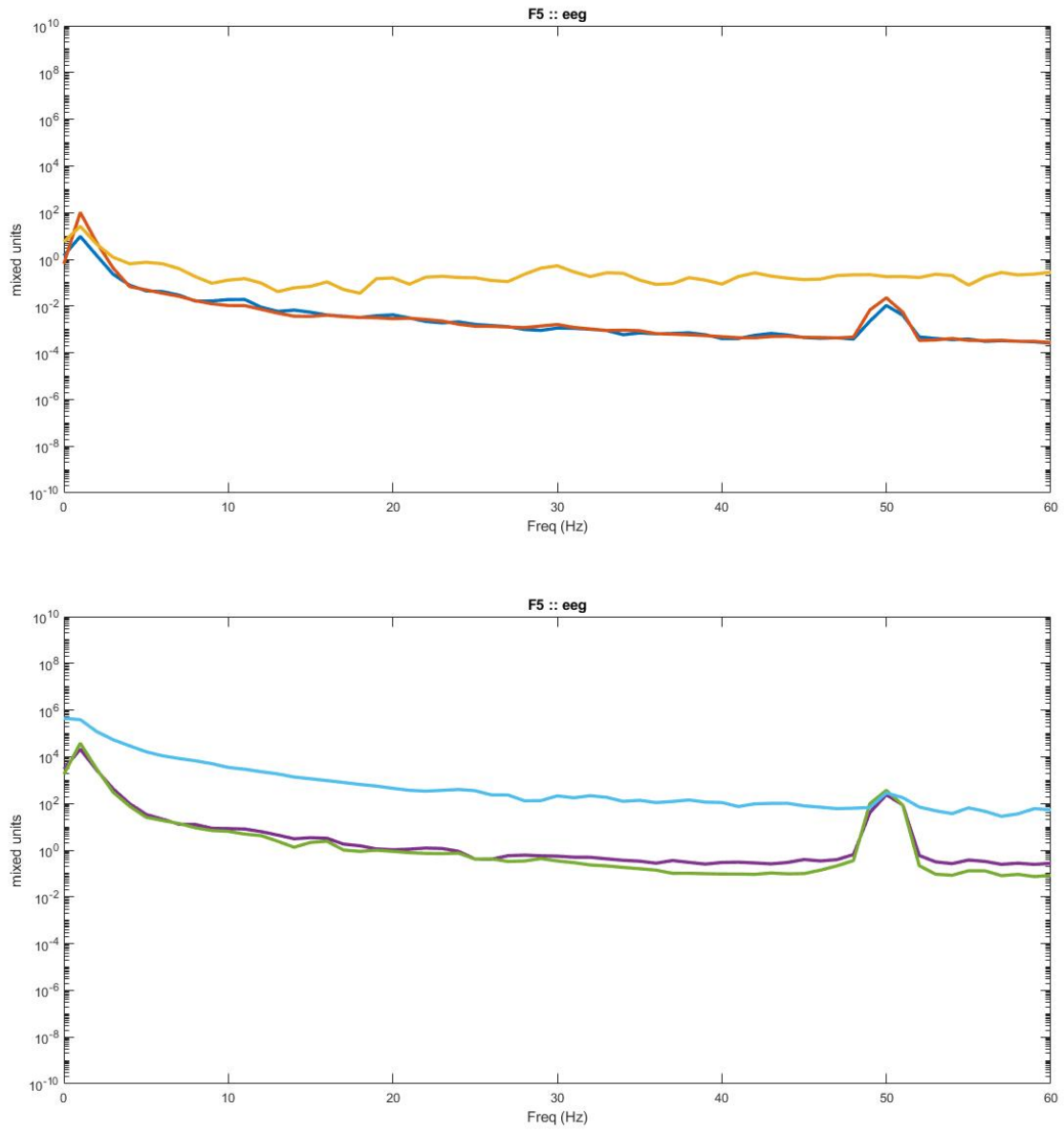


Figure 212. Graph shows electrode location F5. (top) shows software laplacian of electrode EEG. (bottom) shows electrode EEG

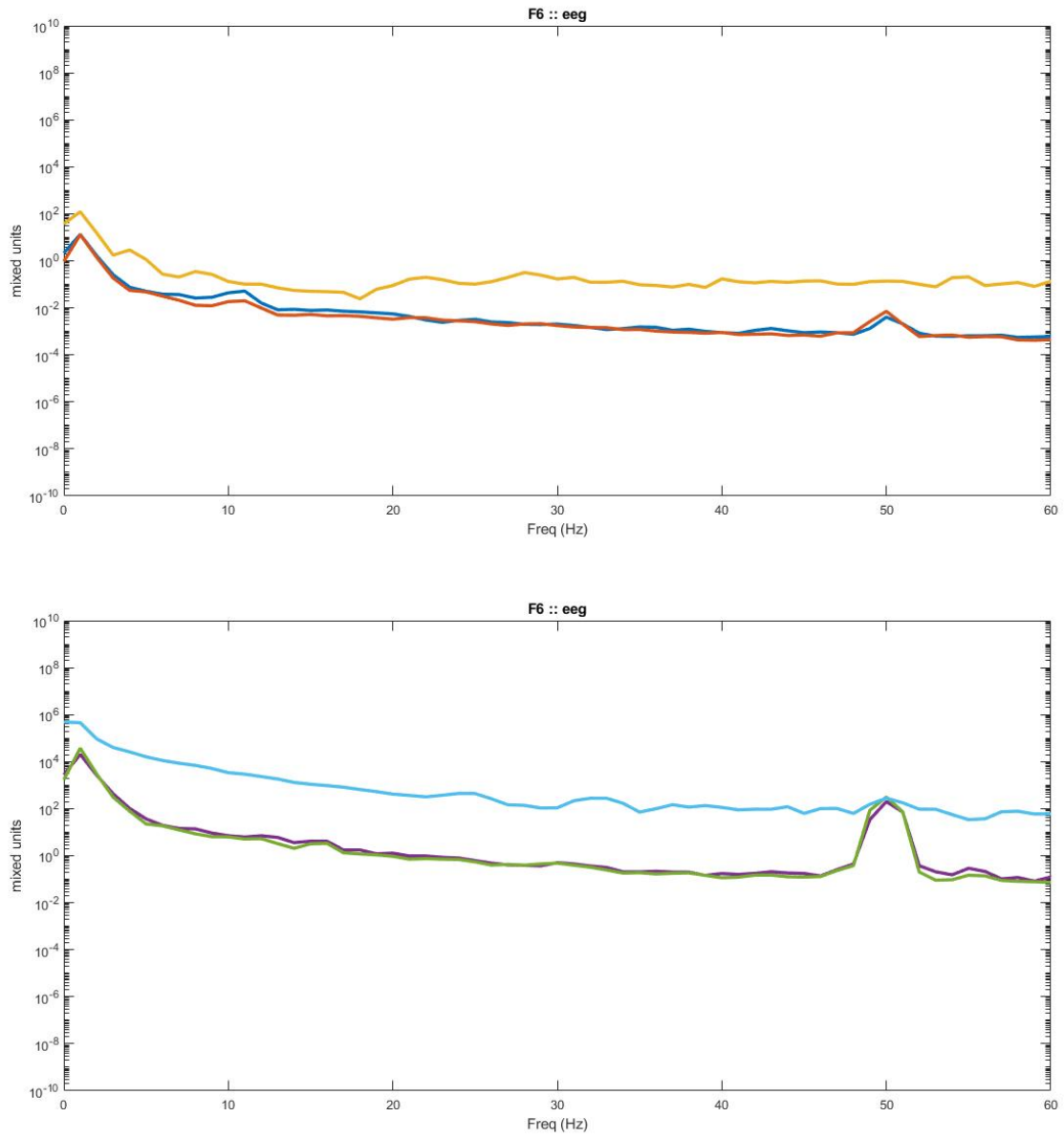


Figure 213. Graph shows electrode location F6. (top) shows software laplacian of electrode EEG. (bottom) shows electrode EEG

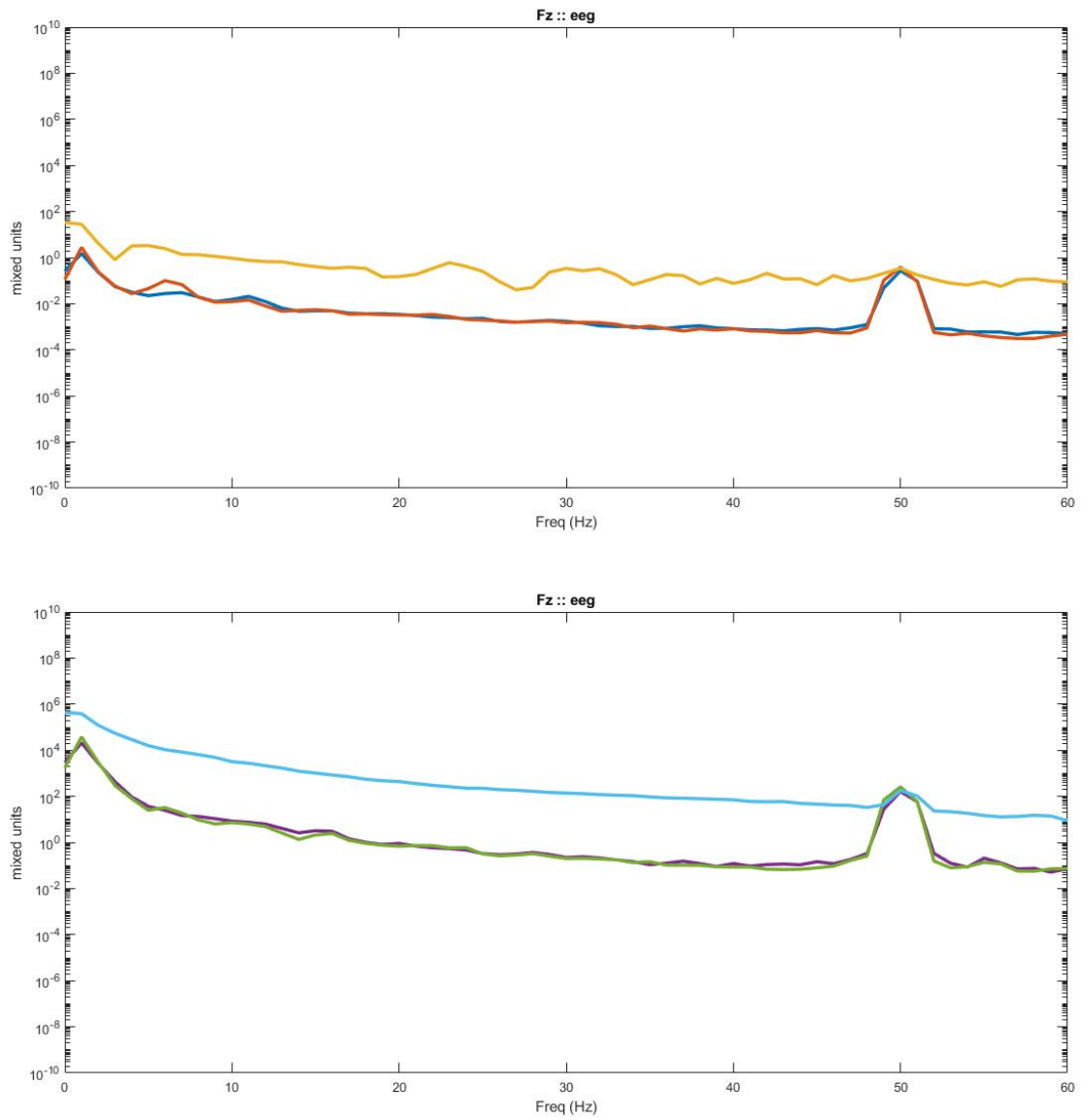


Figure 214. Graph shows electrode location Fz. (top) shows software laplacian of electrode EEG. (bottom) shows electrode EEG

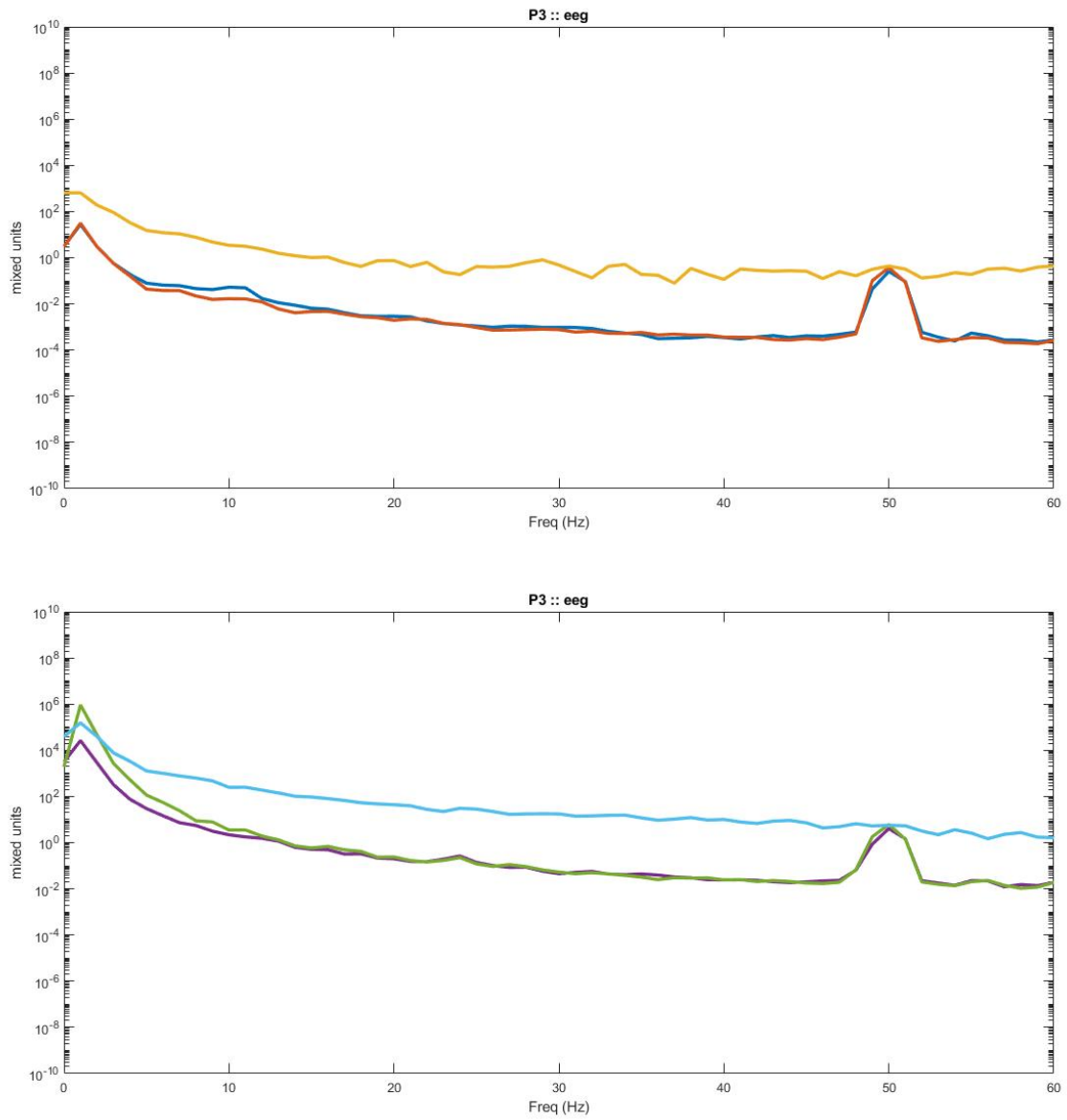


Figure 215. Graph shows electrode location P3. (top) shows software laplacian of electrode EEG. (bottom) shows electrode EEG

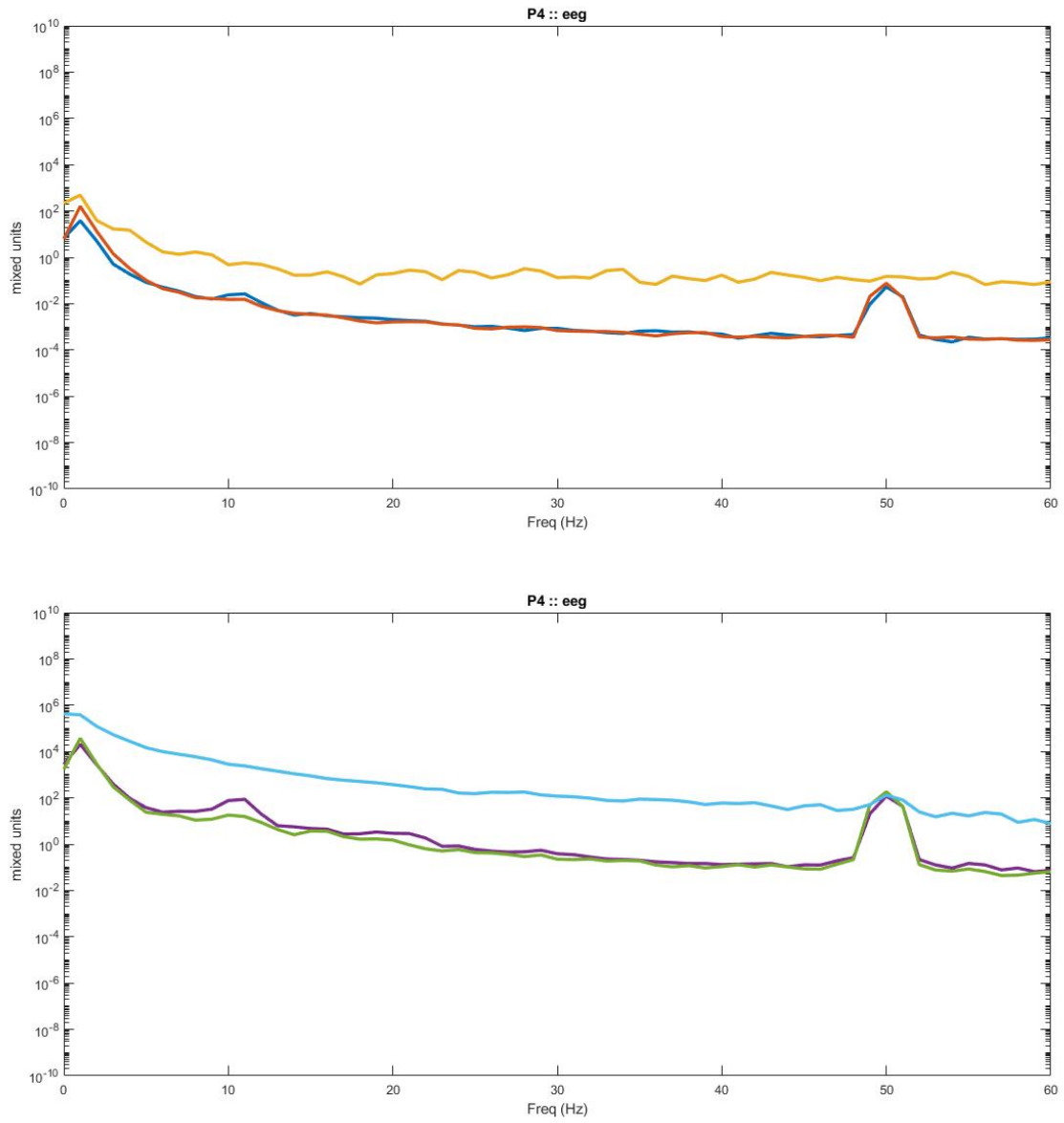


Figure 216. Graph shows electrode location P4. (top) shows software laplacian of electrode EEG. (bottom) shows electrode EEG

9.2.9.3. Dry comb electrodes with ring electrodes used on subject with short, stiff curly hair

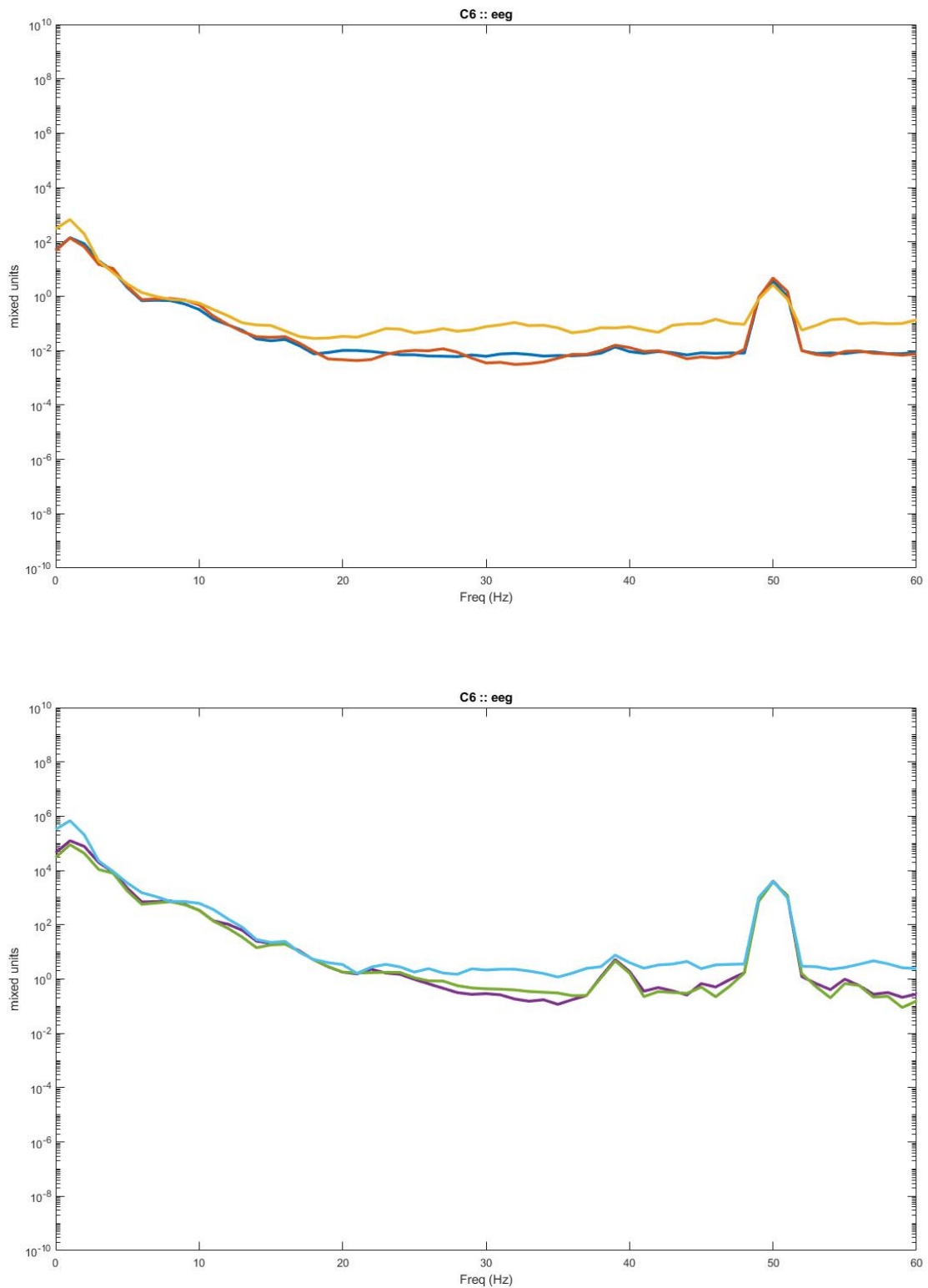


Figure 217. Graph shows electrode location C6. (top) shows software laplacian of electrode EEG. (bottom) shows electrode EEG

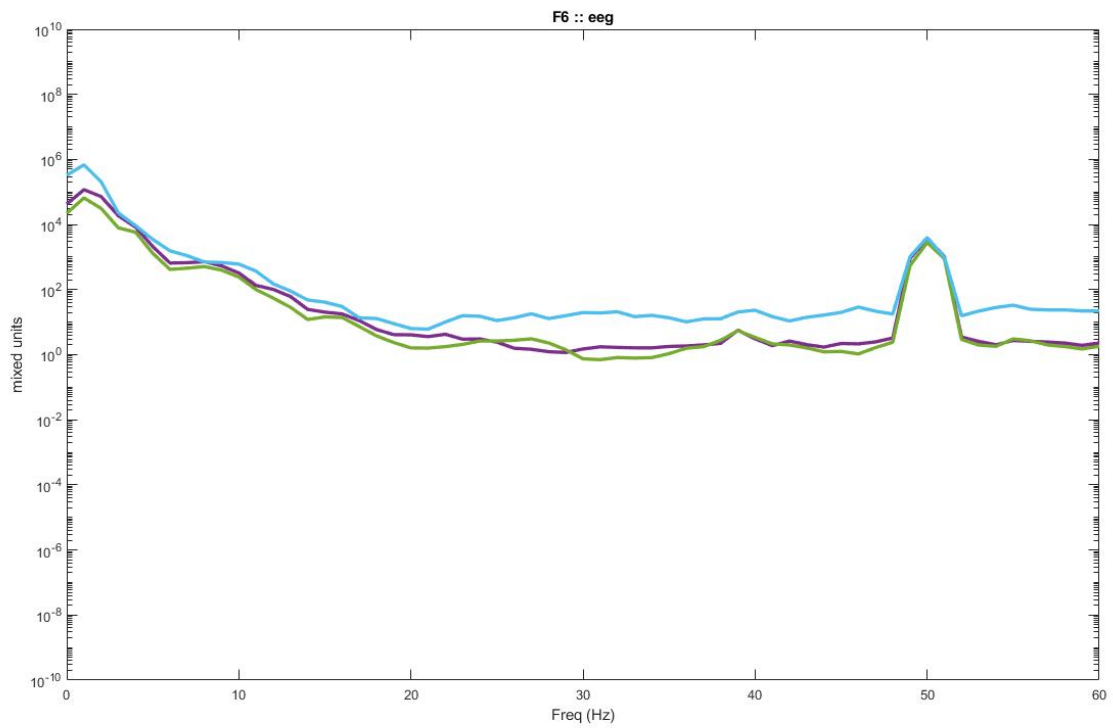
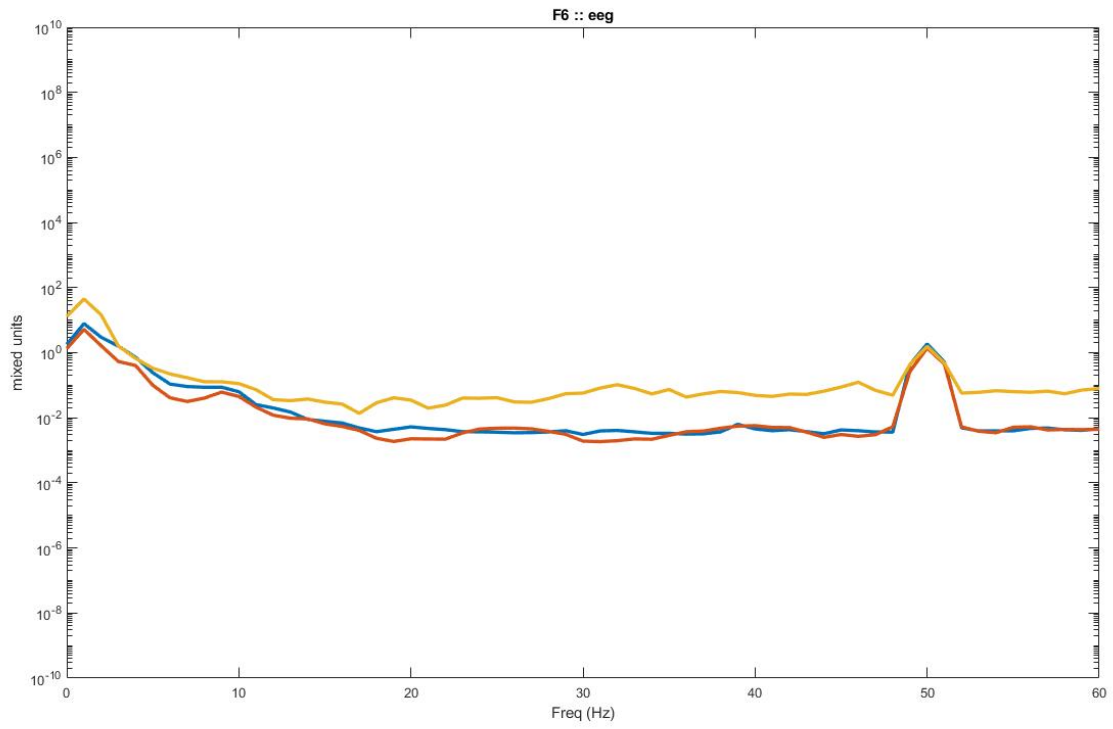


Figure 218. Graph shows electrode location F6. (top) shows software laplacian of electrode EEG. (bottom) shows electrode EEG

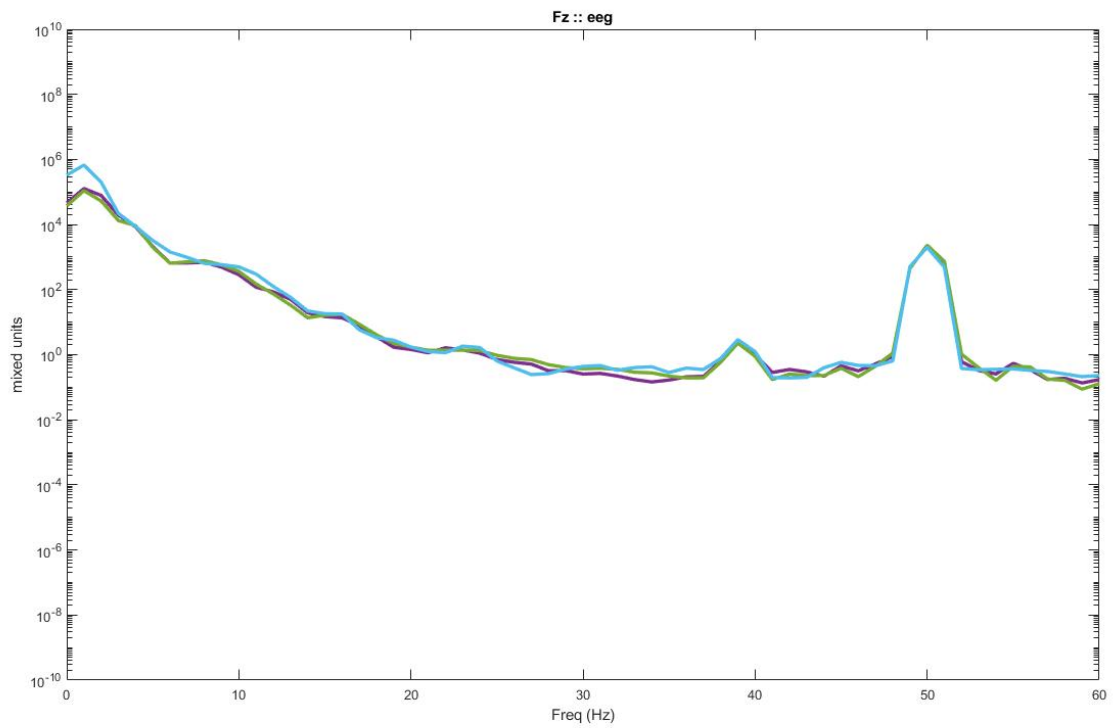
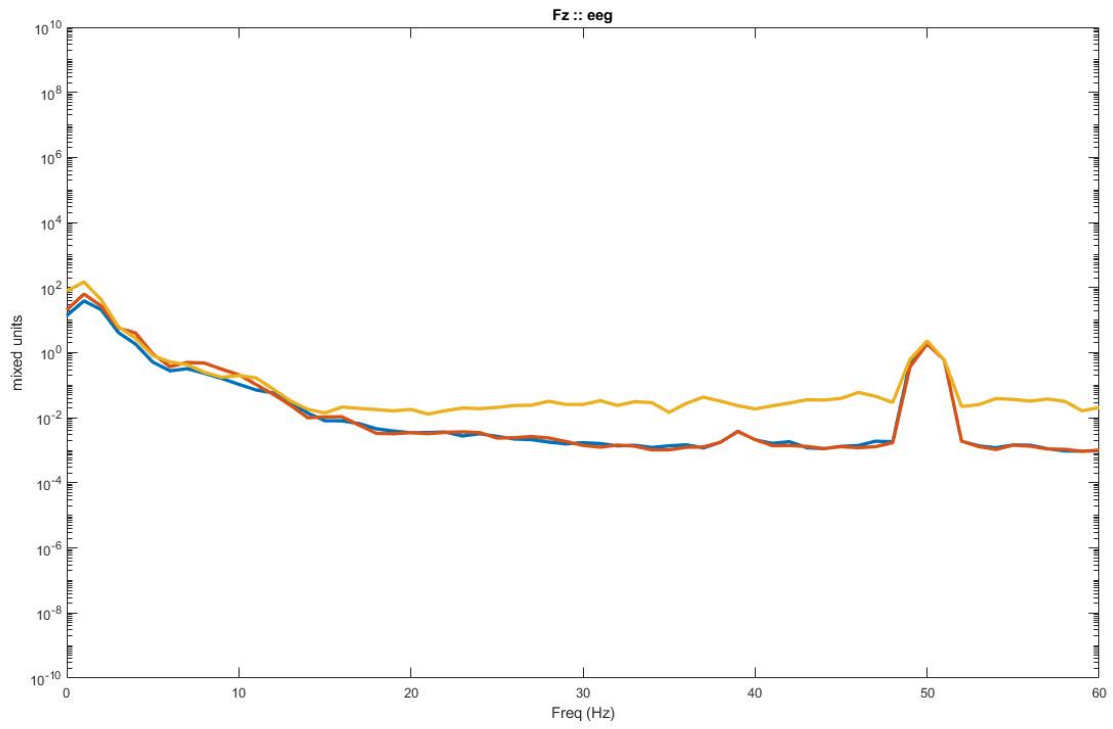


Figure 219. Graph shows electrode location Fz. (top) shows software laplacian of electrode EEG. (bottom) shows electrode EEG

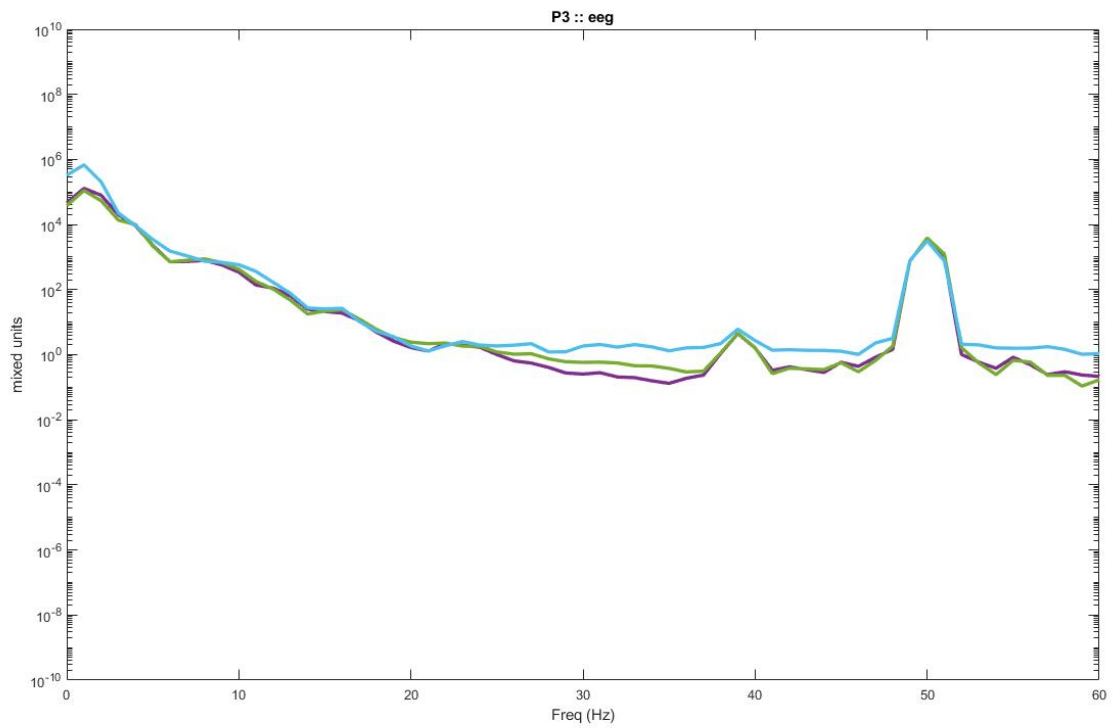
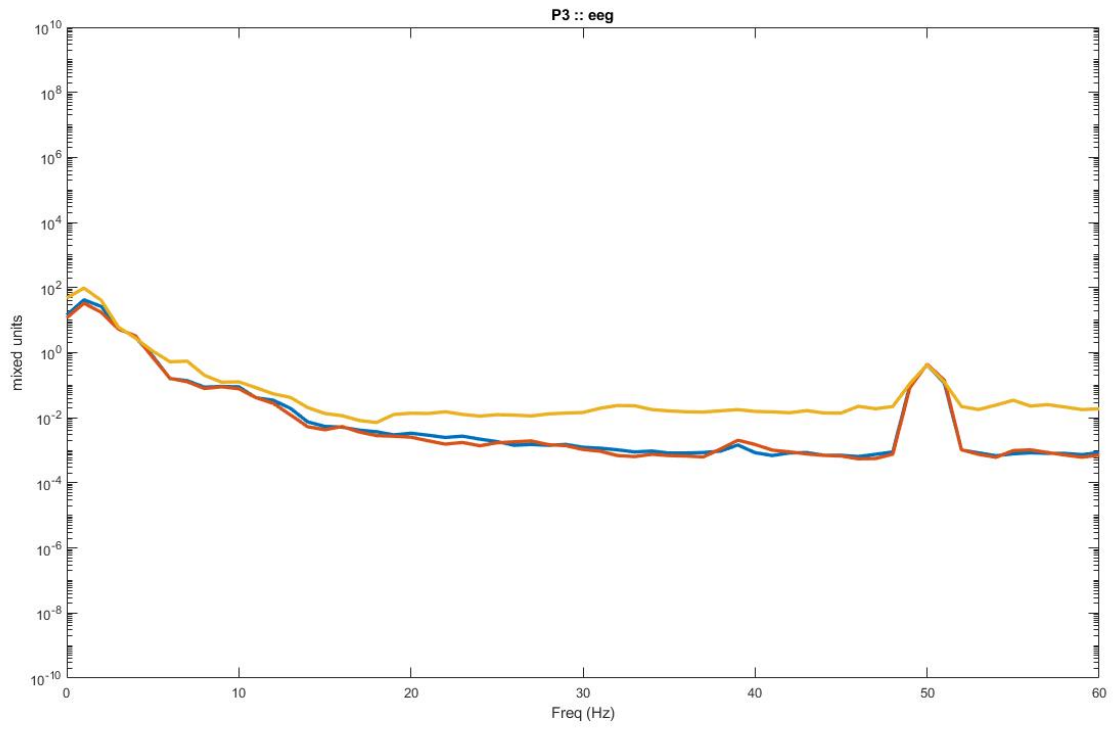


Figure 220. Graph shows electrode location P3. (top) shows software laplacian of electrode EEG. (bottom) shows electrode EEG

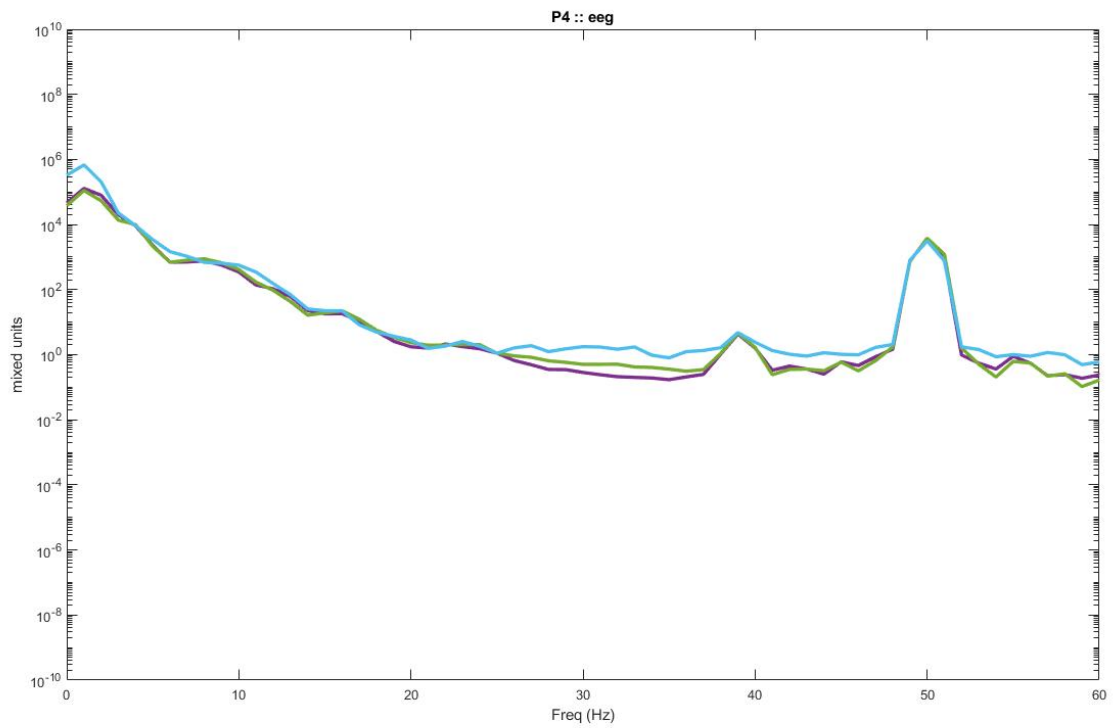
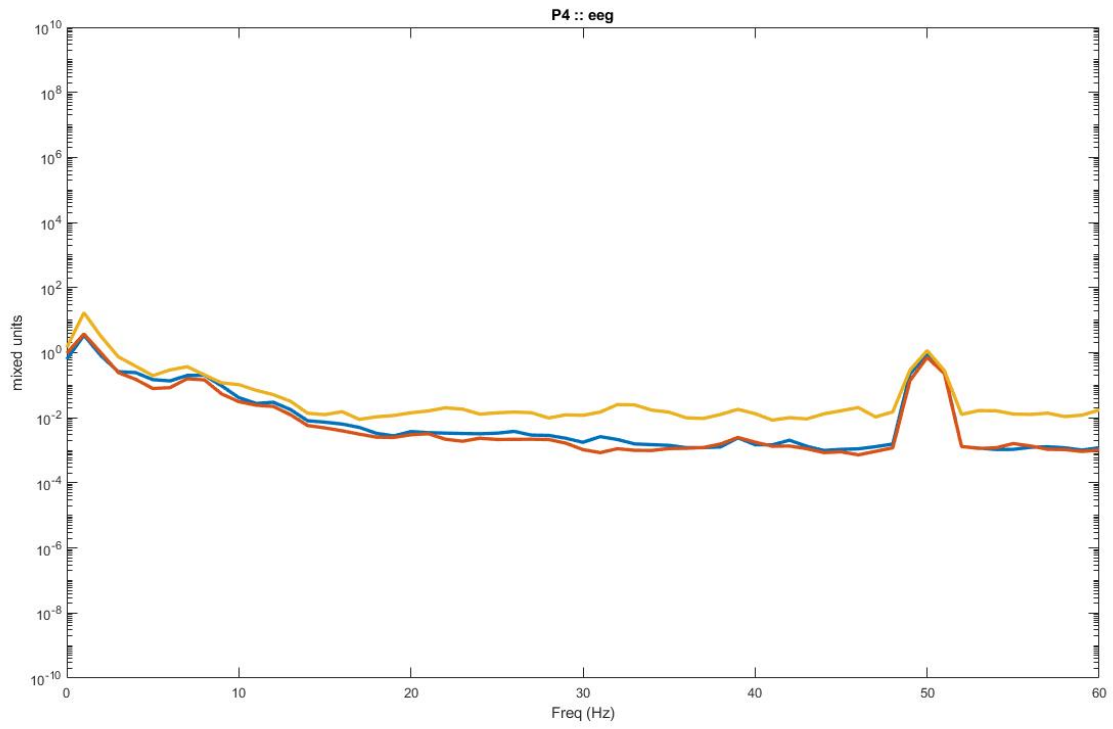


Figure 221. Graph shows electrode location P4. (top) shows software laplacian of electrode EEG. (bottom) shows electrode EEG